

NASA  
CR  
3634  
c.1

# NASA Contractor Report 3634

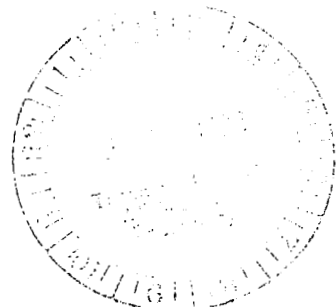
LOAN COPY: RETURN TO  
TECHNICAL LIBRARY, KEESLER

TECH LIBRARY KAFB, NM  
0062150

## Mean-Flow Measurements of the Flow Field Diffusing Bend

O. J. McMillan

CONTRACT NAS3-22113  
NOVEMBER 1982





NASA Contractor Report 3634

# Mean-Flow Measurements of the Flow Field Diffusing Bend

O. J. McMillan  
*Nielsen Engineering & Research, Inc.*  
*Mountain View, California*

Prepared for  
Lewis Research Center  
under Contract NAS3-22113

**NASA**

National Aeronautics  
and Space Administration

**Scientific and Technical  
Information Branch**

1982



## TABLE OF CONTENTS

	Page
SYMBOLS.....	v
SUMMARY.....	1
INTRODUCTION.....	2
APPARATUS AND PROCEDURES.....	3
RESULTS AND DISCUSSION.....	10
Mean Velocity Profiles - Initial Station.....	10
Turbulence Intensity Profiles - Initial Station.....	11
Wall Static Pressures.....	13
Five-Hole Probe Data.....	14
CONCLUDING REMARKS .....	19
APPENDIX A - ARTIFICIAL THICKENING OF THE INLET BOUNDARY LAYERS.....	21
APPENDIX B - CALIBRATION OF THE BOUNDARY-LAYER AND FIVE-HOLE PROBES.....	23
APPENDIX C - TABULATED DATA.....	28
REFERENCES.....	86
TABLES.....	87
FIGURES.....	92



## SYMBOLS

A	constant in hot-wire calibration, eq. (15)
B	constant in hot-wire calibration, eq. (15)
AR	overall area ratio of the diffusing bend, $AR = w_2/w_1$
$AR_x$	local area ratio of the diffusing bend $AR_x = (w_{cv} + w_{cc})/w_1$
AS	aspect ratio of the diffusing bend, $AS = h/w_1$
C	constant in the law of the wall/law of the wake, eq. (14)
$C_f$	skin-friction coefficient, $C_f = 2(u^*/u_\infty)^2$
$C_p$	static-pressure coefficient, $C_p = (p - p_{ref})/q_{ref}$
$C_{pitch}$	five-hole-probe pitch coefficient, eq. (5)
$C_{static}$	five-hole-probe static-pressure coefficient, eq. (8)
$C_{total}$	five-hole-probe total-pressure coefficient, eq. (7)
$C_{yaw}$	five-hole-probe yaw coefficient, eq. (6)
d	diameter of sensing head of five-hole probe, mm
De	Dean number, $De = Re \left( \frac{\frac{1}{2}w_1}{r_c} \right)^{\frac{1}{2}}$
e	output of hot-wire anemometer, volts
G	equilibrium shape factor, $G = \int_0^\delta \left( \frac{u_\infty - u}{u^*} \right)^2 d(\hat{y}/\Delta)$
h	test section height, cm
H	shape factor, $H = \delta^*/\theta$
N	length of circular-arc reference line of diffusing bend, cm
p	static pressure, Pascals

$p_T$	total pressure, Pascals
$\bar{p}$	mean pressure from the yaw-sensing holes of the five-hole probe, eq. (9), Pascals
$q_{ref}$	free-stream dynamic pressure at the initial station
$r_c$	radius of curvature of reference line of diffusing bend
$R_\delta$	Reynolds number based on $u_\infty$ and $\delta$
$R_\theta$	Reynolds number based in $u_\infty$ and $\theta$
$Re$	Reynolds number based on $u_\infty$ and $w_1$
$Re_{bl}$	Reynolds number based on $u_\infty$ and the height of the opening in the boundary-layer probe tip
$Re_{5h}$	Reynolds number based on $u_\infty$ and $d$
$u$	time-average streamwise velocity, m/sec
$u'$	fluctuating component of streamwise velocity, m/sec
$u^*$	wall shear velocity, $u^* = \sqrt{\tau_w/\rho}$ , m/sec
$u^+$	velocity in wall units, $u^+ = u/u^*$
$V$	magnitude of the mean-velocity vector as determined by the five-hole probe, eq. (10), m/sec
$V_{cont}$	one-dimensional through-flow velocity, eq. (13), m/sec
$V_x, V_y, V_z$	components of mean-velocity vector in x, y, z directions, eq. (12), m/sec
$w$	width of test section measured normal to reference line, cm; also wake function, eq. (14)
$w_{cc}, w_{cv}$	distance from reference line to concave or convex wall, respectively, of test section, measured normal to reference line, cm
$x, y, z$	orthogonal curvilinear coordinates, fig. 3, cm
$\hat{y}$	distance from a wall to the geometric center of the opening in the tip of the boundary-layer probe, cm

$\hat{y}^+$	distance from a wall in wall units, $\hat{y}^+ = \hat{y} u^*/\nu$
$\hat{z}$	coordinate specifying location of boundary-layer traverse, Table 2, cm
$\alpha$	pitch angle in the x, y, z system, eq. (12), deg.
$\alpha_p$	pitch angle relative to five-hole-probe tip axis, eq. (4), deg.
$\beta$	yaw angle relative to axis of five-hole-probe tip, fig. 7, deg.
$\delta$	boundary-layer thickness, cm
$\delta^*$	displacement thickness, $\delta^* = \int_0^\delta (u_\infty - u)/u_\infty d\hat{y}$ , cm
$\Delta$	Clouser thickness, $\Delta = \int_0^\delta (u_\infty - u)/u^* d\hat{y}$ , cm
$\theta$	yaw angle of five-hole-probe tip axis relative to test-section reference line, fig. 7, deg.;
	also, momentum thickness $\theta = \int_0^\delta \frac{u}{u_\infty} (1 - \frac{u}{u_\infty}) d\hat{y}$ , cm
$\kappa$	constant in law of the wall/law of the wake, eq. (14)
$\nu$	kinematic viscosity, $m^2/sec$
$\Pi$	Coles wake parameter, eq. (14)
$\rho$	density, $kg/m^3$
$\tau_w$	wall shear stress, Pascals

Subscripts:

p1	plenum
ref	pertaining to the initial station (x = 0)
1	entry channel
2	tailpipe



$\infty$	free stream
cv	convex side
cc	concave side

## SUMMARY

An experimental program to provide high-quality time-average measurements suitable for comparison with calculations of the low-speed turbulent flow in a diffusing bend is described. The apparatus and instrumentation used are discussed in detail. The measurements were made in a closed-loop wind tunnel, the test section of which consists of parallel top and bottom walls and curved diverging side walls. The turning of the center line of this channel is  $40^\circ$ , the area ratio is 1.5, and the ratios of height and center-line length to throat width are 1.5 and 3, respectively. The diffusing bend is preceded and followed by straight, constant-area sections in which measurements were also made. The inlet boundary layers on the parallel walls are artificially thickened and occupy approximately 30% of the channel height; those on the side walls develop naturally and are about half as thick.

The test program was conducted with the inlet free-stream speed held constant at about 30 m/sec. Measurements include: inlet boundary-layer mean-velocity and turbulence-intensity profiles, wall static pressures, and flow-field surveys at six cross sections. The inlet boundary-layer mean-flow measurements were made with a miniature flattened Pitot probe, the intensity measurements with a single-sensor hot wire anemometer. The flow-field surveys were made using a five-hole probe; maps of the velocity-vector and static-pressure fields at the survey locations are provided.

The mean flow field in the diffusing bend is dominated by a pair of counter-rotating streamwise vortices, set up by the cross-stream pressure gradient in the bend which balances the centrifugal force of the fluid as it is turned. The low-speed fluid in the boundary layers on the straight walls is forced towards the convex wall by this pressure gradient, continuity then requiring that high-speed fluid in the central portion of the channel flow towards the concave wall. The modest diffusion present here is manifested as a general deceleration of this flow pattern; the diffuser was designed to avoid any significant separation, and no reverse flow was encountered.

## INTRODUCTION

The continued evolution of the techniques of computational fluid dynamics and turbulence modeling, coupled with the dramatic increases in the power of modern computers, has made for the first time the detailed calculation of certain classes of complex turbulent flows at least thinkable (see, for example, ref. 1). While the full three-dimensional calculation including viscous effects of the flow within the blade passages of turbomachines is not yet practical, the calculation of flows with some of the important features is. These somewhat simplified flows, besides being "building blocks" for turbomachine flows are often also of fundamental interest in themselves. There is, therefore, a need for careful experiments which document such flows at a level of detail sufficient to allow the evaluation and to guide the development of the various methods proposed for their computation.

One example of such a building-block flow is the low-speed turbulent flow through a duct with strong curvature. While obviously many of the complications of an actual turbomachine flow are missing here, included is the effect important in turbomachines of strong secondary flows which are driven by the pressure gradient caused by the curvature of the mean flow. It is also, of course, an interesting flow in its own right, applicable in many practical situations. In a recent experiment (ref. 2), measurements of the longitudinal and radial components of mean velocity and the corresponding normal and Reynolds stresses were made for such a flow in a square duct with inlet boundary layers 15% of the duct width. While the transverse component of mean velocity and associated turbulence quantities were not measured, these measurements still form a benchmark for the evaluation of relevant computational methods.

It is the purpose of the present report to present time-average flow-field measurements in a situation which adds one more physical phenomenon important in turbomachine flows to those included in the experiment of ref. 2; i.e., an adverse pressure gradient. In this work, we present (without extensive analysis) time-average measurements for the flow in a  $40^\circ$  diffusing bend; details of all three mean-velocity components and the static pressure field determined by a five-hole probe, as well as wall static pressures, are included. Because it was desired that there be no appreciable regions of separation in this flow, the overall amount of diffusion incorporated was conservatively selected utilizing the data of reference 3. The diffusion is accomplished by wall divergence in the plane of the bend; the other two walls remain parallel. Incorporating another element important in turbomachine flows, the boundary layers on the parallel walls are artificially thickened to encompass approximately 30% of the passage height; those on

the curved walls are naturally developing and about half as thick.

The following section describes the apparatus, the instrumentation and the procedures used to secure the data. The measurements themselves are presented and briefly discussed in the next section followed by a few concluding remarks. Appendices are included describing the artificial thickening of the inlet boundary layers and the calibration of the probes used; a final appendix contains the tabulated data.

## APPARATUS AND PROCEDURES

The experiment was performed in the Nielsen Engineering & Research, Inc. Water/Wind Tunnel using air as the working fluid. A schematic of this facility as adapted for this test is shown in figure 1, wherein the following major features are identified, starting with the fan (1) and proceeding in the flow direction. A section of honeycomb (0.95 cm cell size, 7.6 cm thick) is located in the 76.2-cm-diameter bottom leg of the tunnel at (2) in order to reduce the swirl of the air entering the turning vanes in the vertical elbow. To further condition the flow, a series of screens and an additional section of honeycomb is located in the 137-cm-diameter plenum (3) as shown in figure 2. Downstream of the plenum, an 8:1 contraction (4) and a 183-cm-long entry channel (5) precede the test section (6). The vertical dimension of the 35.3-cm-wide entry channel increases from 51 cm at the upstream end to 52.8 cm at the downstream end to provide an approximately constant pressure in this section, which is used as the test section in the normal configuration of this tunnel. A diffusing rectangular-to-round transition piece (7) and a return bend (8) complete the flow loop. The belt-driven fan is powered by a 60 kw electric motor (9).

The test section is shown in more detail in figure 3, which also shows the main coordinate system and some of the nomenclature used in this report, as well as the overall features of the diffusing bend. The origin of the coordinate system is at the center, laterally, of the top inside surface of the flow channel approximately one channel-width upstream of the location where the curvature begins. The coordinate system is curvilinear: the x direction is tangent to the reference line throughout the bend and the y and z coordinates are normal to this line. In this report, measurement locations are sometimes referred to by station number: a station is a plane normal to the reference line over which measurements are made and is identified by its x coordinate (which is measured in centimeters) made nondimensional by the length 5.08 cm.

Figure 3 shows that the diffusing bend is preceded in the test section by an upstream length of straight, constant-area channel, and is followed by a straight, constant-area tailpipe which leads to the transition piece. The "Initial Station," where all inlet conditions were measured, is located in the constant-area channel approximately one diffuser throat-width ( $w_1$ ) upstream of the beginning of the bend. The "Reference Line" of the diffusing bend shown in this figure is a circular arc of  $r_c = 152.8$  cm radius tangent to the center lines of the upstream and downstream constant-area sections. The test section is of uniform height,  $h = 52.83 \pm 0.43$  cm. The nominal positions of the side walls in the bend were determined by applying a linear increase in channel width  $w$  (measured normal to the reference line) along the reference line, reaching the overall area ratio at the end of the turning. To avoid excessive bending stress in the side walls, these side-wall positions were modified slightly; the resulting area and "half-width" distributions are compared to the nominal values in figures 4(a) and 4(b), respectively. Post-fabrication inspection showed that the side walls are everywhere within 0.15 cm of their desired location.

The bottom and side walls of the test section are transparent to aid in the conduct of the test and to allow for possible future flow-visualization studies. The bottom wall is 1.9-cm-thick acrylic, while the curved side walls are of 0.95-cm-thick polycarbonate resin. To ensure that these curved side walls have the desired shape, they are fastened to ribs made of 1.9-cm-thick aluminum plate which run the length of the test section at the top and bottom of each of the side walls. These ribs were machined to the required shape using a numerically controlled mill. The top wall is formed from a series of rectangular and circular-sector pieces made of 0.95-cm aluminum tooling plate. This allows the traversing apparatus which provides for remote positioning of the five-hole probe in the  $y$  and  $z$  directions to be located at a number of preselected streamwise locations.

A photograph of the test section is presented in figure 5. The view is looking upstream at the convex side from slightly above; the downstream transition piece and several top pieces have been removed for the photograph. The vertical cylinders shown in this photograph are the "pillars" which connect the top and bottom aluminum ribs for each wall. The pillars are located outside the transparent side walls. Also shown are the braces which were found to be necessary to correct a slight warpage of the convex (CV) wall; no similar problem existed on the concave (CC) wall, which has less curvature and hence smaller bending stresses.

This experiment was conducted with the free-stream dynamic pressure at the initial station ( $q_{ref}$ ) held constant at 543 Pa ( $\pm 1\%$ ) which corresponds to a free-stream velocity ( $u_\infty$ ) at this location of approximately 30.5 m/sec, a Reynolds number ( $Re = u_\infty w_1 / \nu$ ) of 670,000, and a Dean number [ $De = Re(\frac{1}{2}w_1/r_c)^{\frac{1}{2}}$ ] of 228,000.

To avoid possible low-frequency oscillations in the tunnel caused by wandering laminar-to-turbulent transition in the contraction downstream of the plenum, a 0.5-mm-thick trip was placed on all four walls of the contraction approximately 56 cm upstream of its end. Further, to provide the desired artificially thickened boundary layers on the top and bottom walls, an additional trip was provided on these walls at the junction of the contraction and the entry channel. These trips are in the form of bars 0.69 cm high and 0.81 cm in streamwise extent; they are immediately followed by 40.6 cm of 20 grit sandpaper (3M Resinite Open Coat Silicon Carbide Floor Surfacing Paper). The development of this means of artificially thickening the boundary layers is described in Appendix A.

In this investigation, four types of measurements were taken: (1) mean profiles of the boundary layers at the initial station; (2) turbulence-intensity profiles at the initial station; (3) wall static pressures throughout the test section; and (4) mean-velocity and static-pressure surveys of the entire cross section at six streamwise stations. The streamwise locations of the cross sections surveyed are shown in Table 1. Except for the turbulence-intensity measurements, all of the data in this experiment were acquired and reduced during testing with the aid of a DEC PDP 11/23 computer and are stored on a magnetic tape formatted as recommended in reference 4. To insure that the mean data were in fact stationary, all of the inputs to the analog-to-digital converter of the computer were low-pass filtered (cutoff frequency of 5Hz) and a 20-second averaging period was used, during which 2000 samples of each measurand were taken. The data point was saved only if the average  $q_{ref}$  during that particular sampling period was within the specified tolerance; otherwise the fan speed was adjusted and the data point repeated. During the acquisition of the mean-velocity and intensity profiles at the initial station,  $q_{ref}$  was sensed directly using a Kiel probe in the free stream. For the remainder of the testing, to avoid adverse influences of the Kiel probe's wake, this probe was removed and  $q_{ref}$  was obtained by calibration from the observed pressure drop between the plenum and the last wall tap in the entry channel.

The mean boundary-layer profiles ( $u$  vs.  $\hat{y}$ ) were acquired using a flattened Pitot probe of external height 0.24 mm and width 0.94 mm with the opening in the probe tip 0.08 mm high. These profiles were measured at 12 discrete locations at  $x = 0$

(3 profiles on each wall) using a traverser which provided for accurate remote control of the position of the probe tip relative to the wall. The traverse location on a given wall is specified in terms of the  $\hat{z}$  coordinate, which is related to the main coordinate system of figure 3 as shown in Table 2. At each traverse location, the probe was carefully aligned in yaw with the free stream by maximizing the signal from the probe in accord with the probe calibration (Appendix B). The total pressure from the Pitot probe was referenced against the local static pressure (determined using a series of pressure taps located at the initial station) on a carefully calibrated differential pressure transducer. The velocity was calculated from this measured dynamic pressure using the air density corresponding to plenum conditions. The air temperature in the plenum was continuously monitored using a calibrated thermister, while the local barometric pressure and humidity were updated twice daily during testing.

At two of the locations at which Pitot-probe measurements were made, turbulence intensity profiles ( $\sqrt{u'^2}/u_\infty$  vs  $\hat{y}$ ) were also measured. These data were taken using a constant-temperature hot-wire anemometer (TSI 1010A) operated at an overheat ratio of 1.6. A standard, commercially available boundary-layer probe (TSI 1218) was used, supported in the same traverser as was the Pitot probe. This probe has a single platinum-plated tungsten sensor 0.005 mm in diameter oriented normal to the flow. The unlinearized output from the anemometer was calibrated in the tunnel before each profile, and care was taken that the tunnel's temperature change during data acquisition was acceptably small. The computer was not used for these measurements; instead, mean and rms values of the fluctuating anemometer voltage were obtained using an integrating digital voltmeter and a true rms voltmeter, respectively. The normalized turbulence intensity was calculated from these values in the conventional way, as is described in the Results section. For these measurements, a 10-second averaging time was found to be sufficient.

Wall static pressure taps are distributed throughout the test section. These taps are 1 mm diameter and were connected through Scanivalves to differential pressure transducers, the reference sides of which were connected to the average pressure at the initial station ( $p_{ref}$ ). On each Scanivalve,  $p_{ref}$  was also connected to the home port (port 0) and the plenum static pressure ( $p_{p1}$ ) was connected to port 1. This allowed calculation of the static pressure coefficient at each tap independent of the particular calibration coefficients for the transducers involved and further minimized the impact of the already very small zero drift in the instrumentation as follows. The pressure coefficient

is defined to be

$$C_p = \frac{p - p_{ref}}{q_{ref}} \quad (1)$$

which can be written

$$C_p = \left( \frac{p - p_{ref}}{p_{p1} - p_{ref}} \right) \left( \frac{p_{p1} - p_{ref}}{q_{ref}} \right) \quad (2)$$

For this experiment, in which  $q_{ref}$  was held constant, the second term on the right hand side of equation (2) is a constant with measured value 0.9914. Thus, if  $C(I)$  is the average signal in arbitrary units from the pressure transducer for the  $I$ th port of the Scanivalve, and if the calibration of the transducer is taken to be linear, with  $p_{ref}$  on the reference side of the transducer and on port 0 and  $p_{p1}$  on port 1, one can write

$$C_p(I) = 0.9914 \frac{C(I) - C(0)}{C(1) - C(0)} \quad (3)$$

without the use of the calibration coefficients themselves. Equation (3) then also eliminates effects of zero drift up to the beginning of the cycling of the Scanivalve. This equation was used to calculate the pressure coefficients presented in this report.

The mean-velocity and static-pressure surveys of the entire cross sections were done using a commercially available five-hole probe (United Sensor DC-125-36). This probe is sketched in figure 6, which shows the numbers assigned to the five pressure ports, the sign conventions for pitch angle ( $\alpha_p$ ) and yaw angle ( $\beta$ ) relative to the probe axis, and the sleeve which was added to the probe support stem to prevent excessive deflection and vibration of the probe during use. The end of sleeve was  $27d$  (or nine sleeve diameters) from the tip to minimize interference from this source. The probe was supported by a traverser mounted in place of one of the top-wall pieces, as previously discussed. An O-ring seal was provided on the sleeved support stem to prevent leakage; this seal precluded positioning the probe tip any closer to the top wall than approximately  $27d$ .

The probe, which was fully calibrated in an open jet as discussed in Appendix B, was operated with an automatic nulling circuit on the yaw pressure differential ( $p_3 - p_2$ ). At each survey point, this circuit was used to rotate the probe about the stem axis until  $p_3 - p_2 \approx 0$ , at which time the circuit was disabled and the data point taken (using the 20-second averaging



time, as previously described). The resulting angle of the axis of the probe tip relative to the tangent to the channel reference line at the streamwise location of the survey in question is defined to be  $\theta$ , and any small residual average yaw pressure differential is converted to a yaw angle relative to the probe tip axis ( $\beta$ ) using the calibration relations presented below. Thus, the yaw angle of the velocity vector relative to the tangent to the channel reference line at any streamwise location is  $\theta + \beta$ , as shown in figure 7. The pitch angle of the velocity vector in tunnel coordinates ( $\alpha$ ) is related to the pitch angle relative to the probe tip axis by the empirical blockage correction

$$\alpha = \alpha_p + 0.83y/h \quad (4)$$

which is discussed further in the Results section.

The calibration of the five-hole probe is in terms of the following definitions:

$$C_{pitch} = \frac{p_4 - p_5}{p_1 - \bar{p}} \quad (5)$$

$$C_{yaw} = \frac{p_3 - p_2}{p_1 - \bar{p}} \quad (6)$$

$$C_{total} = \frac{p_1 - p_T}{p_1 - \bar{p}} \quad (7)$$

$$C_{static} = \frac{\bar{p} - p}{p_1 - \bar{p}} \quad (8)$$

$$\bar{p} = \frac{p_2 + p_3}{2} \quad (9)$$

At each survey point, differential pressure transducers were used to determine  $p_3 - p_2$ ,  $p_1 - p_2$ ,  $p_4 - p_5$  and  $p_2 - p_{ref}$ . This allowed calculation of  $C_{pitch}$  and  $C_{yaw}$ , with which the calibration curves presented in Appendix B were entered to determine  $\alpha_p$  and  $\beta$  and the corresponding values of  $C_{total}$  and  $C_{static}$ . Then

$$V = \left\{ \frac{2}{\rho} [(p_1 - \bar{p})(C_{static} - C_{total} + 1)] \right\}^{1/2} \quad (10)$$

$$C_p = [(p_2 - p_{ref}) + (p_3 - p_2)/2 - (p_1 - \bar{p})C_{static}] / q_{ref} \quad (11)$$

and resolving the velocity vector into its components,

$$\left. \begin{aligned} V_x &= V \cos\alpha \cos(\theta + \beta) \\ V_y &= -V \sin\alpha \\ V_z &= V \cos\alpha \sin(\theta + \beta) \end{aligned} \right\} \quad (12)$$

A convenient reference used to normalized these velocity-survey results is related to the free-stream velocity at the initial station  $[u_{ref} = (2q_{ref}/\rho)^{1/2}]$  through the one-dimensional continuity equation:

$$V_{cont} = \left\{ \begin{array}{ll} u_{ref} & 0 \leq x \leq 35.6 \\ u_{ref}/[1 + (AR-1)(x-35.6)/N] & 35.6 < x \leq 142.2 \\ u_{ref}/AR & x > 142.2 \end{array} \right\} \quad (13)$$

The estimated experimental uncertainties for the results derived in this investigation are given in Table 3. The method of reference 5 has been used to calculate the way in which the estimated uncertainties in the actual measurands propagate into calculated quantities. The values given in Table 3 are estimated to be valid for all the measurements presented, with the exception of a few points in the surveys at the end of the bend and in the tailpipe (stations 28 and 38, respectively). At these points, the combination of low velocity, large flow angles and increased unsteadiness increases somewhat the estimated uncertainty for some of the values derived from the five-hole probe, perhaps doubling the uncertainty in velocity magnitude to  $\pm 4\%$  and increasing the estimated uncertainty in  $\theta + \beta$  to  $\pm 1.5^\circ$ .

As is discussed further in the Results section, the effects of probe deflection and blockage on the five-hole probe as immersed in a "normal" free-stream/boundary-layer flow (such as exists at the initial station) are accounted for by direct calibration, and wall-proximity/viscous effects are avoided by not

approaching too close to a wall. These phenomena are therefore encompassed in the foregoing uncertainty estimates. However, without recourse to a less intrusive measurement technique, it is impossible to rule out the possibility of additional probe interference effects in the complicated three-dimensional flows measured here. A similar cautionary note is appropriate with respect to the effects of varying turbulence intensity on the calibration of the five-hole probe, a subject which is beyond the scope of the present investigation.

## RESULTS AND DISCUSSION

### Mean Velocity Profiles - Initial Station

Velocity profiles in the boundary layers at the initial station were measured at three transverse locations on each wall and are shown in figures 8(a)-(d). Tabulated data for these profiles are given in Appendix C. In figure 8, the arrow connected to the symbol for each profile indicates the boundary-layer thickness ( $\delta$ ) for that profile as calculated in the fitting procedure to the law of the wall/law of the wake described below. A high degree of uniformity is indicated among the profiles for the bottom wall [fig. 8(a)] and among those for the top wall [fig. 8(b)], although close inspection reveals that the average boundary-layer thickness on the bottom wall is slightly less (approximately 0.3 cm) than that on the top. This is so even though identical means were used on these walls to artificially thicken the layers, and is a consequence of the nonuniformity of the naturally evolving layers in the tunnel. This is demonstrated by the profiles on the CV wall [fig. 8(c)] and the CC wall [fig. 8(d)]; on each of these walls, the bottom-most profile is somewhat thinner than the other two, which are essentially identical to each other. Also shown in figure 8(a) is the variation in velocity which is associated with the allowable variation ( $\pm 1\%$ ) in  $q_{ref}$ .

These same profiles plotted in wall variables are shown in figures 9(a)-(d). The shear velocity ( $u^*$ ) necessary to transform the primitive variables into wall variables has been inferred from each profile using the process described by Coles in reference 6. In this procedure, values of  $u^*$  and  $\delta$  are found so that the rms deviation of the profile data from the law of the wall/law of the wake is minimized. The law of the wall/law of the wake is expressed as

$$u^+ = \frac{1}{\kappa} \ln \hat{y}^+ + C + \frac{\Pi}{\kappa} w(\hat{y}/\delta) \quad (14)$$

where

$$u^+ = u/u^*$$

$$\hat{y}^+ = \hat{y}u^*/\nu$$

$$w(\hat{y}/\delta) = 2 \sin^2 \left( \frac{\pi}{2} \frac{\hat{y}}{\delta} \right)$$

and the constants are set at the values recommended in reference 6 ( $\kappa = 0.41$ ,  $C = 5.0$ ). The value of the wake parameter ( $\Pi$ ) is determined from equation (14) evaluated at  $\hat{y} = \delta$ . Following Coles, the range of experimental data used for the fitting process is such that  $\hat{y}^+ > 50$  and  $\hat{y}/\delta < 0.90$ .

Inspection of the profiles of figure 9 indicates an extensive logarithmic region on all four walls and the existence of some wall-proximity/viscous effects on the readings taken using the boundary-layer probe very near the walls. No corrections have been applied to the data to attempt to account for these effects; these few near-wall data points have essentially no effect on the values inferred from the fitting process described above. The top- and bottom-wall profiles [figs. 9(a) and (b), respectively] show a very small wake, in agreement with previous observations of profiles which have evolved after separation and attachment downstream of a trip (ref. 7). In contrast, the naturally developed side-wall profiles [figs. 9(c) and (d)] show a pronounced wake. In all cases, the agreement of the data with equation (14) in the fitted region is excellent, with the largest rms deviation being less than 0.7% of  $u_\infty$ .

For reference, the values of the standard boundary-layer parameters calculated from these profiles during the fitting process are shown in Table 4. Again following Coles (ref. 6), the integral parameters  $\delta^*$  and  $\theta$  have been calculated using standard functions instead of data for  $\hat{y}^+ < 50$ . As is discussed in Appendix A, these profiles show evidence of being in "local equilibrium", i.e., the parameters calculated from these profiles have approximately the same relation among themselves as do those for equilibrium flows in which  $\Pi$  is constant in the streamwise direction.

#### Turbulence Intensity Profiles - Initial Station

At the center lines of the top and CV walls at the initial station, profiles of the streamwise component of turbulence intensity were measured using a hot-wire probe with its single wire held normal to the stream. The output from the anemometer

was assumed to follow the relation

$$e^2 = A + Bu^{.45} \quad (15)$$

where A and B were determined by direct calibration just prior to each profile. The turbulence intensity at each profile point was determined from

$$\frac{\sqrt{u'^2}}{u_\infty} = 4.44 e \sqrt{e'^2} (e^2 - A)^{1.22} / (e_\infty^2 - A)^{2.22} \quad (16)$$

with  $\sqrt{e'^2}$  measured directly using a true rms voltmeter.

A comparison of the mean profiles measured with the hot wire during this process with the Pitot-probe profiles shown previously in figures 8(b) and (c) is shown in figure 10. In this figure,  $\hat{y}$  for the profiles from the hot-wire as well as from the Pitot-probe has been normalized by the boundary-layer thickness determined from the fit of the Pitot-probe data to the law of the wall/law of the wake. The profiles measured with the two types of probe agree quite well as shown in figure 10, with the discrepancy being well within the combined estimated uncertainty interval. As is evident in figure 10, only the outer regions of the boundary layers were accessible with the hot-wire probe used because of the shape of the prongs which support the sensor. The profiles shown were acquired with the probe protruding though the wall being traversed; an attempt was made to get nearer to this wall by extending the probe through the opposite wall, but this was unsuccessful due to excessive vibration of the probe support stem.

The measured intensity profiles are shown in figure 11. For reference, Kebanoff's profile measurements of the stream-wise intensity on a flat plate at zero incidence in a free stream of very low intensity (0.02%) are reproduced from reference 8. The present data indicate a free-stream turbulence intensity of approximately 1.2%, but for  $\hat{y}/\delta < 0.5$ , where the influence of the free-stream turbulence intensity lessens, the present data seem to be approaching the flat-plate data, as expected. In spite of this apparent good agreement near the wall, it should be noted that the measured free-stream value of 1.2% is somewhat higher than was anticipated; the combination of honeycomb and screens in the plenum described earlier was expected to provide less free-stream turbulence. Because when these data were taken, no instrumentation was available to frequency-analyze the hot-wire signals, the possibility exists that a portion of the measured intensity is due to probe vibration. The probe

experienced no visually apparent vibration, but because of the lack of spectrum analysis, these data should be treated with some caution.

### Wall Static Pressures

Figure 12 shows the variation of the wall static pressure coefficients with streamwise distance as determined from the taps located on the center lines of the CV and CC walls and on the reference line of the top and bottom walls. Indicated on the figure are the four major regions in which data were acquired: (1) the entry channel, which had slightly increasing height to provide for approximately constant pressure, (2) the upstream constant-area portion of the test section, (3) the diffusing bend itself, and (4) the constant-area tailpipe. As indicated earlier, fairing of the wall contours was necessary at the beginning and end of the diffusing bend, so that the increase in the channel spanwise dimension began and ended at slightly different locations on the CV and CC walls; these locations are marked with the vertical arrows in figure 12.

This figure indicates that approximately constant pressure was achieved in the entry channel, that the upstream influence of the curvature of the  $40^\circ$  bend extended almost to the initial station (station 0), and that the downstream influence extended almost to the last data station in the tailpipe. Little variation exists in the data from the top- and bottom-wall taps at the channel reference line.

There are two predominant features of the pressure distribution in the diffusing bend: (1) an overall increase with streamwise position of the mean pressure level due to the area increase, and (2) the cross-stream gradient in reaction to the centrifugal force of the flow as it is turned. The balance of these effects results in a continually adverse pressure gradient up to about station 26 on the CC wall followed by a mild acceleration as the flow relaxes in the tailpipe, whereas on the CV wall there is an initial region of acceleration up to about station 8, which is then followed by a continuing adverse pressure gradient all the way to the exit of the tailpipe.

More detail on the cross-channel variation of static pressure as measured at the wall at several stations is shown in figures 13(a)-(f). In each of these figures, the  $z$ -location of the measurement is normalized using the diffuser inlet width,  $w_1$ , and the side-wall locations are indicated by the vertical lines with cross-hatching.

Generally, only a small top-to-bottom variation is apparent in the readings taken at a given  $z/w_1$ , except at the CV wall. This variation in the y-direction as measured on the CV and CC walls is shown in figure 14(a)-(f). Here, the y coordinate of the measurement location is normalized using the channel height, h. Examination of these figures reveals that at the CV wall, there is a transition from one pattern which exists early in the bend (stations 7 and 14) to another which exists at the end of the bend and at the end of the tailpipe (stations 28 and 38, respectively). The earlier pattern has a "dip" in the middle, whereas the later one has a characteristic "w" shape. The persistence of this "w" pattern in the static pressures measured in the interior of the flow field as well as its relation to the flow pattern deduced from the five-hole-probe measurements is discussed below. In figure 14(e), it is shown that the CV-wall measurements were taken slightly downstream of those on the CC wall. This was required by the presence of a pillar on the CV wall at station 28.

Tabulated values of the measured wall static pressure coefficients are contained in Appendix C.

#### Five-Hole Probe Data

While the probe had previously been fully calibrated in an open jet (Appendix B), the effects of area blockage, wall proximity and immersion in a boundary layer remained to be accounted for. With respect to the effect of probe blockage in the confined area of the test section, with the probe fully extended at station 0, it occupies about 2.4% of the cross-sectional area of the flow channel. While this figure decreases uniformly to about 1.8% at the end of the diffuser, and while it is less if the probe is not fully extended, area-blockage effects could not be ruled out a priori, and an additional calibration step was conducted with the probe in place at station 0. Calibration at this location was possible because the boundary-layer and wall-static-pressure data already presented give a good indication of the flow field which exists at this station; underlying this procedure is the supposition that the careful construction of the tunnel described earlier produces uniform flow parallel to the tunnel axis in the potential core at station 0.

In this additional calibration step, several profiles were taken in each of which the probe traversed a line of constant  $z$ . The resulting measurements were then evaluated on the basis of previous measurements and, in the potential core, the expected uniform parallel flow. For example, the measured profiles of the pitch angle relative to the probe axis ( $\alpha_p$ ) are shown in figures 15(a)-(g). These figures show that at

all z locations, as the probe is extended, the flow at the probe tip is directed continuously more downward. These data are well represented by the relation

$$\alpha_p = -0.83 y/h \quad (17)$$

which straight line is reproduced on all the parts of figure 15. This variation is interpreted to be due to probe blockage, and flow parallel to the tunnel axis is obtained from the traverse data by the use of equation (17) to form the expression already given as equation (4). Application of equation (4) to the five-hole-probe profile data at station 0 yields an average pitch angle in the potential core considerably less than  $0.1^\circ$ , in accord with our expectations, and equation (4) has been applied to all of the five-hole-probe data presented herein.

The indicated yaw-angle variation at station 0 was also examined [fig. 16(a)-(g)]. In this case, while some variation is evident with a general trend of  $\theta + \beta$  increasing slightly with increasing  $y/h$ , the physical mechanism which could cause this variation is not clear. A small-amplitude large-scale streamwise vortical motion could presumably produce approximately the yaw-angle variations of figure 16, but such a motion is precluded by the plenum honeycomb. For this reason, it was not judged suitable to attempt to correct these data. Even so, the average indicated yaw angle in the potential core at station 0 is approximately  $0.2^\circ$ , an acceptably small value well within the estimated uncertainty for this variable.

With area-blockage effects on the indicated direction of the flow thus accounted for, it remained to investigate possible effects on the indicated static pressure and velocity magnitude. The static-pressure profiles to be shown later show no systematic discrepancies and agree with measured wall static pressures within the uncertainty of the data, so no correction has been applied to this variable. The question of velocity magnitude has been addressed by reproducing some of the initial-station boundary-layer profiles with the five-hole probe, three on the bottom wall, and one at the center of the CV wall. These results are shown in figures 17(a) and (b), and allow assessment not only of area-blockage effects but also wall-proximity and viscous effects. It is seen that until the tip of the five-hole probe is approximately  $10d$  from a wall, its indicated velocity agrees with that from the boundary-layer probe to within the estimated uncertainty; thereafter, the discrepancy increases considerably. We have therefore concluded that except within about  $10d$  of a wall, there is no correction required for velocity magnitude; closer than this to a wall, a correction is required, but no correction that is valid throughout the flow field in the test section (which has strongly three-dimensional wall layers)



is known. Because the data from the five-hole probe near a wall at the remaining stations to be surveyed would therefore be subject to unknown but probably unacceptably large errors, it was decided that the resources available for testing would be best applied by concentrating on the interior region at least  $10d$  from all walls; accordingly, no data were taken with the probe closer than this to a wall at the remaining survey stations.

With the preliminaries accomplished, we proceed to the presentation of the data at the six cross sections surveyed, as identified in Table 1. All of the data acquired are tabulated in Appendix C. Selected portions of these data have been plotted and are discussed next.

Figures 18(a)-(f) show the measured cross-flow velocity vectors at the six measurement stations. The cross-flow velocity is defined to be the vector sum of  $V_y$  and  $V_z$ , and has been normalized using the local one-dimensional through-flow velocity,  $V_{cont}$  [see eqs. (12) and (13)]. The scale for these normalized vectors is the same in each of these figures, as shown. The dashed lines in these figures delimit the region which is  $10d$  from the CV, bottom, and CC walls; because the probe could not be traversed this close to the top wall, no dashed line is shown there.

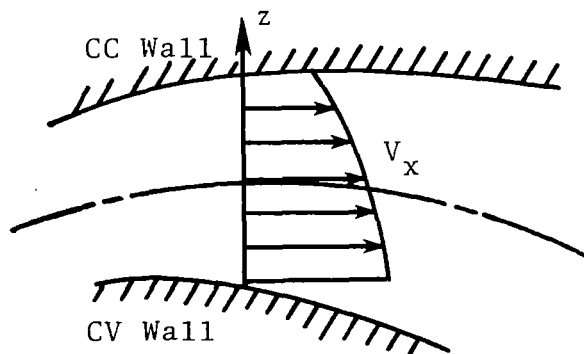
At station 0 [fig. 18(a)], the deviation from axial flow is small, as has been guaranteed by the secondary calibration conducted at this location. Figure 18(b) shows that at the start of the bend (station 7), there is a crossflow towards the CV wall which is fairly uniform from top-to-bottom. This pattern is a consequence of the fairing of the diffuser walls and the entry channel: at station 7, figure 4(b) shows that  $w_{CV}$  (the distance from the channel reference line to the CV wall) has already increased from the entry-channel value while  $w_{CC}$  has not. Because of this asymmetric area increase, one would expect the yaw angle of the flow at this cross section to vary from  $0^\circ$  at the CC wall to the local CV wall angle ( $-3.6^\circ$ ). In general agreement with this expectation, the measured yaw angle ( $\theta + \beta$ ) at the closest profile to the CC wall ( $z = 13.97$ ) is about  $-0.7^\circ$ , while at the nearest profile to the CV wall ( $z = -13.97$ ) the average measured value is about  $-3.1^\circ$ . Any upstream influence at this station of the pressure-gradient-driven secondary flow in the bend is masked by this effect.

At the remaining stations, the development of the pressure-gradient-driven secondary flow and its gradual domination over the asymmetric-area-increase-driven cross flow is shown, with detail lacking at the top wall because of the previously cited limitations on probe travel. The indication is that the flow is qualitatively symmetric top-to-bottom (the degree of quantitative symmetry is about as expected given the discrepancy in the entering top- and bottom-wall boundary-layer thicknesses), so in this

discussion attention is largely focused on the bottom half-channel. As the flow proceeds through the bend, the apparent centroid of the streamwise vorticity near the bottom wall moves towards the CV wall, with this centroid lifting off the bottom wall by the end of the tailpipe in a manner reminiscent of the smoke-visualization photographs of ref. 9. This vortical pattern is the dominant feature of the flow in the bend, and is a direct result of the cross-stream pressure gradient caused by the turning of the flow. The cross-stream gradient causes the slowly moving fluid in the top- and bottom-wall boundary layers to move towards the CV wall; continuity then requires the flow in the center of the channel to flow towards the CC wall. The region near the center of the CC wall will be discussed after the profiles of the axial velocity component, which are shown next.

In figures 19, 20 and 21, profiles of  $V_x/V_{cont}$  are shown for stations 0, 28, and 38, respectively. To allow comparison of the profiles at each station, they have been plotted together with the abscissas offset as shown. The location of the bottom wall is indicated by the line with the cross-hatching. At station 0 (fig. 19), the flow in the potential core is seen to be quite uniform, as was suggested by the boundary-layer and static-pressure data presented earlier.

At the end of the bend [figs. 20(a) and (b)], the main features of the axial velocity profiles result from the equilibrium established at this station between two opposing factors: (1) potential-flow effects which results in a transverse gradient in  $V_x$  with the highest velocity at the CV wall (see sketch below); and (2) effects of the pressure-gradient-driven secondary flow, which is made possible by the boundary layers on the top and bottom walls, and which results in the accumulation of low-speed fluid at the CV wall with the subsequent displacement of high-speed flow towards the CC wall. The profiles of figs. 20(a) and (b) are formed in accord with the balancing of these effects.



Potential-flow  $V_x$  Distribution

The non-uniform regions in the central portions of the profiles for  $z > 15.2$  in fig. 20(b) show an additional effect which will be discussed further in connection with fig. 21(c).

The axial-velocity profiles at the end of the tailpipe [station 38, figs. 21(a)-(c)] show how this balance between potential and viscous effects is affected by the relaxation of the cross-stream pressure gradient, with the attendant continued adverse pressure gradient on the CV wall and favorable gradient on the CC wall. For example, the local maximum which exists at the channel center line near the CV wall at station 28 has disappeared in the profiles nearest this wall at station 38, but persists in profiles a bit farther away ( $-15.2 \leq z \leq -10.2$ ). In the remainder of the cross section, the flow is essentially uniform outside the boundary layers, with the exception of the anomalous region again concentrated in the central portion of the profiles near the CC wall [fig. 21(c)].

After the secondary flow has developed in the bend, the expected pattern near the CC wall is as follows: with respect to the cross flow, a stagnation point should exist at each station near the center line of this wall; the axial velocities in this region should deviate on the high side from the potential distribution shown in the previous sketch. However, the current measurements of the cross-flow-velocity and axial-velocity fields in this region show quite a different pattern. Referring back to figure 19, the axial velocity profile at  $z = 13.3$  at the initial station shows a barely perceptible disturbance near the center of the passage, which has been amplified by the adverse pressure gradient in the bend so that by station 28, a pronounced defect is evident [fig. 20(b)] which persists to the end of the tailpipe [fig. 21(c)]. The cross-flow distributions of fig. 18 show a developing imbedded vortical region near the center line of the CC wall. Analysis of the possible causes of these patterns led to the suspicion that they might be the manifestation of the wake of the plenum thermister, which was located on the horizontal center line of the plenum on the CC side of the tunnel.

To establish if this was in fact the case, the thermister was moved to another location in the plenum and a portion of the measurements at station 38 were repeated. The resulting axial velocity profiles are also shown in figure 21(c), and indicate that when the thermister is moved, the disturbance disappears. This figure also shows that the thermister wake is reasonably localized near the center line of the CC wall when the thermister is in its normal position. Figures 22(a) and (b) show the effect of moving the thermister on the cross-flow velocity vectors. In figure 22(a), the cross-flow vectors at station 38 for  $z > 10$  are shown with the plenum thermister removed from the center line of the CC wall, and it is seen that the imbedded vortical region

near the CC-wall center line in figure 18(f) is replaced by the expected cross-flow stagnation. In figure 22(b), figures 18(f) and 22(a) are overlaid to demonstrate that, just as was concluded from the axial-velocity profiles, the region influenced by the thermister wake does not extend far from the center line of the CC wall. Although this wake is an undesirable contaminant of the basic flow field of interest, its limited extent and comparatively favorable location should minimize its adverse impact on the usefulness of the data.

One of the important design goals for the current experiment was that there was to be no appreciable separation or back-flow in the bend, in order to avoid placing excessive demands on the computational methods to be evaluated using the data. Examination of the axial velocity profiles of figures 20 and 21 suggests that this goal was achieved, for there is no indication of reverse flow anywhere in the measurements. In order to substantiate this, a flow-visualization study was performed on the bottom wall, and the resulting carbon-black pattern also showed no separation.

The final data derived from the five-hole probe are static pressure coefficients in the flow field. In figures 23, 24, and 25, static pressure profiles are shown at stations 0, 28, and 38, respectively. At all of these stations, the variation with  $y$  at a given  $z$  position is relatively small and extrapolation to the wall values shown in these figures by the solid symbols seems reasonable.

#### CONCLUDING REMARKS

The predominant feature of the mean flow in the  $40^\circ$  diffusing bend is a set of counter-rotating streamwise vortices, similar to the situation in a curved duct with no area increase (ref. 2). These vortices are set up by the existence of the cross-stream pressure gradient in the bend which balances the centrifugal force of the fluid as it is turned. Low-speed fluid in the boundary layers on the top and bottom walls is forced towards the convex wall by the pressure gradient, and continuity then requires that high-speed fluid in the central portion of the channel flow towards the concave wall. The modest area increase of the current experiment superimposes a general deceleration on this flow pattern. These results combined with those in the relaxation region in the tailpipe downstream of the bend should provide a significantly challenging test case for three-dimensional calculation methods.

A localized region in the flow near the center line of the concave wall is influenced by the wake of the thermister which was located in the plenum of the tunnel. Although this wake is

an undesirable contaminant of the present measurements, its extent is limited and comparisons with calculations should not be particularly confused by it.

## APPENDIX A

### ARTIFICIAL THICKENING OF THE INLET BOUNDARY LAYERS

A series of profile measurements is presented here which was made in the process of developing the final means used to thicken the inlet boundary layers on the top and bottom walls to the desired thickness of from 7-10 cm. All of these measurements were made at the center line of the bottom wall at the initial station ( $x = 0$ ), although the wall treatments to be described were applied to both top and bottom walls.

The boundary layer was measured under four conditions: (1) no wall treatment -- the boundary layer is the one which naturally evolves on the smooth wall; (2) a 40.6 cm length of 20 grit sandpaper is glued to the wall with its upstream edge at the junction of the contraction and the entry channel; (3) just upstream of the sandpaper, a trip approximately 0.76 cm high by 0.32 cm in streamwise extent is placed across the channel; and (4) this trip is replaced with the final trip geometry (0.69 cm high by 0.81 cm in streamwise extent). The free stream velocity is 30.5 m/sec in all cases.

The measured profiles are shown in figure 26, in which the boundary layer thickness resulting from the fit to the law of the wall/law of the wake is indicated by the arrow marked with the appropriate symbol. It is seen that in going from case (1) to (3), a boundary layer of thickness in the desired range was achieved. However, the boundary layer of case (3) was of the absolute maximum thickness that could be accommodated with the existing boundary-layer traverser - any small variation towards a thicker profile at other measurement locations at station 0 would exceed its capability. Therefore, the final trip height was somewhat less [case(4)]. Also, in fabricating the final trip, more streamwise length was provided to facilitate its mounting to the entry-channel wall. The final profile (sandpaper plus 0.69 cm trip) is seen to have a thickness in the required range.

The same profiles are shown in wall variables in figure 27. For all of the different thickening procedures, a considerable extent of logarithmic region is evident; the profiles differ primarily in this figure by the extent of their wake components, the thicker the profiles, the less the wake. The friction velocities used to define these wall variables were derived from the fitting procedure to the law of the wall/law of the wake described in the text. The profile parameters calculated from the fitting procedure are listed in Table 5.

The artificially augmented thickness of the top- and bottom-wall boundary layers was to be achieved while maintaining as much as possible of the structure of a boundary layer of this same thickness which had grown naturally on a smooth wall. It is known (see, for example, ref. 10) that this can be achieved to a fairly high order of turbulence statistics if it is possible to tune a three-dimensional tripping device for the specified application. However, resources to develop such a trip were not available in this program; the 183 cm length of entry channel was provided instead to allow at least partial equilibration of the profiles generated by the simpler devices actually employed. A measure of the degree of "naturalness" of the resulting profiles at station 0 is available by comparing the values of certain of the profile parameters of Table 5 to those which exist for "equilibrium profiles" (profiles for a flow in which  $\Pi$  is constant at subsequent streamwise positions). This is done in figure 28 which is reproduced from reference 6. The lines on this figure show  $C_f$  vs.  $R_\theta$  as calculated from the local friction law which follows from the law of the wall/law of the wake. The small filled symbols are from several previous experiments identified in ref. 6. In this figure, it is seen that the parameters for the present profiles have the same relation among themselves as do those for equilibrium profiles, and that the present profiles are therefore in satisfactory "local" equilibrium.

## APPENDIX B

### CALIBRATION OF THE BOUNDARY-LAYER AND FIVE-HOLE PROBES

The wind tunnel of figure 1 was used as an open-return facility prior to the installation of the entry channel, test section, transition piece and return bend for the purpose of these calibrations. A special calibration fixture was fabricated which allowed mounting of either of these probes at the approximate center of the free jet issuing from the 8:1 contraction approximately 46 cm downstream from the end of the contraction. This fixture allowed the probe being calibrated to be rotated in pitch about its tip, allowing the calibration to be done at a fixed location in the free jet.

#### The Boundary-Layer Probe

This probe consists of a short length of hypodermic tubing (0.71 mm O.D. x 0.36 mm I.D.) bent to the general shape illustrated in figure 29 and soldered to a 3.18 mm O.D. support stem. The tip of the probe (which is flattened and filed as described in the text) is approximately 18 tubing-diameters upstream of the support-stem axis and approximately 8 support-stem diameters away from the support stem itself to avoid interference from this quarter.

The sensitivity to misalignment in pitch or yaw of this probe as well as its dependence on Reynolds number was investigated. The output from the boundary-layer probe was referenced to the output from a standard Kiel probe using one of the differential pressure transducers available for this test; the reference Kiel probe was placed in the free jet at a location where the stagnation pressure is equal to that at the boundary-layer-probe tip. The pitch and yaw calibrations were conducted at approximately 30 m/sec, the specified free-stream speed at the inlet reference station for the diffusing bend.

The results of the pitch calibration are shown in figure 30, which were obtained after first maximizing the output of the boundary-layer probe with respect to yaw. In this figure,  $\hat{p}_T$  is the total pressure from the boundary-layer probe,  $p_T$  the true total pressure from the reference Kiel probe;  $q$  the reference dynamic head determined from the Kiel probe and a wall static tap located near the nozzle exit, and  $\alpha_p$  is the indicated pitch angle (fig. 29), measured from the probe support-stem axis. The probe was fabricated so that when  $\alpha_p = 0$ , the flattened tip has a slight positive pitch with respect to the velocity vector; in this way, when the probe is in use near a wall (with the stem protruding through the wall), the position of the tip relative to the wall can be determined unambiguously. The results of



figure 30 indicate that the pitch of the tip is a few degrees, as desired, and the sensitivity to pitch of the probe is such that when the probe is mounted with its stem normal to a wall, the indicated total pressure is within 0.5% of the true value (0.25% in velocity).

The sensitivity of the boundary-layer probe to yaw (with  $\alpha_p \approx 0$  is shown in figure 31. In this figure,  $\hat{\beta}$  is the angle of a reference bar attached to the probe stem at an arbitrary orientation with respect to the tip. The actual value of  $\hat{\beta}$  is thus unimportant, but changes in  $\hat{\beta}$  are equal to changes in the actual yaw angle ( $\beta$ ). In practice, the output of the probe is maximized by rotating the probe about the axis of its stem; figure 31 shows that the probe characteristic has a large enough yaw "plateau" so that this is not difficult.

Figure 32 shows the lack of sensitivity of the probe ( $\alpha_p \approx \beta \approx 0$ ) to the Reynolds number over a 2:1 range. The length used to form the Reynolds number is the height of the opening at the probe tip. This Reynolds number range encompasses the values which will be encountered in the boundary-layer traverses.

### The Five-Hole Probe

Because the 5-hole probe is operated in this experiment with the output from its yaw-sensing pressure ports approximately balanced, the calibration procedure is considerably simplified from the general case wherein all the probe coefficients must be determined as functions of yaw as well as pitch. In our case, the coefficients depend only on pitch, with allowance made for the possibility of a small correction due to slight yaw, as described in the text. Accordingly, the probe was calibrated in the same fixture as was used for the boundary-layer probe, again using the free jet from the wind-tunnel nozzle. Using this fixture, the probe can be pitched about its tip, as previously described; additionally, at each pitch angle, the probe can be yawed approximately  $\pm 5^\circ$  relative to its null position to determine the effect of small yaw misalignment. Because of the probe's construction (fig. 6), the axis of rotation for this yawing motion also passes through the probe tip, so the entire calibration occurs at one point in the jet.

The calibration is done using the definitions shown as equations (5)-(9) in the text. In these relations  $p_T$  is the true total pressure and  $p$  is the static pressure at the probe location, as determined by a standard Kiel probe and the nozzle-exit wall tap, respectively.

The bulk of the calibration was conducted at 30 m/sec, which corresponds to a Reynolds number based on probe-tip diameter of approximately 6300, and these results are discussed first. An important dependence of the calibration on Reynolds number was determined, and those results follow.

The variation at  $Re_{5h} = 6300$  of  $C_{pitch}$ ,  $C_{total}$  and  $C_{static}$  over a wide range of pitch angles is shown in figures 33, 34, and 35, respectively. The data points shown were determined with the probe nulled in yaw, and several repeat runs are included to establish the consistency and repeatability of the calibration. The effect on the coefficients of yawing the probe over a range of approximately  $\pm 5^\circ$  is shown by the bars in these figures. In figure 33, the change in  $C_{pitch}$  caused by yawing the probe at constant  $\alpha_p$  has been translated into an apparent change in  $\alpha_p$  using the  $\beta = 0$  calibration curve. For  $|\alpha_p| < 20^\circ$ , figure 33 indicates that this range of yaw results in an indicated change of up to approximately  $\pm 0.5^\circ$  in pitch; for  $|\alpha_p| \geq 20^\circ$ , an indicated change of up to  $\pm 1^\circ$  in pitch is observed. Because these values are of the same order as the repeatability of the calibration, no correction for this effect is warranted. The behavior of  $C_{total}$  (fig. 34) and  $C_{static}$  (fig. 35) with pitch angle is very smooth and regular. The behavior of  $C_{pitch}$  (fig. 33) is considerably less so, and is presumably caused by small asymmetries and irregularities in the manufacture of the probe tip; the results of figure 33 are powerful indicators of the need to individually calibrate probes of this type.

In contrast to the behavior of the pitch coefficient, the variation of the yaw coefficient with  $\beta$  at  $\alpha_p \approx 0^\circ$  is seen to be very linear (fig. 36). In this figure,  $\hat{\beta}$  is again the angle of a reference bar fixed to the probe stem for the purposes of determining yaw sensitivity, so the actual value of  $\hat{\beta}$  is unimportant; from figure 36, it is seen that  $\partial C_{yaw} / \partial \beta = .0375 \text{ deg}^{-1}$  for  $\alpha_p \approx 0^\circ$ . While the probe was being calibrated in pitch, the approximately  $\pm 5^\circ$  variation in yaw about the null position previously described allowed determination of the effect of  $\alpha_p$  on  $C_{yaw} / \partial \beta$ . These results are shown in figure 37. When the 5-hole probe is used to determine the velocity vector in the diffusing bend, a non-zero value for  $C_{yaw}$  is converted to a yaw angle relative to the probe tip by means of the following relations:

$$\left. \begin{aligned} \frac{\partial C_{yaw}}{\partial \beta} \Big|_{\alpha_p \neq 0} &= \left[ \frac{\partial C_{yaw}}{\partial \beta} \Big/ \left( \frac{\partial C_{yaw}}{\partial \beta} \right) \Big|_{\alpha_p = 0} \right] (.0375 \text{ deg}^{-1}) \\ \beta &= C_{yaw} \Big/ \frac{\partial C_{yaw}}{\partial \beta} \end{aligned} \right\} (18)$$

where the first factor on the right hand side of the first of equations (18) is taken from figure 37.

All of the preceding results were obtained at a Reynolds number corresponding to the free-stream speed at the bend reference inlet station. It was expected that the effects of Reynolds number on this calibration would be small over the range of velocities anticipated in the diffusing bend, but this question was investigated during the calibration procedure. Unfortunately, it was determined that our expectation was incorrect for pitch angles outside the range  $|\alpha_p| \lesssim 10^\circ$ .

Figure 38 shows the dependence of the pitch coefficient on probe-tip Reynolds number for three values of pitch outside this range. In figure 38(a), at  $\alpha_p = 20.0^\circ$ , bistable characteristics with a region of hysteresis are shown. In taking the data for this figure, the natural transition to the lower leg of the curve with Reynolds number decreasing was not determined, but at  $Re_{5h} \approx 5500$ , stable operation on either leg of the curve was possible. Switching from one leg to another could be achieved by touching the rear of the probe (thereby damping the small vibration which was present) or by momentarily interrupting the airstream upstream of the probe. It is believed that this behavior is indicative of a switch in flow regime on the probe from a regime corresponding to the lower leg of the calibration where the flow is completely attached, to a regime corresponding to the upper leg where there is a region of "nose separation" on the probe. In figures 38(b) and (c), at  $\alpha_p = 15.0^\circ$  and  $-15.1^\circ$ , respectively, somewhat different behavior is shown wherein there is no hysteresis and no bistable behavior, but a relatively large Reynolds-number dependence persists. At pitch angles below  $10^\circ$ , a lesser effect of Reynolds number was observed. Figure 39 shows the values of pitch coefficient obtained for all values of  $Re_{5h}$  studied for  $-10 < \alpha_p < 10^\circ$ ; the solid line shown is the  $Re_{5h} = 6300$  "best-fit" line for this angle range reproduced from figure 33 (note the expanded scale in figure 39). All but two of the data points in figure 39 fall within the  $\pm 0.5^\circ$  band previously used to bound the uncertainty in this calibration in this range, and this band is therefore felt to adequately encompass the effects of Reynolds number as well, except near  $\alpha_p = 10^\circ$  where the effects of  $Re_{5h}$ -variation and small yaw misalignment fall in the range of  $+1^\circ$  to  $-0.5^\circ$ . The effects of Reynolds number on  $C_{total}$  and  $C_{static}$  are also with the variations shown by the bands which were previously used to define the effects of non-zero  $\beta$  in figures 34 and 35; for these coefficients, this is true for the whole range of pitch angles studied.

From these observations, it is clear that to use this probe for  $Re_{5h} < 6300$  and  $|\alpha_p| > 10^\circ$ , empirical  $Re_{5h}$  corrections would have to be determined every few degrees in pitch, and some means

would have to be developed to guarantee operation on some particular leg of the calibration curve wherever bistable operation is possible. This is not judged to be feasible; this probe is therefore recommended for general use only for  $-10^\circ \leq \alpha_p \leq 10^\circ$ , and for higher pitch angles, only at constant Reynolds number. The flow field measured in the current experiment was such that the probe could be used following these guidelines.

APPENDIX C  
TABULATED DATA

This appendix has 3 sections: Mean Boundary-Layer Profiles, Wall Static Pressure Coefficients, and Five-Hole Probe Data. Each section is begun with an explanation of the data included and the nomenclature used in the computer-generated tables.

Mean Boundary Layer Profiles

In the following tables, each profile has an identification number of form MMDDNN, where MM and DD are the month and day, respectively, on which the profile was measured and NN is a running index of the profiles taken on that day. Thus, profile 120901 is the first profile taken on December 9th. The computer-printed variables are defined as follows:

WALLID	wall identification (B, T, CV, or CC)
IDQ	identification number of transducer used for $q_{ref}$
IDPROB	identification number of transducer used for the boundary-layer probe
XSTAT	station number
ZHAT	$\hat{z}$
YCOR	reading of linear displacement transducer on the boundary-layer probe traverser with the probe contacting the wall (cm). Used in calculating $\hat{y}$
YCL	distance from the wall to the center of the probe opening with the probe contacting the wall (cm). Used in calculating $\hat{y}$
USTAR	$u^*$
DELTA	$\delta$
CAPPI	$\Pi$
RMS	RMS deviation of the data from the law of the wall/ law of the wake in $u^+$ units
L, M	identification numbers of first and last profile points included in the fitting process.
NU	$\nu$
UINF	$u_\infty$
K	$\kappa$

C	C
I	profile point identification number
YH	$\hat{y}$
YH/DELTA	$\hat{y}/\delta$
YHPLUS	$\hat{y}^+$
U	u
UPLUS	$u^+$

FINAL RESULTS FOR PROFILE 121101

WALLID	IDQ	IDPROB	XSTAT	ZHAT	YCOR	YCL			
CC	5	6	0.00	39.624	12.5131	0.0119			
USTAR	DELTA	CAPP1	RMS	L	M	NU	UINF	K	C
1.150	3.485	0.511	0.144	2	12	0.1599E-04	30.58	0.41	5.00
I	YH	YH/DELTA	YHPLUS	U	UPLUS	(UINF-U)/UINF	(UINF-U)/USTAR		
1	0.0226	0.006	16.23	15.630	13.59	0.489	12.997		
2	0.1161	0.033	83.55	18.627	16.19	0.391	10.392		
3	0.2037	0.058	146.55	19.884	17.29	0.350	9.299		
4	0.3285	0.094	236.33	21.090	18.33	0.310	8.251		
5	0.4407	0.126	317.01	21.950	19.08	0.282	7.502		
6	0.6198	0.178	445.88	22.875	19.89	0.252	6.699		
7	0.7808	0.224	561.68	23.783	20.67	0.222	5.910		
8	1.0900	0.313	784.07	24.954	21.69	0.184	4.891		
9	1.3546	0.389	974.44	25.958	22.57	0.151	4.018		
10	1.9264	0.553	1385.75	27.767	24.14	0.092	2.446		
11	2.4974	0.717	1796.51	29.167	25.36	0.046	1.229		
12	3.0689	0.881	2207.63	30.175	26.23	0.013	0.352		
13	3.6317	1.042	2612.46	30.538	26.55	0.001	0.037		
14	4.2110	1.208	3029.17	30.581	26.58	0.000	0.000		

FINAL RESULTS FOR PROFILE 121402

WALLID	IDQ	IDPROB	XSTAT	ZHAT	YCOR	YCL			
CC	5	6	0.00	26.416	12.5119	0.0119			
USTAR	DELTA	CAPPI	RMS	L	M	NU	UINF	K	C
1.088	4.425	0.710	0.098	2	14	0.1608E-04	30.44	0.41	5.00
I	YH	YH/DELTA	YHPLUS	U	UPLUS	(UINF-U)/UINF	(UINF-U)/USTAR		
1	0.0279	0.006	18.86	13.807	12.70	0.546	15.290		
2	0.1408	0.032	95.26	17.840	16.40	0.414	11.581		
3	0.2559	0.058	173.08	19.189	17.64	0.370	10.341		
4	0.3756	0.085	254.06	20.161	18.54	0.338	9.447		
5	0.4941	0.112	334.25	20.898	19.22	0.313	8.769		
6	0.7994	0.181	540.77	22.303	20.51	0.267	7.478		
7	1.0772	0.243	728.75	23.344	21.47	0.233	6.521		
8	1.3760	0.311	930.83	24.345	22.39	0.200	5.600		
9	1.6562	0.374	1120.40	25.187	23.16	0.172	4.826		
10	1.9422	0.439	1313.88	26.058	23.96	0.144	4.025		
11	2.2198	0.502	1501.70	26.834	24.67	0.118	3.311		
12	2.5023	0.566	1692.78	27.418	25.21	0.099	2.775		
13	3.0563	0.691	2067.58	28.661	26.35	0.058	1.632		
14	3.6357	0.822	2459.49	29.596	27.21	0.028	0.772		
15	4.1984	0.949	2840.17	30.104	27.68	0.011	0.304		
16	4.7826	1.081	3235.40	30.386	27.94	0.002	0.045		
17	5.3659	1.213	3629.94	30.435	27.99	0.000	0.000		



FINAL RESULTS FOR PROFILE 121003

WALLID	IDQ	IDPROB	XSTAT	ZHAT	YCOR	YCL			
CC	5	6	0.00	13.208	12.5255	0.0119			
USTAR	DELTA	CAPPI	RMS	L	M	NU	UINF	K	C
1.113	4.277	0.611	0.167	2	12	0.1602E-04	30.60	0.41	5.00
I	YH	YH/DELTA	YHPLUS	U	UPLUS	(UINF-U)/UINF	(UINF-U)/USTAR		
1	0.0415	0.010	28.81	15.762	14.16	0.485	13.329		
2	0.0992	0.023	68.91	17.527	15.74	0.427	11.744		
3	0.1585	0.037	110.14	18.543	16.65	0.394	10.832		
4	0.2797	0.065	194.38	19.917	17.89	0.349	9.597		
5	0.3921	0.092	272.45	20.758	18.64	0.322	8.842		
6	0.5100	0.119	354.41	21.495	19.31	0.298	8.180		
7	0.7968	0.186	553.69	22.804	20.48	0.255	7.005		
8	1.3907	0.325	966.38	24.815	22.29	0.189	5.198		
9	1.9580	0.458	1360.61	26.545	23.84	0.133	3.645		
10	2.5131	0.588	1746.33	27.956	25.11	0.087	2.378		
11	3.0739	0.719	2136.01	29.214	26.24	0.045	1.248		
12	3.6453	0.852	2533.02	30.027	26.97	0.019	0.518		
13	4.2017	0.982	2919.69	30.323	27.23	0.009	0.252		
14	4.8002	1.122	3335.58	30.540	27.43	0.002	0.057		
15	5.3671	1.255	3729.51	30.603	27.49	0.000	0.000		

FINAL RESULTS FOR PROFILE 120902

WALLID	IDQ	IDPROB	XSTAT	ZHAT	YCOR	YCL			
CV	5	6	0.00	39.624	12.5273	0.0119			
USTAR	DELTA	CAPPI	RMS	L	M	NU	UINF	K	C
1.173	3.190	0.491	0.077	2	13	0.1633E-04	30.82	0.41	5.00
I	YH	YH/DELTA	YHPLUS	U	UPLUS	(UINF-U)/UINF	(UINF-U)/USTAR		
1	0.0391	0.012	28.09	16.102	13.72	0.478	12.546		
2	0.0951	0.030	68.31	18.227	15.53	0.409	10.736		
3	0.1550	0.049	111.37	19.455	16.58	0.369	9.689		
4	0.2108	0.066	151.47	20.279	17.28	0.342	8.986		
5	0.2785	0.087	200.10	21.043	17.93	0.317	8.335		
6	0.3415	0.107	245.37	21.614	18.42	0.299	7.849		
7	0.3974	0.125	285.52	22.082	18.82	0.284	7.450		
8	0.4590	0.144	329.79	22.543	19.21	0.269	7.054		
9	0.5159	0.162	370.70	22.930	19.54	0.256	6.728		
10	0.6093	0.254	581.54	24.508	20.89	0.205	5.383		
11	1.3931	0.437	1000.97	26.810	22.85	0.130	3.421		
12	1.9496	0.611	1400.88	28.501	24.29	0.075	1.980		
13	2.5110	0.787	1804.28	29.860	25.45	0.031	0.822		
14	3.0568	0.958	2196.47	30.525	26.01	0.010	0.256		
15	3.6493	1.144	2622.17	30.701	26.16	0.004	0.105		
16	4.2177	1.322	3030.62	30.799	26.25	0.001	0.022		
17	4.7883	1.501	3440.58	30.825	26.27	0.000	0.000		

33

FINAL RESULTS FOR PROFILE 121401

WALLID	IDQ	IDPROB	XSTAT	ZHAT	YCOR	YCL			
CV	5	6	0.00	26.416	12.5060	0.0119			
USTAR	DELTA	CAPPI	RMS	L	M	NU	UINF	K	C
1.130	3.727	0.580	0.035	2	12	0.1603E-04	30.55	0.41	5.00
I	YH	YH/DELTA	YHPLUS	U	UPLUS	(UINF-U)/UINF	(UINF-U)/USTAR		
1	0.0367	0.010	25.90	15.014	13.28	0.509	13.749		
2	0.1326	0.036	93.46	18.240	16.14	0.403	10.894		
3	0.2403	0.064	169.39	19.803	17.52	0.352	9.511		
4	0.3744	0.100	263.93	21.093	18.66	0.310	8.370		
5	0.4982	0.134	351.24	21.995	19.46	0.280	7.572		
6	0.7875	0.211	555.21	23.393	20.70	0.234	6.335		
7	1.0812	0.290	762.26	24.520	21.70	0.197	5.338		
8	1.3735	0.369	968.40	25.528	22.59	0.164	4.445		
9	1.6587	0.445	1169.47	26.429	23.38	0.135	3.648		
10	1.9227	0.516	1355.58	27.269	24.13	0.107	2.905		
11	2.5019	0.671	1763.94	28.715	25.41	0.060	1.626		
12	3.0561	0.820	2154.69	29.735	26.31	0.027	0.723		
13	3.6292	0.974	2558.71	30.465	26.96	0.003	0.078		
14	4.2045	1.128	2964.32	30.574	27.05	-0.001	-0.019		
15	4.7853	1.284	3373.80	30.552	27.03	0.000	0.000		

FINAL RESULTS FOR PROFILE 121001

WALLID IDQ IDPROB XSTAT ZHAT YCOR YCL  
 CV 5 6 0.00 13.208 12.5308 0.0119

USTAR DELTA CAPPI RMS L M NU UINF K C  
 1.133 3.800 0.557 0.100 2 11 0.1603E-04 30.55 0.41 5.00

I	YH	YH/DELTA	YHPLUS	U	UPLUS	(UINF-U)/UINF	(UINF-U)/USTAR
1	0.0462	0.012	32.62	15.962	14.09	0.478	12.879
2	0.0998	0.026	70.49	17.723	15.65	0.420	11.324
3	0.1609	0.042	113.65	18.788	16.59	0.385	10.384
4	0.2802	0.074	197.93	20.207	17.84	0.339	9.131
5	0.4027	0.106	284.44	21.288	18.80	0.303	8.176
6	0.5112	0.135	361.12	21.982	19.41	0.280	7.564
7	0.7967	0.210	562.80	23.406	20.66	0.234	6.307
8	1.3954	0.367	985.72	25.593	22.60	0.162	4.376
9	1.9600	0.516	1384.48	27.335	24.13	0.105	2.837
10	2.5047	0.659	1769.25	28.642	25.29	0.062	1.683
11	3.0855	0.812	2179.54	29.692	26.21	0.028	0.756
12	3.6540	0.962	2581.11	30.262	26.72	0.009	0.253
13	4.2253	1.112	2984.66	30.479	26.91	0.002	0.061
14	4.7907	1.261	3384.06	30.515	26.94	0.001	0.029
15	5.3789	1.416	3799.54	30.549	26.97	0.000	0.000

35

FINAL RESULTS FOR PROFILE 121102

WALLID	IDQ	IDPROB	XSTAT	ZHAT	YCOR	YCL			
T	5	6	0.00	9.826	12.5308	0.0119			
USTAR	DELTA	CAPPI	RMS	L	M	NU	UINF	K	C
1.134	7.605	0.162	0.173	2	18	0.1595E-04	30.34	0.41	5.00
I	YH	YH/DELTA	YHPLUS	U	UPLUS	(UINF-U)/UINF	(UINF-U)/USTAR		
1	0.0444	0.006	31.58	16.173	14.26	0.467	12.495		
2	0.1062	0.014	75.56	18.153	16.01	0.402	10.749		
3	0.1603	0.021	114.01	19.070	16.81	0.372	9.940		
4	0.2857	0.038	203.16	20.530	18.10	0.323	8.653		
5	0.4021	0.053	285.97	21.448	18.91	0.293	7.844		
6	0.5183	0.068	368.61	22.100	19.49	0.272	7.269		
7	0.8165	0.107	580.69	23.233	20.48	0.234	6.270		
8	1.1036	0.145	784.93	23.998	21.16	0.209	5.596		
9	1.3972	0.184	993.70	24.633	21.72	0.188	5.036		
10	1.9554	0.257	1390.74	25.671	22.63	0.154	4.120		
11	2.5289	0.333	1798.61	26.368	23.25	0.131	3.506		
12	3.0809	0.405	2191.22	27.094	23.89	0.107	2.865		
13	3.6500	0.480	2595.94	27.713	24.43	0.087	2.320		
14	4.2201	0.555	3001.44	28.246	24.90	0.069	1.850		
15	4.7924	0.630	3408.44	28.819	25.41	0.050	1.345		
16	5.4053	0.711	3844.33	29.309	25.84	0.034	0.912		
17	5.9700	0.785	4245.95	29.704	26.19	0.021	0.565		
18	6.5814	0.865	4680.78	30.027	26.48	0.010	0.280		
19	7.1852	0.945	5110.26	30.214	26.64	0.004	0.115		
20	7.8066	1.027	5552.19	30.344	26.75	0.000	0.000		

FINAL RESULTS FOR PROFILE 121103

WALLID	IDQ	IDPROB	XSTAT	ZHAT	YCOR	YCL			
T	5	6	0.00	0.000	12.5161	0.0119			
USTAR	DELTA	CAPP1	RMS	L	M	NU	UINF	K	C
1.136	7.912	0.202	0.110	2	17	0.1627E-04	30.67	0.41	5.00
I	YH	YH/DELTA	YHPLUS	U	UPLUS	(UINF-U)/UINF	(UINF-U)/USTAR		
1	0.0308	0.004	21.53	15.238	13.41	0.503	13.588		
2	0.1397	0.018	97.52	18.666	16.43	0.391	10.570		
3	0.2618	0.033	182.81	20.298	17.87	0.338	9.133		
4	0.3832	0.048	267.58	21.280	18.73	0.306	8.269		
5	0.5006	0.063	349.54	22.027	19.39	0.282	7.611		
6	0.7993	0.101	558.14	23.228	20.45	0.243	6.554		
7	1.0825	0.137	755.89	23.963	21.09	0.219	5.907		
8	1.3795	0.174	963.28	24.673	21.72	0.196	5.282		
9	1.9401	0.245	1354.70	25.766	22.68	0.160	4.320		
10	2.4987	0.316	1744.77	26.503	23.33	0.136	3.671		
11	3.0668	0.388	2141.40	27.129	23.88	0.116	3.120		
12	3.6392	0.460	2541.14	27.795	24.47	0.094	2.534		
13	4.2157	0.533	2943.64	28.396	25.00	0.074	2.005		
14	4.7805	0.604	3338.05	28.879	25.42	0.059	1.580		
15	5.3600	0.677	3742.70	29.370	25.85	0.042	1.147		
16	5.9516	0.752	4155.81	29.798	26.23	0.029	0.771		
17	6.5648	0.830	4583.93	30.187	26.57	0.016	0.428		
18	7.1789	0.907	5012.79	30.411	26.77	0.009	0.231		
19	7.7656	0.981	5422.45	30.542	26.89	0.004	0.116		
20	8.4015	1.062	5866.42	30.673	27.00	0.000	0.000		

FINAL RESULTS FOR PROFILE 121104

WALLID	IDQ	IDPROB	XSTAT	ZHAT	YCOR	YCL			
T	5	6	0.00	-8.826	12.4990	0.0119			
USTAR	DELTA	CAPPI	RMS	L	M	NU	UINF	K	C
1.144	7.414	0.179	0.115	2	17	0.1619E-04	30.60	0.41	5.00
I	YH	YH/DELTA	YHPLUS	U	UPLUS	(UINF-U)/UINF	(UINF-U)/USTAR		
1	0.0473	0.006	33.44	16.180	14.15	0.471	12.611		
2	0.1261	0.017	89.05	18.527	16.20	0.395	10.559		
3	0.2501	0.034	176.69	20.329	17.78	0.336	8.984		
4	0.3720	0.050	262.74	21.416	18.73	0.300	8.033		
5	0.4923	0.066	347.72	22.109	19.33	0.278	7.427		
6	0.7828	0.106	552.93	23.290	20.37	0.239	6.394		
7	1.0735	0.145	758.27	24.228	21.19	0.208	5.574		
8	1.3624	0.184	962.35	24.829	21.71	0.189	5.049		
9	1.9292	0.260	1362.71	25.795	22.56	0.157	4.204		
10	2.4926	0.336	1760.68	26.614	23.27	0.130	3.487		
11	3.0388	0.410	2146.46	27.386	23.95	0.105	2.812		
12	3.6278	0.489	2562.52	28.042	24.52	0.084	2.239		
13	4.1946	0.566	2962.84	28.622	25.03	0.065	1.731		
14	4.7708	0.643	3369.87	29.152	25.49	0.047	1.268		
15	5.3358	0.720	3769.00	29.590	25.87	0.033	0.886		
16	5.9476	0.802	4201.14	29.984	26.22	0.020	0.541		
17	6.5483	0.883	4625.39	30.220	26.42	0.013	0.335		
18	7.1540	0.965	5053.23	30.407	26.59	0.006	0.171		
19	7.7613	1.047	5482.23	30.566	26.73	0.001	0.032		
20	8.3715	1.129	5913.23	30.602	26.76	0.000	0.000		

FINAL RESULTS FOR PROFILE 120802

WALLID	IDQ	IDPROB	XSTAT	ZHAT	YCOR	YCL			
B	5	6	0.00	8.826	12.5279	0.0119			
USTAR	DELTA	CAPPI	RMS	L	M	NU	UINF	K	C
1.141	7.468	0.185	0.182	2	17	0.1615E-04	30.57	0.41	5.00
I	YH	YH/DELTA	YHPLUS	U	UPLUS	(UINF-U)/UINF	(UINF-U)/USTAR		
1	0.0361	0.005	25.52	16.014	14.04	0.476	12.765		
2	0.0904	0.012	63.81	17.870	15.67	0.416	11.138		
3	0.1585	0.021	111.94	19.067	16.72	0.376	10.088		
4	0.2179	0.029	153.85	19.899	17.45	0.349	9.359		
5	0.3757	0.050	265.26	21.182	18.57	0.307	8.234		
6	0.5171	0.069	365.13	22.083	19.36	0.278	7.444		
7	0.8099	0.108	571.92	23.268	20.40	0.239	6.404		
8	1.3833	0.185	976.75	24.722	21.68	0.191	5.130		
9	1.9485	0.261	1375.90	25.729	22.56	0.158	4.247		
10	2.5127	0.336	1774.31	26.566	23.29	0.131	3.513		
11	3.0717	0.411	2169.02	27.342	23.97	0.106	2.832		
12	3.6396	0.487	2570.04	27.982	24.53	0.085	2.272		
13	4.2235	0.566	2982.31	28.585	25.06	0.065	1.743		
14	4.7923	0.642	3383.98	29.103	25.52	0.048	1.289		
15	5.3759	0.720	3796.09	29.611	25.96	0.031	0.844		
16	5.9760	0.800	4219.79	30.011	26.31	0.018	0.493		
17	6.5760	0.881	4643.46	30.235	26.51	0.011	0.296		
18	7.1950	0.963	5080.57	30.460	26.71	0.004	0.099		
19	7.8043	1.045	5510.80	30.579	26.81	-0.000	-0.005		
20	8.4127	1.127	5940.40	30.573	26.81	0.000	0.000		



FINAL RESULTS FOR PROFILE 120801

WALLID      ID@      IDPROB      XSTAT      ZHAT      YCOR      YCL  
 B          5          6          0.00      0.000      12.5308      0.0119

USTAR      DELTA      CAPPI      RMS      L      M      NU      UINF      K      C  
 1.122      7.457      0.286      0.050      2      17      0.1615E-04      30.59      0.41      5.00

I	YH	YH/DELTA	YHPLUS	U	UPLUS	(UINF-U)/UINF	(UINF-U)/USTAR
1	0.0438	0.006	30.44	15.273	13.61	0.501	13.645
2	0.1062	0.014	73.81	17.548	15.64	0.426	11.618
3	0.1532	0.021	106.46	18.459	16.45	0.397	10.806
4	0.2085	0.028	144.82	19.197	17.11	0.372	10.148
5	0.3739	0.050	259.75	20.828	18.56	0.319	8.695
6	0.5230	0.070	363.30	21.792	19.42	0.288	7.836
7	0.8159	0.109	566.77	23.008	20.50	0.248	6.753
8	1.3608	0.182	945.30	24.435	21.77	0.201	5.481
9	1.9509	0.262	1355.24	25.571	22.78	0.164	4.469
10	2.5085	0.336	1742.61	26.403	23.53	0.137	3.728
11	3.0775	0.413	2137.87	27.079	24.13	0.115	3.125
12	3.6528	0.490	2537.54	27.801	24.77	0.091	2.482
13	4.2207	0.566	2932.03	28.385	25.29	0.072	1.962
14	4.7913	0.642	3328.38	28.960	25.80	0.053	1.450
15	5.3754	0.721	3734.13	29.445	26.24	0.037	1.017
16	5.9682	0.800	4145.96	29.845	26.59	0.024	0.661
17	6.6261	0.889	4603.00	30.208	26.92	0.012	0.337
18	7.1907	0.964	4995.18	30.404	27.09	0.006	0.162
19	7.8054	1.047	5422.21	30.527	27.20	0.002	0.053
20	8.4346	1.131	5859.29	30.586	27.25	0.000	0.000

FINAL RESULTS FOR PROFILE 120901

WALLID	IDQ	IDPROB	XSTAT	ZHAT	YCOR	YCL			
B	5	6	0.00	-8.826	12.5267	0.0119			
USTAR	DELTA	CAPPI	RMS	L	M	NU	UINF	K	C
1.146	7.051	0.183	0.115	2	15	0.1625E-04	30.54	0.41	5.00
I	YH	YH/DELTA	YHPLUS	U	UPLUS	(UINF-U)/UINF	(UINF-U)/USTAR		
1	0.0409	0.006	28.81	15.734	13.73	0.485	12.919		
2	0.0962	0.014	67.84	17.856	15.59	0.415	11.067		
3	0.2179	0.031	153.60	19.937	17.40	0.347	9.251		
4	0.3463	0.049	244.13	21.167	18.47	0.307	8.177		
5	0.5188	0.074	365.72	22.296	19.46	0.270	7.192		
6	0.8022	0.114	565.43	23.404	20.43	0.234	6.224		
7	1.3746	0.195	968.89	24.891	21.72	0.185	4.927		
8	1.9462	0.276	1371.83	25.920	22.62	0.151	4.029		
9	2.5132	0.356	1771.50	26.772	23.37	0.123	3.285		
10	3.0694	0.435	2163.54	27.510	24.01	0.099	2.641		
11	3.6453	0.517	2569.48	28.226	24.64	0.076	2.016		
12	4.2109	0.597	2968.14	28.748	25.09	0.059	1.560		
13	4.8088	0.682	3389.61	29.221	25.50	0.043	1.147		
14	5.3859	0.764	3796.39	29.740	25.96	0.026	0.695		
15	5.9563	0.845	4198.46	30.058	26.23	0.016	0.417		
16	6.5760	0.933	4635.27	30.365	26.50	0.006	0.149		
17	7.1968	1.021	5072.88	30.541	26.66	-0.000	-0.004		
18	7.7951	1.106	5494.61	30.536	26.65	0.000	0.000		

## Wall Static Pressure Coefficients

In the following table, the average pressure coefficient measured at each wall tap as well as the location of the tap is given. Several repeat points are included. The taps are grouped first by x value, then by y value; i.e., at a given x, the top-wall taps ( $y = 0$ ) appear first, then the CV- and CC-taps at each increasing y value, followed by the bottom wall taps ( $y = 52.83$ ), which are ordered by increasing z.

X	Y	Z	CP
-139.95	52.83	0.00	-0.0022
-124.71	52.83	0.00	-0.0099
-109.47	52.83	0.00	-0.0143
-78.94	52.83	0.00	-0.0094
-63.70	52.83	0.00	-0.0075
-48.46	52.83	0.00	-0.0052
-47.12	52.83	0.00	-0.0142
-33.22	52.83	0.00	0.0058
-17.98	52.83	0.00	0.0170
-2.54	52.83	0.00	0.0091
0.00	0.00	-15.24	-0.0050
0.00	0.00	-7.62	-0.0023
0.00	0.00	0.00	0.0030
0.00	0.00	7.62	0.0081
0.00	0.00	15.24	0.0130
0.00	3.56	-17.65	-0.0128
0.00	3.56	17.65	0.0117
0.00	8.64	-17.65	0.0001
0.00	8.64	17.65	0.0160
0.00	16.26	-17.65	-0.0040
0.00	16.26	17.65	0.0157
0.00	36.58	-17.65	-0.0049
0.00	36.58	17.65	0.0111
0.00	44.20	-17.65	-0.0040
0.00	44.20	17.65	0.0109
0.00	49.28	-17.65	-0.0023
0.00	49.28	17.65	0.0088
0.00	52.83	-15.24	-0.0014
0.00	52.83	15.24	0.0157
5.08	26.42	-17.65	-0.0045
5.08	26.42	17.65	0.0089
10.16	26.42	-17.65	-0.0104
10.16	26.42	17.65	0.0124
15.24	26.42	-17.65	-0.0205
15.24	26.42	17.65	0.0163
20.32	26.42	-17.65	-0.0512
20.32	26.42	17.65	0.0265
25.40	26.42	-17.65	-0.0879
25.40	26.42	17.65	0.0419
30.48	26.42	-17.70	-0.1229
30.48	26.42	17.65	0.0612
33.02	26.42	-17.78	-0.1312
35.56	3.56	-17.93	-0.1241
35.56	3.56	17.65	0.0807
35.56	8.64	-17.93	-0.1329
35.56	8.64	17.65	0.0871
35.56	16.26	-17.93	-0.1369
35.56	16.26	17.65	0.0865
35.56	26.42	-17.93	-0.1458
35.56	26.42	17.65	0.0916
35.56	36.58	-17.93	-0.1394
35.56	36.58	17.65	0.0903

X	Y	Z	CP
142.24	36.58	23.22	0.4057
142.24	44.20	23.22	0.4086
142.24	49.28	23.22	0.4092
142.24	52.83	-15.24	0.2177
142.24	52.83	0.00	0.2943
142.24	52.83	15.24	0.3764
144.78	3.56	-23.37	0.2415
144.78	8.64	-23.37	0.2153
144.78	16.26	-23.37	0.2230
144.78	26.42	-23.37	0.2292
144.78	36.58	-23.37	0.2219
144.78	44.20	-23.37	0.2112
144.78	49.28	-23.37	0.2409
152.40	26.42	-23.37	0.2393
152.40	26.42	23.37	0.3754
162.56	26.42	-23.37	0.2523
162.56	26.42	23.37	0.3431
172.72	26.42	-23.37	0.2677
172.72	26.42	23.37	0.3188
182.88	26.42	-23.37	0.2822
182.88	26.42	23.37	0.3073
193.04	0.00	-22.86	0.3143
193.04	0.00	-20.32	0.3091
193.04	0.00	-17.78	0.2971
193.04	0.00	-15.24	0.2875
193.04	0.00	-7.62	0.2845
193.04	0.00	0.00	0.2916
193.04	0.00	7.62	0.3043
193.04	0.00	15.24	0.3087
193.04	0.00	17.78	0.3076
193.04	0.00	20.32	0.3093
193.04	0.00	22.86	0.3083
193.04	3.56	-23.37	0.3148
193.04	3.56	23.37	0.3055
193.04	8.64	-23.37	0.2923
193.04	8.64	23.37	0.3032
193.04	16.26	-23.37	0.2863
193.04	16.26	23.37	0.3009
193.04	26.42	-23.37	0.2979
193.04	36.58	-23.37	0.2878
193.04	36.58	23.37	0.2986
193.04	44.20	-23.37	0.2942
193.04	44.20	23.37	0.2997
193.04	49.28	-23.37	0.3234
193.04	49.28	23.37	0.3063
193.04	52.83	-15.24	0.2908
193.04	52.83	0.00	0.2947
193.04	52.83	15.24	0.2993
193.40	26.42	23.37	0.2966

X	Y	Z	CP
35.56	44.20	-17.93	-0.1262
35.56	44.20	17.65	0.0858
35.56	49.28	-17.93	-0.1289
35.56	49.28	17.65	0.0874
35.56	52.83	-15.24	-0.0896
35.56	52.83	0.00	0.0236
35.56	52.83	15.24	0.0825
38.10	26.42	-18.06	-0.1571
38.10	26.42	17.68	0.1031
40.64	26.42	-18.19	-0.1578
40.64	26.42	17.75	0.1307
43.18	26.42	-18.34	-0.1595
43.18	26.42	17.88	1.0912
45.72	26.42	-18.47	-0.1535
45.72	26.42	18.01	0.1677
48.26	26.42	-18.62	-0.1519
48.26	26.42	18.14	0.1883
50.80	26.42	-18.75	-0.1413
50.80	26.42	18.26	0.2062
53.34	26.42	-18.87	-0.1338
53.34	26.42	18.39	0.2214
55.88	26.42	-19.00	-0.1258
55.88	26.42	18.54	0.2350
58.42	26.42	-19.15	-0.1173
58.42	26.42	18.67	0.2488
60.96	26.42	-19.28	-0.1125
60.96	26.42	18.80	0.2618
63.50	26.42	-19.41	-0.1011
63.50	26.42	18.92	0.2723
66.04	26.42	-19.53	-0.0834
66.04	26.42	19.05	0.2818
68.58	26.42	19.20	0.2914
71.12	0.00	-15.24	-0.0094
71.12	0.00	-7.62	0.0682
71.12	0.00	0.00	0.1422
71.12	0.00	7.62	0.2059
71.12	0.00	15.24	0.2633
71.12	0.00	17.78	0.2802
71.12	3.56	-19.81	-0.0421
71.12	3.56	19.33	0.2857
71.12	8.64	-19.81	-0.0559
71.12	8.64	19.33	0.2875
71.12	16.26	-19.81	-0.0627
71.12	16.26	19.33	0.2968
71.12	26.42	-19.81	-0.0672
71.12	26.42	19.33	0.2967
71.12	36.58	-19.81	-0.0603
71.12	36.58	19.33	0.2953
71.12	44.20	-19.81	-0.0491
71.12	44.20	19.33	0.2883
71.12	49.28	-19.81	-0.0400
71.12	49.28	19.33	0.2852

X	Y	Z	CP
71.12	52.83	-15.24	-0.0019
71.12	52.83	0.00	0.1480
71.12	52.83	15.24	0.2696
76.20	26.42	-19.81	-0.0533
76.20	26.42	19.63	0.3072
81.28	26.42	-20.35	-0.0315
81.28	26.42	19.91	0.3261
86.36	26.42	-20.62	-0.0092
86.36	26.42	20.17	0.3417
91.44	26.42	-20.88	0.0148
91.44	26.42	20.45	0.3588
101.60	0.00	-15.24	0.0945
101.60	0.00	-15.24	0.0941
101.60	0.00	-7.62	0.1601
101.60	0.00	-7.62	0.1615
101.60	0.00	0.00	0.2220
101.60	0.00	0.00	0.2241
101.60	0.00	7.62	0.2828
101.60	0.00	7.62	0.2848
101.60	0.00	15.24	0.3521
101.60	0.00	15.24	0.3550
101.60	0.00	17.78	0.3657
101.60	0.00	17.78	0.3676
101.60	0.00	20.32	0.3736
101.60	0.00	20.32	0.3758
101.60	3.56	-21.41	0.0660
101.60	3.56	21.01	0.3749
101.60	8.64	-21.41	0.0617
101.60	8.64	21.01	0.3761
101.60	16.26	-21.41	0.0640
101.60	16.26	21.01	0.3836
101.60	26.42	-21.41	0.0631
101.60	26.42	21.01	0.3855
101.60	36.58	-21.41	0.0670
101.60	36.58	21.01	0.3846
101.60	44.20	-21.41	0.0636
101.60	44.20	21.01	0.3770
101.60	49.28	-21.41	0.0662
101.60	49.28	21.01	0.3763
101.60	52.83	-15.24	0.0999
101.60	52.83	0.00	0.2294
101.60	52.83	15.24	0.3611
111.76	26.42	-21.95	0.1119
111.76	26.42	21.56	0.4001
121.92	26.42	-22.50	0.1610
121.92	26.42	22.10	0.4138
132.08	26.42	-23.04	0.2037
132.08	26.42	22.66	0.4230
142.24	3.56	23.22	0.4034
142.24	8.64	23.22	0.4011
142.24	16.26	23.22	0.4083
142.24	26.42	23.22	0.4040

### Five-Hole Probe Data

For each of the six streamwise stations surveyed\*, these data are listed as a series of profiles at approximately constant  $z$ . Repeat points are included in the profiles. For each  $z$  value, the data are listed in order of increasing  $y$ . The column headings requiring explanation are:

CPITCH	pitch coefficient, $C_{pitch}$
CYAW	yaw coefficient, $C_{yaw}$
VCONT	one dimensional through-flow velocity, $V_{cont}$
VV	$V/V_{cont}$
VX	$V_x/V_{cont}$
VY	$V_y/V_{cont}$
VZ	$V_z/V_{cont}$
CP	pressure coefficient, $C_p$

---

\*The survey planes are identified by the station number which specifies the nominal location. Actual  $x$  values for these planes are given in Table 1.



STATION 0

POINT	Z	Y	CPITCH	CYAW	ALPHA	THETA	BETA	V	VCONT	VV	VX	VY	VZ	CP
1	-16.955	26.471	-0.111	0.006	-1.1	0.2	0.2	25.414	30.740	0.8267	0.8266	0.0160	0.0054	-0.0152
2	-16.243	26.471	-0.091	0.003	-0.5	0.1	0.1	27.663	30.721	0.9004	0.9004	0.0071	0.0024	-0.0125
3	-15.490	26.470	-0.085	0.005	-0.2	0.2	0.1	29.537	30.765	0.9601	0.9601	0.0041	0.0053	-0.0109
4	-14.821	26.472	-0.083	0.002	-0.2	0.4	0.1	30.537	30.735	0.9936	0.9935	0.0034	0.0078	-0.0063
5	-14.103	26.471	-0.078	0.003	-0.0	0.4	0.1	30.944	30.793	1.0049	1.0049	0.0004	0.0093	-0.0050
6	-14.100	26.471	-0.077	0.004	-0.0	0.4	0.1	30.974	30.813	1.0052	1.0052	0.0002	0.0097	-0.0056
7	-13.777	52.135	-0.082	0.007	0.3	0.6	0.2	22.835	30.599	0.7463	0.7462	-0.0034	0.0101	-0.0068
8	-13.247	8.785	-0.070	0.004	-0.1	-0.0	0.1	30.362	30.806	0.9856	0.9856	0.0017	0.0011	-0.0026
9	-13.249	11.313	-0.077	0.004	-0.2	0.0	0.1	30.806	30.786	1.0007	1.0007	0.0042	0.0021	-0.0037
10	-13.247	13.896	-0.079	0.005	-0.3	0.2	0.1	30.900	30.777	1.0040	1.0040	0.0044	0.0062	-0.0044
11	-13.248	16.437	-0.081	0.005	-0.3	-0.0	0.1	30.930	30.787	1.0046	1.0046	0.0046	0.0018	-0.0042
12	-13.246	18.988	-0.083	0.005	-0.3	0.2	0.1	30.946	30.784	1.0053	1.0052	0.0053	0.0053	-0.0051
13	-13.244	21.556	-0.074	0.004	-0.0	0.1	0.1	30.932	30.756	1.0057	1.0057	0.0001	0.0034	-0.0060
14	-13.243	24.089	-0.079	0.003	-0.1	0.0	0.1	31.001	30.798	1.0066	1.0066	0.0015	0.0022	-0.0064
15	-13.245	26.469	-0.076	0.003	0.0	0.4	0.1	30.910	30.738	1.0056	1.0056	-0.0003	0.0082	-0.0038
16	-13.362	26.471	-0.076	0.003	0.0	0.5	0.1	30.891	30.725	1.0054	1.0053	-0.0006	0.0101	-0.0034
17	-13.372	26.472	-0.076	0.003	0.0	0.5	0.1	30.697	30.525	1.0056	1.0056	-0.0006	0.0101	-0.0039
18	-13.373	26.472	-0.075	0.004	0.0	0.5	0.1	30.869	30.679	1.0062	1.0061	-0.0008	0.0104	-0.0041
19	-13.245	26.634	-0.077	0.004	0.0	0.3	0.1	30.978	30.783	1.0064	1.0063	-0.0000	0.0070	-0.0056
20	-13.244	29.202	-0.081	0.003	-0.1	0.4	0.1	30.935	30.734	1.0065	1.0065	0.0013	0.0083	-0.0047
21	-13.243	31.731	-0.077	0.004	0.1	0.6	0.1	30.959	30.764	1.0063	1.0063	-0.0012	0.0117	-0.0027
22	-13.246	34.276	-0.076	0.004	0.1	0.3	0.1	31.043	30.808	1.0076	1.0076	-0.0026	0.0077	-0.0006
23	-13.245	36.858	-0.073	0.004	0.3	0.5	0.1	30.918	30.654	1.0086	1.0086	-0.0046	0.0098	0.0010
24	-13.245	39.412	-0.077	0.005	0.2	0.7	0.1	30.906	30.626	1.0092	1.0090	-0.0035	0.0147	0.0013
25	-13.244	41.947	-0.078	0.004	0.2	0.5	0.1	30.936	30.727	1.0068	1.0067	-0.0037	0.0107	-0.0003
26	-13.245	44.515	-0.082	0.003	0.1	0.7	0.1	30.310	30.712	0.9869	0.9868	-0.0022	0.0134	-0.0044
27	-13.245	45.796	-0.086	0.005	0.0	0.8	0.1	29.752	30.677	0.9699	0.9697	-0.0004	0.0160	-0.0041
28	-13.245	47.074	-0.090	0.004	-0.1	0.7	0.1	29.370	30.798	0.9536	0.9535	0.0014	0.0135	-0.0041
29	-13.245	48.345	-0.093	0.004	-0.2	0.3	0.1	28.881	30.752	0.9392	0.9392	0.0029	0.0064	-0.0050
30	-13.247	49.605	-0.092	0.005	-0.1	-0.0	0.1	27.774	30.766	0.9028	0.9028	0.0016	0.0019	-0.0058
31	-13.245	50.898	-0.098	0.006	0.0	0.1	0.2	25.917	30.797	0.8415	0.8415	-0.0005	0.0037	-0.0073
32	-13.247	52.135	-0.082	0.005	0.3	0.7	0.1	23.050	30.710	0.7506	0.7505	-0.0033	0.0105	-0.0099
33	-8.851	8.723	-0.070	0.003	-0.1	-0.1	0.1	30.722	30.884	0.9947	0.9947	0.0015	0.0004	0.0026
34	-8.854	11.237	-0.072	0.001	-0.1	-0.0	0.0	30.830	30.958	0.9959	0.9959	0.0017	0.0004	0.0033
35	-8.827	13.811	-0.075	0.001	-0.1	0.1	0.0	30.795	30.882	0.9972	0.9972	0.0025	0.0022	0.0001
36	-8.827	16.369	-0.076	0.002	-0.1	0.0	0.0	30.837	30.904	0.9978	0.9978	0.0024	0.0008	-0.0004
37	-8.829	18.920	-0.073	0.001	-0.0	0.2	0.0	30.778	30.834	0.9982	0.9982	0.0004	0.0042	-0.0008
38	-8.830	21.482	-0.074	0.000	-0.0	0.1	0.0	30.763	30.808	0.9985	0.9985	0.0001	0.0022	-0.0007
39	-8.830	24.034	-0.075	0.001	0.0	0.1	0.0	30.714	30.756	0.9986	0.9986	-0.0001	0.0027	-0.0002
40	-8.831	26.574	-0.078	0.003	-0.0	0.4	0.1	30.796	30.808	0.9996	0.9996	0.0003	0.0086	-0.0024
41	-8.831	29.128	-0.078	0.001	0.0	0.3	0.0	30.799	30.819	0.9994	0.9993	-0.0003	0.0058	-0.0009
42	-8.833	31.674	-0.079	0.003	0.0	0.5	0.1	30.818	30.819	1.0000	0.9999	-0.0003	0.0104	-0.0013
43	-8.831	34.216	-0.082	0.003	-0.0	0.7	0.1	30.829	30.817	1.0004	1.0003	0.0004	0.0141	-0.0013
44	-8.831	36.804	-0.083	0.002	-0.0	0.6	0.0	30.783	30.763	1.0006	1.0006	0.0003	0.0106	-0.0014
45	-8.831	39.369	-0.083	0.003	0.0	0.5	0.1	30.849	30.804	1.0014	1.0014	-0.0004	0.0106	-0.0022
46	-8.832	41.898	-0.083	0.001	0.1	0.7	0.0	30.820	30.792	1.0009	1.0008	-0.0011	0.0135	-0.0014
47	-8.834	44.460	-0.085	0.002	0.0	0.8	0.0	30.791	30.758	1.0011	1.0010	-0.0004	0.0139	-0.0019
48	-8.832	45.732	-0.086	0.001	0.0	0.7	0.0	30.709	30.790	0.9974	0.9973	-0.0001	0.0121	-0.0016
49	-8.835	47.031	-0.091	0.002	-0.1	0.6	0.0	30.294	30.766	0.9847	0.9846	0.0020	0.0116	-0.0028
50	-8.833	48.287	-0.093	0.005	-0.2	0.4	0.1	29.481	30.801	0.9572	0.9571	0.0029	0.0094	-0.0034

## STATION 0 (Continued)

POINT	Z	Y	CPITCH	CYAW	ALPHA	THETA	BETA	V	VCONT	VW	VX	VY	VZ	CP
51	-8.833	49.564	-0.095	0.003	-0.2	0.4	0.1	28.273	30.797	0.9180	0.9180	0.0033	0.0074	-0.0059
52	-8.833	50.210	-0.095	0.003	-0.2	0.4	0.1	27.582	30.816	0.8951	0.8950	0.0034	0.0079	-0.0065
53	-8.834	50.860	-0.094	0.002	-0.2	0.4	0.0	26.753	30.845	0.8673	0.8673	0.0026	0.0070	-0.0082
54	-8.834	51.488	-0.093	0.005	-0.1	0.3	0.1	25.783	30.857	0.8356	0.8355	0.0020	0.0064	-0.0096
55	-8.834	52.118	-0.085	0.003	0.1	0.3	0.1	24.254	30.838	0.7865	0.7865	-0.0019	0.0053	-0.0097
56	-8.833	52.738	0.053	0.010	3.9	0.1	0.3	20.496	30.843	0.6645	0.6630	-0.0452	0.0045	0.0023
57	-4.985	52.132	-0.086	0.006	0.1	0.4	0.2	24.363	30.707	0.7934	0.7934	-0.0017	0.0082	-0.0064
58	-4.416	8.775	-0.066	0.002	0.0	-0.3	0.0	30.781	30.784	0.9999	0.9999	-0.0004	-0.0050	0.0064
59	-4.415	11.290	-0.070	0.001	-0.0	-0.1	0.0	30.829	30.789	1.0013	1.0013	0.0007	-0.0018	0.0046
60	-4.416	13.864	-0.071	0.003	-0.0	-0.1	0.1	30.855	30.782	1.0024	1.0024	0.0009	-0.0006	0.0034
61	-4.417	16.420	-0.074	0.003	-0.1	0.1	0.1	30.753	30.632	1.0040	1.0040	0.0012	0.0027	-0.0011
62	-4.415	18.968	-0.071	0.004	0.0	-0.0	0.1	30.825	30.702	1.0040	1.0040	-0.0009	0.0018	0.0020
63	-4.418	21.522	-0.071	0.003	0.1	0.1	0.1	30.793	30.684	1.0035	1.0035	-0.0012	0.0028	0.0025
64	-4.417	24.078	-0.075	0.003	0.0	0.1	0.1	30.847	30.734	1.0037	1.0037	-0.0002	0.0027	0.0028
65	-4.418	26.604	-0.075	0.002	0.0	0.2	0.1	30.824	30.681	1.0047	1.0047	-0.0009	0.0041	0.0016
66	-4.417	29.165	-0.073	0.003	0.1	0.2	0.1	30.817	30.687	1.0042	1.0042	-0.0024	0.0047	0.0027
67	-4.418	31.711	-0.077	0.003	0.1	0.3	0.1	30.845	30.688	1.0051	1.0051	-0.0014	0.0067	0.0017
68	-4.417	34.254	-0.077	0.002	0.1	0.4	0.1	30.865	30.715	1.0049	1.0049	-0.0021	0.0080	0.0013
69	-4.418	36.833	-0.080	0.002	0.1	0.5	0.1	30.855	30.689	1.0054	1.0053	-0.0015	0.0098	0.0025
70	-4.418	39.395	-0.083	0.004	0.0	0.5	0.1	30.825	30.624	1.0066	1.0065	-0.0002	0.0099	0.0011
71	-4.417	41.924	-0.082	0.002	0.1	0.6	0.1	30.780	30.604	1.0058	1.0057	-0.0017	0.0119	0.0021
72	-4.418	44.476	-0.087	0.004	-0.0	0.5	0.1	30.906	30.706	1.0065	1.0065	0.0006	0.0108	0.0012
73	-4.418	44.476	-0.087	0.004	-0.1	0.5	0.1	30.843	30.639	1.0067	1.0066	0.0009	0.0105	0.0010
74	-4.420	44.478	-0.088	0.003	-0.1	0.5	0.1	30.837	30.640	1.0064	1.0064	0.0010	0.0103	0.0014
75	-4.418	45.752	-0.089	0.003	-0.1	0.5	0.1	30.866	30.709	1.0051	1.0050	0.0014	0.0105	0.0013
76	-4.419	47.050	-0.091	0.003	-0.1	0.5	0.1	30.563	30.741	0.9942	0.9942	0.0020	0.0104	0.0003
77	-4.419	48.306	-0.092	0.004	-0.1	0.5	0.1	29.718	30.647	0.9697	0.9696	0.0025	0.0106	-0.0012
78	-4.419	49.580	-0.094	0.004	-0.2	0.6	0.1	28.495	30.644	0.9299	0.9298	0.0028	0.0115	-0.0026
79	-4.418	50.878	-0.094	0.003	-0.2	0.6	0.1	26.917	30.655	0.8781	0.8780	0.0026	0.0109	-0.0042
80	-4.422	52.131	-0.086	0.007	0.1	0.4	0.2	24.328	30.661	0.7935	0.7934	-0.0015	0.0081	-0.0072
81	-0.013	8.708	-0.072	-0.005	-0.1	-0.4	-0.1	30.505	30.807	0.9902	0.9901	0.0023	-0.0092	0.0128
82	-0.013	11.223	-0.075	-0.001	-0.2	-0.2	-0.0	30.660	30.823	0.9947	0.9947	0.0034	-0.0034	0.0082
83	-0.012	13.805	-0.073	-0.003	-0.1	-0.2	-0.1	30.636	30.824	0.9939	0.9939	0.0016	-0.0046	0.0075
84	-0.013	16.352	-0.070	-0.002	0.0	-0.1	-0.1	30.639	30.790	0.9951	0.9951	-0.0004	-0.0027	0.0072
85	-0.014	18.901	-0.077	0.000	-0.1	-0.1	0.0	30.734	30.838	0.9966	0.9966	0.0019	-0.0011	0.0052
86	-0.015	21.462	-0.076	0.002	-0.1	0.0	0.0	30.798	30.874	0.9975	0.9975	0.0010	0.0012	0.0042
87	-0.015	24.016	-0.074	0.003	0.0	0.0	0.1	30.713	30.747	0.9989	0.9989	-0.0006	0.0020	0.0019
88	-0.017	26.558	-0.076	0.001	0.0	0.1	0.0	30.532	30.585	0.9983	0.9982	-0.0006	0.0030	0.0031
89	-0.017	29.107	-0.079	0.004	-0.0	0.1	0.1	30.644	30.653	0.9997	0.9997	0.0003	0.0042	0.0019
90	-0.018	31.670	-0.079	0.001	0.0	0.2	0.0	30.622	30.647	0.9992	0.9992	-0.0006	0.0046	0.0020
91	-0.016	34.198	-0.078	-0.001	0.1	0.3	-0.0	30.601	30.652	0.9983	0.9983	-0.0018	0.0052	0.0032
92	-0.016	36.781	-0.080	-0.001	0.1	0.4	-0.0	30.644	30.685	0.9987	0.9986	-0.0011	0.0073	0.0041
93	-0.017	39.349	-0.084	-0.001	-0.0	0.4	-0.0	30.673	30.703	0.9990	0.9990	0.0003	0.0060	0.0051
94	-0.017	41.879	-0.084	0.002	0.0	0.3	0.1	30.722	30.713	1.0003	1.0003	-0.0004	0.0068	0.0030
95	-0.020	44.432	-0.086	0.002	-0.0	0.3	0.1	30.701	30.703	0.9999	0.9999	0.0000	0.0066	0.0033
96	-0.018	45.710	-0.087	0.002	-0.0	0.6	0.0	30.570	30.703	0.9957	0.9956	0.0005	0.0103	0.0030
97	-0.020	47.009	-0.089	0.002	-0.1	0.5	0.1	30.043	30.690	0.9789	0.9789	0.0010	0.0104	0.0016
98	-0.020	48.282	-0.092	0.003	-0.1	0.5	0.1	29.111	30.670	0.9492	0.9491	0.0025	0.0101	0.0001
99	-0.021	49.540	-0.093	0.002	-0.1	0.6	0.0	27.891	30.718	0.9080	0.9079	0.0023	0.0108	-0.0018
100	-0.020	50.190	-0.092	0.003	-0.1	0.6	0.1	27.135	30.775	0.8817	0.8817	0.0016	0.0105	-0.0023

STATION 0 (Continued)

POINT	Z	Y	CPITCH	CYAW	ALPHA	THETA	BETA	V	VCONT	VV	VX	VY	VZ	CP
101	-0.022	50.843	-0.091	0.003	-0.1	0.7	0.1	26.198	30.711	0.8530	0.8530	0.0010	0.0112	-0.0020
102	-0.022	51.471	-0.091	-0.002	-0.1	0.7	-0.0	25.096	30.735	0.8165	0.8165	0.0010	0.0093	-0.0040
103	-0.025	52.100	-0.084	0.001	0.2	0.7	0.0	23.653	30.804	0.7679	0.7678	-0.0024	0.0104	-0.0055
104	-0.022	52.712	0.050	-0.005	3.8	0.7	-0.1	19.982	30.783	0.6491	0.6476	-0.0435	0.0064	-0.0043
105	4.007	8.769	-0.067	0.004	-0.0	-0.5	0.1	30.616	30.677	0.9980	0.9980	0.0000	-0.0071	0.0114
106	4.388	8.771	-0.065	0.006	0.0	-0.5	0.2	30.683	30.724	0.9987	0.9987	-0.0007	-0.0059	0.0126
107	4.389	11.284	-0.071	0.004	-0.1	-0.4	0.1	30.701	30.686	1.0005	1.0005	0.0011	-0.0059	0.0099
108	4.389	13.862	-0.070	0.004	0.0	-0.3	0.1	30.760	30.719	1.0013	1.0013	-0.0000	-0.0040	0.0088
109	4.390	16.412	-0.073	0.005	-0.0	-0.3	0.1	30.772	30.703	1.0022	1.0022	0.0008	-0.0039	0.0059
110	4.390	18.958	-0.073	0.004	-0.0	-0.4	0.1	30.776	30.693	1.0027	1.0027	0.0001	-0.0044	0.0061
111	4.390	21.517	-0.074	0.003	-0.0	-0.2	0.1	30.779	30.702	1.0025	1.0025	0.0001	-0.0018	0.0050
112	4.390	24.064	-0.075	0.002	0.0	-0.2	0.1	30.699	30.604	1.0031	1.0031	-0.0003	-0.0021	0.0063
113	4.389	26.604	-0.076	0.002	0.0	0.1	0.0	30.663	30.548	1.0038	1.0038	-0.0004	0.0017	0.0052
114	4.390	29.152	-0.077	0.002	0.0	0.1	0.0	30.737	30.625	1.0036	1.0036	-0.0007	0.0022	0.0055
115	4.389	31.697	-0.079	0.004	0.0	0.1	0.1	30.791	30.645	1.0048	1.0048	-0.0006	0.0036	0.0043
116	4.389	34.240	-0.080	0.001	0.0	0.3	0.0	30.758	30.621	1.0045	1.0045	-0.0008	0.0058	0.0056
117	4.386	36.816	-0.080	0.003	0.1	0.2	0.1	30.753	30.582	1.0056	1.0056	-0.0016	0.0046	0.0034
118	4.386	39.386	-0.081	0.002	0.1	0.3	0.1	30.669	30.512	1.0051	1.0051	-0.0017	0.0063	0.0046
119	4.385	41.918	-0.081	0.004	0.1	0.3	0.1	30.866	30.688	1.0058	1.0058	-0.0021	0.0066	0.0037
120	4.385	44.464	-0.079	0.003	0.2	0.2	0.1	30.880	30.742	1.0045	1.0045	-0.0042	0.0058	0.0044
121	4.387	45.741	-0.079	0.004	0.2	0.3	0.1	30.510	30.595	0.9972	0.9972	-0.0041	0.0069	0.0040
122	4.385	47.038	-0.084	0.002	0.1	0.4	0.0	29.827	30.557	0.9761	0.9761	-0.0020	0.0074	0.0050
123	4.384	48.292	-0.087	0.001	0.0	0.5	0.0	28.810	30.477	0.9453	0.9453	-0.0004	0.0086	0.0036
124	4.385	49.564	-0.090	0.005	-0.0	0.4	0.1	27.598	30.472	0.9057	0.9057	0.0007	0.0084	-0.0000
125	4.386	50.862	-0.092	0.004	-0.1	0.4	0.1	26.088	30.471	0.8562	0.8562	0.0014	0.0071	0.0004
126	4.387	52.119	-0.086	0.003	0.1	0.2	0.1	23.562	30.494	0.7727	0.7727	-0.0015	0.0038	-0.0013
127	8.809	8.722	-0.061	0.001	0.1	-0.4	0.0	30.468	30.821	0.9885	0.9885	-0.0024	-0.0069	0.0152
128	8.809	11.217	-0.067	0.001	0.1	-0.4	0.0	30.520	30.804	0.9908	0.9908	-0.0013	-0.0069	0.0139
129	8.810	13.806	-0.069	0.002	0.0	-0.4	0.0	30.505	30.751	0.9920	0.9920	-0.0001	-0.0064	0.0122
130	8.809	16.352	-0.071	0.003	-0.0	-0.2	0.1	30.602	30.797	0.9937	0.9937	0.0008	-0.0017	0.0092
131	8.811	18.900	-0.071	0.002	-0.0	-0.2	0.0	30.660	30.861	0.9935	0.9935	0.0001	-0.0035	0.0102
132	8.809	21.471	-0.073	0.003	0.0	-0.2	0.1	30.681	30.860	0.9942	0.9942	-0.0007	-0.0030	0.0096
133	8.810	24.006	-0.075	0.002	0.0	-0.1	0.0	30.742	30.903	0.9948	0.9948	-0.0002	-0.0009	0.0083
134	8.811	26.557	-0.078	0.000	-0.0	-0.1	0.0	30.775	30.924	0.9952	0.9952	0.0005	-0.0016	0.0098
135	8.811	29.117	-0.080	0.002	-0.0	0.2	0.1	30.797	30.904	0.9965	0.9965	0.0006	0.0048	0.0085
136	8.809	31.653	-0.081	0.001	-0.0	0.2	0.0	30.773	30.897	0.9960	0.9960	0.0007	0.0042	0.0102
137	8.810	34.199	-0.080	0.002	0.0	0.2	0.0	30.746	30.867	0.9961	0.9961	-0.0004	0.0044	0.0105
138	8.810	36.781	-0.080	0.003	0.1	0.2	0.1	30.752	30.826	0.9976	0.9976	-0.0014	0.0053	0.0085
139	8.809	39.344	-0.084	0.002	-0.0	0.2	0.1	30.864	30.950	0.9972	0.9972	0.0003	0.0048	0.0096
140	8.810	41.876	-0.082	0.003	0.1	0.3	0.1	30.813	30.892	0.9974	0.9974	-0.0018	0.0071	0.0095
141	8.810	44.448	-0.086	0.002	-0.0	0.3	0.1	30.836	30.913	0.9975	0.9975	0.0001	0.0068	0.0084
142	8.812	45.725	-0.087	0.001	-0.0	0.2	0.0	30.719	30.927	0.9933	0.9933	0.0001	0.0045	0.0092
143	8.810	47.001	-0.091	0.002	-0.1	0.3	0.1	30.259	30.900	0.9793	0.9792	0.0022	0.0065	0.0074
144	8.811	48.276	-0.094	0.003	-0.2	0.4	0.1	29.396	30.886	0.9518	0.9517	0.0037	0.0077	0.0053
145	8.815	49.531	-0.094	0.001	-0.2	0.5	0.0	28.137	30.908	0.9104	0.9103	0.0030	0.0088	0.0061
146	8.814	50.181	-0.095	0.001	-0.2	0.5	0.0	27.449	30.936	0.8873	0.8872	0.0031	0.0084	0.0056
147	8.810	50.834	-0.095	0.002	-0.2	0.6	0.0	26.525	30.910	0.8581	0.8581	0.0029	0.0101	0.0044
148	8.811	51.477	-0.094	-0.000	-0.2	0.5	-0.0	25.497	30.885	0.8255	0.8255	0.0023	0.0068	0.0037
149	8.813	52.143	-0.088	0.004	0.0	0.5	0.1	23.816	30.774	0.7739	0.7739	-0.0005	0.0089	0.0028
150	8.813	52.713	0.038	-0.003	3.5	0.3	-0.1	20.054	30.744	0.6523	0.6510	-0.0402	0.0027	0.0121

## STATION 0 (Concluded)

POINT	Z	Y	CPITCH	CYAW	ALPHA	THETA	BETA	V	VCONT	VV	VX	VY	VZ	CP
151	13.251	8.748	-0.068	0.004	-0.0	-0.4	0.1	29.401	30.501	0.9639	0.9639	0.0004	-0.0046	0.0135
152	13.160	8.757	-0.068	0.002	-0.0	-0.4	0.1	29.526	30.609	0.9646	0.9646	0.0007	-0.0062	0.0106
153	13.166	8.757	-0.068	0.005	-0.0	-0.4	0.1	29.640	30.716	0.9650	0.9649	0.0004	-0.0045	0.0111
154	13.155	8.760	-0.068	0.003	-0.0	-0.4	0.1	29.543	30.632	0.9645	0.9644	0.0004	-0.0059	0.0125
155	13.251	11.263	-0.071	0.001	-0.1	-0.4	0.0	30.113	30.474	0.9881	0.9881	0.0014	-0.0061	0.0106
156	13.250	13.835	-0.074	0.001	-0.1	-0.4	0.0	30.366	30.414	0.9984	0.9984	0.0019	-0.0064	0.0125
157	13.250	16.390	-0.078	0.002	-0.2	-0.4	0.1	30.412	30.387	1.0008	1.0008	0.0033	-0.0060	0.0118
158	13.250	18.936	-0.075	0.001	-0.1	-0.2	0.0	30.394	30.356	1.0013	1.0013	0.0014	-0.0030	0.0123
159	13.249	21.482	-0.079	0.003	-0.1	-0.2	0.1	30.596	30.502	1.0031	1.0031	0.0024	-0.0019	0.0102
160	13.249	24.044	-0.082	0.003	-0.2	0.2	0.1	30.575	30.514	1.0020	1.0020	0.0032	0.0052	0.0113
161	13.244	25.308	-0.083	0.003	-0.2	-0.3	0.1	30.603	30.611	0.9997	0.9997	0.0035	-0.0041	0.0103
162	13.230	26.332	-0.077	0.006	0.0	-0.7	0.2	30.520	30.727	0.9933	0.9932	-0.0001	-0.0086	0.0099
163	13.250	26.566	-0.076	0.001	0.0	-0.6	0.0	30.372	30.538	0.9946	0.9945	-0.0006	-0.0099	0.0094
164	13.248	26.586	-0.075	0.001	0.0	-0.6	0.0	30.295	30.488	0.9936	0.9936	-0.0008	-0.0103	0.0109
165	13.243	27.888	-0.072	0.003	0.2	-0.1	0.1	30.636	30.595	1.0013	1.0013	-0.0027	-0.0003	0.0101
166	13.250	29.128	-0.078	0.001	0.0	0.4	0.0	30.623	30.521	1.0034	1.0033	-0.0001	0.0075	0.0132
167	13.251	31.672	-0.081	0.002	-0.0	0.3	0.1	30.534	30.411	1.0040	1.0040	0.0008	0.0071	0.0151
168	13.250	34.215	-0.082	0.002	-0.0	0.2	0.1	30.574	30.435	1.0046	1.0046	0.0007	0.0038	0.0188
169	13.248	36.775	-0.088	0.003	-0.2	0.1	0.1	30.754	30.589	1.0054	1.0054	0.0032	0.0037	0.0194
170	13.245	39.357	-0.087	0.002	-0.1	0.3	0.1	30.735	30.572	1.0053	1.0053	0.0018	0.0067	0.0192
171	13.248	41.886	-0.086	0.002	-0.0	0.2	0.1	30.694	30.577	1.0039	1.0038	0.0005	0.0040	0.0187
172	13.247	44.439	-0.089	0.002	-0.1	0.3	0.0	30.250	30.505	0.9916	0.9916	0.0019	0.0055	0.0175
173	13.246	45.720	-0.090	0.002	-0.1	0.3	0.0	29.770	30.500	0.9761	0.9760	0.0018	0.0064	0.0163
174	13.247	47.008	-0.094	0.002	-0.2	0.4	0.1	29.347	30.521	0.9615	0.9615	0.0039	0.0082	0.0149
175	13.245	48.266	-0.098	0.003	-0.3	0.7	0.1	28.975	30.678	0.9445	0.9444	0.0054	0.0126	0.0134
176	13.246	49.535	-0.099	0.003	-0.3	0.9	0.1	27.866	30.572	0.9115	0.9113	0.0054	0.0154	0.0137
177	13.244	50.837	-0.095	0.005	-0.2	0.7	0.1	25.888	30.503	0.8487	0.8486	0.0029	0.0128	0.0120
178	13.244	52.092	-0.085	0.009	0.1	0.1	0.2	23.048	30.624	0.7526	0.7526	-0.0019	0.0045	0.0095

STATION 7

POINT	Z	Y	CPITCH	CYAW	ALPHA	THETA	BETA	V	VCONT	W	VX	VY	VZ	CP
1	-13.989	8.800	-0.084	0.002	-0.5	-3.6	0.1	31.405	30.861	1.0176	1.0157	0.0090	-0.0620	-0.0935
2	-13.970	11.303	-0.085	0.002	-0.5	-3.4	0.1	32.278	30.841	1.0466	1.0448	0.0092	-0.0609	-0.0985
3	-13.973	13.998	-0.086	0.002	-0.5	-3.1	0.1	32.630	30.818	1.0588	1.0572	0.0089	-0.0568	-0.1022
4	-13.973	16.534	-0.087	0.002	-0.5	-3.4	0.1	32.715	30.800	1.0622	1.0604	0.0089	-0.0613	-0.1037
5	-13.976	19.067	-0.083	0.003	-0.3	-3.1	0.1	32.736	30.788	1.0633	1.0618	0.0056	-0.0570	-0.1071
6	-13.975	21.598	-0.077	0.002	-0.1	-3.3	0.1	32.735	30.764	1.0641	1.0624	0.0016	-0.0606	-0.1082
7	-13.977	24.145	-0.080	0.002	-0.1	-3.4	0.1	32.772	30.760	1.0654	1.0637	0.0023	-0.0612	-0.1108
8	-13.976	26.671	-0.079	0.002	-0.0	-3.1	0.1	32.754	30.742	1.0654	1.0639	0.0007	-0.0570	-0.1124
9	-13.977	29.218	-0.079	0.002	-0.0	-3.1	0.1	32.702	30.717	1.0646	1.0631	0.0004	-0.0562	-0.1146
10	-13.978	31.770	-0.072	0.001	0.2	-3.0	0.0	32.667	30.703	1.0639	1.0625	-0.0042	-0.0552	-0.1148
11	-13.978	34.298	-0.071	0.004	0.3	-3.2	0.1	32.716	30.685	1.0662	1.0646	-0.0051	-0.0570	-0.1147
12	-13.978	36.863	-0.066	0.003	0.5	-3.0	0.1	32.689	30.685	1.0653	1.0639	-0.0084	-0.0549	-0.1143
13	-13.984	39.392	-0.069	0.002	0.4	-2.9	0.1	32.676	30.676	1.0652	1.0639	-0.0078	-0.0516	-0.1139
14	-13.983	41.921	-0.070	0.003	0.4	-2.8	0.1	32.368	30.663	1.0556	1.0543	-0.0082	-0.0509	-0.1140
15	-13.984	44.479	-0.070	0.004	0.5	-2.9	0.1	31.347	30.633	1.0233	1.0220	-0.0085	-0.0508	-0.1154
16	-13.983	45.717	-0.071	0.003	0.5	-2.9	0.1	31.079	30.860	1.0071	1.0058	-0.0080	-0.0502	-0.1158
17	-13.985	47.015	-0.072	0.003	0.5	-3.0	0.1	30.729	30.833	0.9966	0.9953	-0.0079	-0.0515	-0.1150
18	-13.986	48.241	-0.072	0.003	0.5	-3.5	0.1	30.356	30.821	0.9849	0.9832	-0.0080	-0.0579	-0.1130
19	-13.987	49.529	-0.072	0.003	0.5	-3.7	0.1	29.248	30.794	0.9498	0.9478	-0.0082	-0.0607	-0.1130
20	-11.440	8.826	-0.076	0.003	-0.3	-3.4	0.1	32.162	30.954	1.0390	1.0373	0.0047	-0.0597	-0.0669
21	-11.439	11.397	-0.081	0.003	-0.3	-3.3	0.1	32.293	30.947	1.0435	1.0418	0.0064	-0.0583	-0.0709
22	-11.440	13.946	-0.082	0.002	-0.3	-3.3	0.1	32.296	30.903	1.0451	1.0434	0.0063	-0.0584	-0.0740
23	-11.439	16.498	-0.082	0.003	-0.3	-3.4	0.1	32.357	30.902	1.0471	1.0453	0.0057	-0.0603	-0.0779
24	-11.440	19.016	-0.079	0.002	-0.2	-3.2	0.1	32.450	30.975	1.0476	1.0460	0.0031	-0.0581	-0.0798
25	-11.438	21.590	-0.080	0.002	-0.2	-3.2	0.1	32.469	30.959	1.0488	1.0473	0.0029	-0.0567	-0.0811
26	-11.438	24.129	-0.075	0.004	0.0	-3.4	0.1	32.478	30.941	1.0497	1.0479	-0.0002	-0.0601	-0.0830
27	-11.440	26.637	-0.073	0.002	0.1	-3.1	0.1	32.474	30.923	1.0502	1.0487	-0.0021	-0.0555	-0.0846
28	-11.438	29.204	-0.072	0.002	0.2	-3.1	0.1	32.479	30.915	1.0506	1.0491	-0.0030	-0.0557	-0.0847
29	-11.437	31.754	-0.077	0.005	0.1	-3.2	0.1	32.490	30.910	1.0511	1.0497	-0.0017	-0.0556	-0.0857
30	-11.437	34.234	-0.078	0.003	0.1	-3.0	0.1	32.484	30.896	1.0514	1.0501	-0.0017	-0.0527	-0.0867
31	-11.437	36.826	-0.074	0.003	0.2	-3.0	0.1	32.549	30.952	1.0516	1.0503	-0.0043	-0.0531	-0.0862
32	-11.435	39.372	-0.073	0.003	0.3	-2.9	0.1	32.536	30.940	1.0516	1.0502	-0.0055	-0.0527	-0.0856
33	-11.433	41.883	-0.079	0.004	0.2	-2.8	0.1	32.529	30.935	1.0515	1.0504	-0.0035	-0.0494	-0.0854
34	-11.435	44.456	-0.076	0.004	0.3	-2.7	0.1	32.444	30.934	1.0488	1.0477	-0.0059	-0.0483	-0.0841
35	-11.433	45.736	-0.077	0.003	0.3	-2.7	0.1	32.256	30.919	1.0432	1.0421	-0.0054	-0.0482	-0.0861
36	-11.430	47.013	-0.078	0.006	0.3	-2.9	0.2	31.752	30.903	1.0275	1.0262	-0.0053	-0.0497	-0.0852
37	-11.429	48.279	-0.080	0.002	0.3	-3.2	0.1	30.864	30.879	0.9995	0.9980	-0.0046	-0.0539	-0.0864
38	-11.448	49.533	-0.081	0.001	0.3	-3.5	0.0	29.592	30.939	0.9565	0.9547	-0.0042	-0.0576	-0.0870
39	-7.631	8.802	-0.075	0.002	-0.2	-3.3	0.1	31.652	30.857	1.0257	1.0241	0.0041	-0.0573	-0.0324
40	-7.630	11.395	-0.078	0.003	-0.3	-3.2	0.1	31.756	30.835	1.0299	1.0283	0.0046	-0.0568	-0.0366
41	-7.630	13.962	-0.073	0.003	-0.1	-3.2	0.1	31.790	30.820	1.0315	1.0299	0.0016	-0.0567	-0.0403
42	-7.629	16.501	-0.074	0.003	-0.1	-3.1	0.1	31.803	30.806	1.0324	1.0309	0.0013	-0.0550	-0.0421
43	-7.628	19.022	-0.076	0.003	-0.1	-3.1	0.1	31.821	30.800	1.0332	1.0317	0.0018	-0.0546	-0.0437
44	-7.626	21.588	-0.074	0.003	-0.0	-3.1	0.1	31.829	30.789	1.0338	1.0324	0.0001	-0.0546	-0.0451
45	-7.624	24.132	-0.074	0.003	0.0	-3.0	0.1	31.840	30.763	1.0350	1.0336	-0.0008	-0.0536	-0.0473
46	-7.628	26.644	-0.077	0.003	0.0	-3.0	0.1	31.813	30.735	1.0351	1.0337	-0.0002	-0.0536	-0.0471
47	-7.624	29.211	-0.077	0.003	0.0	-2.9	0.1	31.833	30.733	1.0358	1.0345	-0.0007	-0.0518	-0.0484
48	-7.621	31.749	-0.077	0.003	0.1	-2.9	0.1	31.947	30.829	1.0363	1.0350	-0.0017	-0.0516	-0.0489
49	-7.621	34.249	-0.079	0.003	0.1	-2.7	0.1	31.932	30.809	1.0365	1.0354	-0.0013	-0.0477	-0.0490
50	-7.617	36.838	-0.076	0.003	0.2	-2.7	0.1	31.905	30.775	1.0367	1.0356	-0.0035	-0.0478	-0.0493

## STATION 7 (Continued)

POINT	Z	Y	CPITCH	CYAW	ALPHA	THETA	BETA	V	VCONT	VW	VX	VY	VZ	CP
51	-7.618	39.383	-0.077	0.003	0.2	-2.7	0.1	31.900	30.769	1.0367	1.0356	-0.0035	-0.0477	-0.0496
52	-7.615	41.870	-0.076	0.003	0.3	-2.6	0.1	31.910	30.772	1.0370	1.0359	-0.0047	-0.0466	-0.0497
53	-7.614	44.439	-0.078	0.003	0.2	-2.7	0.1	31.886	30.765	1.0364	1.0354	-0.0045	-0.0465	-0.0497
54	-7.618	45.762	-0.081	0.003	0.2	-2.7	0.1	31.342	30.579	1.0250	1.0239	-0.0032	-0.0470	-0.0497
55	-7.610	47.014	-0.083	0.003	0.1	-2.9	0.1	31.382	30.749	1.0206	1.0193	-0.0026	-0.0508	-0.0501
56	-7.610	48.255	-0.087	0.004	0.0	-2.9	0.1	30.110	30.553	0.9855	0.9844	-0.0005	-0.0480	-0.0514
57	-7.614	49.544	-0.088	0.004	0.0	-3.4	0.1	29.325	30.698	0.9553	0.9537	-0.0005	-0.0548	-0.0528
58	-3.831	8.827	-0.071	0.002	-0.1	-3.2	0.1	31.137	30.873	1.0085	1.0070	0.0020	-0.0551	-0.0053
59	-3.807	11.342	-0.075	0.003	-0.2	-3.1	0.1	31.258	30.860	1.0129	1.0115	0.0035	-0.0527	-0.0097
60	-3.807	14.006	-0.075	0.004	-0.2	-3.1	0.1	31.269	30.846	1.0137	1.0123	0.0027	-0.0526	-0.0117
61	-3.809	16.528	-0.077	0.003	-0.1	-3.1	0.1	31.294	30.852	1.0143	1.0129	0.0026	-0.0529	-0.0131
62	-3.808	19.070	-0.078	0.002	-0.1	-3.1	0.0	31.292	30.837	1.0147	1.0133	0.0024	-0.0536	-0.0153
63	-3.808	21.603	-0.076	0.004	-0.1	-3.1	0.1	31.303	30.820	1.0157	1.0143	0.0011	-0.0527	-0.0167
64	-3.807	24.132	-0.076	0.004	0.0	-3.1	0.1	31.313	30.809	1.0164	1.0150	-0.0000	-0.0527	-0.0175
65	-3.809	26.678	-0.076	0.005	0.0	-3.0	0.1	31.308	30.803	1.0164	1.0151	-0.0004	-0.0501	-0.0181
66	-3.810	29.229	-0.073	0.003	0.2	-3.0	0.1	31.318	30.787	1.0172	1.0160	-0.0027	-0.0511	-0.0189
67	-3.808	31.758	-0.073	0.002	0.2	-2.9	0.1	31.299	30.776	1.0170	1.0158	-0.0032	-0.0496	-0.0198
68	-3.808	34.298	-0.078	0.002	0.1	-2.7	0.1	31.297	30.762	1.0174	1.0163	-0.0018	-0.0477	-0.0202
69	-3.809	36.873	-0.075	0.003	0.2	-2.8	0.1	31.287	30.745	1.0176	1.0165	-0.0037	-0.0476	-0.0210
70	-3.808	39.402	-0.078	0.003	0.2	-2.8	0.1	31.286	30.734	1.0179	1.0168	-0.0032	-0.0478	-0.0214
71	-3.810	41.914	-0.077	0.003	0.2	-2.7	0.1	31.229	30.704	1.0171	1.0161	-0.0043	-0.0456	-0.0213
72	-3.810	44.457	-0.082	0.004	0.1	-2.7	0.1	31.265	30.730	1.0174	1.0164	-0.0021	-0.0457	-0.0214
73	-3.813	45.715	-0.084	0.003	0.1	-2.7	0.1	31.179	30.724	1.0148	1.0137	-0.0018	-0.0458	-0.0212
74	-3.810	47.027	-0.085	0.005	0.1	-2.8	0.1	30.811	30.707	1.0034	1.0023	-0.0012	-0.0461	-0.0233
75	-3.811	48.246	-0.089	0.005	-0.0	-2.9	0.1	30.204	30.909	0.9772	0.9761	0.0004	-0.0466	-0.0252
76	-3.814	49.507	-0.091	0.005	-0.1	-3.1	0.1	28.993	30.908	0.9380	0.9367	0.0016	-0.0494	-0.0261
77	0.010	8.761	-0.072	0.002	-0.1	-3.0	0.0	30.147	30.407	0.9914	0.9901	0.0023	-0.0513	0.0184
78	-0.016	8.762	-0.070	0.003	-0.1	-3.0	0.1	30.505	30.498	1.0002	0.9989	0.0014	-0.0510	0.0195
79	0.007	11.283	-0.074	0.004	-0.2	-2.9	0.1	30.296	30.397	0.9967	0.9955	0.0030	-0.0490	0.0146
80	-0.014	11.287	-0.073	0.003	-0.1	-2.9	0.1	30.649	30.496	1.0050	1.0038	0.0025	-0.0496	0.0158
81	-0.014	13.984	-0.072	0.002	-0.1	-2.8	0.1	30.683	30.502	1.0059	1.0048	0.0012	-0.0480	0.0142
82	-0.001	16.535	-0.073	0.003	-0.0	-2.8	0.1	30.713	30.516	1.0065	1.0053	0.0006	-0.0475	0.0125
83	-0.005	19.043	-0.075	0.003	-0.1	-2.8	0.1	30.736	30.521	1.0070	1.0059	0.0011	-0.0479	0.0107
84	-0.005	21.592	-0.076	0.003	-0.1	-2.7	0.1	30.734	30.505	1.0075	1.0065	0.0010	-0.0459	0.0104
85	-0.007	24.156	-0.075	0.003	0.0	-2.7	0.1	30.750	30.506	1.0080	1.0070	-0.0003	-0.0462	0.0086
86	-0.005	26.683	-0.075	0.003	0.1	-2.7	0.1	30.757	30.497	1.0085	1.0075	-0.0012	-0.0461	0.0078
87	-0.007	29.210	-0.074	0.003	0.1	-2.6	0.1	30.773	30.495	1.0091	1.0081	-0.0023	-0.0441	0.0071
88	-0.007	31.775	-0.073	0.003	0.2	-2.6	0.1	30.769	30.478	1.0095	1.0086	-0.0032	-0.0443	0.0061
89	-0.007	34.284	-0.074	0.002	0.2	-2.5	0.1	30.746	30.468	1.0091	1.0082	-0.0037	-0.0435	0.0059
90	-0.008	36.857	-0.076	0.003	0.2	-2.5	0.1	30.761	30.471	1.0095	1.0086	-0.0034	-0.0433	0.0057
91	-0.009	39.398	-0.077	0.003	0.2	-2.4	0.1	30.774	30.455	1.0105	1.0096	-0.0038	-0.0416	0.0056
92	-0.010	41.907	-0.077	0.002	0.2	-2.5	0.1	30.756	30.446	1.0102	1.0093	-0.0044	-0.0420	0.0043
93	-0.011	44.459	-0.079	0.004	0.2	-2.4	0.1	30.710	30.435	1.0090	1.0082	-0.0042	-0.0409	0.0030
94	-0.007	45.910	-0.081	0.005	0.2	-2.2	0.1	30.334	30.574	0.9922	0.9915	-0.0031	-0.0358	0.0024
95	-0.006	47.000	-0.083	0.005	0.1	-2.3	0.1	29.778	30.576	0.9739	0.9732	-0.0025	-0.0369	-0.0003
96	-0.009	47.016	-0.082	0.005	0.2	-2.3	0.1	29.839	30.438	0.9803	0.9796	-0.0032	-0.0381	0.0020
97	-0.007	48.243	-0.085	0.004	0.1	-2.4	0.1	28.774	30.579	0.9410	0.9402	-0.0015	-0.0379	-0.0005
98	-0.015	49.550	-0.085	0.004	0.1	-2.7	0.1	27.710	30.619	0.9050	0.9041	-0.0017	-0.0408	-0.0022
99	3.807	8.777	-0.067	0.004	-0.0	-2.6	0.1	30.197	30.739	0.9823	0.9814	0.0004	-0.0429	0.0376
100	3.810	11.400	-0.073	0.003	-0.1	-2.5	0.1	30.301	30.733	0.9859	0.9850	0.0021	-0.0417	0.0353

STATION 7 (Continued)

POINT	Z	Y	CPITCH	CYAW	ALPHA	THETA	BETA	V	VCONT	VW	VX	VY	VZ	CP
101	3.808	13.958	-0.073	0.003	-0.1	-2.5	0.1	30.308	30.712	0.9869	0.9860	0.0015	-0.0420	0.0329
102	3.808	16.504	-0.075	0.003	-0.1	-2.5	0.1	30.311	30.715	0.9868	0.9859	0.0019	-0.0417	0.0317
103	3.807	19.033	-0.075	0.004	-0.1	-2.4	0.1	30.312	30.666	0.9884	0.9876	0.0010	-0.0394	0.0305
104	3.809	21.603	-0.075	0.004	-0.0	-2.4	0.1	30.332	30.682	0.9886	0.9878	0.0004	-0.0396	0.0300
105	3.808	24.126	-0.077	0.004	-0.0	-2.3	0.1	30.357	30.682	0.9894	0.9886	0.0006	-0.0387	0.0288
106	3.808	26.647	-0.077	0.004	-0.0	-2.2	0.1	30.513	30.815	0.9902	0.9895	0.0001	-0.0363	0.0285
107	3.811	29.218	-0.076	0.003	0.1	-2.2	0.1	30.509	30.803	0.9905	0.9898	-0.0010	-0.0365	0.0281
108	3.809	31.757	-0.078	0.003	0.0	-2.1	0.1	30.510	30.790	0.9909	0.9903	-0.0008	-0.0348	0.0269
109	3.810	34.240	-0.078	0.004	0.1	-2.1	0.1	30.503	30.779	0.9910	0.9904	-0.0014	-0.0347	0.0267
110	3.808	36.828	-0.078	0.004	0.1	-2.1	0.1	30.488	30.751	0.9915	0.9909	-0.0024	-0.0344	0.0257
111	3.807	39.379	-0.079	0.003	0.2	-2.1	0.1	30.482	30.738	0.9917	0.9910	-0.0027	-0.0349	0.0250
112	3.809	41.888	-0.080	0.004	0.2	-2.1	0.1	30.462	30.719	0.9916	0.9910	-0.0030	-0.0345	0.0238
113	3.809	44.420	-0.077	0.002	0.3	-2.1	0.1	30.413	30.703	0.9905	0.9899	-0.0049	-0.0352	0.0239
114	3.809	45.719	-0.078	0.003	0.3	-2.1	0.1	30.161	30.694	0.9826	0.9820	-0.0049	-0.0345	0.0229
115	3.808	47.017	-0.082	0.005	0.2	-2.1	0.1	29.501	30.691	0.9612	0.9607	-0.0030	-0.0330	0.0220
116	3.808	48.271	-0.085	0.004	0.1	-2.2	0.1	28.503	30.686	0.9289	0.9282	-0.0013	-0.0341	0.0201
117	3.856	49.534	-0.088	0.005	0.0	-2.4	0.1	27.226	30.661	0.8880	0.8873	-0.0002	-0.0356	0.0186
118	7.607	8.761	-0.063	0.003	0.1	-2.3	0.1	29.639	30.450	0.9734	0.9726	-0.0017	-0.0375	0.0557
119	7.616	11.282	-0.069	0.002	-0.0	-2.2	0.1	29.752	30.433	0.9776	0.9769	0.0004	-0.0365	0.0528
120	7.616	13.976	-0.073	0.005	-0.1	-2.2	0.1	29.781	30.440	0.9784	0.9777	0.0014	-0.0359	0.0505
121	7.613	16.542	-0.073	0.004	-0.1	-2.2	0.1	29.796	30.444	0.9787	0.9781	0.0010	-0.0355	0.0498
122	7.613	19.072	-0.072	0.003	0.0	-2.1	0.1	29.790	30.425	0.9791	0.9786	-0.0001	-0.0341	0.0493
123	7.616	21.583	-0.073	0.004	0.0	-2.1	0.1	29.812	30.429	0.9797	0.9792	-0.0007	-0.0337	0.0478
124	7.617	24.137	-0.075	0.004	0.0	-2.1	0.1	29.827	30.435	0.9800	0.9794	-0.0003	-0.0340	0.0479
125	7.615	26.668	-0.078	0.003	-0.0	-2.0	0.1	29.843	30.438	0.9804	0.9799	0.0002	-0.0322	0.0468
126	7.617	29.214	-0.079	0.003	-0.0	-1.9	0.1	29.852	30.415	0.9815	0.9810	0.0002	-0.0309	0.0455
127	7.617	31.771	-0.076	0.003	0.1	-1.8	0.1	29.849	30.411	0.9815	0.9811	-0.0018	-0.0288	0.0438
128	7.618	34.302	-0.078	0.006	0.1	-1.8	0.2	29.847	30.396	0.9819	0.9815	-0.0015	-0.0277	0.0435
129	7.613	36.847	-0.078	0.004	0.1	-1.7	0.1	29.827	30.367	0.9822	0.9818	-0.0025	-0.0280	0.0427
130	7.614	39.395	-0.081	0.004	0.1	-1.8	0.1	29.844	30.370	0.9827	0.9822	-0.0013	-0.0288	0.0425
131	7.615	41.903	-0.082	0.004	0.1	-1.7	0.1	29.831	30.340	0.9832	0.9829	-0.0016	-0.0270	0.0418
132	7.617	44.477	-0.082	0.004	0.1	-1.7	0.1	29.813	30.337	0.9827	0.9824	-0.0021	-0.0272	0.0406
133	7.616	45.715	-0.085	0.004	0.1	-1.7	0.1	29.908	30.595	0.9775	0.9772	-0.0012	-0.0269	0.0391
134	7.613	47.013	-0.087	0.003	0.0	-1.7	0.1	29.393	30.609	0.9603	0.9599	-0.0001	-0.0267	0.0390
135	7.617	48.246	-0.091	0.006	-0.1	-1.7	0.2	28.472	30.603	0.9304	0.9300	0.0015	-0.0254	0.0368
136	7.616	49.522	-0.091	0.004	-0.1	-1.9	0.1	27.148	30.595	0.8873	0.8869	0.0013	-0.0273	0.0347
137	11.435	8.776	-0.060	0.002	0.2	-1.7	0.1	29.121	30.595	0.9518	0.9514	-0.0029	-0.0271	0.0676
138	11.436	11.290	-0.070	0.004	-0.0	-1.7	0.1	29.485	30.603	0.9634	0.9631	0.0008	-0.0265	0.0663
139	11.435	13.982	-0.074	0.003	-0.1	-1.8	0.1	29.666	30.596	0.9696	0.9692	0.0020	-0.0284	0.0665
140	11.436	16.534	-0.076	0.004	-0.1	-1.7	0.1	29.661	30.565	0.9704	0.9700	0.0022	-0.0268	0.0656
141	11.434	19.062	-0.079	0.005	-0.2	-1.6	0.1	29.689	30.568	0.9713	0.9709	0.0031	-0.0243	0.0645
142	11.434	21.595	-0.076	0.004	-0.1	-1.5	0.1	29.697	30.575	0.9713	0.9710	0.0009	-0.0240	0.0640
143	11.434	24.138	-0.074	0.005	0.0	-1.4	0.1	29.699	30.558	0.9719	0.9717	-0.0007	-0.0211	0.0625
144	11.434	26.684	-0.078	0.005	-0.0	-1.9	0.1	29.637	30.554	0.9700	0.9695	0.0003	-0.0298	0.0625
145	11.434	29.213	-0.082	0.004	-0.1	-1.2	0.1	29.730	30.554	0.9730	0.9729	0.0021	-0.0177	0.0608
146	11.435	31.775	-0.083	0.005	-0.1	-1.2	0.1	29.716	30.511	0.9739	0.9738	0.0016	-0.0180	0.0602
147	11.436	34.292	-0.085	0.004	-0.1	-1.2	0.1	29.728	30.522	0.9740	0.9738	0.0022	-0.0181	0.0593
148	11.435	36.866	-0.085	0.003	-0.1	-1.2	0.1	29.715	30.494	0.9745	0.9743	0.0014	-0.0185	0.0586
149	11.435	39.386	-0.083	0.004	0.0	-1.2	0.1	30.018	30.779	0.9753	0.9751	-0.0005	-0.0182	0.0572
150	11.435	41.904	-0.087	0.004	-0.1	-1.2	0.1	29.926	30.666	0.9759	0.9757	0.0014	-0.0183	0.0557

## STATION 7 (Concluded)

POINT	Z	Y	PITCH	CYAW	ALPHA	THETA	BETA	V	VCONT	VW	VX	VY	VZ	CP
151	11.437	44.472	-0.090	0.006	-0.1	-1.2	0.2	29.771	30.647	0.9714	0.9713	0.0021	-0.0171	0.0545
152	11.433	45.712	-0.093	0.003	-0.2	-1.2	0.1	29.563	30.636	0.9650	0.9648	0.0036	-0.0183	0.0534
153	11.433	47.008	-0.095	0.003	-0.3	-1.1	0.1	29.171	30.644	0.9519	0.9518	0.0043	-0.0163	0.0519
154	11.433	48.245	-0.097	0.003	-0.3	-1.0	0.1	28.385	30.629	0.9267	0.9266	0.0051	-0.0142	0.0499
155	11.431	49.522	-0.098	0.005	-0.3	-0.9	0.1	26.973	30.617	0.8810	0.8809	0.0047	-0.0122	0.0485
156	13.965	8.769	-0.070	0.003	-0.1	-1.3	0.1	26.534	30.739	0.8632	0.8630	0.0014	-0.0178	0.0691
157	13.965	11.402	-0.078	0.004	-0.3	-1.2	0.1	27.294	30.722	0.8884	0.8883	0.0041	-0.0164	0.0683
158	13.964	13.974	-0.080	0.005	-0.3	-1.2	0.1	27.957	30.711	0.9104	0.9102	0.0044	-0.0165	0.0700
159	13.965	16.497	-0.080	0.004	-0.2	-1.1	0.1	28.899	30.691	0.9416	0.9415	0.0039	-0.0153	0.0705
160	13.965	19.035	-0.081	0.004	-0.2	-0.9	0.1	29.025	30.681	0.9460	0.9459	0.0039	-0.0140	0.0713
161	13.965	21.591	-0.084	0.005	-0.3	-1.0	0.1	29.240	30.671	0.9533	0.9532	0.0046	-0.0138	0.0697
162	13.963	24.132	-0.084	0.003	-0.2	-0.9	0.1	29.235	30.664	0.9534	0.9533	0.0041	-0.0130	0.0694
163	13.965	26.639	-0.082	0.005	-0.1	-1.2	0.1	27.778	30.660	0.9060	0.9058	0.0021	-0.0162	0.0664
164	13.967	29.213	-0.079	0.003	-0.0	-0.6	0.1	29.256	30.649	0.9545	0.9545	0.0003	-0.0089	0.0664
165	13.965	31.752	-0.083	0.003	-0.1	-0.6	0.1	29.428	30.633	0.9607	0.9606	0.0014	-0.0093	0.0666
166	13.965	34.255	-0.084	0.004	-0.1	-0.6	0.1	29.164	30.612	0.9527	0.9527	0.0015	-0.0087	0.0646
167	13.967	36.835	-0.086	0.003	-0.1	-0.6	0.1	29.187	30.590	0.9541	0.9541	0.0020	-0.0089	0.0632
168	13.968	39.379	-0.086	0.003	-0.1	-0.6	0.1	29.386	30.687	0.9576	0.9576	0.0014	-0.0081	0.0610
169	13.969	41.872	-0.087	0.003	-0.1	-0.5	0.1	28.782	30.679	0.9382	0.9381	0.0015	-0.0072	0.0596
170	13.967	44.440	-0.090	0.005	-0.1	-0.6	0.1	27.679	30.647	0.9032	0.9031	0.0021	-0.0080	0.0567
171	13.967	45.714	-0.092	0.006	-0.2	-0.7	0.2	26.898	30.636	0.8777	0.8776	0.0029	-0.0089	0.0552
172	13.965	46.992	-0.099	0.006	-0.4	-0.7	0.2	26.431	30.631	0.8629	0.8628	0.0058	-0.0087	0.0535
173	13.965	48.290	-0.105	0.006	-0.6	-0.4	0.2	26.404	30.613	0.8625	0.8625	0.0084	-0.0041	0.0529
174	13.936	49.522	-0.108	0.005	-0.6	-0.0	0.1	26.128	30.610	0.8536	0.8535	0.0095	0.0021	0.0540



STATION 14

56

POINT	Z	Y	CPITCH	CYAW	ALPHA	THETA	BETA	V	VCONT	VW	VX	VY	VZ	CP
1	-15.241	8.804	-0.129	0.003	-2.0	-1.7	0.1	29.175	27.644	1.0554	1.0543	0.0369	-0.0299	-0.0065
2	-15.243	11.313	-0.118	0.004	-1.6	-1.5	0.1	30.132	27.672	1.0889	1.0882	0.0303	-0.0258	-0.0116
3	-15.244	13.991	-0.110	0.005	-1.3	-1.3	0.1	30.786	27.647	1.1136	1.1130	0.0248	-0.0238	-0.0129
4	-15.246	16.537	-0.107	0.005	-1.1	-1.5	0.1	31.019	27.621	1.1230	1.1225	0.0223	-0.0261	-0.0141
5	-15.245	19.068	-0.104	0.002	-1.0	-1.3	0.1	31.052	27.616	1.1244	1.1240	0.0195	-0.0251	-0.0156
6	-15.244	21.596	-0.091	0.002	-0.5	-1.7	0.1	31.080	27.615	1.1255	1.1250	0.0101	-0.0314	-0.0178
7	-15.247	24.142	-0.088	0.003	-0.4	-1.8	0.1	31.105	27.597	1.1271	1.1266	0.0077	-0.0328	-0.0213
8	-15.250	26.669	-0.084	0.006	-0.2	-1.8	0.2	31.091	27.579	1.1273	1.1269	0.0042	-0.0315	-0.0230
9	-15.251	29.233	-0.076	0.003	0.1	-1.8	0.1	31.032	27.571	1.1255	1.1250	-0.0014	-0.0331	-0.0241
10	-15.248	31.739	-0.060	0.004	0.5	-1.6	0.1	31.020	27.567	1.1253	1.1248	-0.0105	-0.0284	-0.0224
11	-15.248	34.283	-0.058	0.003	0.7	-1.6	0.1	31.030	27.560	1.1259	1.1255	-0.0128	-0.0292	-0.0208
12	-15.248	36.867	-0.045	0.002	1.0	-1.3	0.1	31.004	27.563	1.1248	1.1244	-0.0203	-0.0235	-0.0217
13	-15.248	39.393	-0.047	0.003	1.0	-0.7	0.1	31.135	27.744	1.1222	1.1220	-0.0200	-0.0121	-0.0224
14	-15.251	41.903	-0.044	0.002	1.1	-1.0	0.1	30.495	27.746	1.0990	1.0987	-0.0219	-0.0187	-0.0223
15	-15.253	44.454	-0.033	0.004	1.5	-1.2	0.1	29.472	27.726	1.0630	1.0624	-0.0274	-0.0209	-0.0255
16	-15.252	45.736	-0.027	0.010	1.7	-1.4	0.3	29.132	27.708	1.0514	1.0507	-0.0306	-0.0207	-0.0282
17	-15.252	46.382	-0.024	0.006	1.7	-1.4	0.2	28.952	27.696	1.0454	1.0446	-0.0319	-0.0233	-0.0253
18	-15.255	46.996	-0.023	0.002	1.8	-1.6	0.0	28.721	27.701	1.0368	1.0359	-0.0323	-0.0283	-0.0232
19	-15.254	47.621	-0.023	0.003	1.8	-1.8	0.1	28.371	27.695	1.0244	1.0235	-0.0321	-0.0302	-0.0219
20	-15.254	48.251	-0.025	0.004	1.8	-2.2	0.1	27.826	27.707	1.0043	1.0032	-0.0309	-0.0358	-0.0214
21	-15.256	48.896	-0.030	0.004	1.6	-2.6	0.1	27.218	27.700	0.9826	0.9813	-0.0282	-0.0426	-0.0212
22	-15.256	49.526	-0.035	0.004	1.5	-3.1	0.1	26.576	27.695	0.9596	0.9580	-0.0251	-0.0501	-0.0216
23	-12.729	8.825	-0.103	0.007	-1.1	-1.0	0.2	30.406	27.848	1.0919	1.0916	0.0213	-0.0155	0.0217
24	-12.731	11.392	-0.103	0.003	-1.1	-1.0	0.1	30.670	27.838	1.1017	1.1014	0.0207	-0.0170	0.0216
25	-12.725	13.960	-0.100	0.004	-0.9	-1.0	0.1	30.878	27.963	1.1043	1.1040	0.0180	-0.0164	0.0187
26	-12.727	16.504	-0.100	0.003	-0.9	-1.2	0.1	30.879	27.958	1.1045	1.1041	0.0176	-0.0210	0.0181
27	-12.729	19.022	-0.092	0.005	-0.6	-1.2	0.1	30.902	27.937	1.1061	1.1059	0.0114	-0.0200	0.0143
28	-12.726	21.591	-0.090	0.006	-0.5	-1.2	0.2	30.905	27.907	1.1074	1.1072	0.0095	-0.0197	0.0116
29	-12.728	24.135	-0.081	0.007	-0.2	-1.5	0.2	30.913	27.890	1.1084	1.1081	0.0032	-0.0250	0.0099
30	-12.725	26.639	-0.076	0.008	0.0	-1.2	0.2	30.916	27.880	1.1089	1.1087	-0.0004	-0.0192	0.0072
31	-12.723	29.222	-0.072	0.006	0.2	-1.3	0.2	30.911	27.852	1.1098	1.1096	-0.0037	-0.0217	0.0067
32	-12.723	31.764	-0.071	0.004	0.2	-1.2	0.1	30.988	27.953	1.1086	1.1084	-0.0048	-0.0212	0.0093
33	-12.723	34.255	-0.068	0.005	0.4	-1.0	0.1	30.970	27.939	1.1085	1.1083	-0.0072	-0.0170	0.0084
34	-12.721	36.839	-0.060	0.002	0.6	-0.9	0.1	30.971	27.926	1.1090	1.1089	-0.0123	-0.0157	0.0108
35	-12.725	39.386	-0.058	0.009	0.7	-0.7	0.2	30.964	27.901	1.1098	1.1096	-0.0142	-0.0097	0.0094
36	-12.721	41.871	-0.063	0.004	0.6	-0.5	0.1	30.947	27.905	1.1090	1.1089	-0.0122	-0.0084	0.0096
37	-12.716	44.439	-0.056	0.006	0.9	-0.4	0.2	30.719	27.877	1.1020	1.1018	-0.0167	-0.0052	0.0066
38	-12.714	45.717	-0.052	0.007	1.0	-0.6	0.2	30.353	27.847	1.0900	1.0898	-0.0186	-0.0085	0.0060
39	-12.713	46.362	-0.052	0.006	1.0	-0.8	0.2	30.058	27.842	1.0796	1.0794	-0.0189	-0.0118	0.0062
40	-12.712	46.984	-0.054	0.003	1.0	-1.0	0.1	29.780	27.940	1.0659	1.0656	-0.0177	-0.0179	0.0050
41	-12.711	47.650	-0.053	0.008	1.0	-1.5	0.2	29.293	27.931	1.0487	1.0483	-0.0178	-0.0231	0.0060
42	-12.709	48.257	-0.055	0.006	0.9	-1.9	0.2	28.732	27.932	1.0286	1.0280	-0.0169	-0.0306	0.0065
43	-12.710	48.920	-0.058	0.007	0.9	-2.4	0.2	28.043	27.919	1.0044	1.0036	-0.0155	-0.0385	0.0072
44	-12.710	49.536	-0.060	0.008	0.8	-3.1	0.2	27.401	27.890	0.9825	0.9811	-0.0142	-0.0500	0.0063
45	-10.195	8.831	-0.094	0.003	-0.8	-0.6	0.1	30.011	27.818	1.0789	1.0787	0.0157	-0.0096	0.0516
46	-10.162	11.343	-0.095	0.005	-0.8	-0.6	0.1	30.218	27.808	1.0867	1.0865	0.0156	-0.0089	0.0469
47	-10.164	13.992	-0.094	0.005	-0.8	-0.6	0.1	30.233	27.772	1.0886	1.0885	0.0144	-0.0083	0.0464
48	-10.163	16.533	-0.094	0.007	-0.7	-0.7	0.2	30.231	27.743	1.0897	1.0896	0.0135	-0.0098	0.0435
49	-10.164	19.069	-0.087	0.003	-0.4	-0.7	0.1	30.262	27.788	1.0891	1.0890	0.0084	-0.0125	0.0443
50	-10.166	21.605	-0.084	0.008	-0.3	-0.9	0.2	30.260	27.751	1.0904	1.0903	0.0055	-0.0128	0.0402

STATION 14 (Continued)

POINT	Z	Y	CPITCH	CYAW	ALPHA	THETA	BETA	V	VCONT	VV	VX	VY	VZ	CP
51	-10.164	24.137	-0.080	0.006	-0.1	-1.0	0.2	30.273	27.762	1.0904	1.0903	0.0021	-0.0152	0.0402
52	-10.159	26.676	-0.078	0.005	-0.0	-0.8	0.1	30.352	27.846	1.0900	1.0899	0.0006	-0.0134	0.0380
53	-10.159	29.242	-0.074	0.005	0.1	-0.9	0.1	30.348	27.824	1.0907	1.0906	-0.0023	-0.0137	0.0369
54	-10.157	31.748	-0.072	0.006	0.2	-0.7	0.1	30.329	27.806	1.0907	1.0907	-0.0044	-0.0112	0.0382
55	-10.160	34.295	-0.068	0.004	0.4	-0.4	0.1	30.320	27.797	1.0908	1.0907	-0.0071	-0.0063	0.0378
56	-10.155	36.859	-0.066	0.004	0.5	-0.4	0.1	30.311	27.782	1.0910	1.0910	-0.0088	-0.0063	0.0379
57	-10.156	39.405	-0.064	0.004	0.6	-0.3	0.1	30.308	27.787	1.0907	1.0907	-0.0105	-0.0040	0.0372
58	-10.157	41.910	-0.062	0.003	0.7	-0.1	0.1	30.308	27.770	1.0914	1.0913	-0.0126	-0.0008	0.0369
59	-10.154	44.471	-0.063	0.004	0.7	-0.0	0.1	30.237	27.765	1.0890	1.0890	-0.0128	0.0015	0.0365
60	-10.157	45.709	-0.063	0.003	0.7	-0.1	0.1	30.002	27.770	1.0804	1.0803	-0.0129	-0.0006	0.0361
61	-10.157	46.376	-0.065	0.003	0.6	-0.4	0.1	29.764	27.757	1.0723	1.0722	-0.0120	-0.0065	0.0343
62	-10.155	47.000	-0.066	0.005	0.6	-0.6	0.1	29.404	27.748	1.0597	1.0596	-0.0115	-0.0092	0.0343
63	-10.156	47.630	-0.068	0.006	0.6	-1.1	0.2	28.988	27.739	1.0450	1.0449	-0.0106	-0.0165	0.0343
64	-10.156	48.249	-0.070	0.005	0.5	-1.6	0.1	28.478	27.727	1.0271	1.0267	-0.0094	-0.0262	0.0318
65	-10.156	48.892	-0.072	0.007	0.5	-2.1	0.2	27.908	27.729	1.0065	1.0059	-0.0088	-0.0336	0.0318
66	-10.158	49.541	-0.074	0.003	0.4	-2.8	0.1	27.253	27.723	0.9831	0.9819	-0.0075	-0.0468	0.0310
67	-7.642	8.788	-0.089	0.002	-0.7	-0.1	0.1	29.721	27.780	1.0699	1.0698	0.0123	0.0001	0.0772
68	-7.638	11.409	-0.091	0.004	-0.7	-0.1	0.1	29.871	27.758	1.0761	1.0760	0.0131	0.0007	0.0756
69	-7.637	13.961	-0.089	0.001	-0.6	-0.2	0.0	29.896	27.753	1.0772	1.0772	0.0107	-0.0025	0.0738
70	-7.633	16.510	-0.083	0.003	-0.3	-0.3	0.1	29.993	27.803	1.0788	1.0787	0.0064	-0.0035	0.0720
71	-7.632	19.031	-0.082	0.003	-0.3	-0.3	0.1	29.999	27.798	1.0792	1.0792	0.0053	-0.0044	0.0714
72	-7.631	21.589	-0.083	0.003	-0.3	-0.4	0.1	30.007	27.794	1.0797	1.0796	0.0048	-0.0059	0.0691
73	-7.633	24.131	-0.080	0.002	-0.1	-0.4	0.1	30.008	27.760	1.0810	1.0810	0.0021	-0.0059	0.0674
74	-7.630	26.655	-0.075	0.004	0.0	-0.4	0.1	30.023	27.749	1.0819	1.0819	-0.0008	-0.0053	0.0665
75	-7.628	29.220	-0.078	0.001	0.0	-0.3	0.0	30.020	27.739	1.0822	1.0822	-0.0004	-0.0047	0.0658
76	-7.629	31.757	-0.073	0.002	0.2	-0.2	0.1	30.010	27.744	1.0817	1.0817	-0.0034	-0.0022	0.0654
77	-7.627	34.249	-0.072	0.002	0.3	0.0	0.1	29.980	27.704	1.0821	1.0821	-0.0048	0.0020	0.0651
78	-7.626	36.837	-0.069	0.003	0.4	0.1	0.1	29.975	27.685	1.0827	1.0827	-0.0071	0.0027	0.0661
79	-7.626	39.387	-0.068	0.003	0.4	0.1	0.1	29.990	27.699	1.0827	1.0827	-0.0083	0.0043	0.0648
80	-7.625	41.876	-0.067	0.004	0.5	0.2	0.1	29.977	27.692	1.0825	1.0824	-0.0095	0.0064	0.0657
81	-7.622	44.442	-0.068	0.003	0.5	0.5	0.1	29.910	27.689	1.0802	1.0801	-0.0098	0.0100	0.0670
82	-7.622	45.719	-0.070	0.003	0.5	0.2	0.1	29.712	27.658	1.0742	1.0742	-0.0094	0.0050	0.0651
83	-7.621	46.359	-0.071	0.001	0.5	-0.0	0.0	29.501	27.660	1.0666	1.0665	-0.0090	0.0005	0.0631
84	-7.618	46.985	-0.072	0.005	0.5	-0.4	0.1	29.163	27.644	1.0549	1.0549	-0.0086	-0.0044	0.0618
85	-7.617	47.648	-0.073	0.001	0.4	-0.8	0.0	28.705	27.634	1.0388	1.0386	-0.0081	-0.0135	0.0615
86	-7.614	48.257	-0.075	0.005	0.4	-1.2	0.1	28.185	27.646	1.0195	1.0193	-0.0072	-0.0183	0.0606
87	-7.614	48.917	-0.077	0.003	0.4	-1.8	0.1	27.562	27.623	0.9978	0.9973	-0.0064	-0.0302	0.0596
88	-7.600	49.508	-0.079	0.005	0.3	-2.6	0.1	26.840	27.607	0.9722	0.9713	-0.0051	-0.0415	0.0613
89	-3.805	8.809	-0.083	0.006	-0.5	0.2	0.2	28.973	27.871	1.0395	1.0395	0.0083	0.0075	0.1107
90	-3.807	11.386	-0.085	0.003	-0.5	0.5	0.1	29.169	27.870	1.0466	1.0465	0.0089	0.0104	0.1108
91	-3.806	13.975	-0.086	0.004	-0.5	0.3	0.1	29.188	27.857	1.0478	1.0477	0.0086	0.0084	0.1093
92	-3.808	16.497	-0.082	0.005	-0.3	0.1	0.1	29.213	27.854	1.0488	1.0488	0.0059	0.0053	0.1079
93	-3.807	19.024	-0.082	0.004	-0.3	0.2	0.1	29.301	27.939	1.0487	1.0487	0.0047	0.0055	0.1064
94	-3.808	21.584	-0.079	0.004	-0.1	0.1	0.1	29.299	27.933	1.0489	1.0489	0.0027	0.0035	0.1071
95	-3.807	24.129	-0.078	0.005	-0.1	0.0	0.1	29.312	27.929	1.0495	1.0495	0.0013	0.0030	0.1067
96	-3.807	26.640	-0.078	0.003	-0.0	0.2	0.1	29.328	27.915	1.0506	1.0506	0.0004	0.0050	0.1052
97	-3.808	29.205	-0.075	0.004	0.1	0.2	0.1	29.319	27.898	1.0509	1.0509	-0.0018	0.0055	0.1049
98	-3.807	31.752	-0.074	0.004	0.2	0.3	0.1	29.327	27.893	1.0514	1.0514	-0.0029	0.0076	0.1040
99	-3.810	34.242	-0.074	0.002	0.2	0.4	0.1	29.287	27.860	1.0512	1.0512	-0.0036	0.0083	0.1043
100	-3.808	36.823	-0.074	0.004	0.3	0.6	0.1	29.345	27.874	1.0528	1.0527	-0.0046	0.0121	0.1018

57

STATION 14 (Continued)

POINT	Z	Y	CPITCH	CYAW	ALPHA	THETA	BETA	V	VCONT	VW	VX	VY	VZ	CP
101	-3.809	39.371	-0.073	0.004	0.3	0.6	0.1	29.421	27.932	1.0533	1.0532	-0.0056	0.0128	0.1021
102	-3.809	41.880	-0.072	0.003	0.4	0.8	0.1	29.418	27.938	1.0530	1.0528	-0.0069	0.0155	0.1019
103	-3.810	44.437	-0.070	0.003	0.5	0.8	0.1	29.379	27.933	1.0518	1.0516	-0.0088	0.0163	0.1020
104	-3.809	45.728	-0.070	0.004	0.5	0.7	0.1	29.194	27.929	1.0453	1.0451	-0.0088	0.0146	0.1025
105	-3.812	46.364	-0.072	0.006	0.5	0.5	0.2	28.966	27.911	1.0378	1.0377	-0.0082	0.0121	0.0992
106	-3.811	46.989	-0.073	0.003	0.4	0.3	0.1	28.570	27.904	1.0238	1.0238	-0.0077	0.0067	0.1001
107	-3.812	47.637	-0.075	0.007	0.4	-0.1	0.2	28.108	27.906	1.0072	1.0072	-0.0069	0.0010	0.0983
108	-3.811	48.267	-0.076	0.005	0.4	-0.7	0.1	27.506	27.907	0.9856	0.9856	-0.0065	-0.0097	0.0995
109	-3.813	48.914	-0.078	0.008	0.3	-1.4	0.2	26.833	27.904	0.9616	0.9614	-0.0055	-0.0196	0.0964
110	-3.806	49.543	-0.081	0.002	0.3	-2.0	0.1	25.997	27.890	0.9321	0.9316	-0.0041	-0.0315	0.0975
111	-0.036	8.748	-0.074	0.003	-0.2	0.8	0.1	28.142	27.422	1.0263	1.0261	0.0036	0.0154	0.1476
112	-0.006	11.263	-0.078	0.004	-0.3	0.9	0.1	28.349	27.416	1.0340	1.0339	0.0048	0.0191	0.1460
113	0.000	13.978	-0.077	0.004	-0.2	0.9	0.1	28.393	27.417	1.0356	1.0354	0.0034	0.0184	0.1445
114	0.002	16.545	-0.077	0.005	-0.2	0.8	0.1	28.392	27.414	1.0356	1.0355	0.0030	0.0165	0.1436
115	0.001	19.067	-0.077	0.004	-0.1	0.7	0.1	28.406	27.413	1.0362	1.0361	0.0020	0.0147	0.1427
116	0.003	21.572	-0.079	0.003	-0.1	0.7	0.1	28.409	27.422	1.0360	1.0359	0.0026	0.0138	0.1428
117	0.004	24.150	-0.078	0.004	-0.1	0.7	0.1	28.417	27.413	1.0366	1.0365	0.0013	0.0147	0.1414
118	0.002	26.673	-0.075	0.003	0.0	0.8	0.1	28.428	27.403	1.0374	1.0373	-0.0008	0.0155	0.1408
119	0.005	29.215	-0.074	0.003	0.1	0.8	0.1	28.428	27.390	1.0379	1.0378	-0.0020	0.0164	0.1404
120	0.004	31.755	-0.074	0.004	0.2	0.9	0.1	28.432	27.396	1.0378	1.0376	-0.0029	0.0188	0.1403
121	0.006	34.317	-0.074	0.003	0.2	0.9	0.1	28.444	27.394	1.0383	1.0382	-0.0038	0.0177	0.1398
122	0.005	36.841	-0.075	0.001	0.2	1.1	0.0	28.456	27.400	1.0386	1.0383	-0.0039	0.0210	0.1383
123	0.004	39.400	-0.074	-0.000	0.3	1.3	-0.0	28.462	27.389	1.0392	1.0389	-0.0050	0.0231	0.1391
124	0.004	41.910	-0.075	0.000	0.3	1.3	0.0	28.443	27.393	1.0383	1.0380	-0.0056	0.0245	0.1403
125	0.001	44.463	-0.075	0.003	0.3	1.4	0.1	28.357	27.379	1.0357	1.0353	-0.0060	0.0271	0.1347
126	-0.008	45.718	-0.077	0.005	0.3	1.2	0.1	27.872	27.451	1.0153	1.0150	-0.0052	0.0243	0.1350
127	-0.000	47.018	-0.077	0.002	0.3	0.7	0.1	27.045	27.385	0.9876	0.9875	-0.0054	0.0131	0.1352
128	-0.005	47.656	-0.079	-0.000	0.3	0.4	-0.0	26.577	27.403	0.9697	0.9698	-0.0048	0.0063	0.1332
129	-0.002	48.257	-0.080	0.004	0.3	-0.4	0.1	25.924	27.384	0.9467	0.9467	-0.0042	-0.0043	0.1323
130	-0.003	48.906	-0.081	0.001	0.2	-1.0	0.0	25.276	27.390	0.9228	0.9227	-0.0037	-0.0154	0.1315
131	-0.003	49.529	-0.084	0.004	0.1	-1.7	0.1	24.549	27.402	0.8959	0.8956	-0.0023	-0.0250	0.1310
132	3.852	8.803	-0.064	0.002	0.1	1.2	0.1	27.488	27.534	0.9983	0.9981	-0.0013	0.0227	0.1815
133	3.814	11.317	-0.070	0.004	-0.1	1.3	0.1	27.649	27.524	1.0045	1.0043	0.0010	0.0236	0.1802
134	3.816	13.976	-0.071	0.004	-0.0	1.1	0.1	27.675	27.528	1.0054	1.0051	0.0005	0.0217	0.1802
135	3.815	16.545	-0.074	0.002	-0.1	0.9	0.0	27.652	27.523	1.0047	1.0045	0.0013	0.0173	0.1802
136	3.817	19.053	-0.074	0.002	-0.0	1.0	0.1	27.679	27.515	1.0059	1.0058	0.0006	0.0192	0.1791
137	3.816	21.601	-0.075	0.005	-0.0	1.0	0.1	27.696	27.501	1.0071	1.0069	0.0003	0.0207	0.1764
138	3.813	24.145	-0.077	0.005	-0.0	1.0	0.1	27.698	27.505	1.0070	1.0068	0.0007	0.0203	0.1762
139	3.816	26.682	-0.077	0.004	-0.0	1.3	0.1	27.706	27.497	1.0076	1.0073	0.0001	0.0238	0.1768
140	3.814	29.216	-0.078	0.005	0.0	1.2	0.1	27.708	27.485	1.0081	1.0078	-0.0001	0.0242	0.1754
141	3.816	31.762	-0.082	0.004	-0.1	1.4	0.1	27.693	27.462	1.0084	1.0081	0.0009	0.0258	0.1744
142	3.815	34.290	-0.082	0.004	-0.0	1.4	0.1	27.697	27.453	1.0089	1.0085	0.0005	0.0273	0.1741
143	3.815	36.871	-0.081	0.003	0.0	1.5	0.1	27.724	27.464	1.0095	1.0091	-0.0006	0.0278	0.1725
144	3.815	39.396	-0.082	0.005	0.0	1.7	0.1	27.727	27.448	1.0102	1.0097	-0.0007	0.0316	0.1726
145	3.815	41.906	-0.084	0.004	0.0	1.8	0.1	27.723	27.435	1.0105	1.0100	-0.0006	0.0333	0.1712
146	3.815	44.459	-0.083	0.004	0.1	1.9	0.1	27.642	27.437	1.0075	1.0069	-0.0019	0.0347	0.1691
147	3.817	45.717	-0.084	0.005	0.1	1.8	0.1	27.349	27.438	0.9968	0.9962	-0.0013	0.0334	0.1677
148	3.815	47.013	-0.086	0.005	0.0	1.1	0.1	26.566	27.439	0.9682	0.9679	-0.0005	0.0218	0.1669
149	3.817	47.660	-0.088	0.002	-0.0	0.9	0.1	26.062	27.424	0.9503	0.9502	0.0001	0.0166	0.1653
150	3.815	48.251	-0.089	0.006	-0.0	0.3	0.2	25.486	27.410	0.9298	0.9298	0.0004	0.0076	0.1646

## STATION 14 (Continued)

POINT	Z	Y	CPITCH	CYAW	ALPHA	THETA	BETA	V	VCONT	VW	VX	VY	VZ	CP
151	3.816	48.895	-0.089	0.009	-0.0	-0.4	0.2	24.832	27.420	0.9056	0.9056	0.0006	-0.0028	0.1635
152	3.817	49.523	-0.091	0.003	-0.1	-1.0	0.1	24.120	27.417	0.8797	0.8796	0.0015	-0.0146	0.1626
153	3.813	49.527	-0.091	0.008	-0.1	-1.1	0.2	24.146	27.417	0.8807	0.8806	0.0012	-0.0145	0.1619
154	7.631	8.749	-0.052	0.004	0.4	1.7	0.1	26.786	27.258	0.9827	0.9822	-0.0067	0.0309	0.2108
155	7.622	11.268	-0.061	0.005	0.2	1.7	0.1	26.917	27.245	0.9880	0.9875	-0.0032	0.0319	0.2112
156	7.621	13.986	-0.067	0.006	0.1	1.5	0.1	26.921	27.253	0.9878	0.9874	-0.0011	0.0287	0.2101
157	7.621	16.527	-0.068	0.004	0.1	1.5	0.1	26.933	27.238	0.9888	0.9884	-0.0013	0.0278	0.2084
158	7.624	19.071	-0.068	0.004	0.1	1.6	0.1	26.929	27.248	0.9883	0.9878	-0.0020	0.0297	0.2098
159	7.624	21.580	-0.069	0.005	0.2	1.4	0.1	26.935	27.236	0.9889	0.9886	-0.0026	0.0268	0.2087
160	7.624	24.136	-0.073	0.003	0.1	1.5	0.1	26.951	27.245	0.9892	0.9888	-0.0013	0.0276	0.2085
161	7.624	26.682	-0.078	0.005	-0.0	1.6	0.1	26.953	27.231	0.9898	0.9894	0.0003	0.0292	0.2075
162	7.622	29.209	-0.081	0.002	-0.1	1.7	0.1	26.961	27.230	0.9901	0.9896	0.0012	0.0309	0.2074
163	7.622	31.749	-0.080	0.004	-0.0	1.8	0.1	26.972	27.196	0.9918	0.9912	0.0000	0.0333	0.2057
164	7.622	34.311	-0.083	0.005	-0.0	1.9	0.1	26.972	27.199	0.9916	0.9910	0.0008	0.0355	0.2055
165	7.625	36.852	-0.084	0.005	-0.0	2.0	0.1	26.978	27.199	0.9919	0.9912	0.0008	0.0365	0.2039
166	7.624	39.410	-0.090	0.003	-0.2	2.1	0.1	26.988	27.176	0.9931	0.9924	0.0035	0.0377	0.2036
167	7.623	41.901	-0.092	0.004	-0.2	2.2	0.1	27.009	27.166	0.9942	0.9934	0.0042	0.0407	0.2015
168	7.624	44.467	-0.094	0.004	-0.3	2.3	0.1	26.965	27.167	0.9925	0.9916	0.0047	0.0425	0.2005
169	7.605	45.719	-0.098	0.003	-0.4	2.2	0.1	27.014	27.138	0.9846	0.9838	0.0064	0.0389	0.1994
170	7.626	47.008	-0.100	0.005	-0.4	1.8	0.1	26.310	27.353	0.9619	0.9613	0.0073	0.0327	0.1962
171	7.621	47.602	-0.101	0.006	-0.5	1.7	0.2	25.970	27.424	0.9470	0.9465	0.0076	0.0302	0.1954
172	7.626	48.260	-0.100	0.006	-0.4	1.1	0.2	25.208	27.349	0.9217	0.9215	0.0067	0.0196	0.1946
173	7.625	48.888	-0.101	0.004	-0.4	0.6	0.1	24.508	27.359	0.8958	0.8957	0.0065	0.0107	0.1930
174	7.621	49.517	-0.100	0.005	-0.4	-0.4	0.1	23.663	27.343	0.8654	0.8654	0.0059	-0.0033	0.1924
175	10.165	8.805	-0.039	0.002	0.8	1.9	0.1	26.536	27.529	0.9639	0.9633	-0.0127	0.0323	0.2333
176	10.166	11.393	-0.056	0.004	0.3	1.7	0.1	26.699	27.521	0.9701	0.9697	-0.0057	0.0299	0.2326
177	10.164	13.966	-0.064	0.005	0.1	1.6	0.1	26.748	27.511	0.9723	0.9718	-0.0025	0.0299	0.2319
178	10.162	16.498	-0.067	0.006	0.1	1.8	0.2	26.758	27.513	0.9726	0.9720	-0.0017	0.0339	0.2313
179	10.164	19.029	-0.070	0.006	0.1	1.8	0.1	26.754	27.499	0.9729	0.9724	-0.0011	0.0325	0.2309
180	10.165	21.584	-0.069	0.005	0.1	1.8	0.1	26.850	27.589	0.9732	0.9727	-0.0024	0.0324	0.2310
181	10.161	24.130	-0.064	0.005	0.3	1.7	0.1	26.835	27.580	0.9730	0.9725	-0.0054	0.0307	0.2317
182	10.166	26.649	-0.078	0.006	-0.0	1.4	0.2	26.821	27.573	0.9727	0.9724	0.0006	0.0270	0.2308
183	10.166	29.221	-0.087	0.003	-0.3	2.1	0.1	26.844	27.562	0.9740	0.9733	0.0044	0.0367	0.2303
184	10.163	31.751	-0.086	0.006	-0.2	2.1	0.2	26.854	27.529	0.9755	0.9747	0.0034	0.0381	0.2289
185	10.162	34.237	-0.088	0.006	-0.2	2.2	0.1	26.855	27.531	0.9754	0.9746	0.0036	0.0399	0.2280
186	10.163	36.823	-0.090	0.004	-0.2	2.2	0.1	26.831	27.494	0.9759	0.9751	0.0042	0.0390	0.2259
187	10.163	39.368	-0.091	0.006	-0.2	2.4	0.2	26.855	27.479	0.9773	0.9763	0.0042	0.0428	0.2243
188	10.163	41.880	-0.098	0.006	-0.4	2.4	0.1	26.864	27.474	0.9778	0.9768	0.0076	0.0442	0.2231
189	10.164	44.435	-0.104	0.003	-0.6	2.4	0.1	26.825	27.451	0.9772	0.9762	0.0102	0.0420	0.2235
190	10.161	45.712	-0.109	0.005	-0.8	2.3	0.1	26.723	27.463	0.9730	0.9721	0.0129	0.0411	0.2213
191	10.163	46.991	-0.117	0.005	-1.0	2.2	0.1	26.284	27.451	0.9575	0.9566	0.0167	0.0389	0.2190
192	10.132	47.619	-0.120	0.006	-1.1	2.0	0.2	25.850	27.430	0.9424	0.9416	0.0177	0.0354	0.2158
193	10.161	48.262	-0.122	0.003	-1.1	1.9	0.1	25.280	27.440	0.9213	0.9206	0.0183	0.0311	0.2172
194	10.165	48.892	-0.123	0.005	-1.2	1.5	0.1	24.558	27.439	0.8950	0.8945	0.0184	0.0250	0.2150
195	10.164	49.560	-0.122	0.007	-1.1	0.7	0.2	23.588	27.433	0.8598	0.8596	0.0169	0.0134	0.2129
196	12.733	8.749	-0.030	0.004	1.0	1.9	0.1	24.900	27.521	0.9048	0.9041	-0.0160	0.0313	0.2490
197	12.706	11.247	-0.051	0.006	0.5	1.9	0.2	25.507	27.516	0.9270	0.9263	-0.0074	0.0339	0.2488
198	12.703	13.990	-0.063	0.004	0.2	1.9	0.1	26.106	27.505	0.9492	0.9485	-0.0032	0.0340	0.2509
199	12.705	16.554	-0.068	0.006	0.1	2.1	0.1	26.393	27.495	0.9599	0.9592	-0.0017	0.0375	0.2521
200	12.703	19.076	-0.069	0.005	0.1	2.1	0.1	26.436	27.490	0.9617	0.9609	-0.0017	0.0383	0.2521

STATION 14 (Concluded)

POINT	Z	Y	CPITCH	CYAW	ALPHA	THETA	BETA	V	VCONT	VW	VX	VY	VZ	CP
201	12.705	21.585	-0.067	0.005	0.2	2.0	0.1	26.447	27.489	0.9621	0.9614	-0.0032	0.0363	0.2525
202	12.705	24.125	-0.069	0.005	0.2	2.2	0.1	26.384	27.488	0.9598	0.9590	-0.0031	0.0365	0.2525
203	12.705	25.415	-0.073	0.006	0.1	1.5	0.2	26.079	27.478	0.9491	0.9487	-0.0017	0.0278	0.2510
204	12.699	26.027	-0.074	0.004	0.1	1.1	0.1	25.882	27.535	0.9400	0.9398	-0.0012	0.0194	0.2509
205	12.704	26.668	-0.077	0.003	-0.0	1.2	0.1	25.850	27.475	0.9408	0.9406	0.0001	0.0212	0.2513
206	12.700	27.299	-0.080	0.004	-0.1	1.4	0.1	25.965	27.524	0.9433	0.9430	0.0012	0.0243	0.2498
207	12.702	27.961	-0.083	0.004	-0.2	1.9	0.1	26.213	27.461	0.9546	0.9539	0.0027	0.0341	0.2502
208	12.701	29.199	-0.088	0.006	-0.3	2.3	0.2	26.451	27.465	0.9631	0.9621	0.0050	0.0420	0.2495
209	12.705	31.738	-0.091	0.006	-0.4	2.4	0.2	26.467	27.452	0.9641	0.9631	0.0061	0.0429	0.2492
210	12.704	34.301	-0.092	0.005	-0.4	2.4	0.1	26.468	27.446	0.9644	0.9634	0.0063	0.0423	0.2488
211	12.703	36.845	-0.099	0.005	-0.6	2.4	0.1	26.486	27.444	0.9651	0.9641	0.0095	0.0433	0.2479
212	12.701	39.389	-0.099	0.006	-0.5	2.5	0.1	26.497	27.420	0.9664	0.9653	0.0089	0.0452	0.2451
213	12.702	41.918	-0.100	0.006	-0.5	2.8	0.2	26.405	27.416	0.9631	0.9618	0.0087	0.0490	0.2441
214	12.701	44.465	-0.107	0.005	-0.7	2.5	0.1	25.716	27.409	0.9382	0.9371	0.0113	0.0441	0.2409
215	12.702	45.743	-0.118	0.006	-1.0	2.3	0.2	25.219	27.406	0.9202	0.9191	0.0168	0.0401	0.2387
216	12.699	47.006	-0.137	0.004	-1.7	2.2	0.1	24.807	27.398	0.9054	0.9043	0.0261	0.0371	0.2375
217	12.706	47.623	-0.144	0.008	-1.9	2.1	0.2	24.689	27.445	0.8996	0.8984	0.0293	0.0362	0.2346
218	12.701	48.257	-0.154	0.007	-2.1	2.2	0.2	24.355	27.396	0.8890	0.8876	0.0331	0.0365	0.2350
219	12.702	48.886	-0.159	0.005	-2.2	2.0	0.1	23.939	27.399	0.8737	0.8724	0.0342	0.0326	0.2353
220	12.700	49.516	-0.163	0.008	-2.4	1.7	0.2	23.340	27.394	0.8520	0.8508	0.0350	0.0278	0.2326
221	14.005	26.028	-0.076	0.006	0.0	1.3	0.2	24.219	27.521	0.8800	0.8797	-0.0004	0.0222	0.2585
222	13.973	26.669	-0.078	0.005	-0.0	1.1	0.1	24.303	27.538	0.8825	0.8823	0.0004	0.0183	0.2576
223	13.956	27.300	-0.081	0.007	-0.1	1.4	0.2	24.582	27.529	0.8930	0.8926	0.0017	0.0242	0.2566
224	15.238	8.753	-0.014	0.007	1.4	1.8	0.2	21.188	27.509	0.7702	0.7695	-0.0193	0.0266	0.2587
225	15.239	11.401	-0.035	0.009	0.9	2.2	0.3	21.946	27.518	0.7975	0.7966	-0.0126	0.0347	0.2602
226	15.242	13.955	-0.051	0.003	0.5	2.4	0.1	22.578	27.500	0.8210	0.8202	-0.0072	0.0361	0.2630
227	15.240	16.508	-0.057	0.009	0.4	2.9	0.2	23.946	27.493	0.8710	0.8697	-0.0058	0.0470	0.2642
228	15.242	19.054	-0.063	0.006	0.3	2.6	0.2	24.092	27.496	0.8762	0.8751	-0.0039	0.0429	0.2668
229	15.241	21.607	-0.071	0.005	0.1	2.8	0.1	24.364	27.483	0.8865	0.8854	-0.0014	0.0447	0.2671
230	15.239	24.127	-0.072	0.009	0.1	3.0	0.2	24.333	27.482	0.8854	0.8840	-0.0017	0.0503	0.2654
231	15.241	25.377	-0.074	0.007	0.1	2.0	0.2	22.882	27.479	0.8327	0.8321	-0.0010	0.0324	0.2645
232	15.244	26.012	-0.079	0.005	-0.1	1.3	0.1	22.154	27.540	0.8044	0.8042	0.0007	0.0208	0.2637
233	15.240	26.649	-0.080	0.007	-0.1	1.0	0.2	21.957	27.482	0.7990	0.7988	0.0011	0.0167	0.2638
234	15.243	27.221	-0.082	0.008	-0.1	1.2	0.2	22.159	27.541	0.8046	0.8044	0.0019	0.0192	0.2619
235	15.241	27.956	-0.084	0.009	-0.2	2.2	0.2	23.161	27.468	0.8432	0.8424	0.0026	0.0364	0.2616
236	15.240	29.211	-0.085	0.005	-0.2	3.0	0.1	24.403	27.470	0.8884	0.8870	0.0035	0.0487	0.2634
237	15.239	31.756	-0.090	0.006	-0.3	3.0	0.2	24.784	27.449	0.9029	0.9016	0.0053	0.0494	0.2644
238	15.242	34.254	-0.092	0.005	-0.4	2.8	0.1	24.228	27.453	0.8826	0.8814	0.0056	0.0455	0.2633
239	15.240	36.835	-0.104	0.005	-0.7	2.9	0.1	24.255	27.450	0.8836	0.8823	0.0109	0.0465	0.2622
240	15.239	39.382	-0.111	0.006	-0.9	3.3	0.2	24.549	27.427	0.8951	0.8934	0.0143	0.0536	0.2597
241	15.239	41.871	-0.118	0.007	-1.1	3.4	0.2	23.908	27.423	0.8718	0.8700	0.0169	0.0541	0.2566
242	15.242	44.443	-0.128	0.005	-1.4	3.1	0.1	22.423	27.416	0.8179	0.8163	0.0200	0.0461	0.2522
243	15.239	45.737	-0.137	0.009	-1.7	2.3	0.2	21.340	27.401	0.7788	0.7777	0.0228	0.0339	0.2494
244	15.240	46.994	-0.152	0.006	-2.1	1.4	0.2	20.553	27.402	0.7500	0.7493	0.0272	0.0206	0.2506
245	15.216	47.621	-0.163	0.003	-2.4	1.4	0.1	20.343	27.473	0.7405	0.7396	0.0307	0.0195	0.2489
246	15.239	48.268	-0.172	-0.000	-2.6	1.8	-0.0	20.461	27.401	0.7467	0.7456	0.0341	0.0235	0.2485
247	15.239	48.928	-0.182	0.007	-2.9	2.1	0.2	20.896	27.395	0.7627	0.7612	0.0381	0.0309	0.2471
248	15.174	49.519	-0.187	0.006	-3.0	2.5	0.2	21.125	27.389	0.7713	0.7694	0.0403	0.0358	0.2472

## STATION 20

POINT	Z	Y	CPITCH	CYAW	ALPHA	THETA	BETA	V	VCONT	W	VX	VY	VZ	CP
1	-17.786	8.815	-0.199	0.006	-4.0	-0.7	0.2	24.723	25.814	0.9577	0.9554	0.0665	-0.0094	0.0789
2	-17.787	11.393	-0.191	0.008	-3.7	-0.6	0.2	24.574	25.814	0.9520	0.9499	0.0617	-0.0067	0.0778
3	-17.786	13.955	-0.168	0.004	-3.0	-0.5	0.1	25.334	25.770	0.9831	0.9817	0.0521	-0.0072	0.0784
4	-17.787	16.505	-0.143	0.006	-2.3	-0.4	0.2	26.376	25.782	1.0231	1.0222	0.0416	-0.0044	0.0798
5	-17.787	19.015	-0.125	0.004	-1.7	-0.4	0.1	27.165	25.766	1.0543	1.0538	0.0312	-0.0049	0.0807
6	-17.785	21.587	-0.110	0.006	-1.2	-0.8	0.2	27.571	25.813	1.0681	1.0678	0.0216	-0.0119	0.0813
7	-17.786	22.860	-0.102	0.003	-0.9	-0.8	0.1	27.695	25.609	1.0815	1.0813	0.0166	-0.0137	0.0803
8	-17.785	24.123	-0.096	0.007	-0.7	-0.8	0.2	27.902	25.845	1.0796	1.0795	0.0123	-0.0111	0.0798
9	-17.783	24.127	-0.095	0.006	-0.6	-0.7	0.2	27.791	25.552	1.0876	1.0875	0.0115	-0.0107	0.0801
10	-17.783	25.390	-0.091	0.001	-0.5	-0.7	0.0	27.859	25.881	1.0764	1.0763	0.0086	-0.0135	0.0798
11	-17.782	25.399	-0.088	0.006	-0.4	-0.7	0.2	27.711	25.488	1.0872	1.0871	0.0072	-0.0107	0.0798
12	-17.784	26.025	-0.088	0.002	-0.3	-0.8	0.1	27.780	25.869	1.0739	1.0737	0.0064	-0.0148	0.0771
13	-17.783	26.640	-0.082	0.006	-0.1	-0.9	0.2	27.584	25.525	1.0807	1.0806	0.0027	-0.0144	0.0781
14	-17.783	26.641	-0.084	0.006	-0.2	-0.9	0.2	27.658	25.790	1.0724	1.0723	0.0037	-0.0144	0.0784
15	-17.775	27.307	-0.078	0.004	-0.0	-1.0	0.1	27.537	25.850	1.0653	1.0651	0.0004	-0.0174	0.0760
16	-17.781	27.943	-0.073	0.005	0.1	-1.1	0.1	27.378	25.532	1.0723	1.0722	-0.0027	-0.0187	0.0781
17	-17.784	29.193	-0.064	0.004	0.4	-1.1	0.1	27.341	25.752	1.0617	1.0615	-0.0075	-0.0192	0.0777
18	-17.779	29.209	-0.062	0.004	0.4	-1.1	0.1	27.317	25.522	1.0703	1.0701	-0.0083	-0.0194	0.0779
19	-17.775	30.502	-0.059	0.004	0.6	-1.0	0.1	27.224	25.471	1.0688	1.0686	-0.0104	-0.0174	0.0777
20	-17.786	31.740	-0.047	0.004	0.9	-0.6	0.1	27.299	25.702	1.0622	1.0620	-0.0166	-0.0094	0.0775
21	-17.777	31.847	-0.063	0.004	0.5	-0.5	0.1	27.260	25.492	1.0693	1.0693	-0.0087	-0.0073	0.0795
22	-17.785	32.993	-0.039	0.004	1.1	-0.5	0.1	27.197	25.661	1.0599	1.0597	-0.0210	-0.0069	0.0775
23	-17.786	34.244	-0.032	0.004	1.3	-0.7	0.1	27.244	25.818	1.0552	1.0549	-0.0247	-0.0117	0.0758
24	-17.786	34.286	-0.032	0.005	1.3	-0.7	0.1	27.052	25.682	1.0534	1.0530	-0.0247	-0.0108	0.0768
25	-17.784	35.596	-0.026	0.005	1.5	-0.5	0.1	26.833	25.684	1.0447	1.0443	-0.0279	-0.0070	0.0771
26	-17.782	36.815	-0.019	0.005	1.7	-0.0	0.1	26.750	25.799	1.0369	1.0364	-0.0314	-0.0019	0.0746
27	-17.783	39.340	0.006	0.004	2.5	0.1	0.1	25.989	25.759	1.0089	1.0080	-0.0432	0.0036	0.0715
28	-17.780	41.875	0.033	0.006	3.2	-0.3	0.2	25.016	25.826	0.9686	0.9671	-0.0547	-0.0023	0.0693
29	-17.781	43.174	0.044	0.006	3.5	-0.3	0.2	24.772	25.797	0.9602	0.9584	-0.0592	-0.0024	0.0684
30	-17.785	44.426	0.048	0.003	3.7	-0.2	0.1	24.887	25.784	0.9652	0.9632	-0.0616	-0.0029	0.0670
31	-17.787	45.710	0.048	0.006	3.7	-0.6	0.2	25.008	25.831	0.9681	0.9661	-0.0619	-0.0073	0.0639
32	-17.783	46.369	0.047	0.006	3.7	-0.8	0.2	24.767	25.773	0.9610	0.9589	-0.0614	-0.0114	0.0652
33	-17.784	46.986	0.046	0.005	3.6	-1.1	0.1	24.521	25.833	0.9492	0.9472	-0.0603	-0.0165	0.0637
34	-17.785	47.634	0.044	0.006	3.6	-1.7	0.2	24.141	25.811	0.9353	0.9331	-0.0586	-0.0244	0.0631
35	-17.783	48.263	0.042	0.004	3.6	-2.3	0.1	23.743	25.755	0.9219	0.9194	-0.0573	-0.0347	0.0633
36	-17.782	48.911	0.035	0.002	3.4	-3.1	0.1	23.367	25.760	0.9071	0.9042	-0.0538	-0.0484	0.0626
37	-17.779	49.536	0.027	0.005	3.2	-4.4	0.1	23.050	25.759	0.8948	0.8909	-0.0500	-0.0669	0.0638
38	-16.526	8.796	-0.166	0.003	-3.1	-0.4	0.1	25.929	25.695	1.0091	1.0076	0.0541	-0.0055	0.0888
39	-16.517	11.315	-0.154	0.006	-2.7	-0.3	0.2	26.256	25.707	1.0214	1.0202	0.0480	-0.0022	0.0881
40	-16.514	13.888	-0.132	0.005	-2.0	0.0	0.1	27.131	25.565	1.0612	1.0606	0.0375	0.0024	0.0892
41	-16.516	16.533	-0.115	0.004	-1.4	0.2	0.1	28.219	25.643	1.1005	1.1001	0.0273	0.0054	0.0918
42	-16.517	19.066	-0.107	0.004	-1.1	0.1	0.1	28.791	25.663	1.1219	1.1217	0.0214	0.0047	0.0928
43	-16.517	21.596	-0.096	0.004	-0.7	-0.3	0.1	29.004	25.684	1.1293	1.1292	0.0136	-0.0041	0.0936
44	-16.520	22.872	-0.091	0.003	-0.5	-0.3	0.1	28.936	25.538	1.1330	1.1330	0.0100	-0.0046	0.0923
45	-16.518	24.159	-0.086	0.004	-0.3	-0.4	0.1	28.978	25.510	1.1360	1.1359	0.0065	-0.0058	0.0926
46	-16.519	25.399	-0.087	0.004	-0.3	-0.3	0.1	28.958	25.500	1.1356	1.1356	0.0067	-0.0047	0.0929
47	-16.533	26.024	-0.090	0.003	-0.4	-0.4	0.1	29.062	25.860	1.1238	1.1237	0.0080	-0.0068	0.0880
48	-16.520	26.675	-0.085	0.003	-0.3	-0.4	0.1	28.922	25.613	1.1292	1.1292	0.0049	-0.0069	0.0910
49	-16.478	27.309	-0.082	0.004	-0.1	-0.5	0.1	28.954	25.852	1.1200	1.1200	0.0029	-0.0086	0.0889
50	-16.520	27.972	-0.075	0.005	0.1	-0.6	0.1	28.829	25.708	1.1214	1.1214	-0.0016	-0.0089	0.0905

STATION 20 (Continued)

POINT	Z	Y	CPITCH	CYAW	ALPHA	THETA	BETA	V	VCONT	VW	VX	VY	VZ	CP
51	-16.523	29.199	-0.065	0.003	0.4	-0.6	0.1	28.763	25.682	1.1200	1.1199	-0.0073	-0.0110	0.0898
52	-16.522	30.464	-0.054	0.003	0.7	-0.6	0.1	28.769	25.725	1.1183	1.1182	-0.0135	-0.0094	0.0889
53	-16.523	31.758	-0.045	0.003	0.9	-0.1	0.1	28.822	25.692	1.1219	1.1217	-0.0185	-0.0009	0.0896
54	-16.522	33.007	-0.046	0.003	0.9	-0.0	0.1	28.840	25.673	1.1234	1.1232	-0.0185	0.0009	0.0888
55	-16.526	34.282	-0.042	0.003	1.1	-0.2	0.1	28.730	25.687	1.1185	1.1183	-0.0212	-0.0025	0.0893
56	-16.525	35.592	-0.035	0.003	1.3	-0.0	0.1	28.517	25.644	1.1121	1.1118	-0.0252	0.0017	0.0878
57	-16.525	36.830	-0.029	0.004	1.5	0.5	0.1	28.363	25.678	1.1046	1.1041	-0.0283	0.0117	0.0865
58	-16.527	39.400	-0.018	0.004	1.8	0.7	0.1	27.639	25.632	1.0783	1.0777	-0.0339	0.0145	0.0832
59	-16.526	41.909	0.001	0.004	2.4	0.2	0.1	26.527	25.646	1.0343	1.0334	-0.0427	0.0063	0.0783
60	-16.528	43.191	0.010	0.004	2.6	0.1	0.1	26.182	25.714	1.0182	1.0171	-0.0466	0.0035	0.0770
61	-16.527	44.470	0.016	0.006	2.8	-0.0	0.2	26.097	25.733	1.0141	1.0129	-0.0500	0.0029	0.0745
62	-16.530	45.712	0.018	0.006	2.9	-0.3	0.2	25.916	25.719	1.0077	1.0064	-0.0510	-0.0021	0.0745
63	-16.530	47.009	0.016	0.006	2.9	-0.9	0.2	25.250	25.659	0.9841	0.9827	-0.0492	-0.0124	0.0733
64	-16.532	47.636	0.012	0.010	2.8	-1.6	0.3	24.837	25.620	0.9694	0.9681	-0.0467	-0.0223	0.0722
65	-16.532	48.250	0.007	0.003	2.6	-2.4	0.1	24.618	25.681	0.9586	0.9568	-0.0439	-0.0385	0.0710
66	-16.536	48.879	0.003	0.004	2.5	-3.2	0.1	24.227	25.663	0.9440	0.9417	-0.0415	-0.0512	0.0712
67	-16.533	49.527	-0.005	0.004	2.3	-4.6	0.1	23.807	25.612	0.9295	0.9258	-0.0379	-0.0733	0.0723
68	-15.243	8.802	-0.134	0.004	-2.1	0.0	0.1	26.987	25.659	1.0518	1.0510	0.0394	0.0018	0.1011
69	-15.244	11.324	-0.121	0.003	-1.7	0.4	0.1	27.736	25.705	1.0790	1.0785	0.0319	0.0097	0.1002
70	-15.240	13.893	-0.106	0.005	-1.2	0.6	0.1	28.560	25.709	1.1109	1.1106	0.0223	0.0150	0.1027
71	-15.241	16.457	-0.099	0.004	-0.9	0.6	0.1	29.001	25.710	1.1280	1.1278	0.0175	0.0147	0.1049
72	-15.241	19.047	-0.103	0.004	-1.0	0.7	0.1	29.058	25.699	1.1307	1.1304	0.0193	0.0160	0.1062
73	-15.243	21.603	-0.090	0.003	-0.5	0.4	0.1	29.055	25.678	1.1315	1.1314	0.0095	0.0102	0.1056
74	-15.241	24.166	-0.086	0.003	-0.3	0.0	0.1	29.050	25.680	1.1313	1.1312	0.0060	0.0019	0.1047
75	-15.238	26.023	-0.084	0.004	-0.2	-0.0	0.1	29.274	25.891	1.1307	1.1306	0.0047	0.0021	0.1001
76	-15.244	26.715	-0.081	0.004	-0.1	0.1	0.1	29.032	25.668	1.1311	1.1311	0.0021	0.0037	0.1045
77	-15.224	27.309	-0.080	0.005	-0.1	-0.1	0.1	29.198	25.850	1.1295	1.1295	0.0016	0.0016	0.1017
78	-15.241	27.944	-0.078	0.003	-0.0	0.0	0.1	29.179	25.844	1.1290	1.1290	0.0001	0.0018	0.1006
79	-15.242	29.262	-0.068	0.005	0.3	0.0	0.1	28.995	25.655	1.1302	1.1302	-0.0058	0.0028	0.1031
80	-15.245	31.775	-0.052	0.005	0.8	0.3	0.1	29.000	25.648	1.1307	1.1306	-0.0149	0.0092	0.1032
81	-15.243	34.285	-0.046	0.004	1.0	0.4	0.1	29.063	25.669	1.1322	1.1320	-0.0193	0.0104	0.1023
82	-15.243	36.869	-0.037	0.004	1.2	0.9	0.1	29.024	25.666	1.1308	1.1304	-0.0246	0.0207	0.1004
83	-15.242	39.394	-0.040	0.004	1.2	1.3	0.1	28.774	25.696	1.1198	1.1192	-0.0237	0.0275	0.0966
84	-15.242	41.906	-0.033	0.004	1.4	0.8	0.1	28.022	25.716	1.0896	1.0892	-0.0275	0.0178	0.0917
85	-15.243	43.154	-0.025	0.006	1.7	0.7	0.2	27.617	25.762	1.0720	1.0714	-0.0317	0.0163	0.0894
86	-15.243	44.463	-0.018	0.005	1.9	0.5	0.1	27.244	25.715	1.0595	1.0588	-0.0350	0.0113	0.0872
87	-15.243	45.712	-0.014	0.005	2.0	0.2	0.1	26.943	25.829	1.0431	1.0425	-0.0367	0.0061	0.0866
88	-15.243	47.016	-0.015	0.006	2.0	-0.8	0.2	26.180	25.733	1.0174	1.0167	-0.0357	-0.0109	0.0854
89	-15.242	47.634	-0.018	0.002	1.9	-1.4	0.1	25.859	25.789	1.0027	1.0019	-0.0340	-0.0237	0.0840
90	-15.244	48.260	-0.021	0.011	1.9	-2.2	0.3	25.518	25.823	0.9882	0.9871	-0.0321	-0.0338	0.0841
91	-15.240	48.910	-0.025	0.009	1.8	-3.3	0.2	25.022	25.770	0.9710	0.9692	-0.0299	-0.0512	0.0839
92	-15.244	49.519	-0.032	0.005	1.6	-4.7	0.1	24.568	25.737	0.9546	0.9512	-0.0264	-0.0758	0.0836
93	-13.974	26.024	-0.082	0.004	-0.1	0.3	0.1	29.102	25.898	1.1237	1.1237	0.0028	0.0079	0.1126
94	-13.975	26.670	-0.078	0.004	-0.0	0.4	0.1	29.151	25.943	1.1236	1.1236	0.0003	0.0098	0.1117
95	-13.969	27.309	-0.074	0.004	0.1	0.4	0.1	29.055	25.851	1.1239	1.1239	-0.0020	0.0102	0.1114
96	-13.980	27.944	-0.071	0.003	0.2	0.4	0.1	29.037	25.842	1.1236	1.1236	-0.0035	0.0099	0.1125
97	-12.708	8.826	-0.098	0.004	-0.9	0.7	0.1	28.384	25.796	1.1003	1.1001	0.0182	0.0154	0.1217
98	-12.710	11.378	-0.094	0.003	-0.8	1.1	0.1	28.846	25.785	1.1187	1.1184	0.0154	0.0233	0.1240
99	-12.708	13.967	-0.092	0.004	-0.7	1.1	0.1	28.894	25.759	1.1217	1.1214	0.0131	0.0238	0.1259
100	-12.707	16.496	-0.095	0.004	-0.7	1.0	0.1	28.927	25.791	1.1216	1.1213	0.0146	0.0217	0.1262

## STATION 20 (Continued)

POINT	Z	Y	CPITCH	CYAW	ALPHA	THETA	BETA	V	VCONT	WV	VX	VY	VZ	CP
101	-12.707	19.025	-0.089	0.005	-0.5	0.9	0.1	28.948	25.811	1.1215	1.1213	0.0095	0.0200	0.1256
102	-12.708	21.582	-0.087	0.005	-0.4	0.8	0.1	28.870	25.752	1.1211	1.1209	0.0075	0.0174	0.1268
103	-12.706	24.127	-0.080	0.004	-0.1	0.5	0.1	28.905	25.775	1.1215	1.1214	0.0024	0.0116	0.1258
104	-12.707	26.627	-0.074	0.004	0.1	0.6	0.1	28.877	25.741	1.1218	1.1217	-0.0018	0.0148	0.1256
105	-12.708	29.207	-0.068	0.004	0.3	0.7	0.1	28.858	25.718	1.1221	1.1219	-0.0059	0.0155	0.1254
106	-12.706	31.745	-0.064	0.004	0.4	0.7	0.1	28.841	25.696	1.1224	1.1222	-0.0085	0.0164	0.1257
107	-12.705	34.243	-0.060	0.004	0.6	1.0	0.1	28.890	25.715	1.1235	1.1232	-0.0114	0.0225	0.1243
108	-12.704	36.830	-0.058	0.004	0.7	1.2	0.1	28.954	25.736	1.1250	1.1247	-0.0136	0.0261	0.1206
109	-12.703	39.378	-0.060	0.003	0.7	1.5	0.1	28.966	25.725	1.1260	1.1255	-0.0131	0.0315	0.1200
110	-12.704	41.871	-0.064	0.002	0.6	1.7	0.0	28.880	25.661	1.1254	1.1249	-0.0115	0.0335	0.1157
111	-12.704	43.169	-0.061	0.003	0.7	1.6	0.1	28.798	25.685	1.1212	1.1206	-0.0138	0.0338	0.1146
112	-12.702	44.438	-0.054	0.005	0.9	1.4	0.1	28.432	25.606	1.1103	1.1098	-0.0174	0.0305	0.1124
113	-12.700	45.722	-0.051	0.002	1.0	0.9	0.1	27.867	25.584	1.0893	1.0889	-0.0193	0.0186	0.1109
114	-12.703	46.980	-0.052	0.005	1.0	-0.2	0.1	27.155	25.583	1.0614	1.0613	-0.0188	-0.0011	0.1076
115	-12.703	47.648	-0.051	0.003	1.0	-1.0	0.1	26.654	25.577	1.0421	1.0418	-0.0187	-0.0157	0.1073
116	-12.702	48.275	-0.054	0.008	1.0	-2.0	0.2	26.270	25.650	1.0242	1.0235	-0.0173	-0.0320	0.1062
117	-12.702	48.906	-0.056	0.002	0.9	-3.1	0.1	25.742	25.703	1.0015	0.9999	-0.0159	-0.0538	0.1055
118	-12.686	49.532	-0.058	0.005	0.9	-4.7	0.1	25.084	25.673	0.9770	0.9738	-0.0149	-0.0784	0.1060
119	-10.174	8.826	-0.085	0.005	-0.5	1.2	0.1	28.163	25.704	1.0957	1.0953	0.0102	0.0256	0.1454
120	-10.156	11.338	-0.088	0.004	-0.6	1.5	0.1	28.532	25.752	1.1079	1.1075	0.0113	0.0306	0.1466
121	-10.158	14.001	-0.087	0.005	-0.5	1.5	0.1	28.583	25.820	1.1070	1.1065	0.0101	0.0311	0.1494
122	-10.160	16.536	-0.087	0.004	-0.5	1.4	0.1	28.520	25.774	1.1065	1.1061	0.0092	0.0298	0.1489
123	-10.156	19.069	-0.084	0.003	-0.3	1.3	0.1	28.507	25.766	1.1064	1.1060	0.0063	0.0272	0.1494
124	-10.159	21.601	-0.081	0.004	-0.2	1.0	0.1	28.536	25.776	1.1070	1.1068	0.0035	0.0222	0.1486
125	-10.159	24.146	-0.078	0.004	-0.1	1.0	0.1	28.545	25.785	1.1071	1.1068	0.0014	0.0220	0.1486
126	-10.157	26.678	-0.076	0.005	0.0	1.1	0.1	28.492	25.757	1.1062	1.1059	-0.0007	0.0243	0.1493
127	-10.160	29.247	-0.071	0.003	0.2	1.1	0.1	28.506	25.769	1.1062	1.1060	-0.0040	0.0222	0.1475
128	-10.156	31.758	-0.068	0.004	0.3	1.3	0.1	28.495	25.744	1.1069	1.1065	-0.0064	0.0268	0.1480
129	-10.158	34.304	-0.068	0.004	0.4	1.6	0.1	28.475	25.702	1.1079	1.1074	-0.0073	0.0338	0.1454
130	-10.162	36.852	-0.066	0.003	0.5	1.7	0.1	28.516	25.721	1.1087	1.1081	-0.0090	0.0352	0.1445
131	-10.160	39.406	-0.067	0.002	0.5	1.8	0.1	28.563	25.709	1.1110	1.1104	-0.0093	0.0365	0.1419
132	-10.164	41.918	-0.066	0.004	0.5	2.0	0.1	28.610	25.720	1.1124	1.1115	-0.0104	0.0416	0.1384
133	-10.163	44.476	-0.067	0.004	0.5	2.0	0.1	28.504	25.736	1.1075	1.1068	-0.0106	0.0397	0.1357
134	-10.165	45.717	-0.068	0.005	0.5	1.4	0.1	28.122	25.725	1.0932	1.0927	-0.0103	0.0298	0.1334
135	-10.162	47.016	-0.069	0.003	0.5	0.3	0.1	27.383	25.733	1.0641	1.0640	-0.0099	0.0066	0.1323
136	-10.163	47.628	-0.069	0.008	0.5	-0.7	0.2	26.916	25.730	1.0461	1.0460	-0.0099	-0.0083	0.1309
137	-10.163	48.253	-0.070	0.003	0.5	-1.6	0.1	26.430	25.718	1.0277	1.0273	-0.0093	-0.0270	0.1291
138	-10.166	48.880	-0.072	0.005	0.5	-2.7	0.1	25.790	25.737	1.0021	1.0010	-0.0086	-0.0454	0.1301
139	-10.164	49.535	-0.076	0.006	0.4	-4.2	0.2	25.139	25.752	0.9762	0.9738	-0.0068	-0.0686	0.1277
140	-7.624	8.806	-0.078	0.003	-0.3	1.6	0.1	27.672	25.683	1.0775	1.0770	0.0058	0.0326	0.1693
141	-7.622	11.368	-0.081	0.006	-0.4	1.9	0.2	28.025	25.759	1.0880	1.0872	0.0070	0.0399	0.1701
142	-7.622	13.956	-0.077	0.006	-0.2	1.8	0.1	28.016	25.732	1.0888	1.0881	0.0038	0.0377	0.1711
143	-7.624	16.505	-0.076	0.004	-0.1	1.7	0.1	28.017	25.760	1.0876	1.0871	0.0024	0.0349	0.1694
144	-7.625	19.020	-0.077	0.006	-0.1	1.6	0.2	27.796	25.549	1.0880	1.0874	0.0023	0.0339	0.1703
145	-7.627	21.590	-0.078	0.006	-0.1	1.6	0.2	27.956	25.703	1.0877	1.0871	0.0020	0.0336	0.1695
146	-7.627	24.086	-0.077	0.007	-0.0	1.6	0.2	27.948	25.689	1.0879	1.0874	0.0006	0.0334	0.1686
147	-7.628	26.632	-0.074	0.006	0.1	1.4	0.2	27.996	25.714	1.0887	1.0883	-0.0015	0.0308	0.1685
148	-7.626	29.204	-0.076	0.005	0.1	1.6	0.1	27.953	25.673	1.0888	1.0883	-0.0012	0.0325	0.1692
149	-7.625	31.749	-0.074	0.005	0.2	1.7	0.1	27.953	25.658	1.0895	1.0889	-0.0031	0.0344	0.1684
150	-7.627	34.251	-0.075	0.004	0.2	2.0	0.1	28.057	25.754	1.0894	1.0887	-0.0033	0.0397	0.1678









## STATION 20 (Concluded)

POINT	Z	Y	CPITCH	CYAW	ALPHA	THETA	BETA	V	VCONT	VV	VX	VY	VZ	CP
301	17.783	11.335	0.033	0.014	2.8	2.2	0.4	18.011	25.741	0.6997	0.6982	-0.0337	0.0310	0.3472
302	17.781	13.981	0.020	0.007	2.5	3.4	0.2	19.454	25.799	0.7541	0.7519	-0.0323	0.0473	0.3512
303	17.782	16.543	-0.001	0.006	1.9	4.0	0.2	20.475	25.760	0.7948	0.7922	-0.0265	0.0583	0.3535
304	17.783	19.065	-0.032	0.012	1.1	3.6	0.3	20.444	25.809	0.7921	0.7901	-0.0154	0.0547	0.3549
305	17.780	21.610	-0.058	0.005	0.4	3.9	0.1	20.718	25.764	0.8041	0.8021	-0.0060	0.0569	0.3559
306	17.781	24.144	-0.086	0.011	-0.3	4.0	0.3	20.457	25.790	0.7932	0.7909	0.0043	0.0599	0.3548
307	17.782	25.417	-0.094	0.008	-0.6	1.9	0.2	18.561	25.857	0.7178	0.7173	0.0070	0.0260	0.3532
308	17.800	26.008	-0.091	0.017	-0.4	0.2	0.5	17.846	25.908	0.6888	0.6888	0.0054	0.0080	0.3518
309	17.783	26.690	-0.079	0.019	-0.0	-0.6	0.5	17.404	25.844	0.6735	0.6734	0.0006	-0.0013	0.3520
310	17.799	27.299	-0.072	0.007	0.2	-0.1	0.2	17.742	25.899	0.6850	0.6850	-0.0019	0.0010	0.3508
311	17.784	27.967	-0.065	0.007	0.3	1.4	0.2	18.381	25.864	0.7107	0.7104	-0.0042	0.0191	0.3518
312	17.780	29.203	-0.070	0.011	0.2	3.6	0.3	20.234	25.814	0.7838	0.7820	-0.0032	0.0538	0.3515
313	17.781	31.751	-0.097	0.013	-0.6	4.5	0.3	21.459	25.815	0.8313	0.8283	0.0081	0.0696	0.3555
314	17.779	34.300	-0.116	0.011	-1.2	3.9	0.3	20.557	25.827	0.7960	0.7936	0.0163	0.0590	0.3545
315	17.779	36.878	-0.137	0.013	-1.8	3.3	0.3	20.050	25.828	0.7763	0.7743	0.0245	0.0498	0.3519
316	17.780	39.396	-0.161	0.014	-2.4	4.3	0.4	20.926	25.894	0.8081	0.8047	0.0345	0.0660	0.3498
317	17.780	41.908	-0.188	0.009	-3.2	4.8	0.2	21.034	25.900	0.8121	0.8078	0.0447	0.0712	0.3486
318	17.780	44.485	-0.218	0.010	-3.9	4.5	0.3	19.835	25.894	0.7660	0.7616	0.0525	0.0633	0.3423
319	17.781	45.709	-0.230	0.016	-4.2	3.3	0.5	18.709	25.881	0.7229	0.7193	0.0534	0.0475	0.3411
320	17.781	47.004	-0.227	0.011	-4.1	1.4	0.3	17.177	25.891	0.6634	0.6614	0.0478	0.0203	0.3403
321	17.782	47.650	-0.225	0.016	-4.1	-0.1	0.4	16.423	25.890	0.6344	0.6327	0.0450	0.0038	0.3400
322	17.781	48.241	-0.216	0.021	-3.8	-1.2	0.6	15.790	25.880	0.6101	0.6087	0.0407	-0.0062	0.3395
323	17.782	48.870	-0.208	0.016	-3.6	-1.9	0.4	15.347	25.888	0.5928	0.5915	0.0371	-0.0149	0.3403
324	17.782	49.556	-0.186	0.009	-3.0	-1.7	0.3	15.224	25.884	0.5882	0.5872	0.0305	-0.0145	0.3399















STATION 28 (Concluded)

POINT	Z	Y	CPITCH	CYAW	ALPHA	THETA	BETA	V	VCONT	VV	VX	VY	VZ	CP
301	19.785	27.936	-0.053	0.006	0.7	0.8	0.2	18.601	23.333	0.7972	0.7970	-0.0094	0.0129	0.3755
302	19.816	29.236	-0.047	0.012	0.9	3.6	0.3	19.913	23.214	0.8578	0.8557	-0.0128	0.0587	0.3754
303	19.815	31.750	-0.073	0.009	0.2	6.1	0.2	21.846	23.242	0.9399	0.9343	-0.0032	0.1029	0.3801
304	19.816	34.303	-0.106	0.004	-0.8	5.6	0.1	21.433	23.234	0.9225	0.9178	0.0132	0.0924	0.3812
305	19.817	36.887	-0.134	0.014	-1.7	4.4	0.4	20.463	23.236	0.8807	0.8772	0.0262	0.0732	0.3804
306	19.816	39.395	-0.166	0.010	-2.6	4.6	0.3	20.442	23.257	0.8790	0.8749	0.0399	0.0749	0.3795
307	19.816	41.925	-0.204	0.014	-3.6	5.9	0.4	21.267	23.304	0.9126	0.9054	0.0569	0.0992	0.3777
308	19.816	44.503	-0.248	0.005	-4.8	6.6	0.1	21.367	23.287	0.9175	0.9080	0.0761	0.1076	0.3736
309	19.815	45.721	-0.271	0.005	-6.9	6.2	0.1	20.767	23.256	0.8930	0.8811	0.1080	0.0975	0.3750
310	19.817	47.019	-0.283	0.005	-7.3	5.1	0.2	19.875	23.240	0.8552	0.8447	0.1082	0.0781	0.3723
311	19.815	48.272	-0.276	0.005	-7.1	3.2	0.1	18.804	23.266	0.8082	0.8008	0.0992	0.0461	0.3705
312	19.817	49.551	-0.254	0.010	-5.2	0.6	0.3	17.641	23.300	0.7571	0.7539	0.0685	0.0111	0.3676













STATION 38 (Continued)

POINT	Z	Y	CPITCH	CYAW	ALPHA	THETA	BETA	V	VCONT	VV	VX	VY	VZ	CP
251	-0.000	21.591	-0.044	0.005	0.8	3.0	0.1	25.751	22.895	1.1248	1.1230	-0.0164	0.0607	0.2900
252	0.001	24.135	-0.056	0.006	0.5	3.0	0.2	25.769	22.890	1.1258	1.1240	-0.0102	0.0632	0.2890
253	0.000	26.685	-0.069	0.005	0.2	3.2	0.1	25.775	22.891	1.1260	1.1241	-0.0041	0.0649	0.2893
254	-0.000	29.211	-0.088	0.005	-0.3	3.3	0.1	25.792	22.897	1.1264	1.1244	0.0058	0.0669	0.2886
255	-0.002	31.777	-0.101	0.006	-0.7	3.3	0.2	25.796	22.883	1.1273	1.1252	0.0135	0.0674	0.2874
256	-0.001	34.296	-0.113	0.005	-1.1	3.3	0.1	25.815	22.888	1.1279	1.1256	0.0210	0.0681	0.2865
257	-0.001	36.861	-0.124	0.005	-1.4	3.3	0.1	25.846	22.891	1.1291	1.1268	0.0273	0.0667	0.2854
258	-0.001	39.394	-0.132	0.006	-1.6	3.2	0.2	25.863	22.886	1.1301	1.1277	0.0320	0.0653	0.2837
259	-0.002	41.909	-0.139	0.007	-1.8	2.9	0.2	25.894	22.885	1.1315	1.1292	0.0355	0.0615	0.2826
260	-0.002	44.461	-0.144	0.005	-1.9	2.6	0.1	25.860	22.884	1.1301	1.1281	0.0374	0.0546	0.2817
261	-0.003	45.736	-0.146	0.005	-2.0	2.2	0.1	25.697	22.889	1.1227	1.1210	0.0383	0.0464	0.2802
262	-0.002	47.000	-0.146	0.006	-1.9	1.0	0.2	25.233	22.879	1.1029	1.1020	0.0370	0.0221	0.2788
263	-0.004	48.258	-0.144	0.004	-1.8	-1.2	0.1	24.583	22.888	1.0741	1.0733	0.0345	-0.0206	0.2775
264	-0.005	49.536	-0.138	0.006	-1.6	-4.2	0.2	23.968	22.886	1.0473	1.0443	0.0301	-0.0731	0.2761
265	3.874	8.772	0.006	0.007	2.0	1.3	0.2	25.448	22.988	1.1070	1.1060	-0.0386	0.0279	0.2941
266	3.816	11.338	-0.007	0.009	1.7	1.6	0.2	25.557	22.988	1.1118	1.1107	-0.0322	0.0364	0.2910
267	3.813	13.979	-0.016	0.006	1.5	2.0	0.2	25.564	22.989	1.1120	1.1108	-0.0283	0.0430	0.2920
268	3.812	16.545	-0.030	0.007	1.1	2.1	0.2	25.572	22.997	1.1120	1.1109	-0.0220	0.0453	0.2913
269	3.812	19.077	-0.036	0.006	1.0	2.3	0.2	25.579	22.993	1.1125	1.1112	-0.0196	0.0489	0.2896
270	3.813	21.589	-0.046	0.008	0.8	2.5	0.2	25.591	23.003	1.1125	1.1112	-0.0147	0.0519	0.2915
271	3.815	24.129	-0.058	0.008	0.5	2.7	0.2	25.593	22.996	1.1130	1.1115	-0.0092	0.0562	0.2910
272	3.813	26.670	-0.072	0.009	0.1	2.8	0.2	25.614	23.006	1.1134	1.1118	-0.0027	0.0594	0.2899
273	3.806	29.111	-0.084	0.007	-0.2	2.8	0.2	25.788	23.127	1.1150	1.1135	0.0032	0.0589	0.2904
274	3.811	29.189	-0.083	0.007	-0.2	2.8	0.2	25.788	23.121	1.1153	1.1138	0.0030	0.0587	0.2906
275	3.809	29.203	-0.083	0.009	-0.1	2.9	0.2	25.646	23.002	1.1149	1.1133	0.0026	0.0604	0.2896
276	3.814	31.744	-0.094	0.007	-0.5	3.0	0.2	25.639	23.003	1.1146	1.1129	0.0069	0.0615	0.2906
277	3.811	34.271	-0.107	0.007	-0.9	3.0	0.2	25.655	23.002	1.1153	1.1135	0.0168	0.0611	0.2886
278	3.811	36.833	-0.119	0.009	-1.2	3.0	0.2	25.697	23.002	1.1172	1.1152	0.0237	0.0628	0.2867
279	3.811	39.395	-0.126	0.008	-1.4	2.9	0.2	25.704	22.999	1.1176	1.1156	0.0273	0.0601	0.2864
280	3.811	41.894	-0.131	0.007	-1.6	2.7	0.2	25.706	22.992	1.1180	1.1162	0.0303	0.0573	0.2856
281	3.810	44.463	-0.135	0.009	-1.6	2.5	0.2	25.692	22.999	1.1171	1.1154	0.0321	0.0525	0.2854
282	3.812	45.723	-0.139	0.008	-1.7	2.0	0.2	25.571	22.997	1.1119	1.1106	0.0338	0.0437	0.2839
283	3.811	47.000	-0.141	0.005	-1.8	1.2	0.1	25.256	22.995	1.0983	1.0975	0.0342	0.0257	0.2824
284	3.812	48.252	-0.139	0.007	-1.7	-0.8	0.2	24.741	23.001	1.0757	1.0751	0.0323	-0.0107	0.2825
285	3.810	49.544	-0.132	0.009	-1.5	-3.2	0.3	24.116	23.002	1.0484	1.0467	0.0268	-0.0540	0.2814
286	7.636	8.831	-0.011	0.008	1.5	0.6	0.2	25.887	23.375	1.1074	1.1069	-0.0293	0.0165	0.2954
287	7.625	11.344	-0.020	0.008	1.3	1.2	0.2	25.974	23.361	1.1118	1.1112	-0.0254	0.0268	0.2933
288	7.623	14.000	-0.027	0.009	1.2	1.6	0.2	25.985	23.361	1.1123	1.1116	-0.0227	0.0347	0.2921
289	7.622	16.533	-0.036	0.008	1.0	1.8	0.2	25.982	23.359	1.1123	1.1115	-0.0187	0.0384	0.2919
290	7.624	19.072	-0.041	0.008	0.9	1.9	0.2	25.977	23.347	1.1126	1.1118	-0.0170	0.0407	0.2905
291	7.624	21.599	-0.051	0.006	0.6	2.0	0.2	25.986	23.349	1.1129	1.1121	-0.0121	0.0420	0.2906
292	7.626	24.133	-0.062	0.009	0.4	2.1	0.2	25.980	23.346	1.1128	1.1119	-0.0072	0.0444	0.2910
293	7.624	26.662	-0.073	0.007	0.1	2.2	0.2	26.002	23.343	1.1139	1.1130	-0.0022	0.0465	0.2895
294	7.623	29.232	-0.084	0.009	-0.2	2.3	0.2	26.011	23.339	1.1145	1.1134	0.0036	0.0498	0.2891
295	7.625	31.762	-0.095	0.007	-0.5	2.5	0.2	26.011	23.337	1.1146	1.1133	0.0097	0.0514	0.2887
296	7.622	34.273	-0.103	0.010	-0.7	2.4	0.3	26.024	23.329	1.1155	1.1142	0.0139	0.0525	0.2877
297	7.623	36.843	-0.112	0.008	-1.0	2.5	0.2	26.029	23.323	1.1160	1.1146	0.0191	0.0532	0.2883
298	7.624	39.412	-0.120	0.009	-1.2	2.5	0.2	26.036	23.314	1.1168	1.1152	0.0238	0.0533	0.2868
299	7.623	41.905	-0.122	0.007	-1.3	2.4	0.2	26.064	23.323	1.1175	1.1161	0.0244	0.0513	0.2857
300	7.622	44.462	-0.126	0.010	-1.3	2.2	0.3	26.032	23.309	1.1169	1.1155	0.0257	0.0483	0.2844

## STATION 38 (Continued)

POINT	Z	Y	CPITCH	CYAW	ALPHA	THETA	BETA	V	VCONT	VW	VX	VY	VZ	CP
301	7.623	45.722	-0.126	0.008	-1.3	1.9	0.2	25.932	23.311	1.1124	1.1114	0.0255	0.0408	0.2840
302	7.623	47.037	-0.125	0.007	-1.3	1.1	0.2	25.652	23.309	1.1005	1.0999	0.0243	0.0256	0.2827
303	7.624	48.242	-0.126	0.011	-1.3	-0.1	0.3	25.083	23.301	1.0765	1.0762	0.0239	0.0041	0.2809
304	7.626	49.519	-0.120	0.011	-1.0	-1.9	0.3	24.131	23.302	1.0356	1.0350	0.0188	-0.0291	0.2795
305	11.426	8.814	-0.038	0.006	0.8	0.6	0.2	25.438	23.447	1.0849	1.0847	-0.0149	0.0152	0.2926
306	11.429	11.384	-0.042	0.003	0.7	1.1	0.1	25.778	23.436	1.0999	1.0996	-0.0140	0.0222	0.2920
307	11.428	13.955	-0.042	0.004	0.8	1.4	0.1	25.883	23.429	1.1048	1.1043	-0.0147	0.0297	0.2905
308	11.429	16.507	-0.039	0.004	0.9	1.7	0.1	25.952	23.434	1.1074	1.1068	-0.0170	0.0351	0.2941
309	11.428	19.018	-0.040	0.005	0.9	1.7	0.1	25.936	23.418	1.1075	1.1068	-0.0170	0.0361	0.2900
310	11.428	21.590	-0.047	0.004	0.7	1.6	0.1	25.925	23.413	1.1073	1.1067	-0.0144	0.0339	0.2890
311	11.429	24.119	-0.057	0.004	0.5	1.5	0.1	25.911	23.412	1.1067	1.1063	-0.0097	0.0308	0.2888
312	11.432	26.646	-0.075	0.003	0.1	1.6	0.1	25.915	23.408	1.1071	1.1066	-0.0012	0.0325	0.2879
313	11.430	29.212	-0.093	0.003	-0.5	1.9	0.1	25.943	23.399	1.1087	1.1080	0.0091	0.0390	0.2871
314	11.431	31.745	-0.103	0.005	-0.8	2.1	0.1	25.950	23.391	1.1094	1.1084	0.0152	0.0434	0.2865
315	11.431	34.249	-0.110	0.004	-1.0	2.3	0.1	25.974	23.390	1.1105	1.1093	0.0188	0.0474	0.2863
316	11.431	36.818	-0.116	0.003	-1.1	2.3	0.1	25.962	23.375	1.1107	1.1095	0.0220	0.0466	0.2856
317	11.433	39.377	-0.119	0.005	-1.2	2.3	0.1	25.983	23.379	1.1114	1.1101	0.0226	0.0478	0.2850
318	11.432	41.873	-0.123	0.005	-1.3	2.4	0.1	25.981	23.365	1.1120	1.1106	0.0250	0.0497	0.2856
319	11.430	44.449	-0.122	0.005	-1.2	2.4	0.1	25.882	23.368	1.1076	1.1063	0.0232	0.0485	0.2837
320	11.432	45.709	-0.120	0.004	-1.1	2.2	0.1	25.697	23.361	1.1000	1.0989	0.0215	0.0442	0.2819
321	11.431	46.987	-0.117	0.004	-1.0	1.9	0.1	25.196	23.364	1.0784	1.0776	0.0185	0.0376	0.2793
322	11.432	48.260	-0.114	0.005	-0.9	0.9	0.1	24.296	23.359	1.0401	1.0398	0.0157	0.0184	0.2772
323	11.432	48.926	-0.112	0.008	-0.8	0.0	0.2	23.643	23.359	1.0122	1.0121	0.0142	0.0041	0.2770
324	11.442	49.649	-0.110	0.007	-0.7	-1.3	0.2	22.769	23.352	0.9750	0.9748	0.0121	-0.0188	0.2763
325	15.194	8.807	-0.046	0.005	0.6	0.9	0.1	23.910	23.182	1.0314	1.0312	-0.0102	0.0178	0.2892
326	15.239	11.317	-0.047	0.004	0.6	1.5	0.1	24.873	23.193	1.0724	1.0720	-0.0110	0.0303	0.2883
327	15.240	13.994	-0.041	0.008	0.8	1.6	0.2	25.493	23.199	1.0989	1.0982	-0.0151	0.0347	0.2911
328	15.239	16.532	-0.038	0.005	0.9	1.8	0.1	25.684	23.211	1.1065	1.1058	-0.0177	0.0369	0.2908
329	15.239	19.065	-0.037	0.007	1.0	1.6	0.2	25.678	23.200	1.1068	1.1061	-0.0186	0.0343	0.2888
330	15.239	21.609	-0.034	0.009	1.1	1.4	0.2	25.353	23.211	1.0923	1.0917	-0.0208	0.0304	0.2866
331	15.238	24.142	-0.043	0.008	0.9	0.7	0.2	24.611	23.212	1.0603	1.0600	-0.0163	0.0176	0.2861
332	15.238	25.369	-0.057	0.008	0.5	0.5	0.2	24.297	23.363	1.0400	1.0399	-0.0096	0.0120	0.2882
333	15.238	26.674	-0.080	0.008	-0.1	0.4	0.2	24.235	23.214	1.0440	1.0439	0.0015	0.0118	0.2832
334	15.248	27.953	-0.098	0.005	-0.7	0.8	0.1	24.393	23.344	1.0449	1.0447	0.0119	0.0165	0.2820
335	15.239	29.220	-0.106	0.007	-0.9	1.4	0.2	24.873	23.215	1.0714	1.0709	0.0172	0.0288	0.2840
336	15.240	31.765	-0.110	0.008	-1.0	2.0	0.2	25.605	23.219	1.1028	1.1018	0.0191	0.0425	0.2854
337	15.236	34.295	-0.108	0.007	-0.9	2.0	0.2	25.791	23.213	1.1110	1.1101	0.0175	0.0421	0.2865
338	15.237	36.840	-0.111	0.009	-1.0	2.0	0.2	25.779	23.215	1.1104	1.1095	0.0187	0.0428	0.2872
339	15.234	39.410	-0.119	0.007	-1.2	1.9	0.2	25.743	23.214	1.1089	1.1080	0.0227	0.0398	0.2871
340	15.236	41.904	-0.129	0.009	-1.5	2.2	0.2	25.721	23.211	1.1082	1.1068	0.0287	0.0469	0.2864
341	15.235	44.463	-0.138	0.003	-1.7	2.6	0.1	25.395	23.206	1.0943	1.0926	0.0330	0.0512	0.2833
342	15.235	45.718	-0.137	0.011	-1.7	2.4	0.3	24.986	23.207	1.0767	1.0750	0.0315	0.0509	0.2820
343	15.236	47.020	-0.139	0.013	-1.7	2.0	0.4	24.324	23.212	1.0479	1.0465	0.0318	0.0431	0.2793
344	15.235	48.259	-0.139	0.011	-1.7	1.0	0.3	23.354	23.214	1.0061	1.0053	0.0300	0.0227	0.2775
345	15.234	48.909	-0.138	0.010	-1.7	0.1	0.3	22.769	23.214	0.9808	0.9804	0.0285	0.0066	0.2762
346	15.234	49.535	-0.136	0.007	-1.6	-0.9	0.2	22.326	23.207	0.9620	0.9616	0.0265	-0.0113	0.2773
347	16.496	21.587	-0.035	0.008	1.1	1.5	0.2	25.079	23.360	1.0736	1.0729	-0.0200	0.0314	0.2850
348	16.505	22.873	-0.036	0.006	1.1	1.1	0.2	24.426	23.348	1.0462	1.0457	-0.0192	0.0239	0.2839
349	16.503	24.152	-0.044	0.003	0.9	0.4	0.1	23.739	23.353	1.0166	1.0164	-0.0155	0.0087	0.2821
350	16.503	25.393	-0.061	0.008	0.4	-0.4	0.2	23.316	23.351	0.9985	0.9985	-0.0074	-0.0027	0.2824

## STATION 38 (Continued)

POINT	Z	Y	CPITCH	CYAW	ALPHA	THETA	BETA	V	VCONT	VV	VX	VY	VZ	CP
351	16.506	26.661	-0.081	0.005	-0.1	-0.3	0.1	23.279	23.354	0.9968	0.9963	0.0021	-0.0026	0.2820
352	16.506	27.962	-0.100	0.004	-0.7	0.1	0.1	23.478	23.346	1.0057	1.0056	0.0129	0.0039	0.2852
353	16.508	29.204	-0.108	0.007	-1.0	1.0	0.2	24.144	23.340	1.0344	1.0341	0.0177	0.0220	0.2833
354	16.504	30.464	-0.110	0.007	-1.0	1.8	0.2	24.851	23.357	1.0639	1.0632	0.0189	0.0367	0.2822
355	16.506	31.770	-0.109	0.006	-1.0	2.1	0.2	25.388	23.340	1.0877	1.0867	0.0185	0.0437	0.2809
356	17.807	8.811	-0.014	0.006	1.5	0.7	0.2	23.078	23.298	0.9905	0.9901	-0.0251	0.0144	0.2856
357	17.792	11.408	-0.020	0.009	1.3	1.4	0.2	24.299	23.296	1.0431	1.0423	-0.0237	0.0307	0.2860
358	17.774	13.986	-0.029	0.009	1.1	1.6	0.3	24.944	23.285	1.0713	1.0705	-0.0210	0.0339	0.2872
359	17.770	16.537	-0.039	0.008	0.9	1.5	0.2	25.295	23.293	1.0860	1.0853	-0.0168	0.0330	0.2872
360	17.769	19.069	-0.046	0.005	0.7	1.8	0.1	25.293	23.293	1.0859	1.0852	-0.0137	0.0364	0.2848
361	17.771	21.601	-0.048	0.006	0.7	1.6	0.2	24.529	23.286	1.0534	1.0528	-0.0133	0.0324	0.2815
362	17.772	22.852	-0.046	0.004	0.8	1.1	0.1	23.729	23.286	1.0191	1.0187	-0.0138	0.0218	0.2807
363	17.769	24.149	-0.050	0.006	0.7	-0.1	0.2	22.969	23.283	0.9865	0.9864	-0.0122	0.0013	0.2805
364	17.772	25.385	-0.064	0.008	0.3	-1.2	0.2	22.425	23.277	0.9634	0.9632	-0.0058	-0.0170	0.2796
365	17.771	26.669	-0.082	0.012	-0.2	-1.4	0.3	22.428	23.285	0.9632	0.9630	0.0026	-0.0185	0.2783
366	17.769	27.966	-0.099	0.008	-0.7	-0.5	0.2	22.673	23.282	0.9739	0.9738	0.0120	-0.0052	0.2784
367	17.769	29.196	-0.101	0.006	-0.7	0.9	0.2	23.398	23.278	1.0051	1.0049	0.0131	0.0195	0.2781
368	17.770	30.461	-0.101	0.005	-0.7	1.9	0.1	24.255	23.274	1.0422	1.0415	0.0130	0.0366	0.2795
369	17.772	31.765	-0.102	0.004	-0.7	2.3	0.1	24.922	23.275	1.0707	1.0697	0.0139	0.0449	0.2806
370	17.771	34.296	-0.104	0.007	-0.8	2.2	0.2	25.410	23.270	1.0920	1.0909	0.0148	0.0455	0.2831
371	17.770	36.868	-0.111	0.003	-1.0	1.9	0.1	25.138	23.264	1.0906	1.0798	0.0182	0.0370	0.2834
372	17.773	39.394	-0.125	0.008	-1.4	1.6	0.2	24.995	23.266	1.0743	1.0735	0.0257	0.0336	0.2866
373	17.769	41.903	-0.143	0.007	-1.9	1.9	0.2	25.023	23.261	1.0757	1.0744	0.0363	0.0389	0.2833
374	17.770	44.463	-0.160	0.004	-2.4	2.4	0.1	24.957	23.248	1.0735	1.0716	0.0442	0.0469	0.2815
375	17.771	45.723	-0.170	0.002	-2.6	2.5	0.1	24.681	23.246	1.0617	1.0596	0.0482	0.0472	0.2802
376	17.768	47.022	-0.178	0.005	-2.8	2.1	0.1	24.143	23.237	1.0390	1.0370	0.0508	0.0404	0.2794
377	17.772	48.258	-0.183	0.009	-2.9	1.1	0.2	23.464	23.241	1.0096	1.0080	0.0514	0.0227	0.2782
378	17.770	48.889	-0.183	0.004	-2.9	0.5	0.1	23.058	23.244	0.9920	0.9907	0.0503	0.0110	0.2785
379	17.769	49.537	-0.179	0.010	-2.8	-0.5	0.3	22.661	23.245	0.9749	0.9737	0.0473	-0.0046	0.2786
380	18.795	21.586	-0.059	0.003	0.4	1.9	0.1	24.298	23.358	1.0403	1.0396	-0.0075	0.0355	0.2821
381	18.795	22.861	-0.063	0.003	0.3	1.2	0.1	23.541	23.350	1.0082	1.0079	-0.0058	0.0225	0.2799
382	18.795	24.127	-0.063	0.006	0.3	-0.3	0.2	22.710	23.344	0.9728	0.9728	-0.0058	-0.0027	0.2789
383	18.793	25.399	-0.069	0.017	0.2	-1.6	0.5	22.188	23.339	0.9507	0.9505	-0.0033	-0.0195	0.2789
384	18.796	26.643	-0.081	-0.001	-0.1	-1.7	-0.0	22.067	23.333	0.9457	0.9453	0.0018	-0.0277	0.2773
385	18.794	27.935	-0.089	0.006	-0.4	-0.9	0.2	22.540	23.425	0.9622	0.9621	0.0062	-0.0130	0.2778
386	18.795	29.206	-0.090	0.003	-0.4	0.6	0.1	23.233	23.420	0.9920	0.9919	0.0067	0.0124	0.2778
387	18.794	30.485	-0.089	0.005	-0.3	1.7	0.1	24.050	23.420	1.0269	1.0263	0.0060	0.0339	0.2775
388	18.794	31.646	-0.091	0.004	-0.4	2.3	0.1	24.742	23.416	1.0566	1.0557	0.0067	0.0440	0.2808
389	19.802	8.775	0.040	0.010	2.9	0.3	0.3	22.724	23.161	0.9811	0.9798	-0.0493	0.0088	0.2899
390	19.746	8.778	0.038	0.007	2.8	0.3	0.2	22.704	23.169	0.9799	0.9787	-0.0484	0.0085	0.2896
391	19.816	8.813	0.038	0.001	2.8	0.4	0.0	22.775	23.338	0.9759	0.9747	-0.0482	0.0077	0.2859
392	19.811	11.383	0.015	0.000	2.3	1.3	0.0	23.628	23.332	1.0127	1.0116	-0.0402	0.0226	0.2854
393	19.814	13.970	-0.010	0.007	1.6	1.3	0.2	24.171	23.331	1.0360	1.0353	-0.0293	0.0261	0.2865
394	19.815	16.490	-0.034	0.005	1.0	1.4	0.1	24.435	23.348	1.0466	1.0460	-0.0183	0.0273	0.2863
395	19.811	19.047	-0.059	0.005	0.4	1.7	0.1	24.515	23.324	1.0510	1.0505	-0.0069	0.0331	0.2838
396	19.816	21.580	-0.078	0.003	-0.1	1.9	0.1	23.982	23.313	1.0287	1.0281	0.0018	0.0347	0.2825
397	19.816	22.834	-0.087	0.004	-0.4	1.0	0.1	23.301	23.310	0.9996	0.9994	0.0065	0.0202	0.2787
398	19.815	24.129	-0.082	0.009	-0.2	-0.5	0.3	22.527	23.302	0.9667	0.9667	0.0034	-0.0045	0.2800
399	19.814	25.414	-0.081	0.006	-0.1	-2.0	0.2	21.921	23.295	0.9410	0.9405	0.0023	-0.0297	0.2780
400	19.814	26.673	-0.075	0.007	0.1	-2.2	0.2	21.836	23.284	0.9378	0.9372	-0.0009	-0.0327	0.2783

## STATION 38 (Concluded)

POINT	Z	Y	CPITCH	CYAW	ALPHA	THETA	BETA	V	VCONT	VV	VX	VY	VZ	CP
401	19.816	27.947	-0.074	0.007	0.1	-1.2	0.2	22.198	23.275	0.9538	0.9536	-0.0019	-0.0177	0.2779
402	19.815	29.214	-0.070	0.010	0.2	0.1	0.3	22.871	23.271	0.9828	0.9828	-0.0039	0.0066	0.2782
403	19.814	30.436	-0.069	0.008	0.3	1.6	0.2	23.720	23.277	1.0191	1.0185	-0.0051	0.0328	0.2799
404	19.818	31.751	-0.079	0.005	0.0	2.2	0.1	24.321	23.253	1.0460	1.0451	-0.0005	0.0423	0.2795
405	19.817	34.234	-0.099	0.002	-0.6	2.1	0.0	24.584	23.249	1.0574	1.0566	0.0110	0.0393	0.2821
406	19.817	36.822	-0.118	0.007	-1.2	1.6	0.2	24.118	23.240	1.0378	1.0371	0.0217	0.0320	0.2814
407	19.818	39.368	-0.140	0.008	-1.9	1.2	0.2	23.728	23.229	1.0214	1.0206	0.0337	0.0247	0.2811
408	19.816	41.876	-0.157	0.011	-2.3	1.5	0.3	23.874	23.216	1.0283	1.0270	0.0414	0.0315	0.2809
409	19.814	43.177	-0.168	0.008	-2.6	1.8	0.2	24.132	23.281	1.0366	1.0349	0.0469	0.0357	0.2816
410	19.815	44.447	-0.178	0.008	-2.8	2.0	0.2	24.183	23.268	1.0393	1.0373	0.0515	0.0401	0.2815
411	19.817	45.730	-0.191	0.002	-3.2	2.1	0.1	24.151	23.259	1.0383	1.0360	0.0576	0.0388	0.2810
412	19.817	46.987	-0.204	0.001	-3.5	1.9	0.0	23.759	23.247	1.0220	1.0196	0.0623	0.0345	0.2801
413	19.814	48.279	-0.210	0.007	-3.7	1.1	0.2	23.277	23.229	1.0021	0.9998	0.0640	0.0225	0.2798
414	19.797	49.539	-0.208	0.007	-3.6	-0.3	0.2	22.562	23.211	0.9720	0.9701	0.0606	-0.0017	0.2789

STATION 38 - Plenum Thermister Moved to Center Line of Top Wall

POINT	Z	Y	CPITCH	CYAW	ALPHA	THETA	BETA	V	VCONT	VV	VX	VY	VZ	CP
1	11.437	26.664	-0.075	0.004	0.1	1.8	0.1	25.725	23.219	1.1079	1.1073	-0.0010	0.0364	0.2858
2	11.438	29.214	-0.084	0.005	-0.2	1.8	0.1	25.741	23.221	1.1085	1.1079	0.0031	0.0371	0.2856
3	11.437	31.763	-0.093	0.005	-0.4	1.8	0.1	25.741	23.219	1.1086	1.1080	0.0085	0.0373	0.2856
4	11.436	34.295	-0.104	0.006	-0.7	1.8	0.2	25.747	23.208	1.1094	1.1087	0.0144	0.0376	0.2854
5	11.435	36.862	-0.111	0.005	-1.0	1.9	0.1	25.756	23.213	1.1095	1.1087	0.0184	0.0387	0.2838
6	15.243	16.482	-0.039	0.007	0.9	1.1	0.2	25.551	23.151	1.1037	1.1033	-0.0170	0.0243	0.2883
7	15.242	19.054	-0.047	0.006	0.7	0.8	0.2	25.552	23.160	1.1033	1.1030	-0.0134	0.0193	0.2881
8	15.240	21.593	-0.056	0.005	0.5	0.9	0.1	25.556	23.164	1.1033	1.1031	-0.0096	0.0189	0.2867
9	15.242	24.134	-0.064	0.005	0.3	1.1	0.1	25.615	23.162	1.1059	1.1056	-0.0061	0.0238	0.2853
10	15.241	25.401	-0.067	0.006	0.2	1.1	0.2	25.616	23.160	1.1061	1.1058	-0.0047	0.0254	0.2861
11	15.263	26.646	-0.074	0.006	0.1	1.3	0.2	25.575	23.206	1.1021	1.1018	-0.0015	0.0272	0.2843
12	15.242	26.683	-0.072	0.006	0.1	1.2	0.1	25.601	23.164	1.1052	1.1049	-0.0025	0.0253	0.2861
13	15.241	27.964	-0.077	0.006	0.0	1.3	0.2	25.590	23.139	1.1059	1.1056	-0.0003	0.0276	0.2839
14	15.241	29.197	-0.082	0.008	-0.1	1.2	0.2	25.625	23.162	1.1064	1.1060	0.0019	0.0266	0.2852
15	15.239	31.767	-0.093	0.005	-0.4	1.2	0.1	25.632	23.166	1.1065	1.1062	0.0081	0.0260	0.2834
16	15.242	34.293	-0.098	0.004	-0.6	1.3	0.1	25.640	23.152	1.1075	1.1071	0.0111	0.0263	0.2842
17	15.241	36.855	-0.107	0.006	-0.8	1.4	0.2	25.649	23.151	1.1079	1.1073	0.0161	0.0309	0.2847
18	15.241	39.406	-0.114	0.004	-1.0	1.4	0.1	25.623	23.147	1.1070	1.1064	0.0193	0.0295	0.2862
19	15.242	41.883	-0.121	0.004	-1.2	1.7	0.1	25.591	23.141	1.1059	1.1051	0.0234	0.0346	0.2863
20	15.240	44.460	-0.124	0.005	-1.3	2.1	0.1	25.201	23.142	1.0890	1.0879	0.0240	0.0428	0.2794
21	15.240	45.726	-0.122	0.009	-1.2	2.1	0.2	24.681	23.130	1.0671	1.0660	0.0217	0.0435	0.2776
22	15.237	47.006	-0.122	0.010	-1.2	1.6	0.3	23.951	23.124	1.0358	1.0351	0.0208	0.0330	0.2762
23	15.237	48.266	-0.119	0.013	-1.1	0.5	0.4	22.994	23.124	0.9944	0.9941	0.0183	0.0153	0.2753
24	15.238	49.526	-0.117	0.004	-1.0	-1.1	0.1	21.988	23.122	0.9509	0.9507	0.0159	-0.0171	0.2746
25	17.775	13.967	-0.021	0.004	1.3	1.2	0.1	24.801	23.302	1.0643	1.0637	-0.0248	0.0242	0.2858
26	17.777	16.491	-0.028	0.008	1.2	0.8	0.2	24.853	23.307	1.0663	1.0659	-0.0219	0.0195	0.2855
27	17.780	19.031	-0.039	0.005	0.9	0.6	0.1	24.704	23.304	1.0601	1.0598	-0.0169	0.0145	0.2842
28	17.777	21.585	-0.051	0.004	0.6	0.6	0.1	24.697	23.295	1.0602	1.0600	-0.0118	0.0132	0.2877
29	17.776	22.856	-0.056	0.002	0.5	0.8	0.1	24.754	23.279	1.0634	1.0632	-0.0096	0.0151	0.2853
30	17.775	24.132	-0.059	0.004	0.5	0.8	0.1	24.787	23.309	1.0634	1.0632	-0.0085	0.0167	0.2886
31	17.776	25.388	-0.064	0.006	0.3	0.9	0.2	24.800	23.287	1.0650	1.0648	-0.0064	0.0201	0.2831
32	17.776	26.644	-0.069	0.007	0.2	0.9	0.2	24.782	23.281	1.0645	1.0643	-0.0039	0.0209	0.2826
33	17.775	27.940	-0.075	0.005	0.1	0.9	0.1	24.748	23.280	1.0630	1.0629	-0.0016	0.0198	0.2825
34	17.775	29.210	-0.081	0.005	-0.1	1.0	0.1	24.760	23.277	1.0637	1.0635	0.0011	0.0210	0.2825
35	17.774	30.484	-0.087	0.006	-0.3	0.9	0.2	24.779	23.276	1.0645	1.0643	0.0047	0.0205	0.2822
36	17.778	31.752	-0.092	0.004	-0.4	1.0	0.1	24.801	23.279	1.0654	1.0651	0.0075	0.0209	0.2828
37	17.779	34.268	-0.102	0.009	-0.7	1.2	0.2	25.007	23.310	1.0728	1.0724	0.0130	0.0260	0.2823
38	17.775	36.838	-0.111	0.005	-1.0	1.4	0.1	25.001	23.298	1.0731	1.0726	0.0181	0.0279	0.2829
39	17.778	39.387	-0.122	0.005	-1.3	1.4	0.1	24.921	23.301	1.0695	1.0693	0.0236	0.0295	0.2822
40	17.775	41.862	-0.134	0.007	-1.6	1.7	0.2	24.971	23.285	1.0724	1.0714	0.0306	0.0348	0.2812
41	17.776	44.437	-0.146	0.005	-2.0	2.1	0.1	24.591	23.274	1.0566	1.0552	0.0361	0.0408	0.2796
42	17.775	45.697	-0.154	0.001	-2.2	2.1	0.0	24.206	23.282	1.0397	1.0382	0.0390	0.0383	0.2776
43	17.777	47.036	-0.157	0.005	-2.2	1.6	0.1	23.555	23.273	1.0121	1.0109	0.0395	0.0299	0.2758
44	17.778	48.290	-0.163	0.015	-2.4	0.3	0.4	22.796	23.247	0.9806	0.9797	0.0406	0.0121	0.2750
45	17.796	49.525	-0.153	0.003	-2.1	-1.0	0.1	21.942	23.247	0.9439	0.9431	0.0343	-0.0160	0.2751
46	19.785	13.969	0.001	0.012	1.9	0.7	0.3	23.841	23.318	1.0224	1.0217	-0.0344	0.0183	0.2860
47	19.813	16.503	-0.020	0.010	1.4	0.5	0.3	23.682	23.321	1.0155	1.0151	-0.0247	0.0138	0.2842
48	19.811	19.050	-0.036	0.002	1.0	0.3	0.1	23.389	23.315	1.0032	1.0030	-0.0177	0.0062	0.2824
49	19.811	21.611	-0.048	0.009	0.7	0.3	0.2	23.430	23.312	1.0050	1.0049	-0.0127	0.0095	0.2820
50	19.813	22.860	-0.056	0.004	0.5	0.6	0.1	23.546	23.307	1.0102	1.0101	-0.0091	0.0126	0.2814

POINT	Z	Y	CPITCH	CYAW	ALPHA	THETA	BETA	V	VCONT	VV	VX	VY	VZ	CP
51	19.812	24.144	-0.060	0.010	0.4	0.6	0.3	23.632	23.306	1.0140	1.0138	-0.0077	0.0153	0.2812
52	19.811	25.390	-0.065	0.008	0.3	0.6	0.2	23.657	23.298	1.0154	1.0153	-0.0055	0.0149	0.2798
53	19.813	26.682	-0.071	0.007	0.2	0.7	0.2	23.647	23.291	1.0153	1.0151	-0.0028	0.0160	0.2793
54	19.811	27.960	-0.078	0.010	-0.0	0.6	0.3	23.593	23.291	1.0130	1.0128	0.0003	0.0154	0.2800
55	19.813	29.216	-0.085	0.004	-0.2	0.7	0.1	23.597	23.285	1.0134	1.0133	0.0036	0.0146	0.2797
56	19.811	30.455	-0.095	0.005	-0.5	0.7	0.1	23.511	23.290	1.0095	1.0093	0.0091	0.0150	0.2800
57	19.811	31.788	-0.101	0.008	-0.7	0.9	0.2	23.666	23.286	1.0163	1.0161	0.0122	0.0201	0.2800
58	19.804	34.269	-0.112	0.010	-1.0	0.9	0.3	23.618	23.176	1.0191	1.0187	0.0185	0.0207	0.2793
59	19.811	34.296	-0.117	0.008	-1.2	1.1	0.2	23.717	23.275	1.0190	1.0185	0.0210	0.0237	0.2799
60	19.804	36.800	-0.128	0.002	-1.5	1.1	0.1	23.628	23.165	1.0200	1.0194	0.0268	0.0216	0.2774
61	19.798	39.379	-0.140	0.010	-1.9	0.8	0.3	23.395	23.097	1.0129	1.0122	0.0334	0.0185	0.2792
62	19.808	41.894	-0.159	0.009	-2.4	1.2	0.2	23.615	23.105	1.0221	1.0209	0.0423	0.0254	0.2785
63	19.808	44.414	-0.180	0.010	-2.9	1.7	0.3	23.783	23.116	1.0289	1.0269	0.0521	0.0348	0.2784
64	19.807	45.732	-0.193	0.006	-3.2	1.7	0.2	23.770	23.112	1.0285	1.0263	0.0578	0.0328	0.2776
65	19.804	46.994	-0.204	0.009	-3.5	1.4	0.2	23.498	23.123	1.0163	1.0140	0.0619	0.0283	0.2780
66	19.806	48.267	-0.213	0.007	-3.7	0.5	0.2	23.014	23.107	0.9960	0.9938	0.0650	0.0124	0.2753
67	19.805	49.530	-0.206	0.010	-3.5	-0.6	0.3	22.364	23.129	0.9669	0.9651	0.0593	-0.0056	0.2780

## REFERENCES

1. Proceedings, 1980-81 AFOSR-HTMM-Stanford Conference on Complex Turbulent Flows, Vols. I-III. Kline, S. J., Cantwell, B. J., et al., editors. Stanford University, 1982.
2. Taylor, A. M. K. P., Whitelaw, J. H., and Yianneskis, M.: Measurements of Laminar and Turbulent Flow in a Curved Duct with Thin Inlet Boundary Layers. NASA CR 3367, January 1981.
3. Fox, R. W. and Kline, S. J.: Flow Regime Data and Design Methods for Curved Subsonic Diffusers. Rept. PD-6, Dept. of Mech. Eng., Stanford University, August 1960.
4. Cantwell, B.: The Data Library. In Proceedings, 1980-81 AFOSR-HTMM-Stanford Conference on Complex Turbulent Flows. Vol. I, Objectives, Evaluation of Data, Specification of Test Cases, Discussion and Position Papers. Stanford University, 1982.
5. Kline, S. J. and McClintock, F. A.: The Description of Uncertainties in Single Sample Experiments. Mechanical Engineering, January 1953.
6. Coles, D. E.: The Young Person's Guide to the Data. In Proceedings, Computation of Turbulent Boundary Layers - 1968 AFOSR-IFP-Stanford Conference. Vol. II, Computed Data, D. E. Coles, E. A. Hirst, editors, Stanford University, 1969, pp. 1-45.
7. Coles, D.: The Law of the Wake in the Turbulent Boundary Layer. JFM, Vol. 1, July 1956, pp. 191-226.
8. Klebanoff, P. S.: Characteristics of Turbulence in a Boundary Layer with Zero Pressure Gradient. NACA TR 1247, 1955.
9. Herzig, H. Z., Hansen, A. G., and Costello, G. R.: A Visualization Study of Secondary Flows in Cascades. NACA Report 1163, 1954.
10. Ligrani, P. M. and Moffat, R. J.: Artificially Thickening a Smooth-Wall Turbulent Boundary Layer. AIAA Journal, Vol. 17, No. 8, August 1979, pp. 907-910.

Table 1.- Streamwise Location of Survey Planes

<u>Nominal Location (Station Number)</u>	<u>x (cm)</u>
0	0.06
7	35.69
14	71.53
20	101.79
28	142.52
38	193.16



Table 2.- Boundary-Layer Traverse Coordinate  
System Transformations ( $x = 0$ )

Top Wall

$$y = \hat{y}$$

$$z = \hat{z}$$

Bottom Wall

$$y = 52.83 - \hat{y}$$

$$z = \hat{z}$$

Convex Wall

$$y = \hat{z}$$

$$z = \hat{y} - 17.65$$

Concave Wall

$$y = \hat{z}$$

$$z = 17.65 - \hat{y}$$

Table 3.- Estimated Experimental Uncertainty  
of Measured Quantities

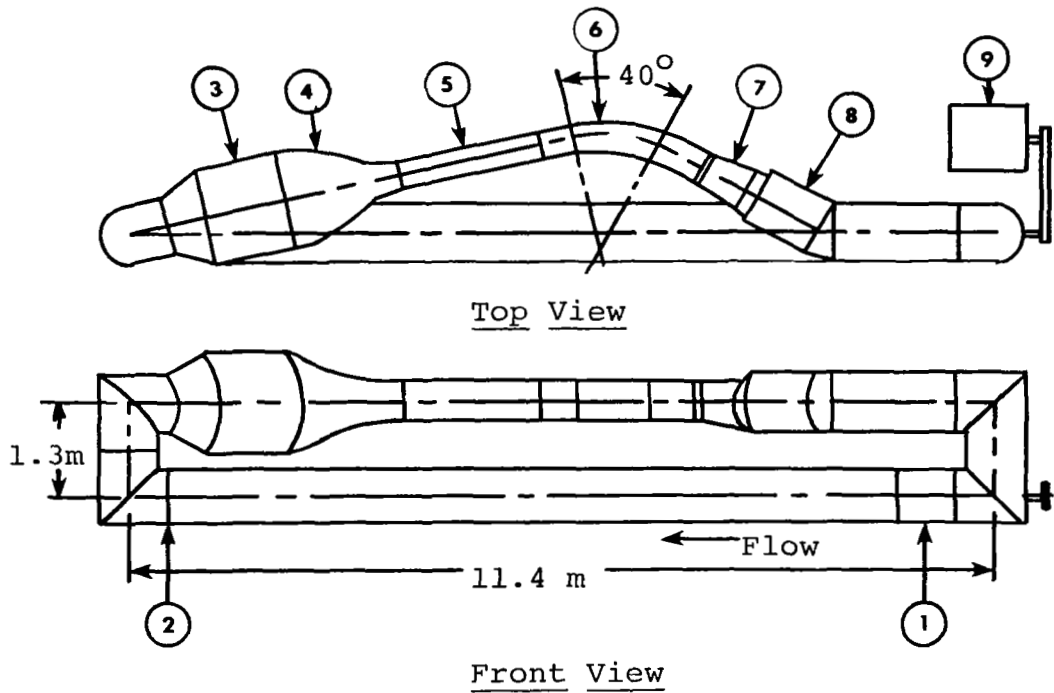
<u>Quantity</u>	<u>Estimated Uncertainty (20:1 odds)</u>
x, y, z, $\hat{z}$	$\pm 0.13$ cm
$\hat{y}$	$\pm 0.005$ cm
u (boundary-layer probe)	$\pm 1\%$
u (hot wire)	$\pm 5\%$
$\sqrt{u'^2}/u_\infty$	$\pm 8\%$
$C_p$ (wall taps)	$\pm 0.006$
$C_p$ (5-hole probe)	$\pm 0.008$
V	$\pm 2\%$
$\theta + \beta$	$\pm 0.5^\circ$
$\alpha$	$\pm 0.5^\circ$

Table 4.- Boundary-Layer Parameters, Initial Station

Wall	$\hat{z}$ (cm)	$u^*$ (mps)	$C_f$	$\delta$ (cm)	$\delta^*$ (cm)	$\theta$ (cm)	H	G	$\Pi$	$\Delta$ (cm)	$R_\delta$	$R_\theta$
B	-8.83	1.15	0.00282	7.05	0.772	0.610	1.27	5.59	0.183	20.58	14509	11464
B	0	1.12	0.00269	7.46	0.868	0.681	1.27	5.86	0.286	23.64	16423	12889
B	8.83	1.14	0.00278	7.47	0.816	0.645	1.27	5.63	0.185	21.89	15454	12206
T	-8.83	1.14	0.00279	7.41	0.809	0.641	1.26	5.56	0.179	21.66	15298	12121
T	0	1.14	0.00274	7.91	0.869	0.688	1.26	5.62	0.202	23.45	16377	12971
T	8.83	1.13	0.00279	7.60	0.819	0.650	1.26	5.53	0.162	21.91	15582	12362
CV	13.21	1.13	0.00275	3.80	0.544	0.407	1.34	6.79	0.557	14.67	10361	7753
CV	26.42	1.13	0.00274	3.73	0.534	0.397	1.34	6.92	0.580	14.42	10169	7567
CV	39.62	1.17	0.00290	3.19	0.450	0.337	1.33	6.56	0.491	11.81	8488	6368
CC	13.21	1.11	0.00265	4.28	0.625	0.466	1.34	7.00	0.611	17.19	11945	8905
CC	26.42	1.09	0.00255	4.42	0.669	0.495	1.35	7.29	0.710	18.72	12665	9365
CC	39.62	1.15	0.00283	3.48	0.488	0.364	1.34	6.72	0.511	12.96	9323	6967

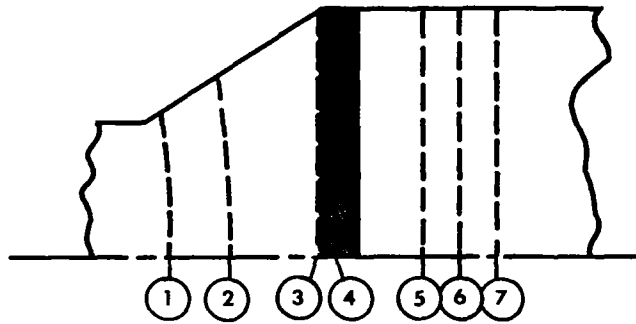
Table 5.- Boundary-Layer Parameters

<u>Wall Treatment</u>	<u>Plotting Symbol</u>	<u>u*</u> (mps)	<u>C<sub>f</sub></u>	<u>δ</u> (cm)	<u>δ*</u> (cm)	<u>θ</u> (cm)	<u>H</u>	<u>G</u>	<u>Π</u>	<u>Δ</u> (cm)	<u>R<sub>δ</sub></u>	<u>R<sub>θ</sub></u>
None	○	1.12	0.00263	4.27	0.630	0.467	1.35	7.13	0.646	17.32	11636	8626
None	△	1.11	0.00261	4.38	0.640	0.475	1.35	7.13	0.645	17.70	12069	8957
Sandpaper	●	1.11	0.00262	5.23	0.721	0.544	1.32	6.77	0.545	19.89	13601	10265
Sandpaper and 0.76 cm trip	◇	1.13	0.00271	10.04	1.019	0.818	1.24	5.32	0.116	27.66	19232	15462
Sandpaper and 0.69 cm trip	▽	1.12	0.00269	7.46	0.868	0.681	1.27	5.86	0.286	23.64	16423	12889



- |                    |                     |
|--------------------|---------------------|
| 1. Fan             | 6. Test Section     |
| 2. Honeycomb       | 7. Transition Piece |
| 3. Plenum          | 8. Return Bend      |
| 4. 8:1 Contraction | 9. Drive Motor      |
| 5. Entry Channel   |                     |

Figure 1.- Schematic of wind tunnel.



1. 8 Mesh x 0.43 mm Wire Screen
- 2 & 3. 20 Mesh x 0.33 mm Wire Screen
4. Honeycomb, 0.64 mm Cell x 10.2 cm Thick  
x 0.08 mm Wall Thickness
- 5, 6 & 7. 36 Mesh x 0.17 mm Wire Screen

Figure 2.- Plenum details.

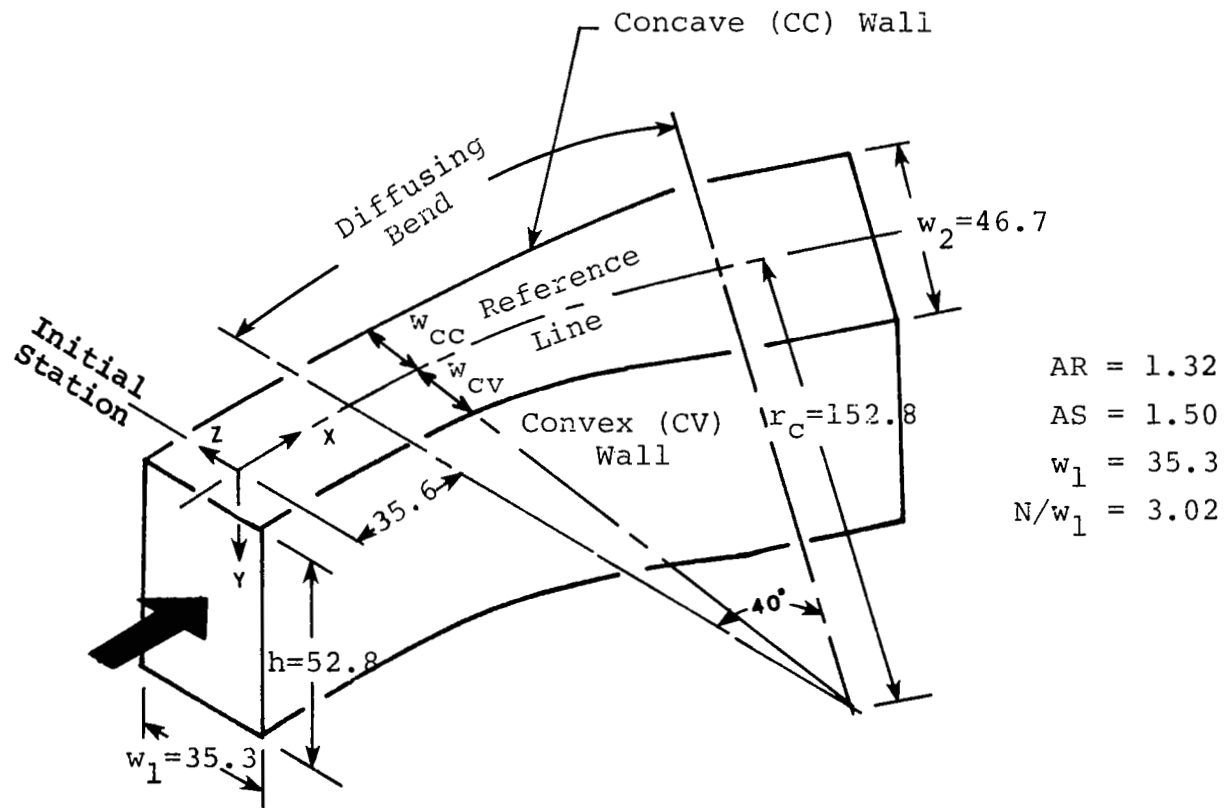
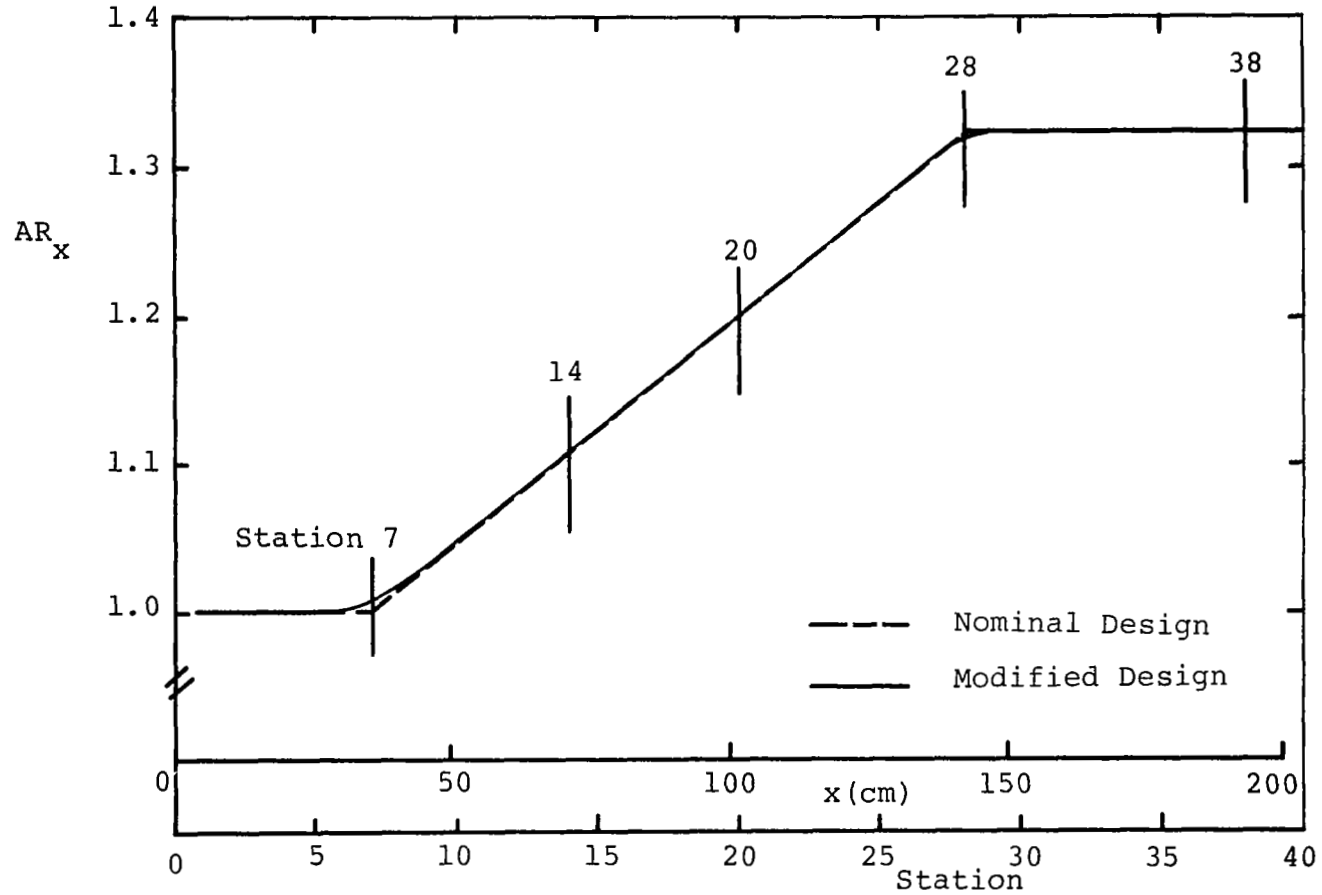


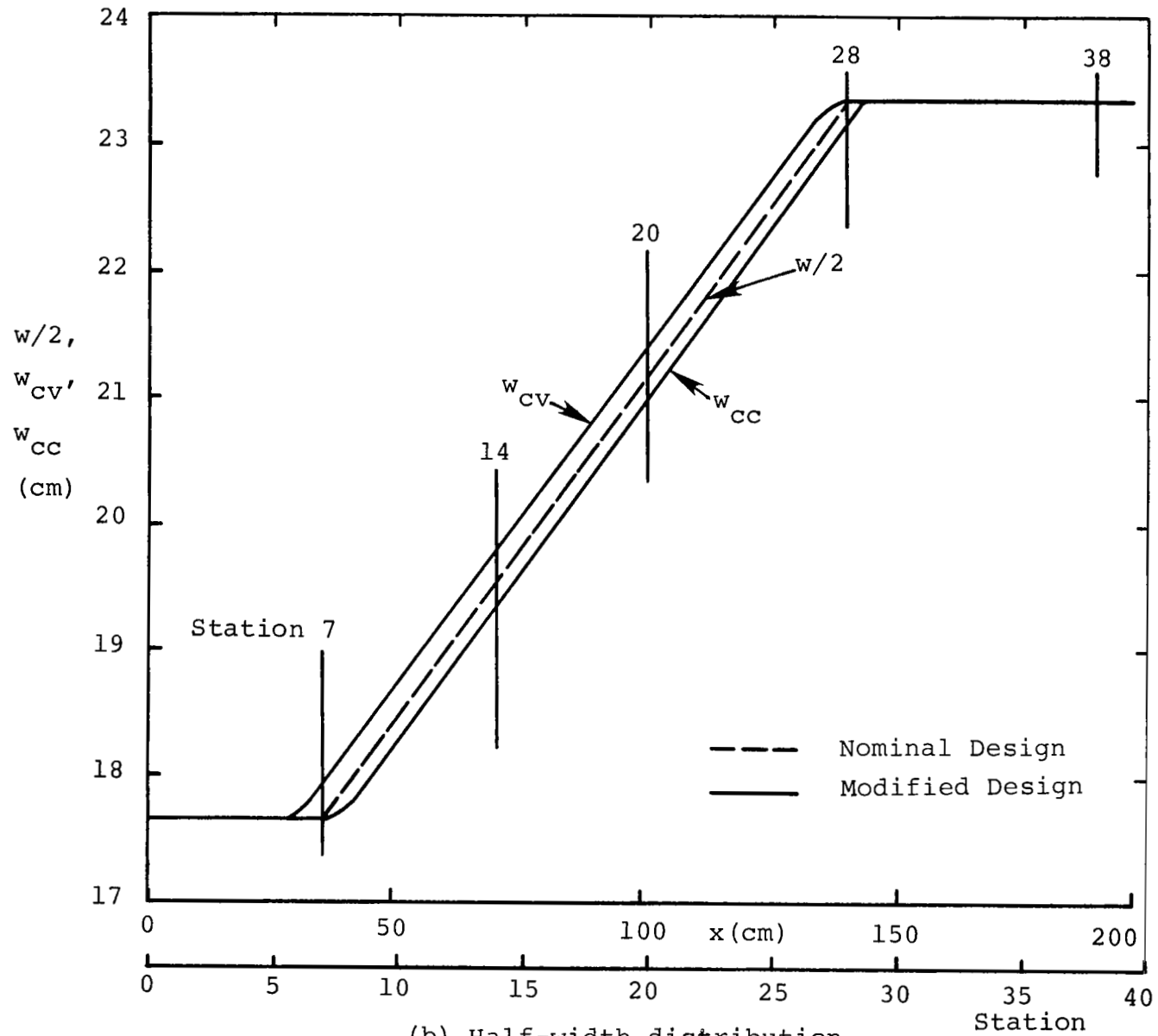
Figure 3.- Test-section details (dimensions in cm).



(a) Area ratio distribution

Figure 4.- Nominal and modified characteristics of the diffusing bend.





(b) Half-width distribution

Figure 4.- (Concluded)

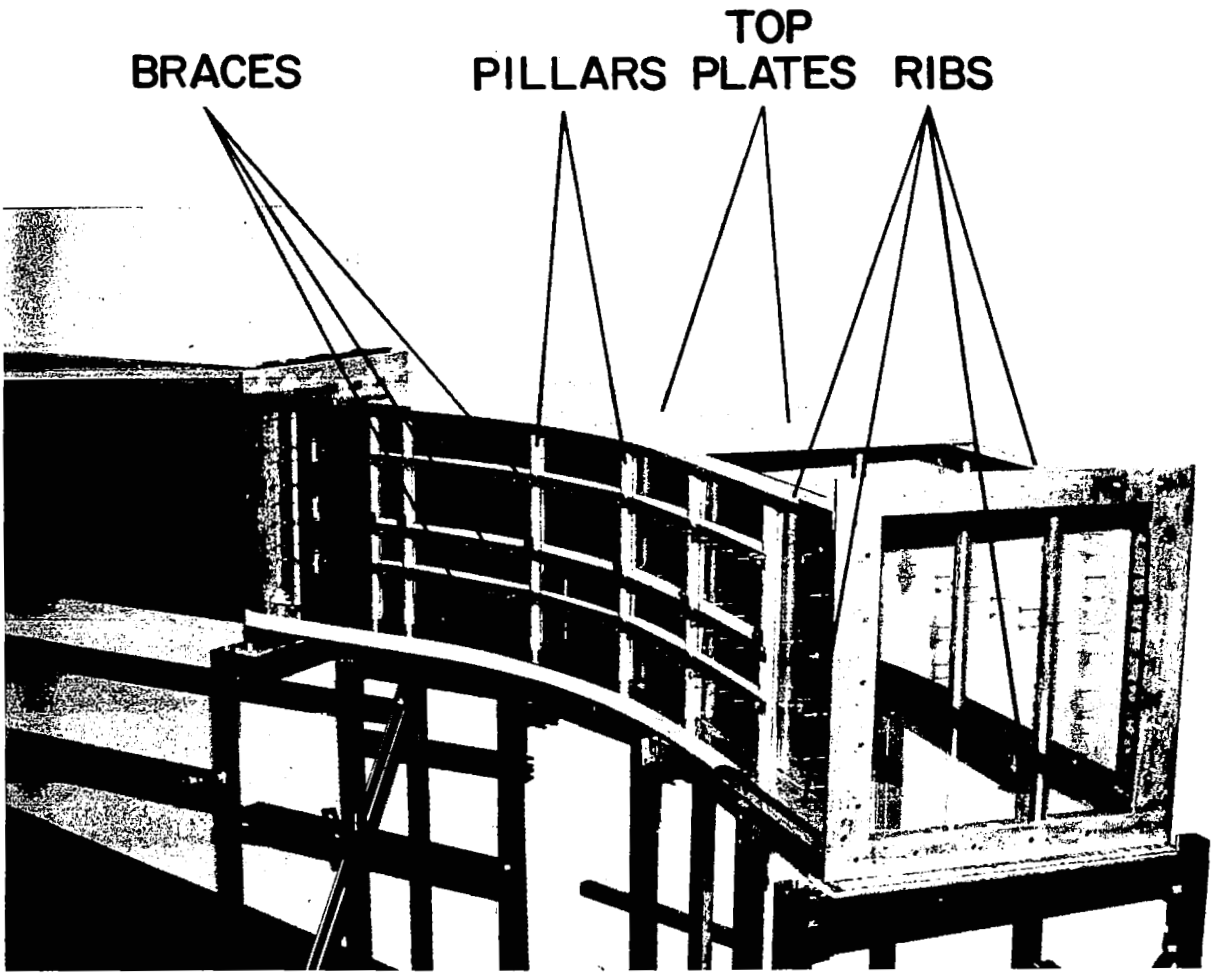
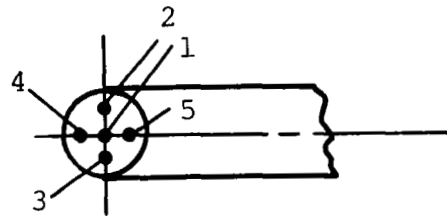


Figure 5. - Test Section



$$p_4 > p_5, \alpha_p > 0$$

$$p_3 > p_2, \beta > 0$$

Enlarged schematic of tip  
looking at front of probe.

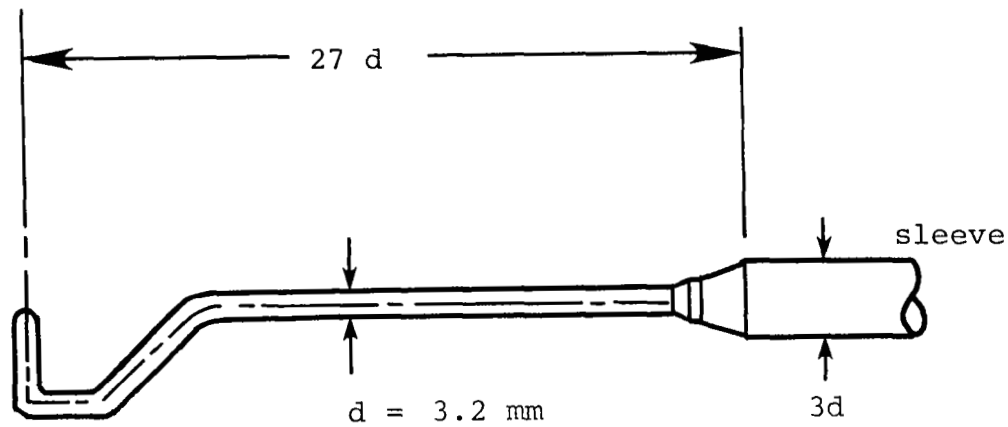


Figure 6.- Five-hole probe.

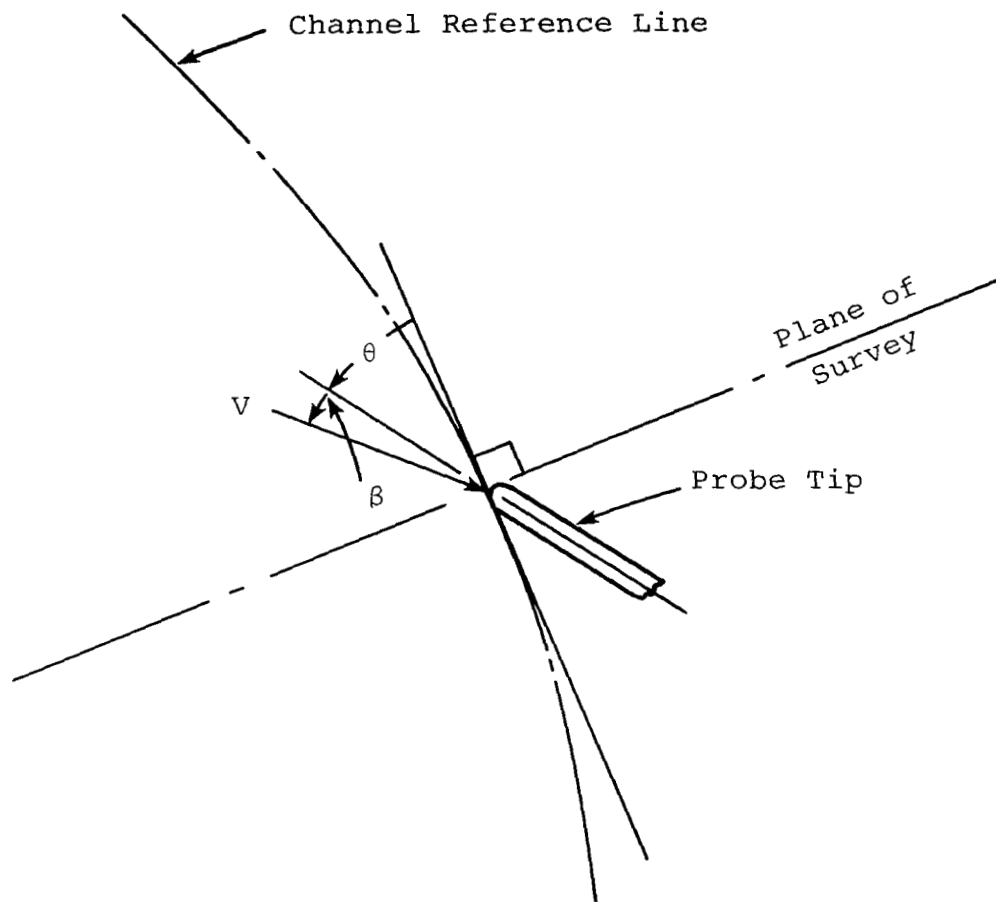


Figure 7.- Yaw-angle definitions (view from top of channel).

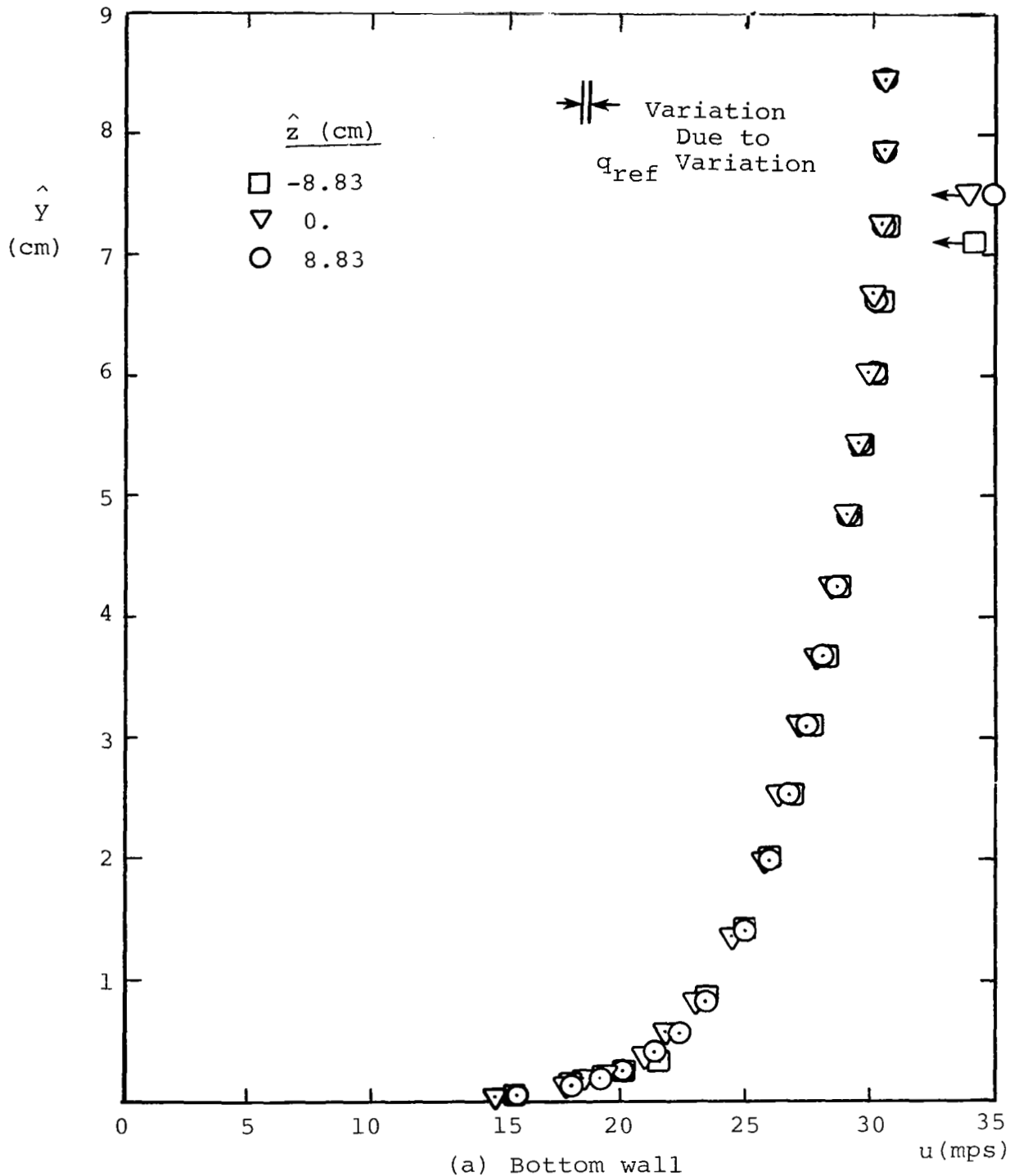


Figure 8.- Boundary-layer mean velocity profiles ( $u$  vs.  $\hat{y}$ ) at the initial station.

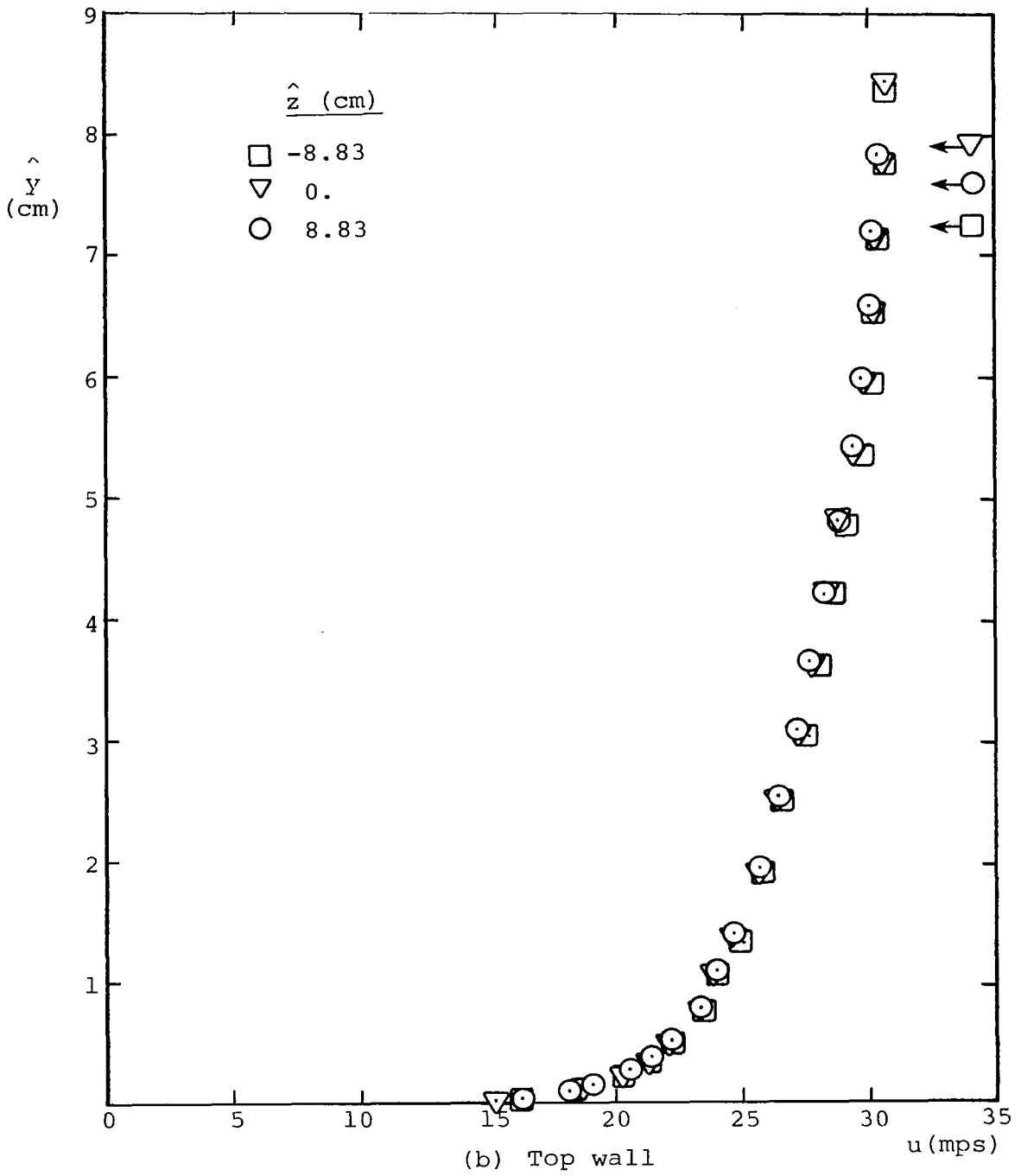


Figure 8.- (Continued)

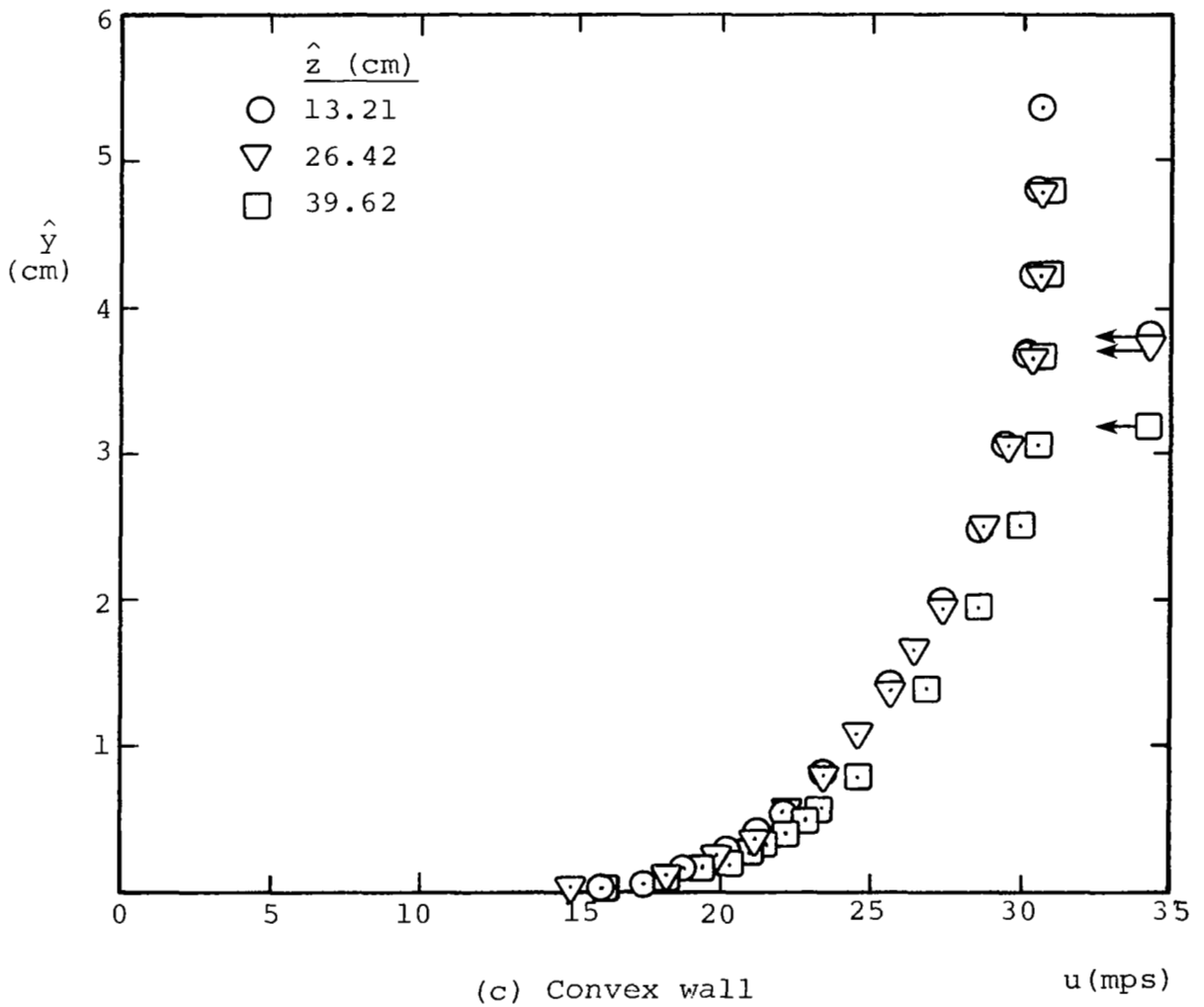
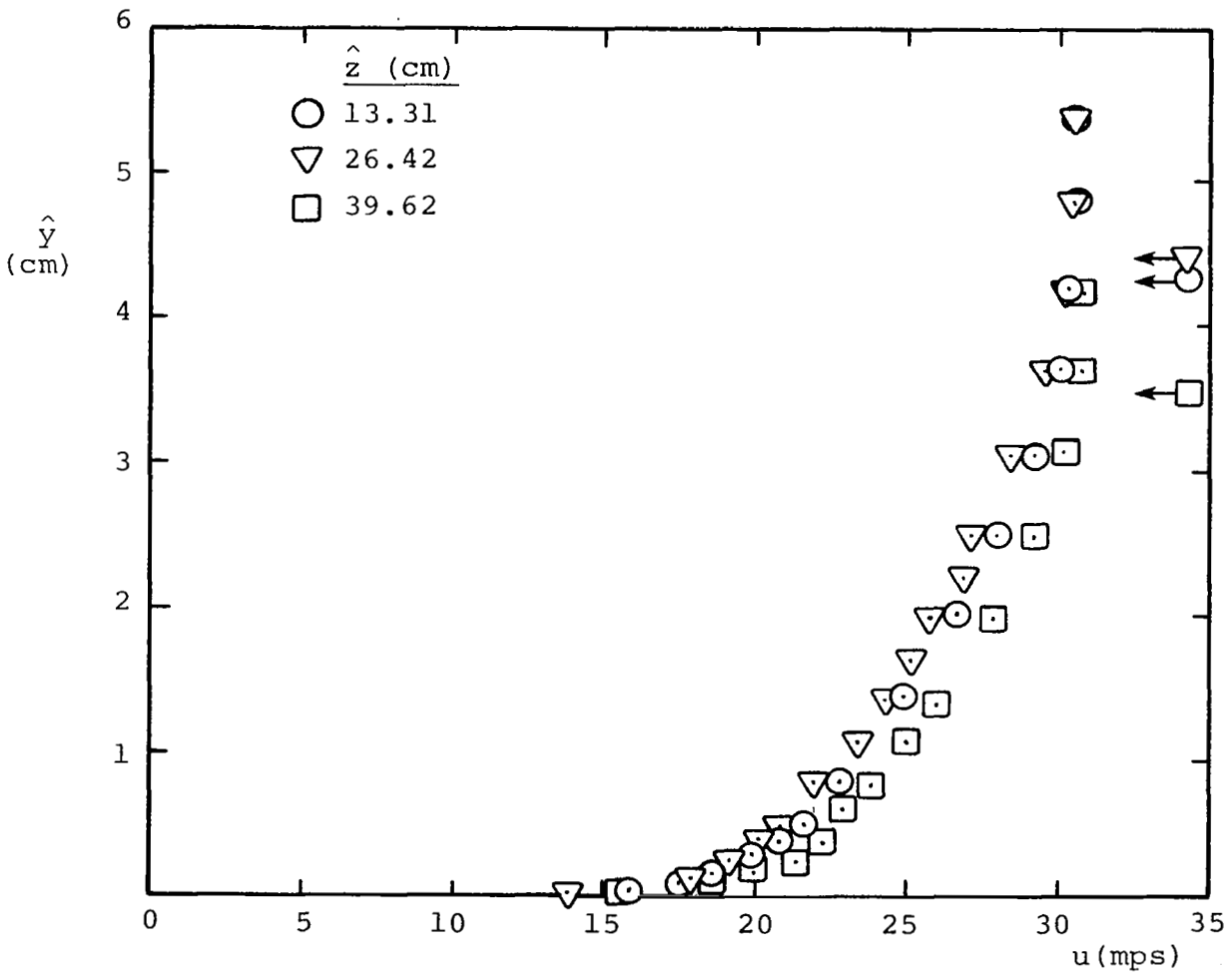


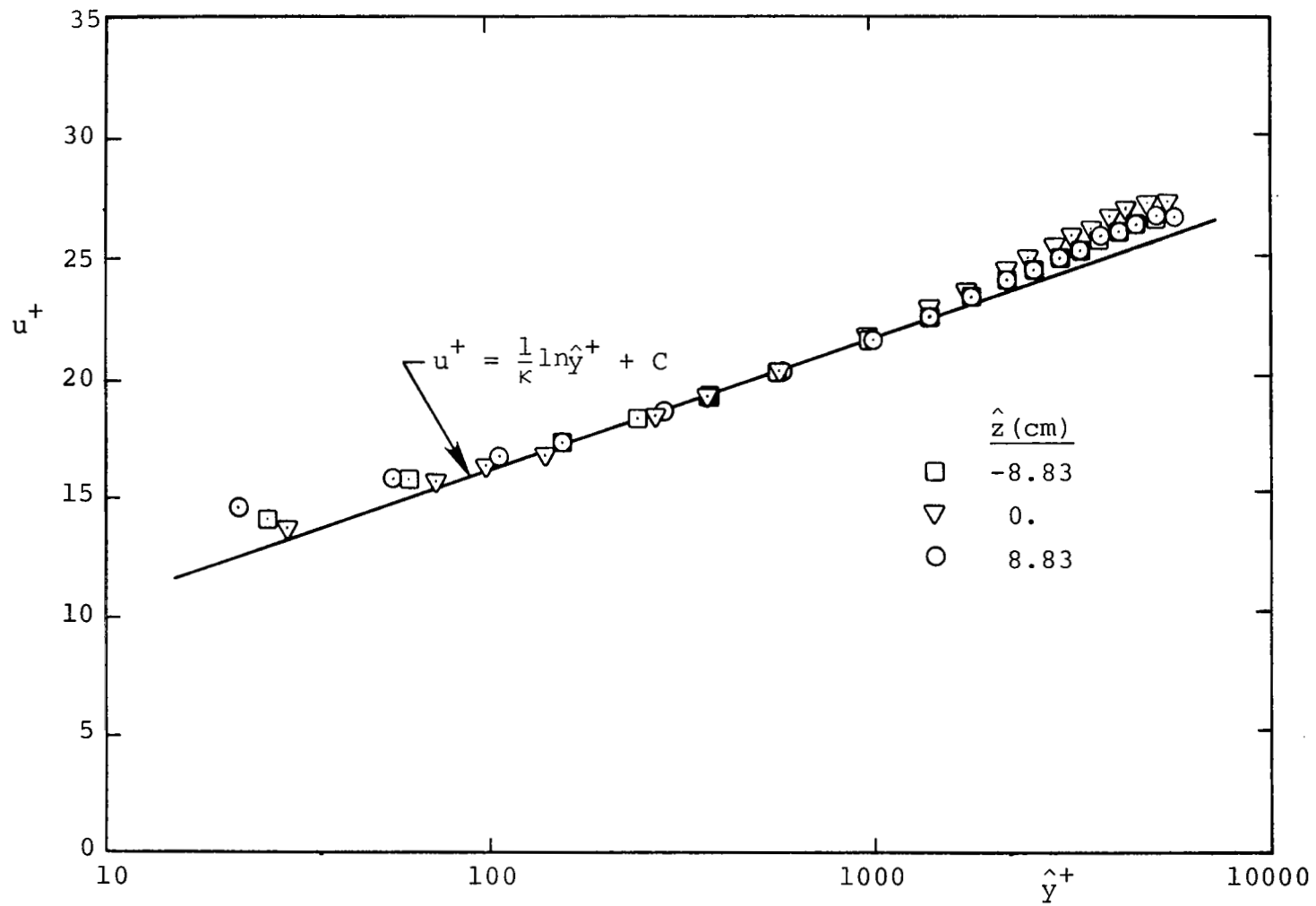
Figure 8.- (Continued)



(d) Concave wall

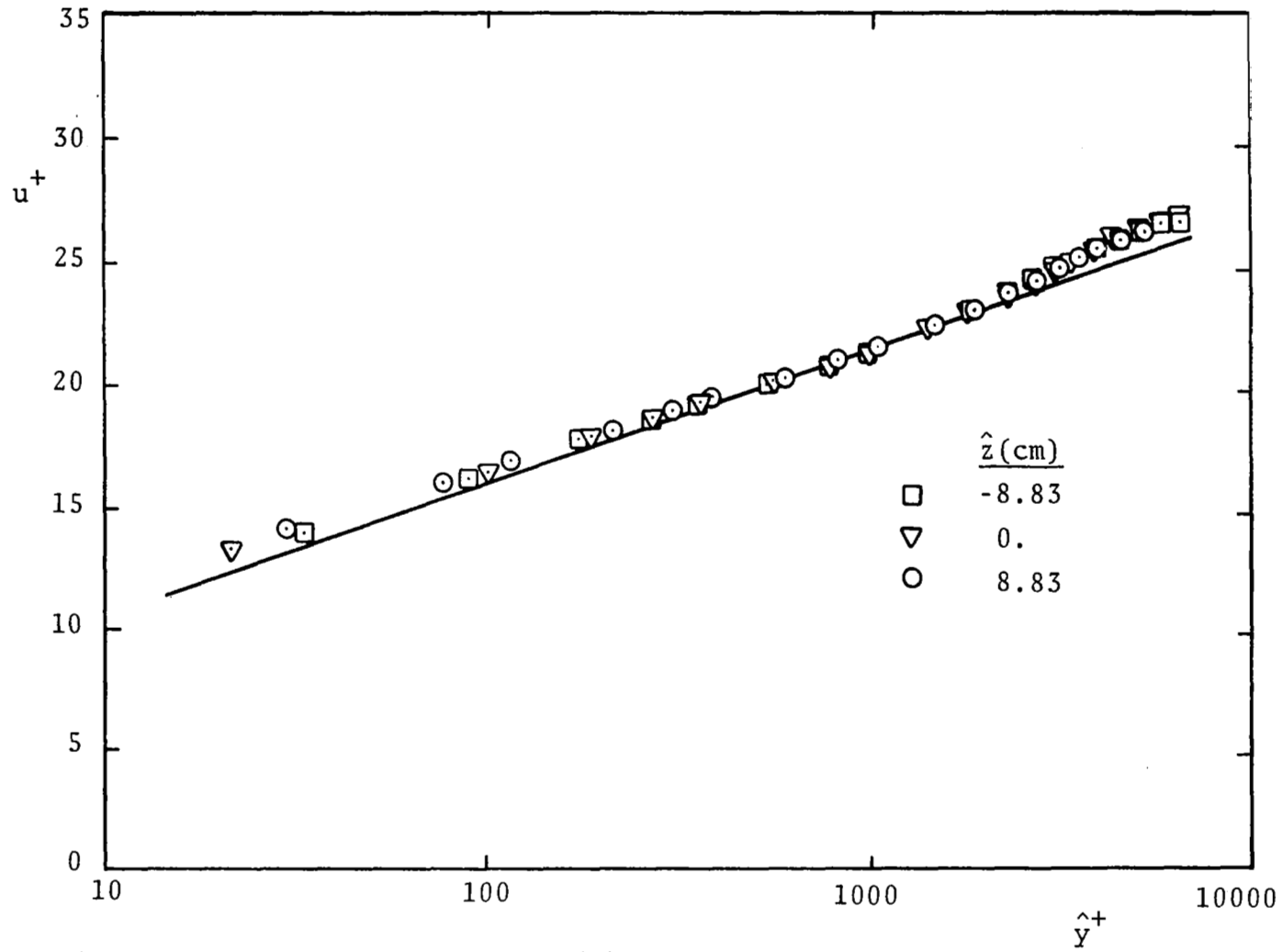
Figure 8.- (Concluded)





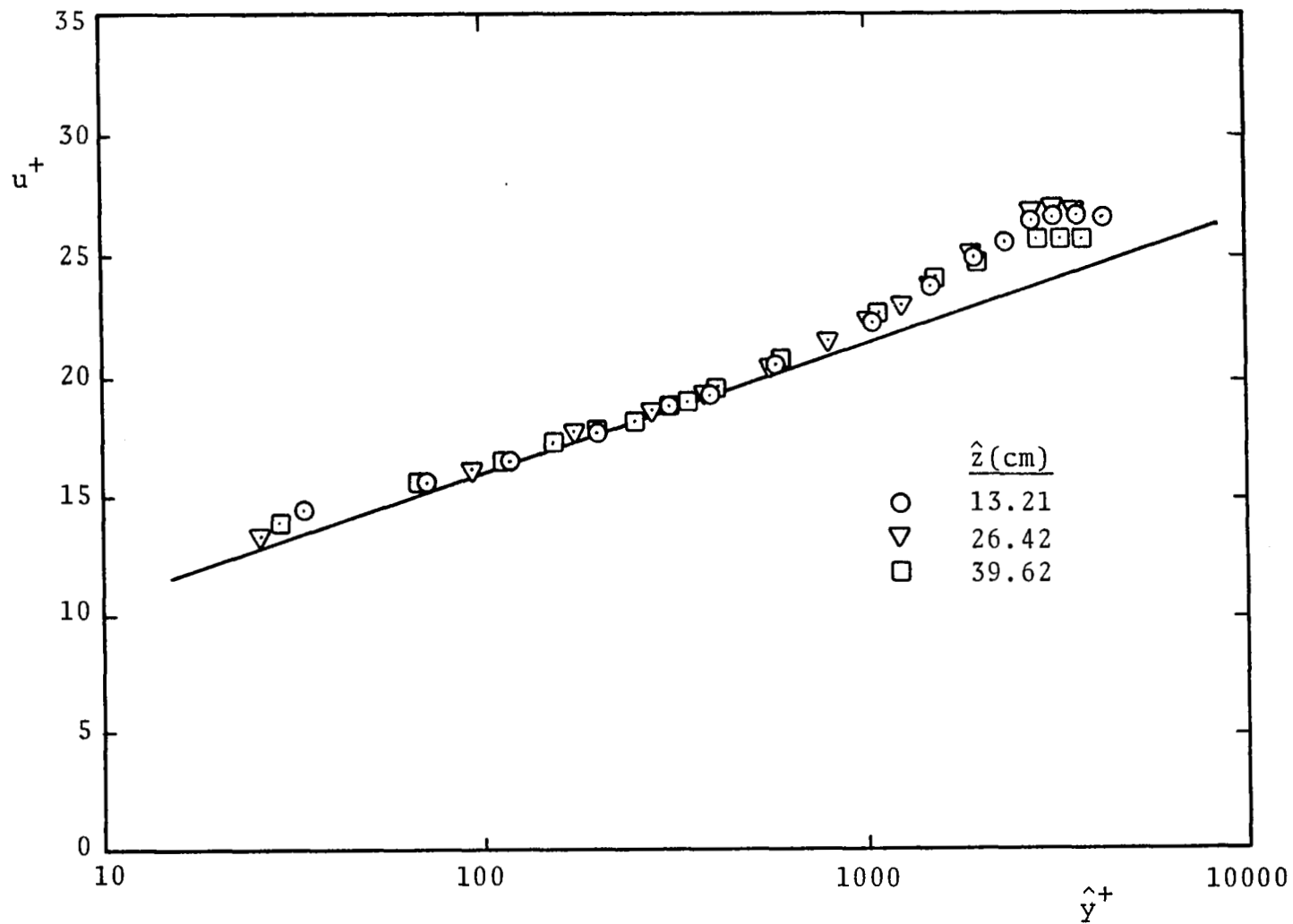
(a) Bottom wall

Figure 9.- Boundary-layer mean velocity profiles (wall variables) at the initial station



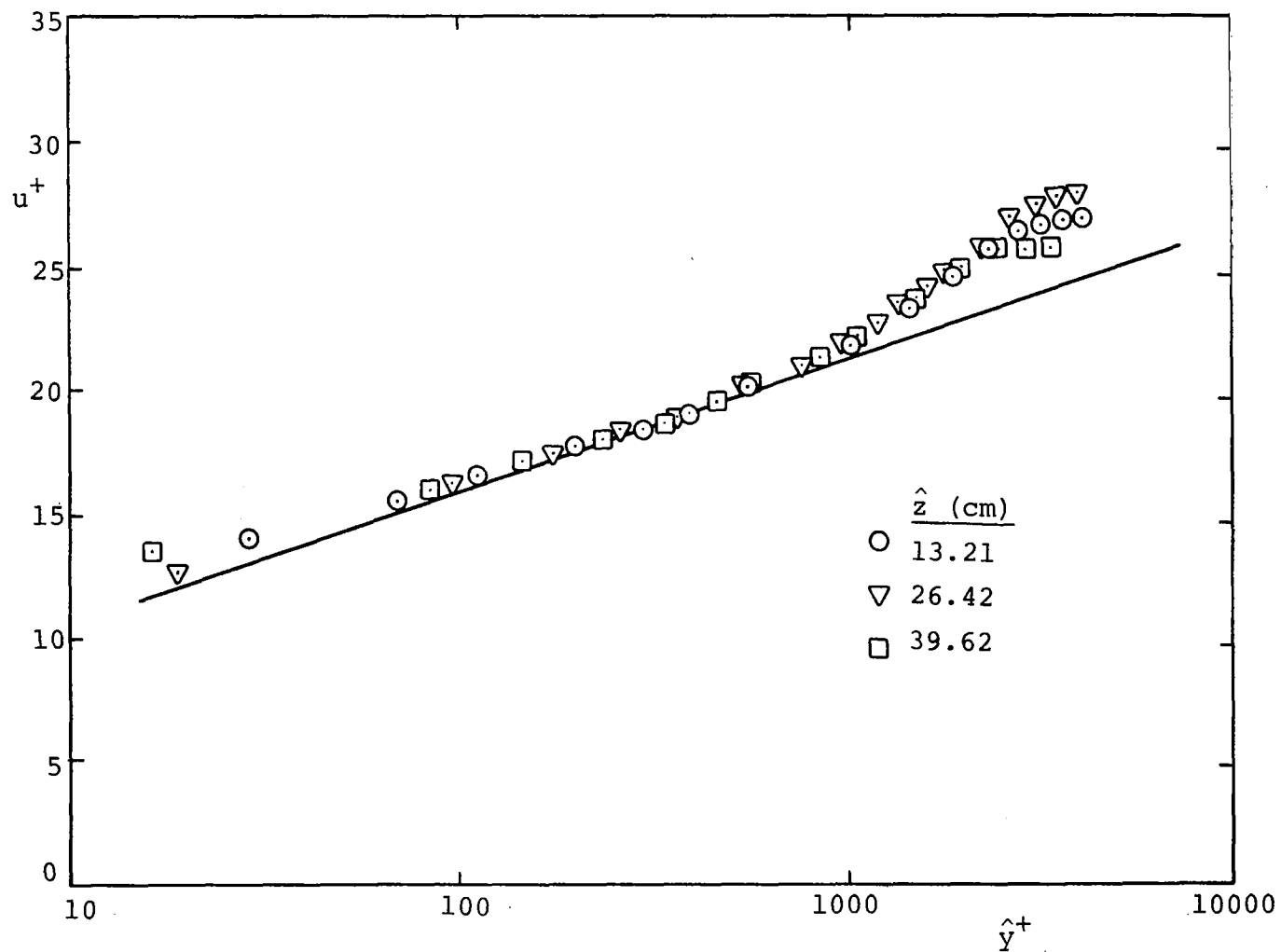
(b) Top wall

Figure 9.- (Continued)



(c) Convex wall

Figure 9.- (Continued)



(d) Concave wall

Figure 9.- (Concluded)

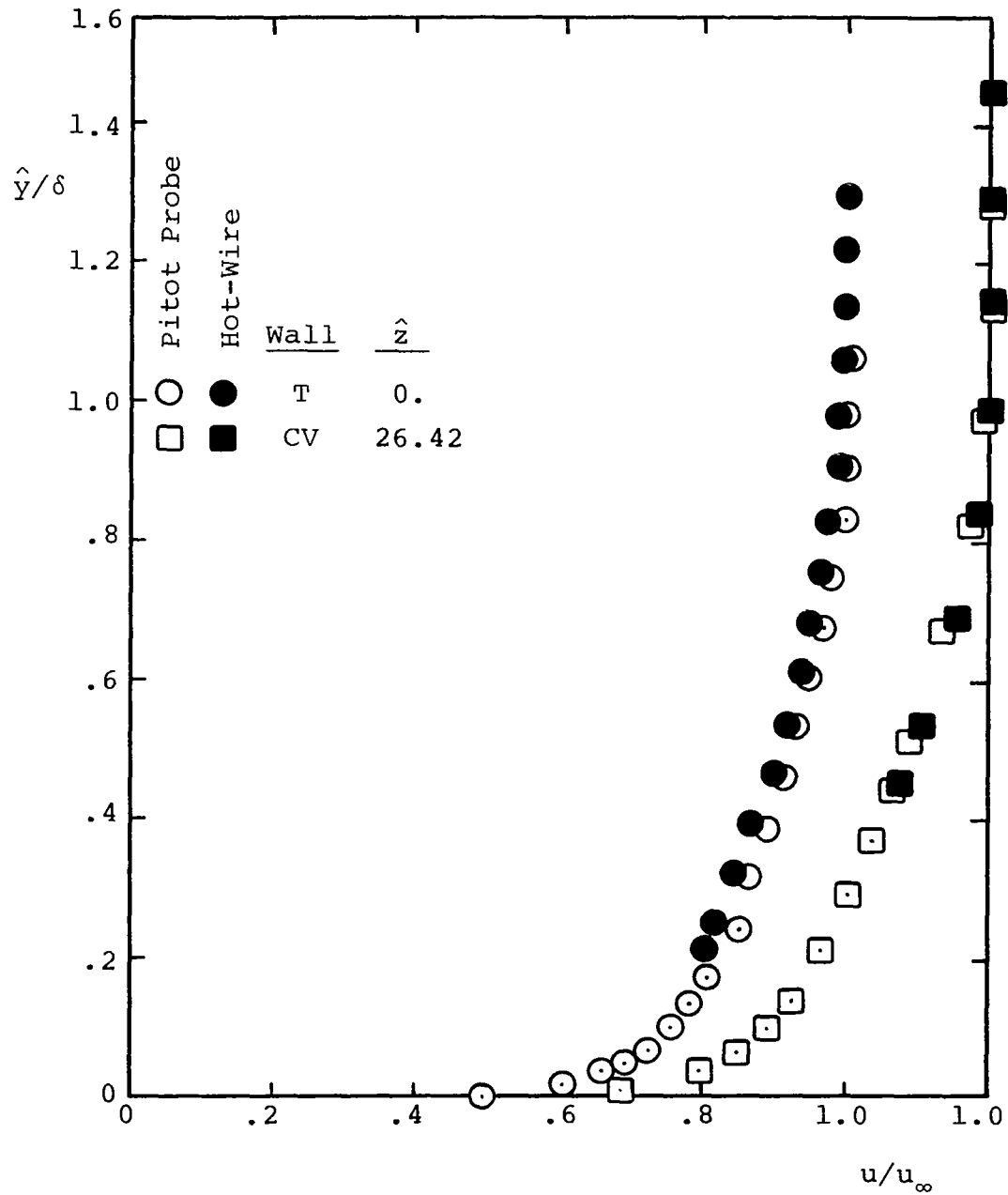


Figure 10.- Boundary-layer mean velocity profiles at the initial station. Pitot probe vs. hot-wire probe. (Note the shifted origin for the CV-wall data.)

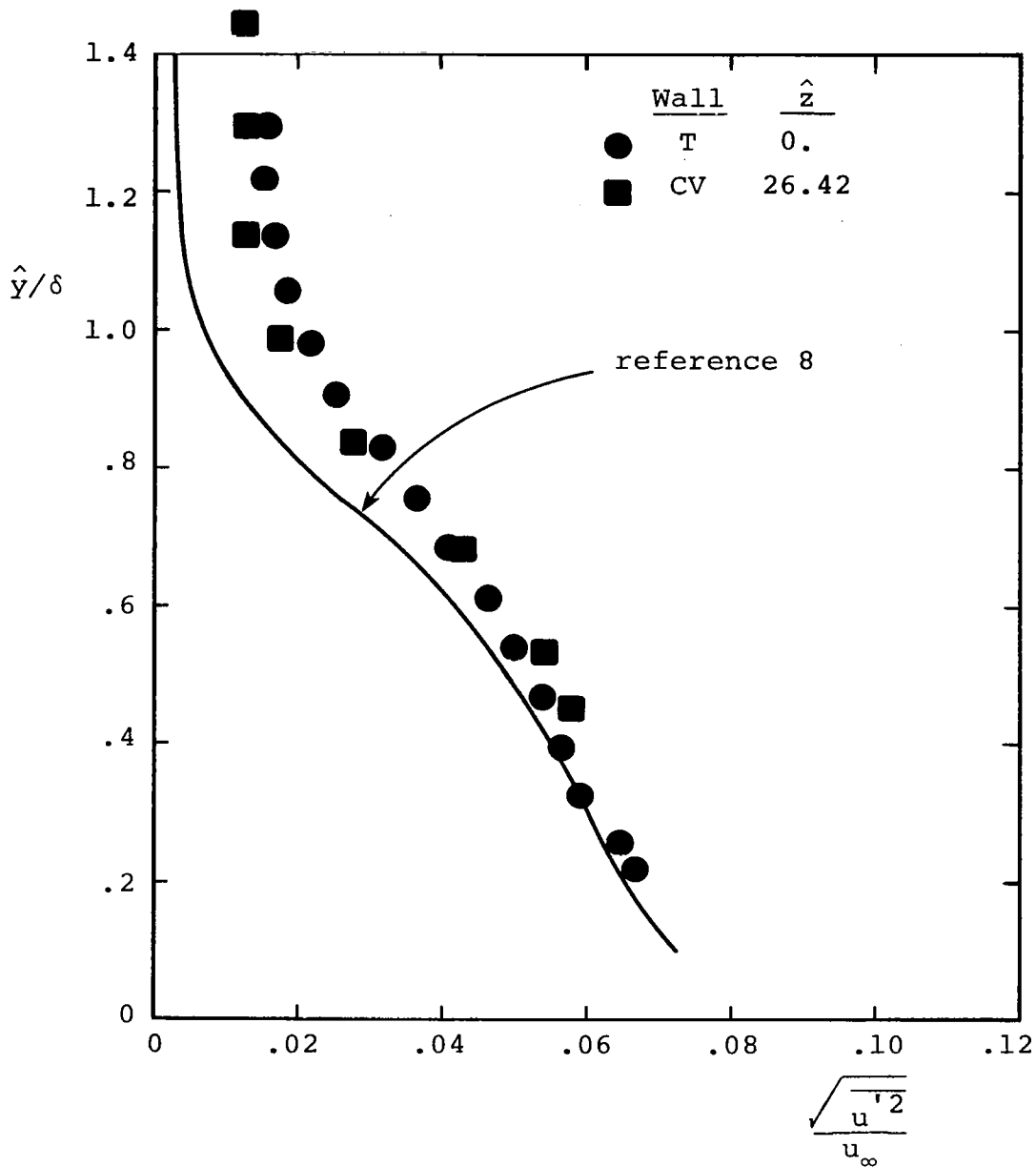


Figure 11.- Boundary-layer streamwise turbulence intensity profiles at the initial station.

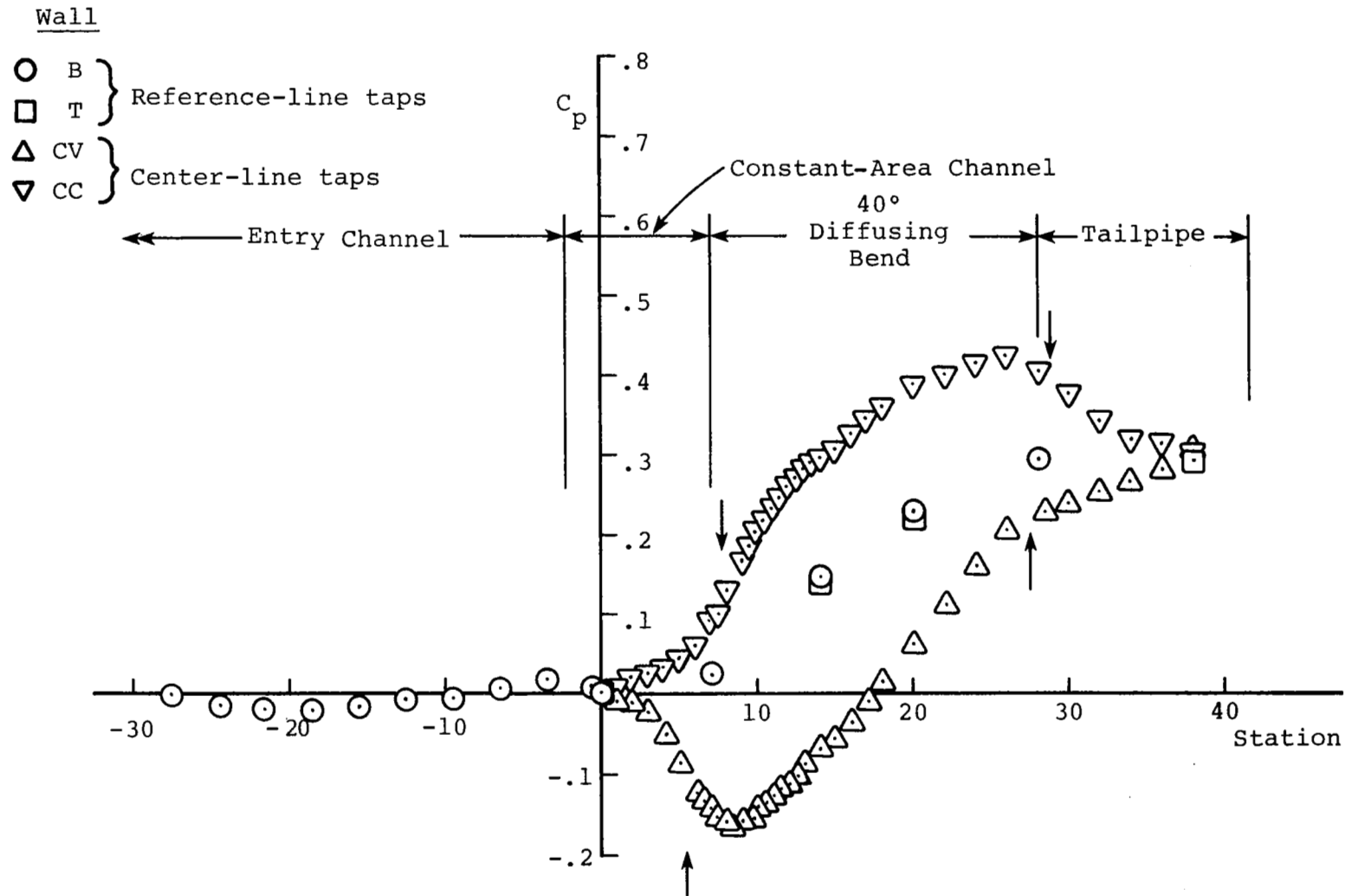
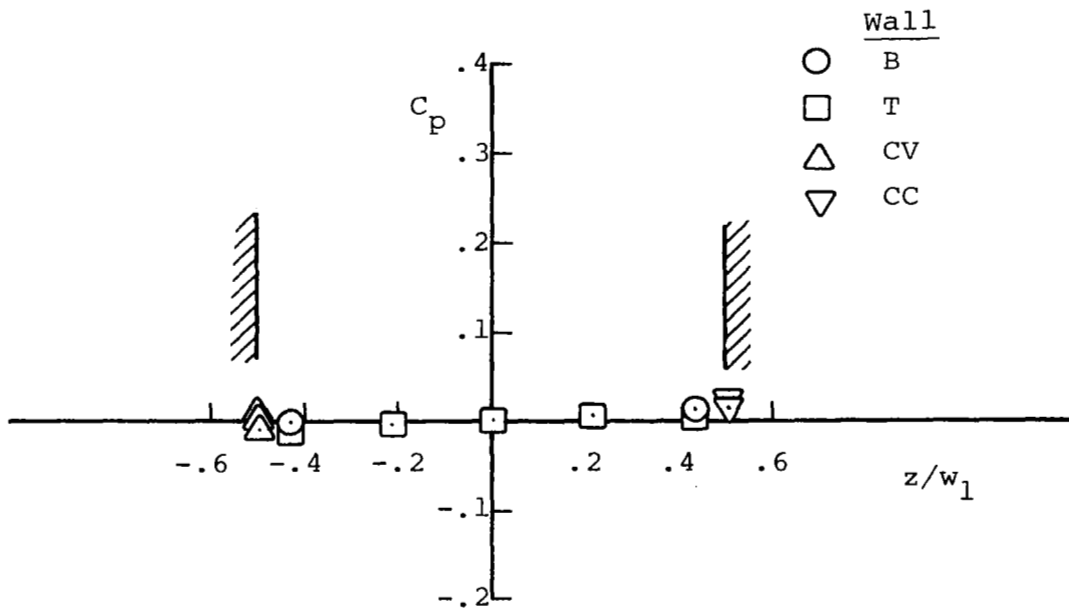
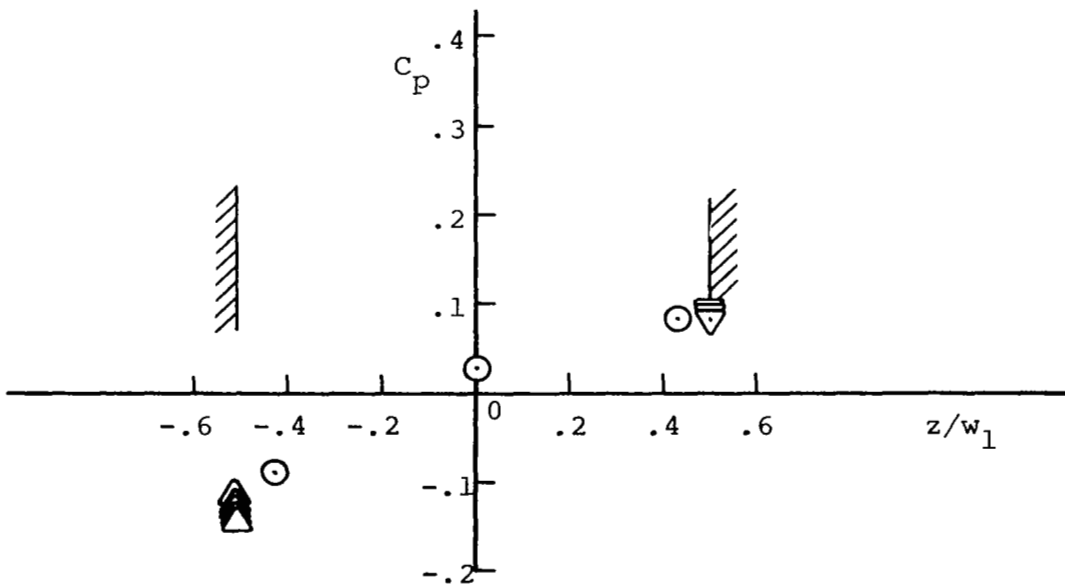


Figure 12.- Wall static pressure coefficients.



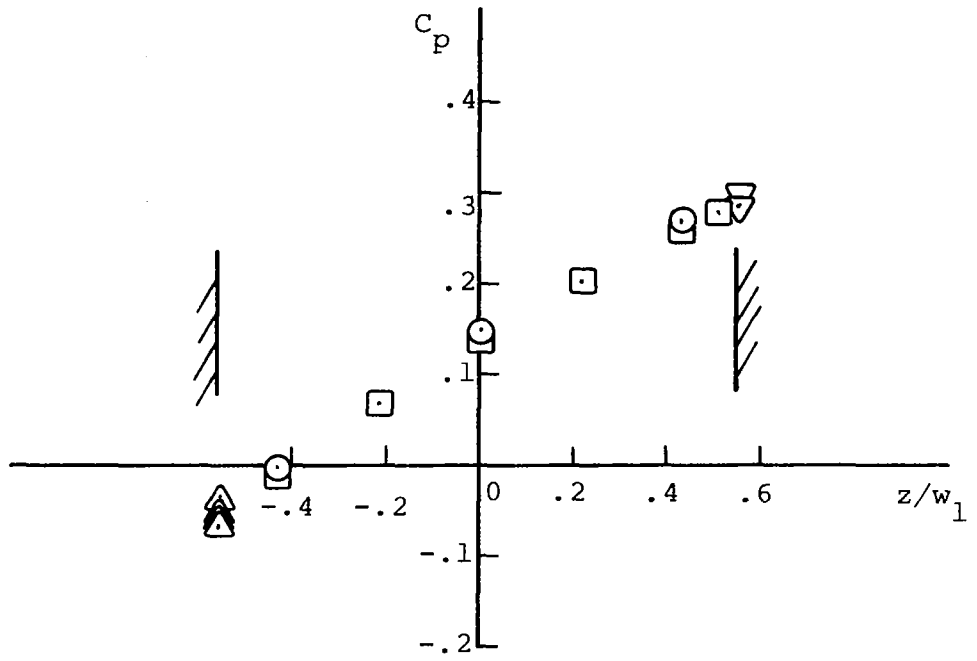
(a) Station 0



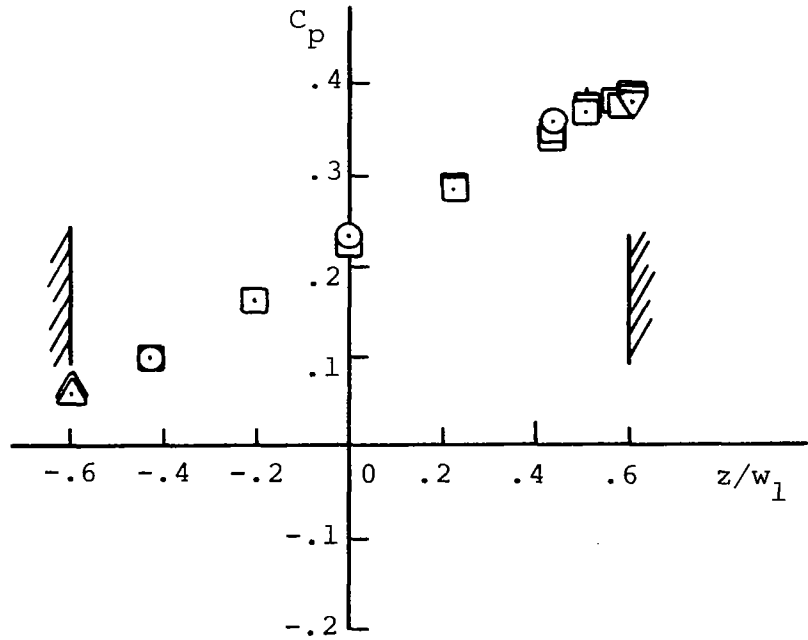
(b) Station 7

Figure 13.- Cross-channel variation in wall static pressure coefficients.



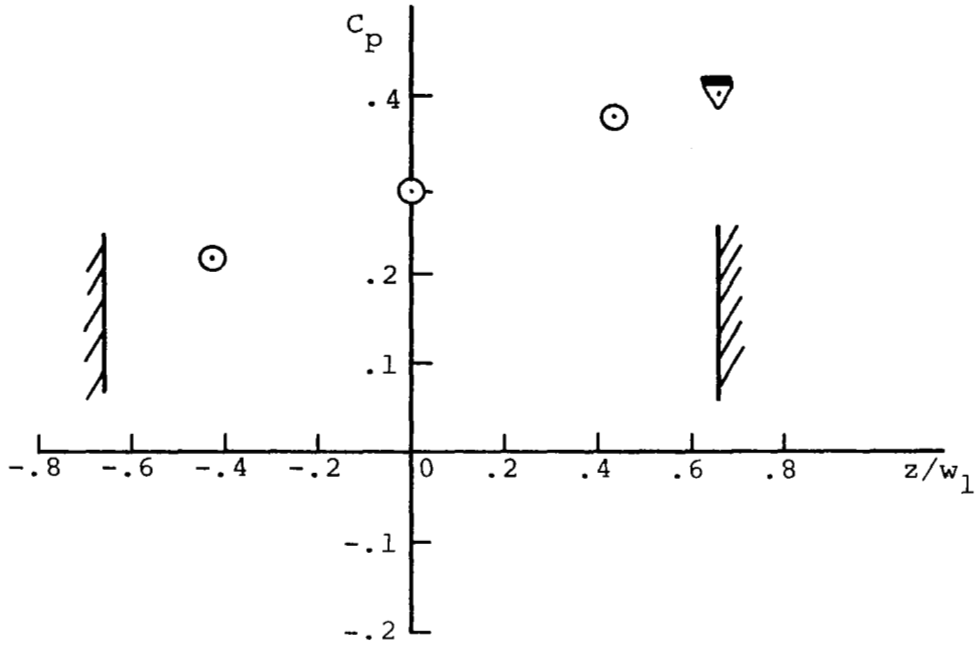


(c) Station 14

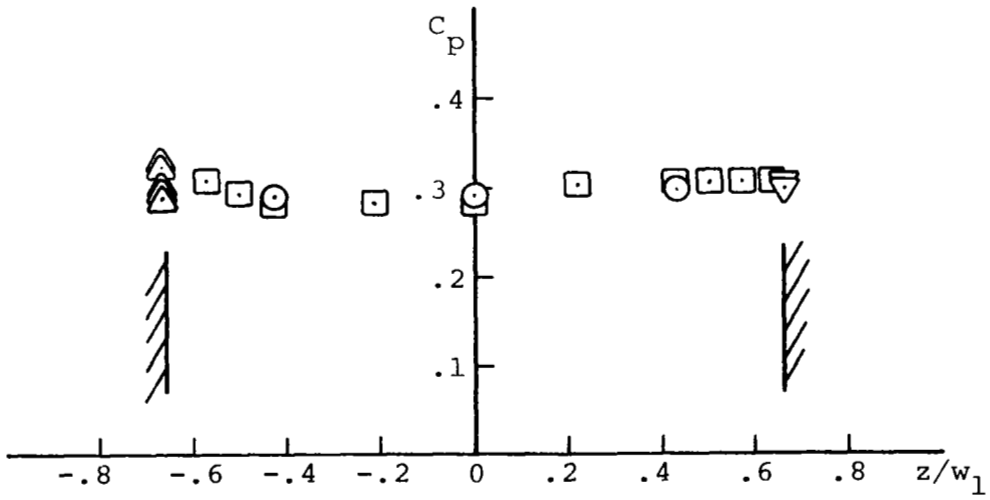


(d) Station 20

Figure 13.- (Continued)

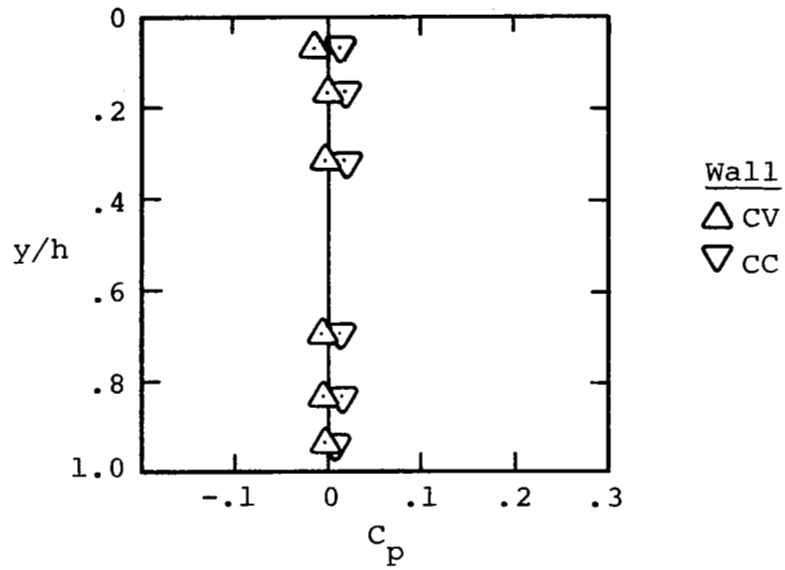


(e) Station 28

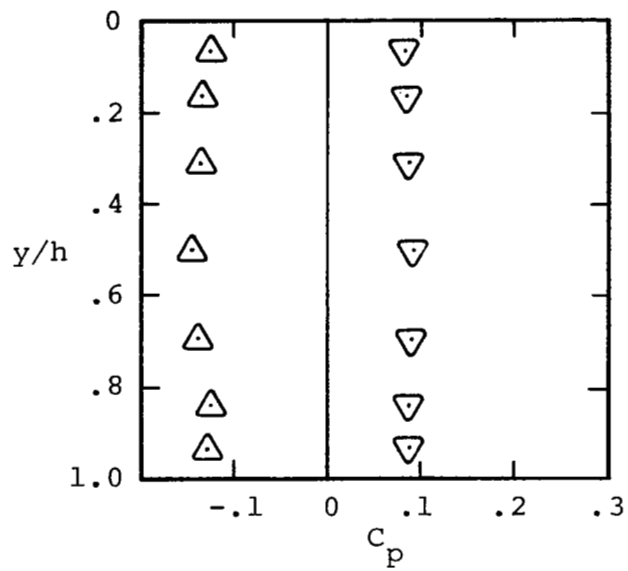


(f) Station 38

Figure 13.- (Concluded)

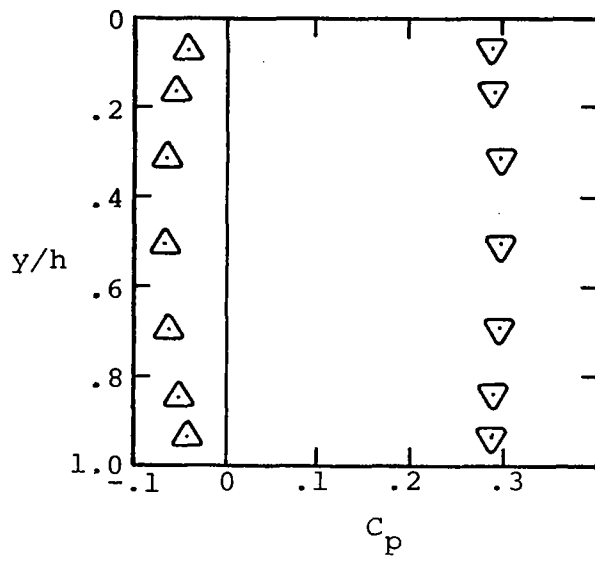


(a) Station 0

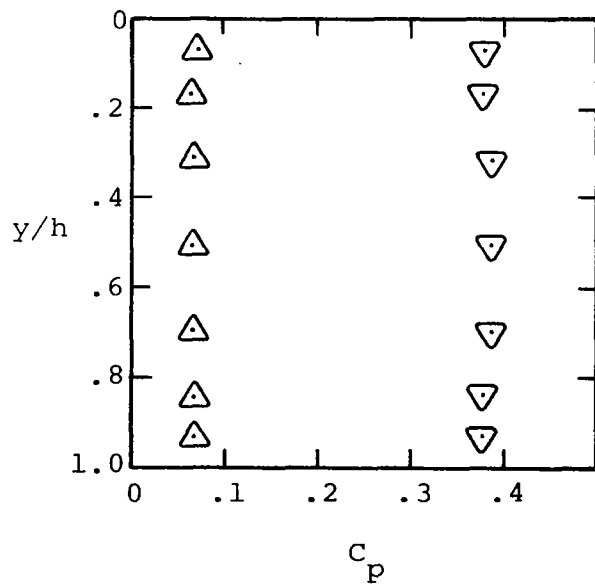


(b) Station 7

Figure 14.- Vertical variation in wall static pressure coefficients.

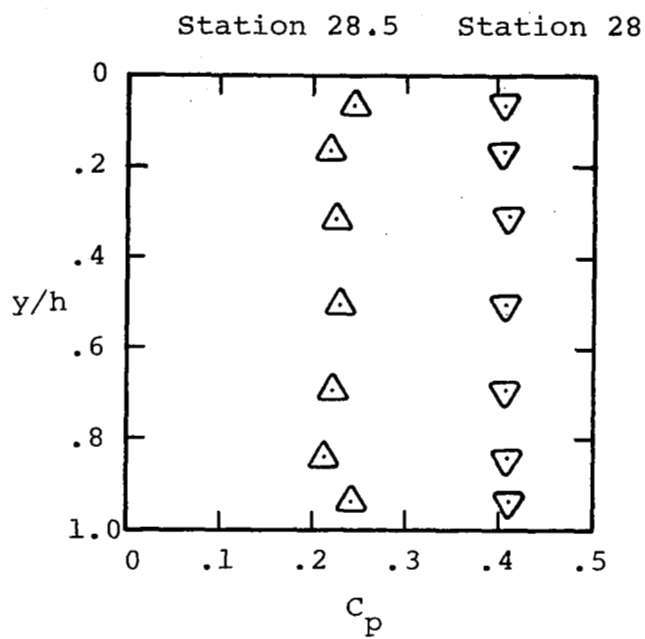


(c) Station 14

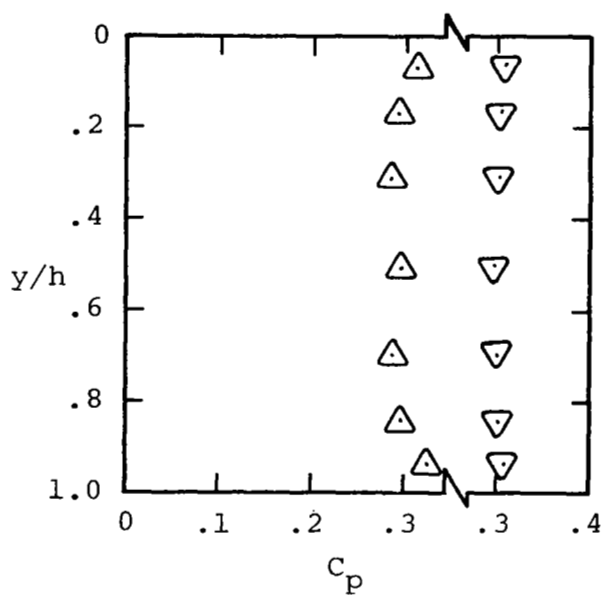


(d) Station 20

Figure 14.- (Continued)

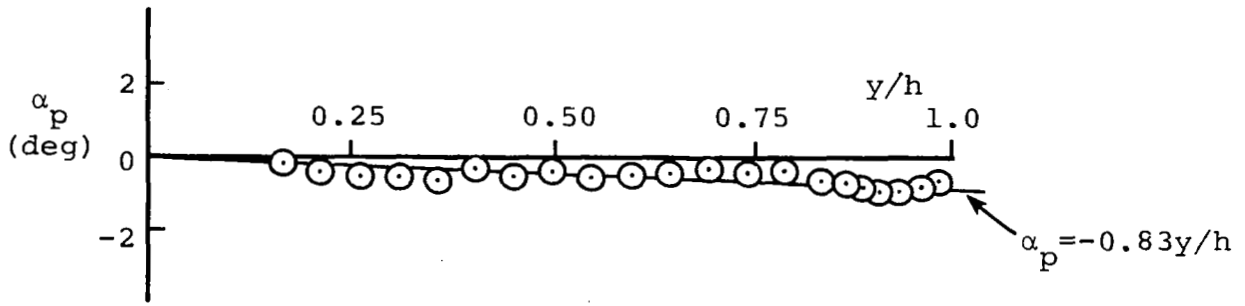


(e) Stations 28 and 28.5

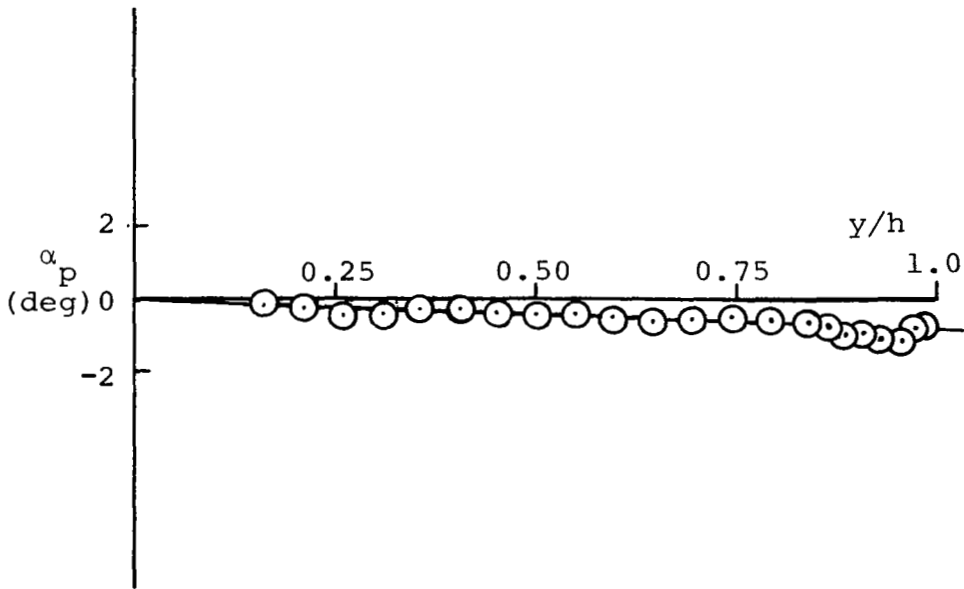


(f) Station 38

Figure 14.- (Concluded)

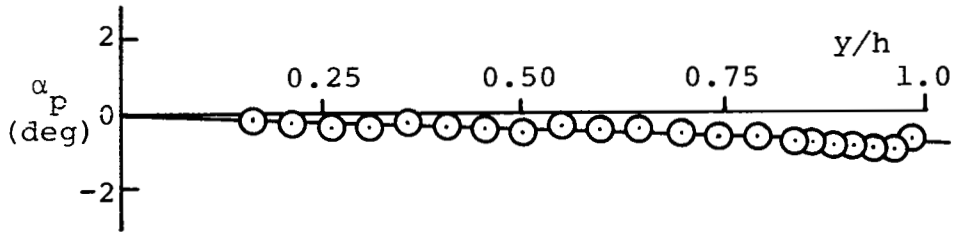


(a)  $z/w_1 = -0.375$

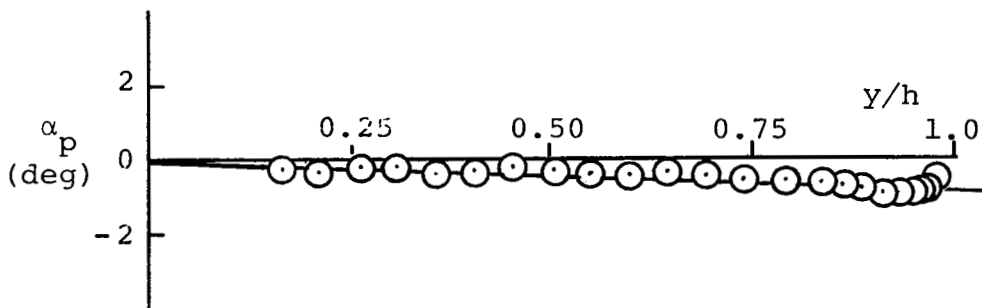


(b)  $z/w_1 = -0.25$

Figure 15.- Profiles of  $\alpha_p$  at the initial station.

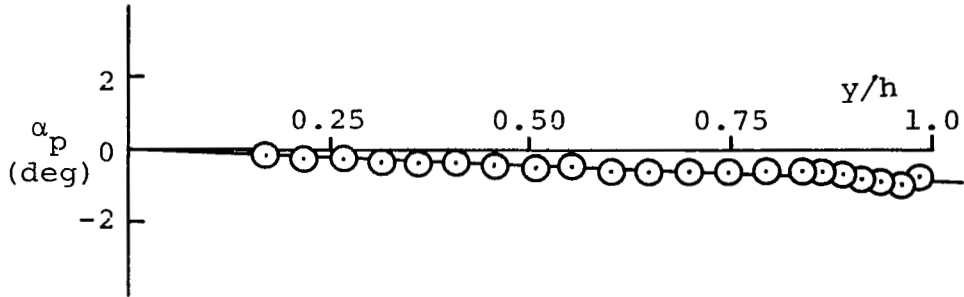


(c)  $z/w_1 = -0.125$

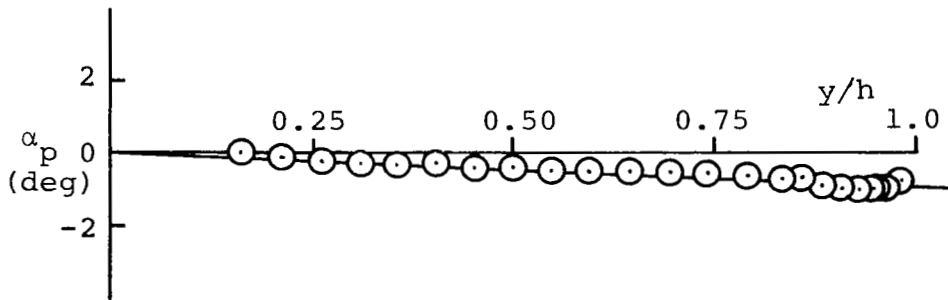


(d)  $z/w_1 = 0$

Figure 15.- (Continued)



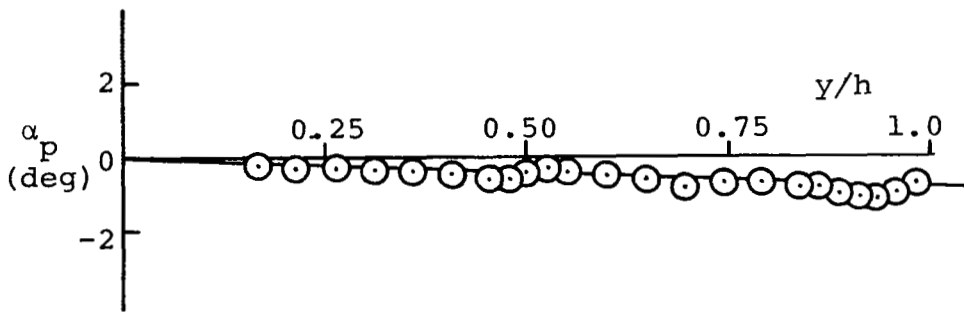
(e)  $z/w_1 = 0.125$



(f)  $z/w_1 = 0.25$

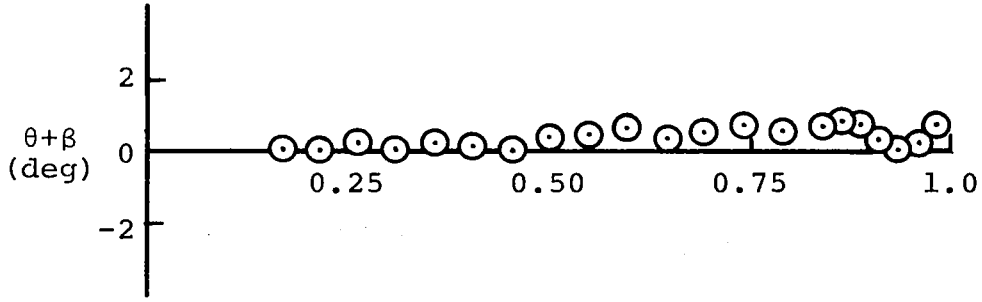
Figure 15.- (Continued)



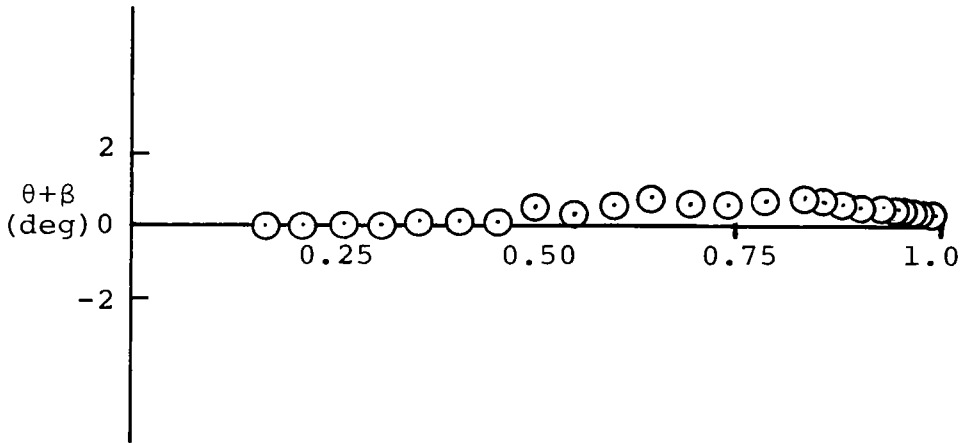


(g)  $z/w_1 = 0.375$

Figure 15.- (Concluded)

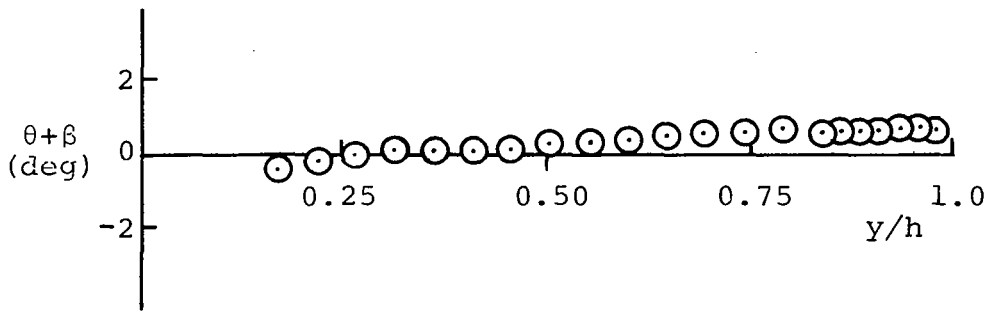


(a)  $z/w_1 = -0.375$

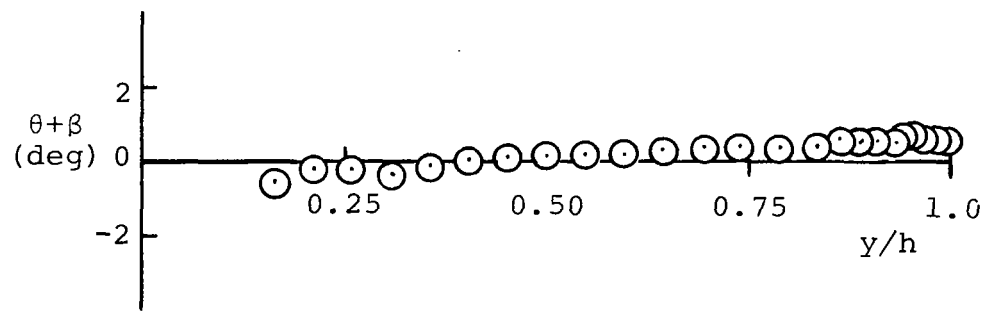


(b)  $z/w_1 = -0.25$

Figure 16.- Profiles of  $\theta + \beta$  at the initial station.

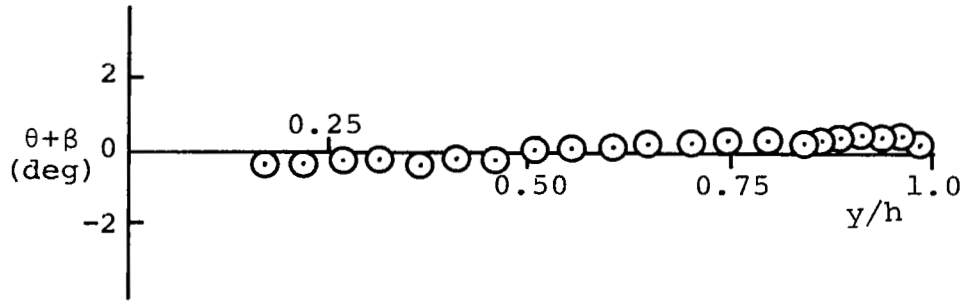


(c)  $z/w_1 = -0.125$

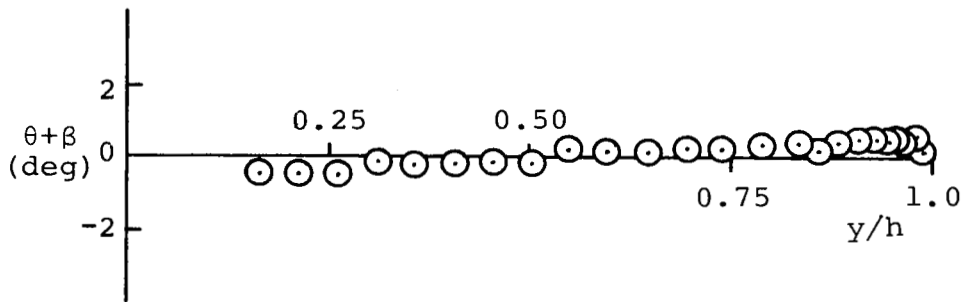


(d)  $z/w_1 = 0$

Figure 16.- (Continued)

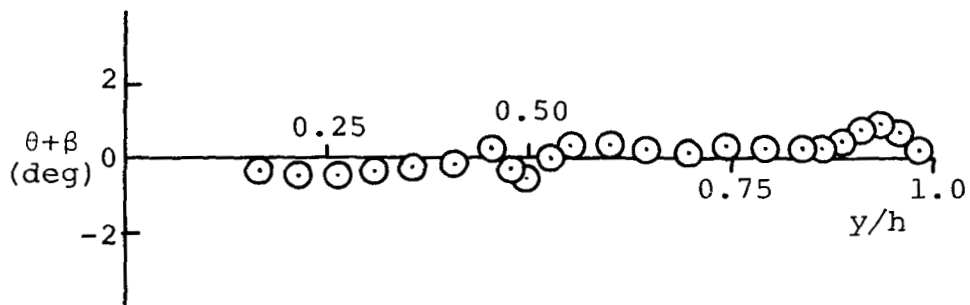


(e)  $z/w_1 = 0.125$



(f)  $z/w_1 = 0.25$

Figure 16.- (Continued)



(g)  $z/w_1 = 0.375$

Figure 16.- (Concluded)

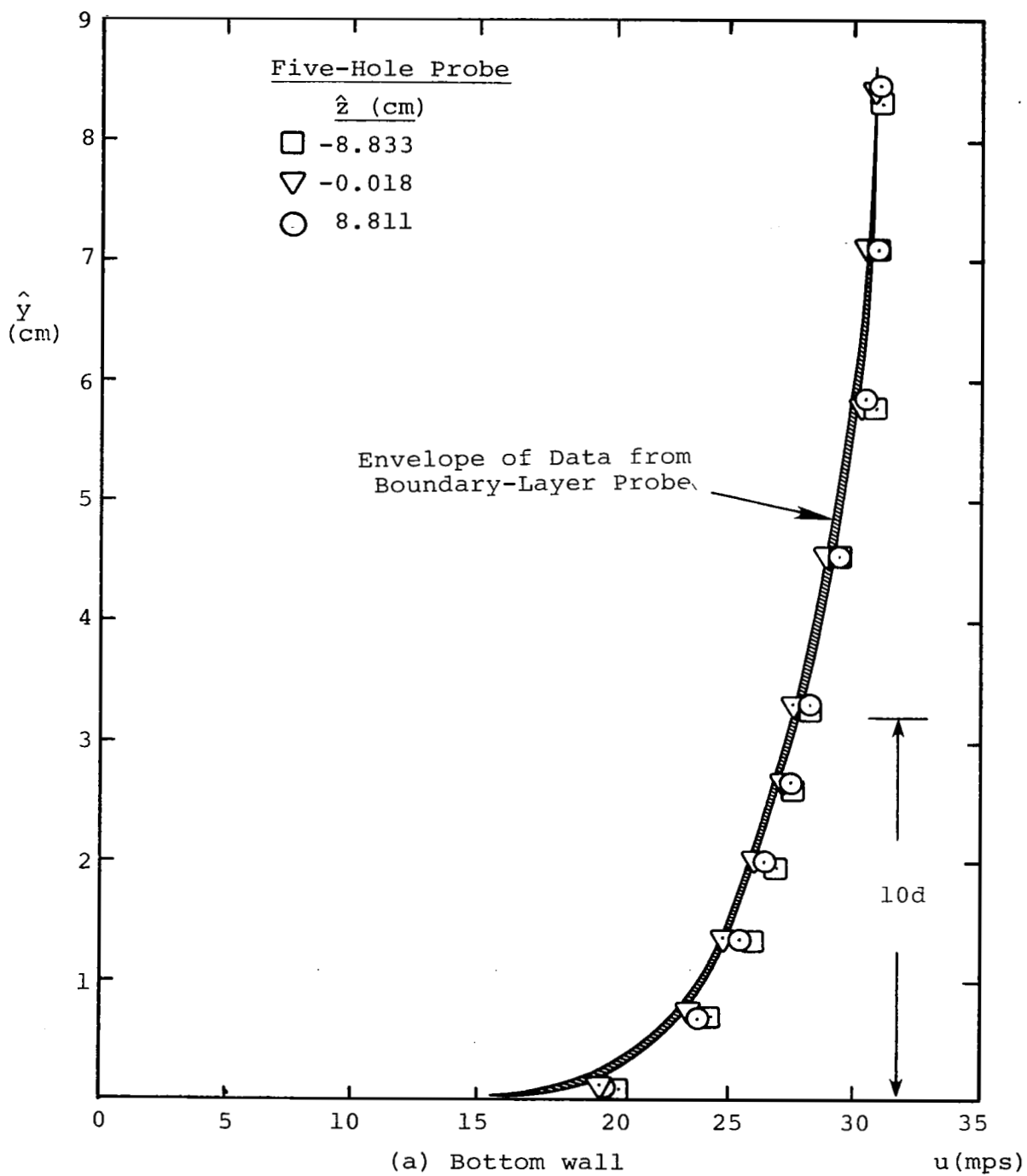


Figure 17.- Comparison of initial-station boundary-layer profiles as measured by the boundary-layer and five-hole probes.

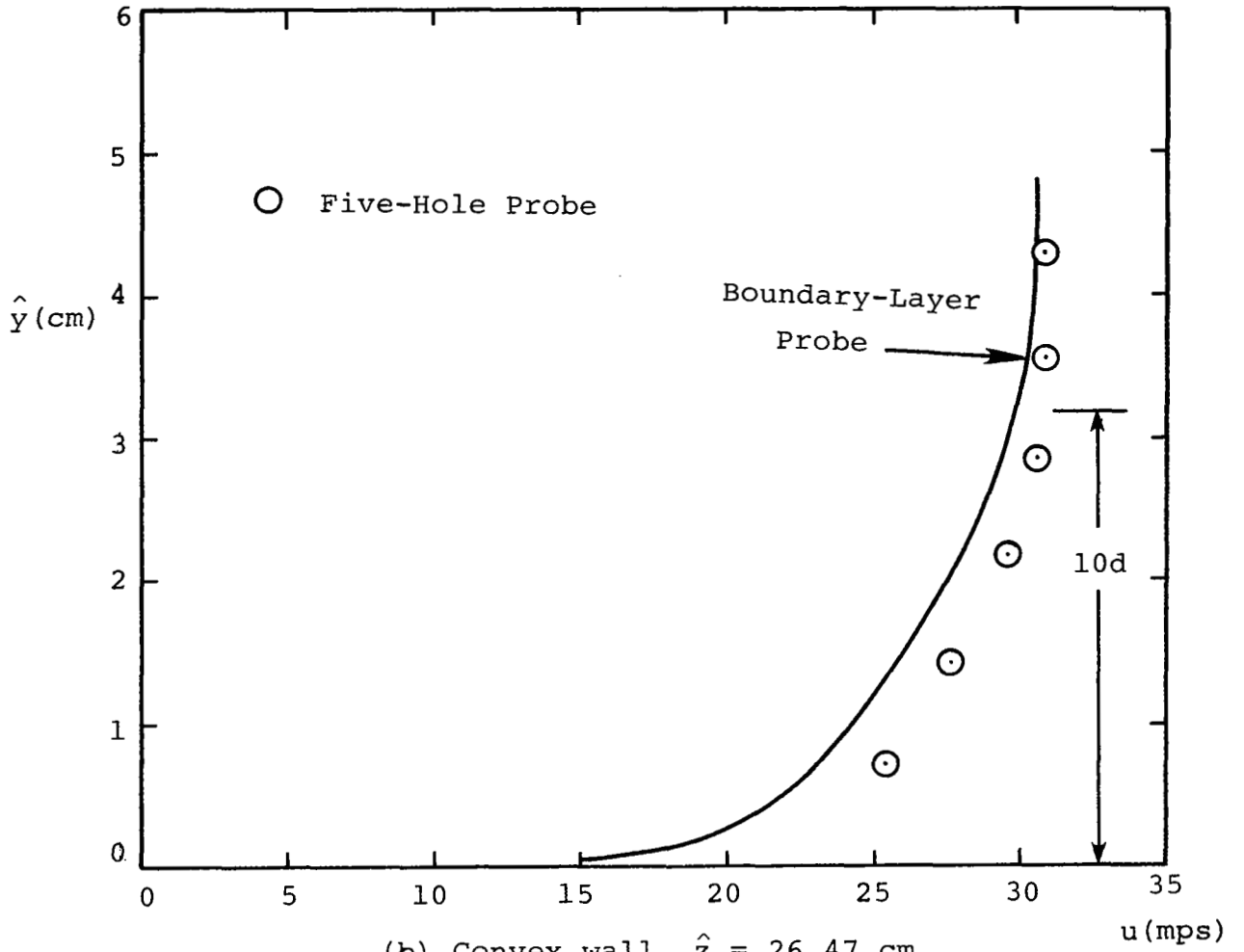
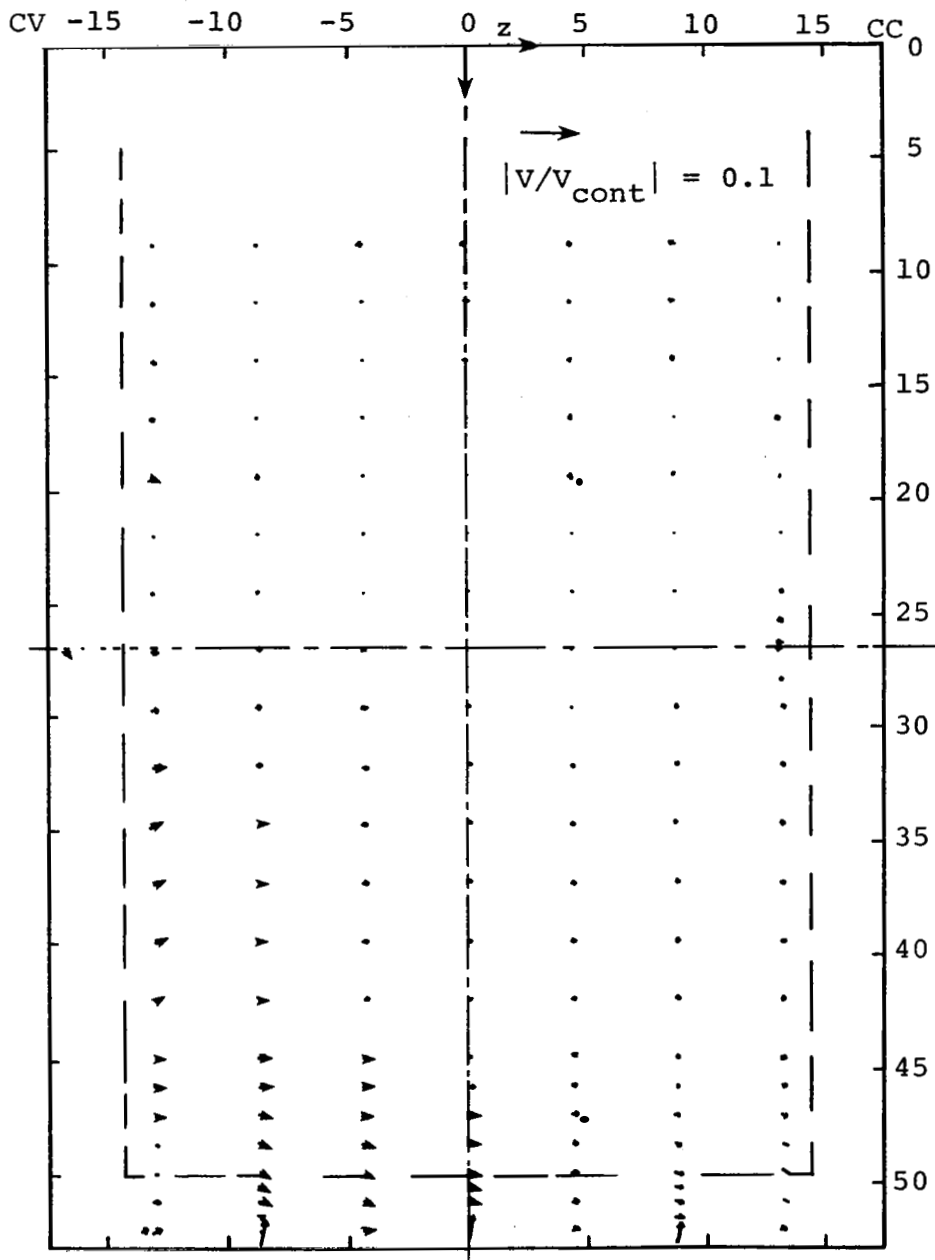


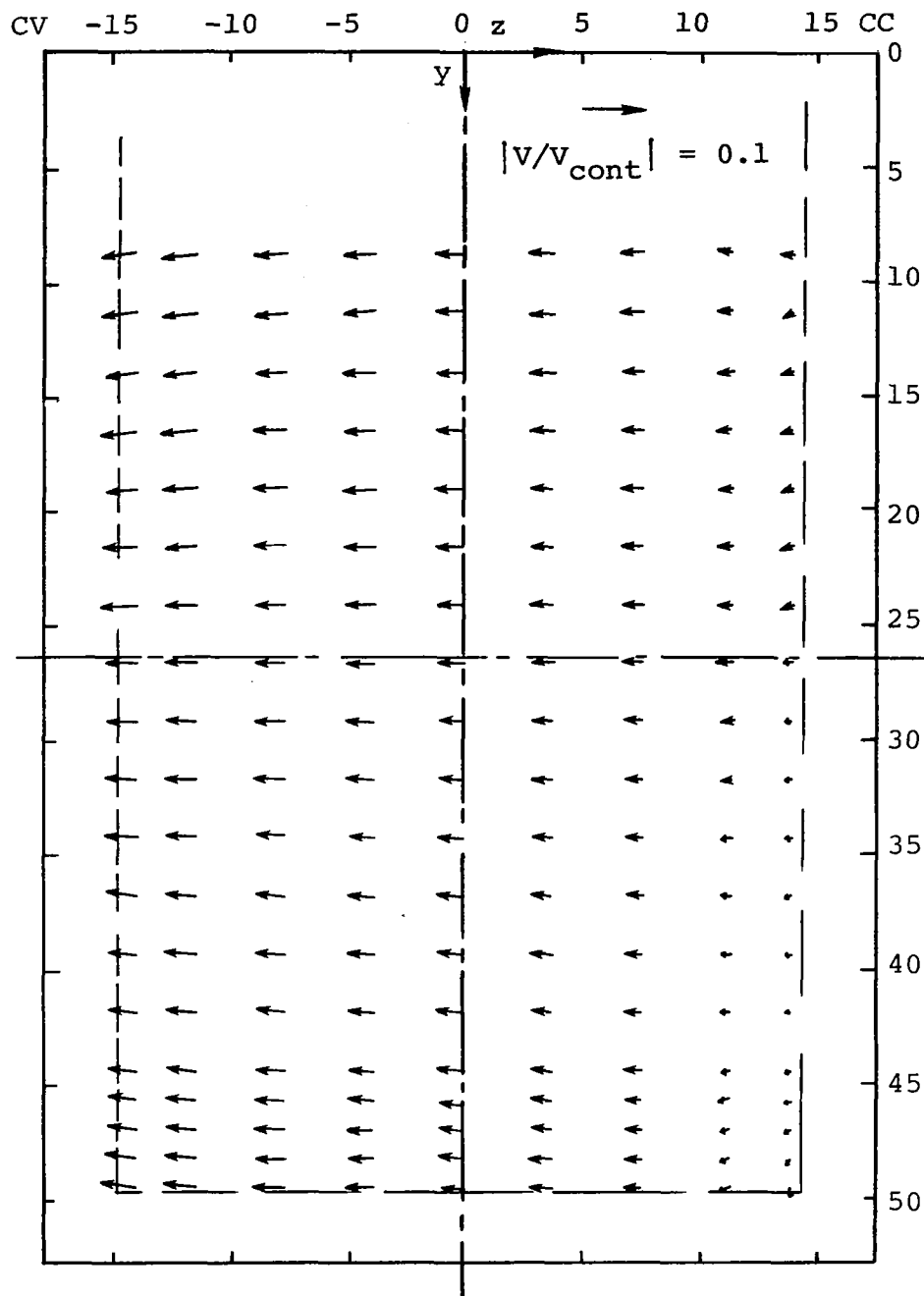
Figure 17.- (Concluded)



(a) Station 0, average  $V_{\text{cont}} = 30.7$  mps

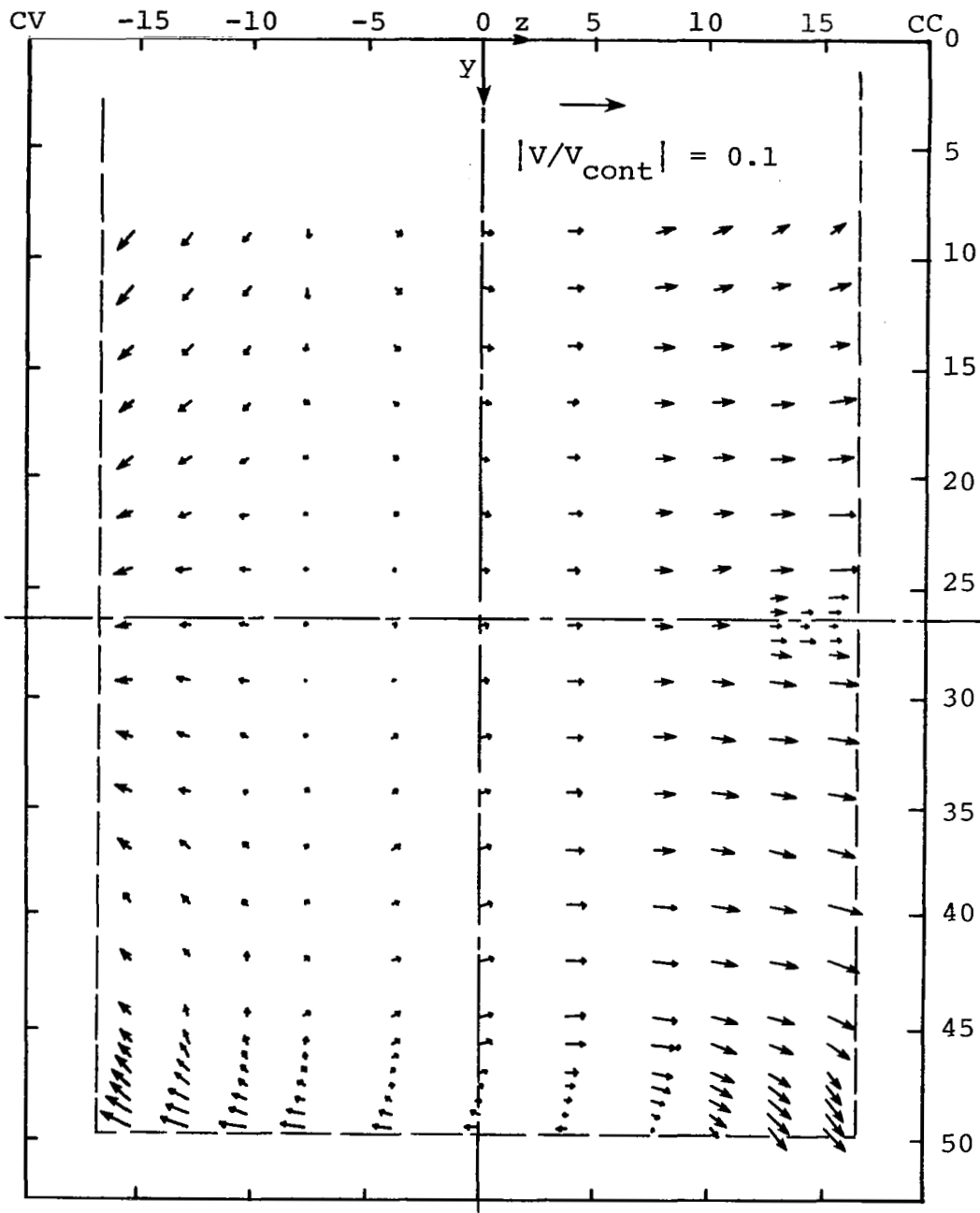
Figure 18.- Cross-flow velocity vectors  
The view is looking upstream.





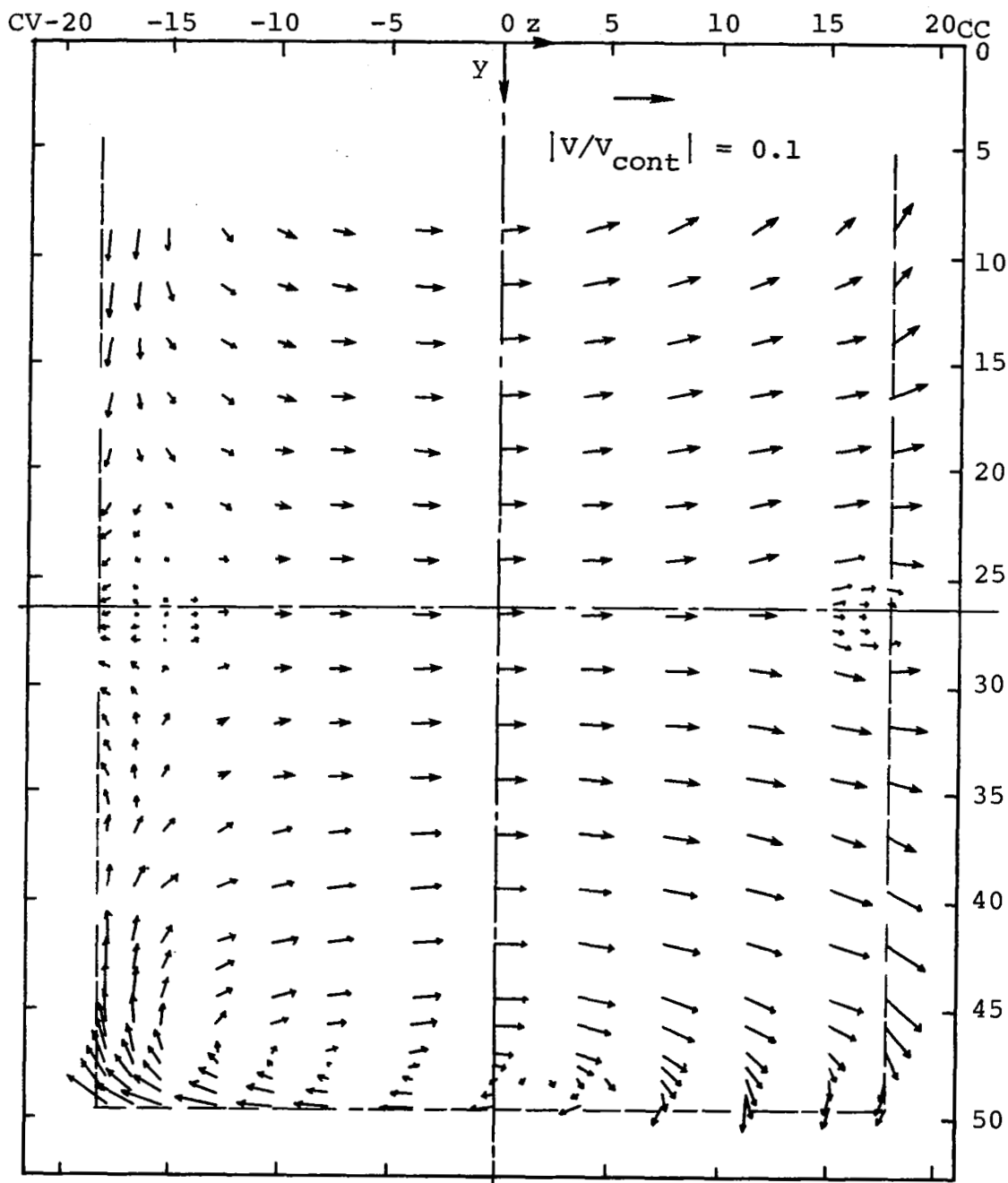
(b) Station 7, average  $V_{cont} = 30.7$  mps

Figure 18.- (Continued)



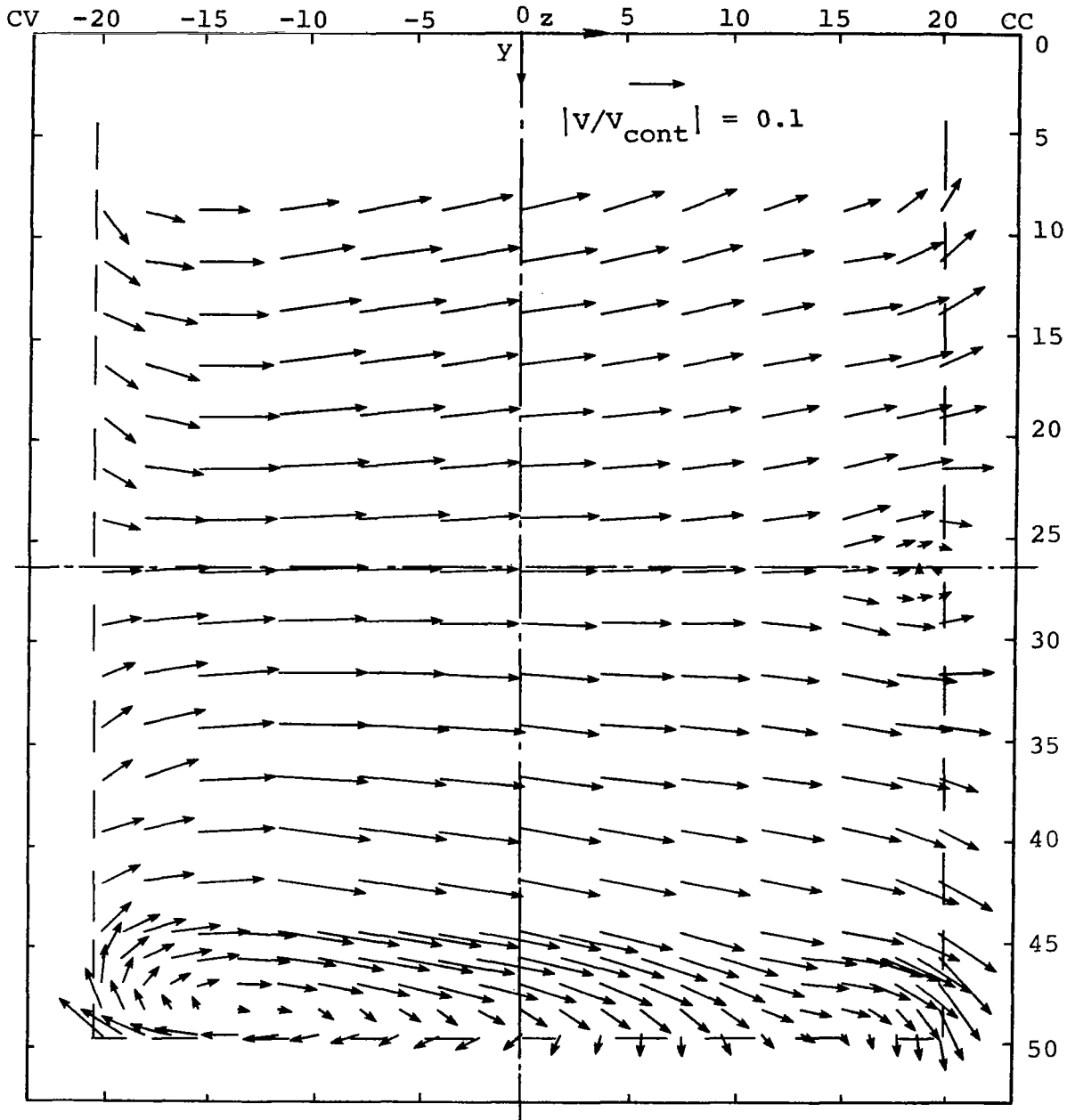
(c) Station 14, average  $V_{cont} = 27.6$  mps

Figure 18.- (Continued)



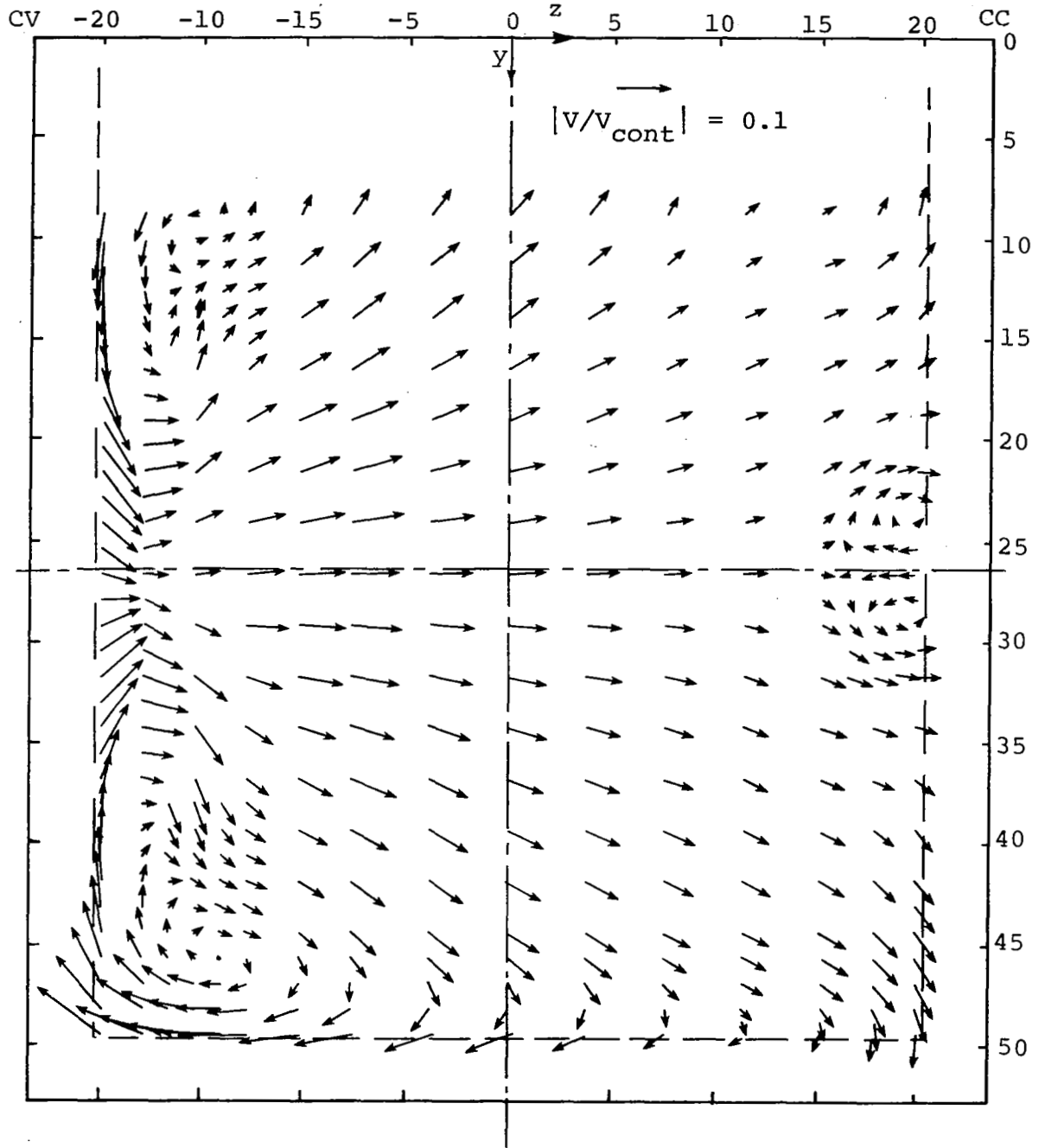
(d) Station 20, average  $V_{cont} = 25.7$  mps

Figure 18.- (Continued)



(e) Station 28, average  $V_{cont} = 23.2$  mps

Figure 18.- (Continued)



(f) Station 38, average  $V_{cont} = 23.2$  mps

Figure 18.- (Concluded)

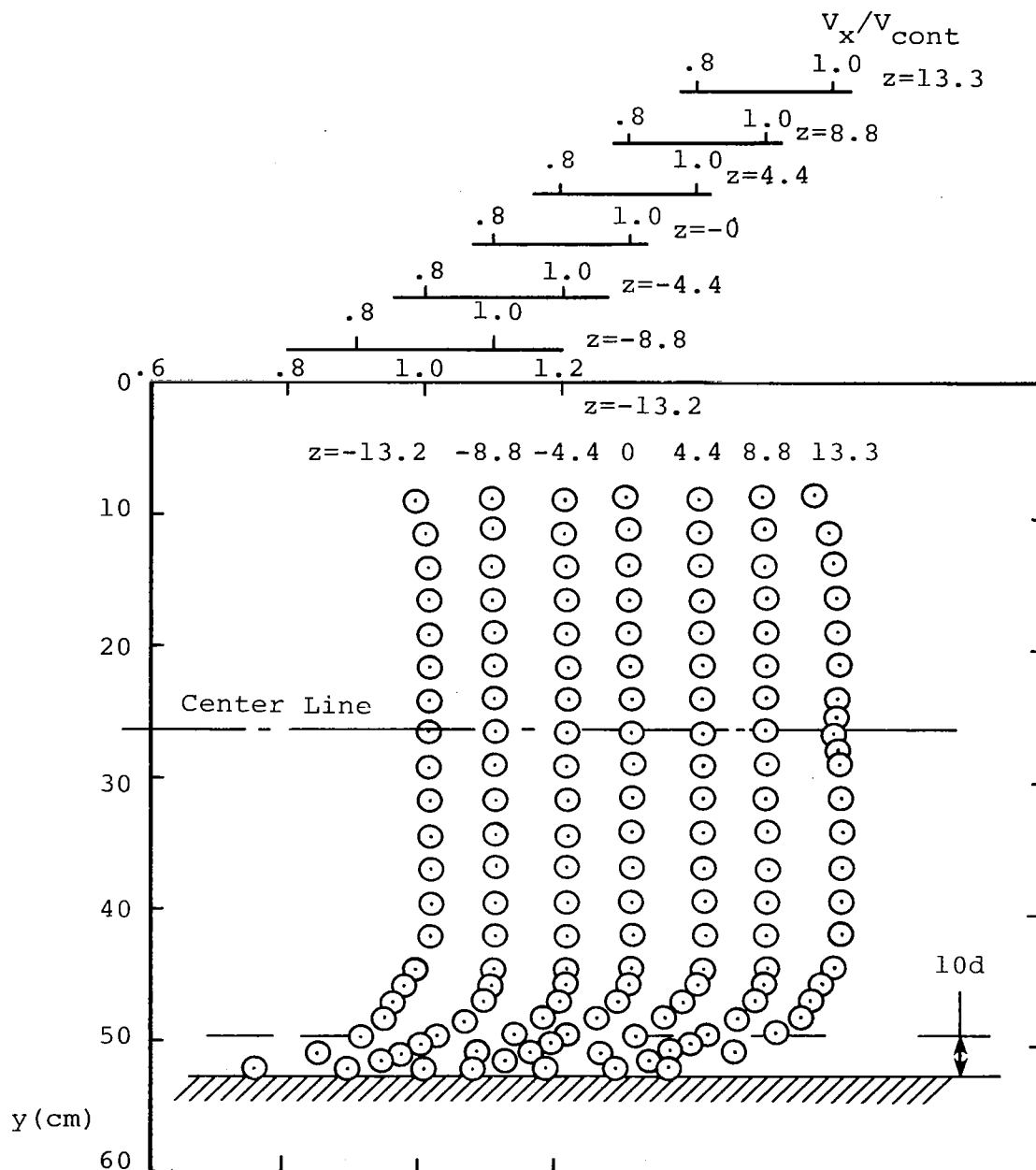
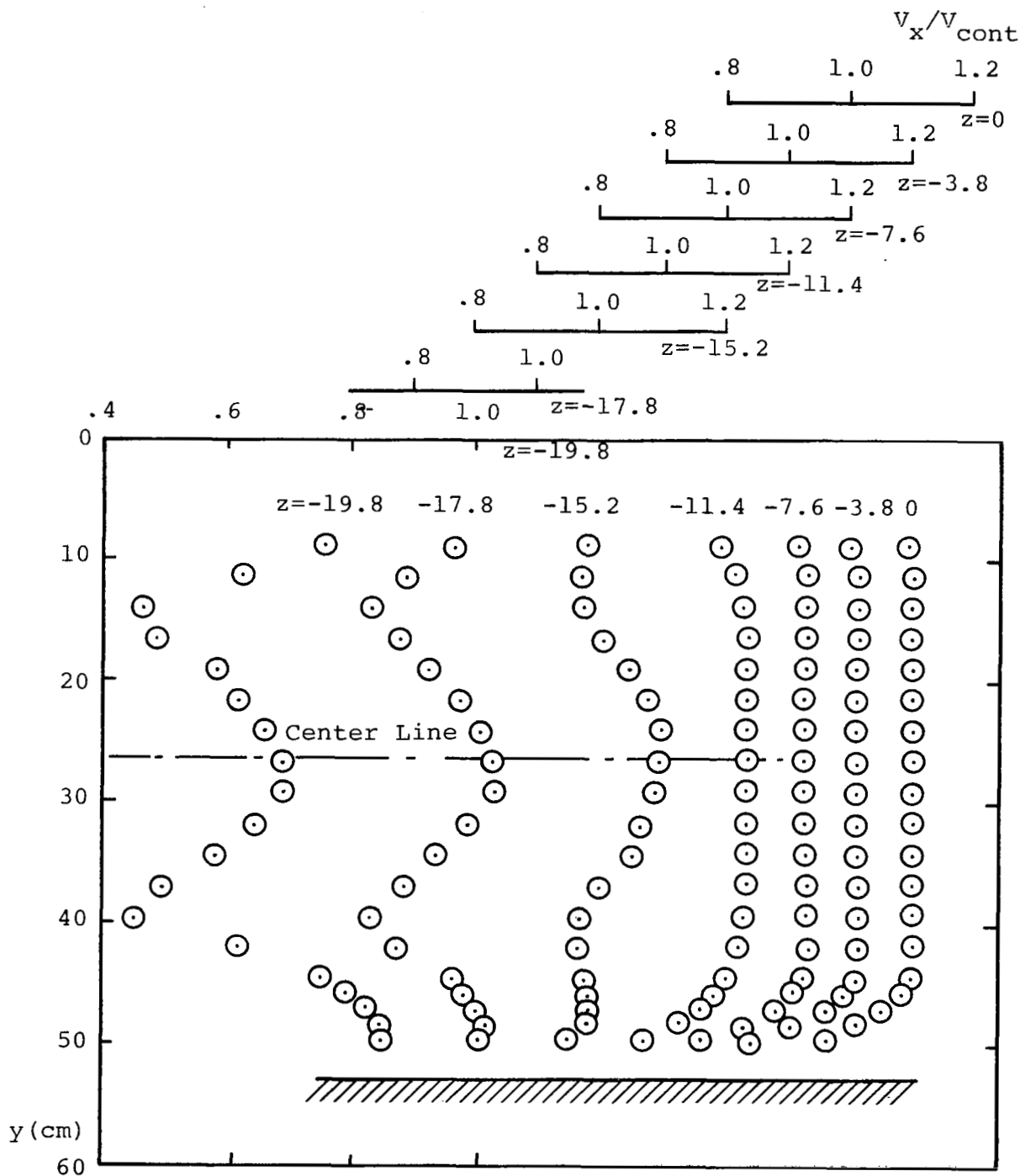
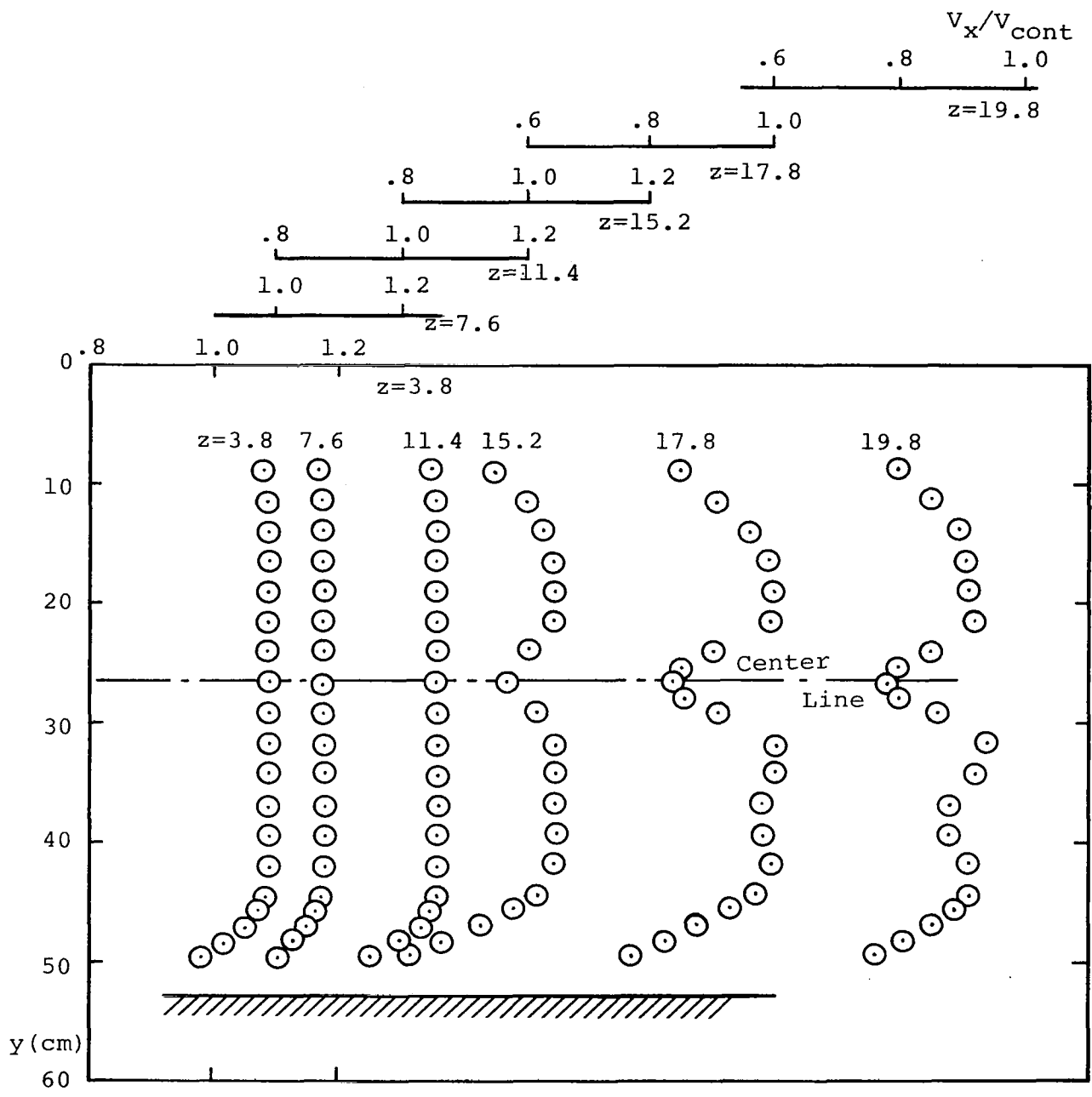


Figure 19.- Axial velocity profiles, station 0.  
Average  $V_{cont} = 30.7$  mps.



(a)  $z \leq 0$

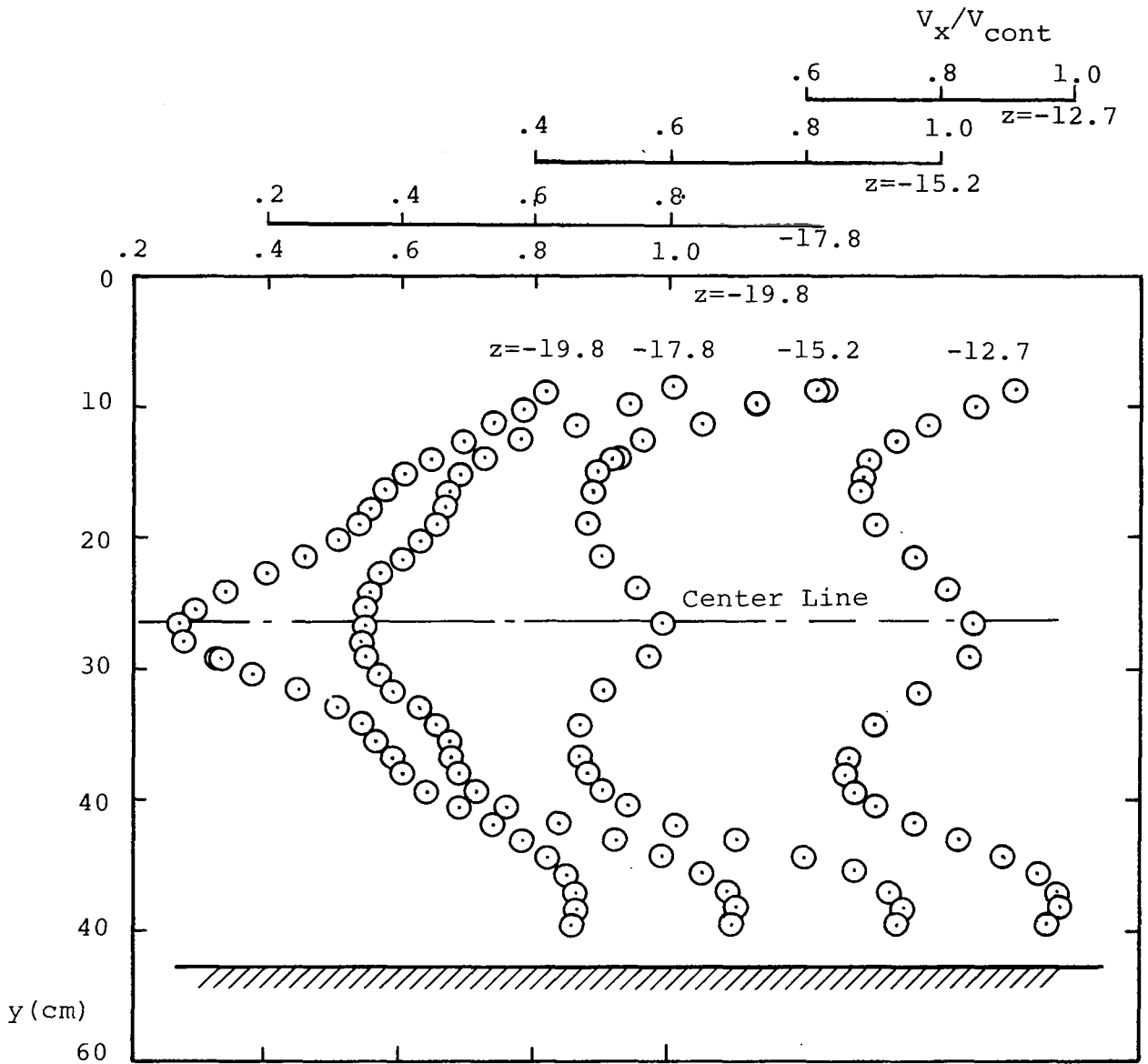
Figure 20.- Axial velocity profiles, station 28.  
Average  $V_{cont} = 23.2$  mps.



(b)  $z > 0$

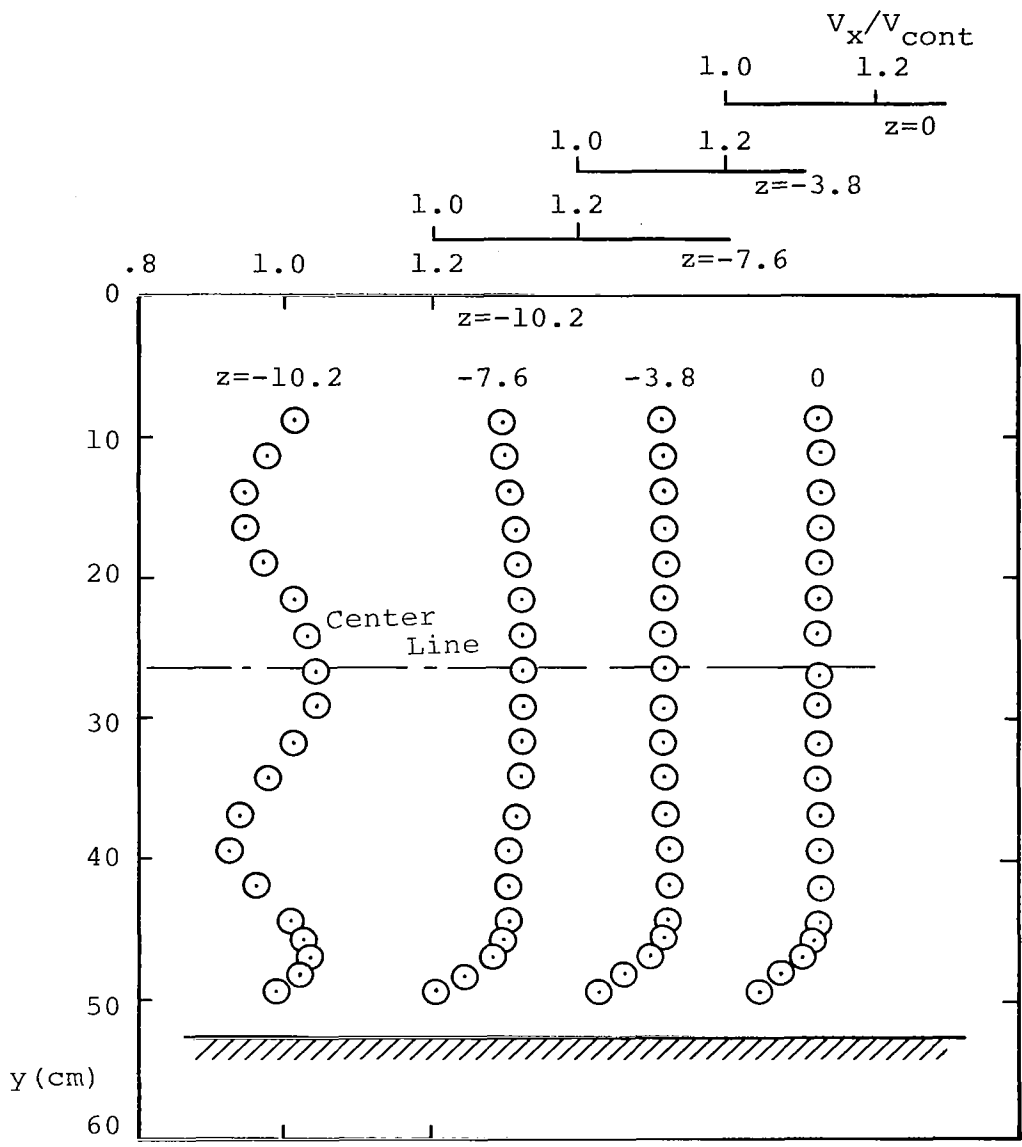
Figure 20.- (Concluded)





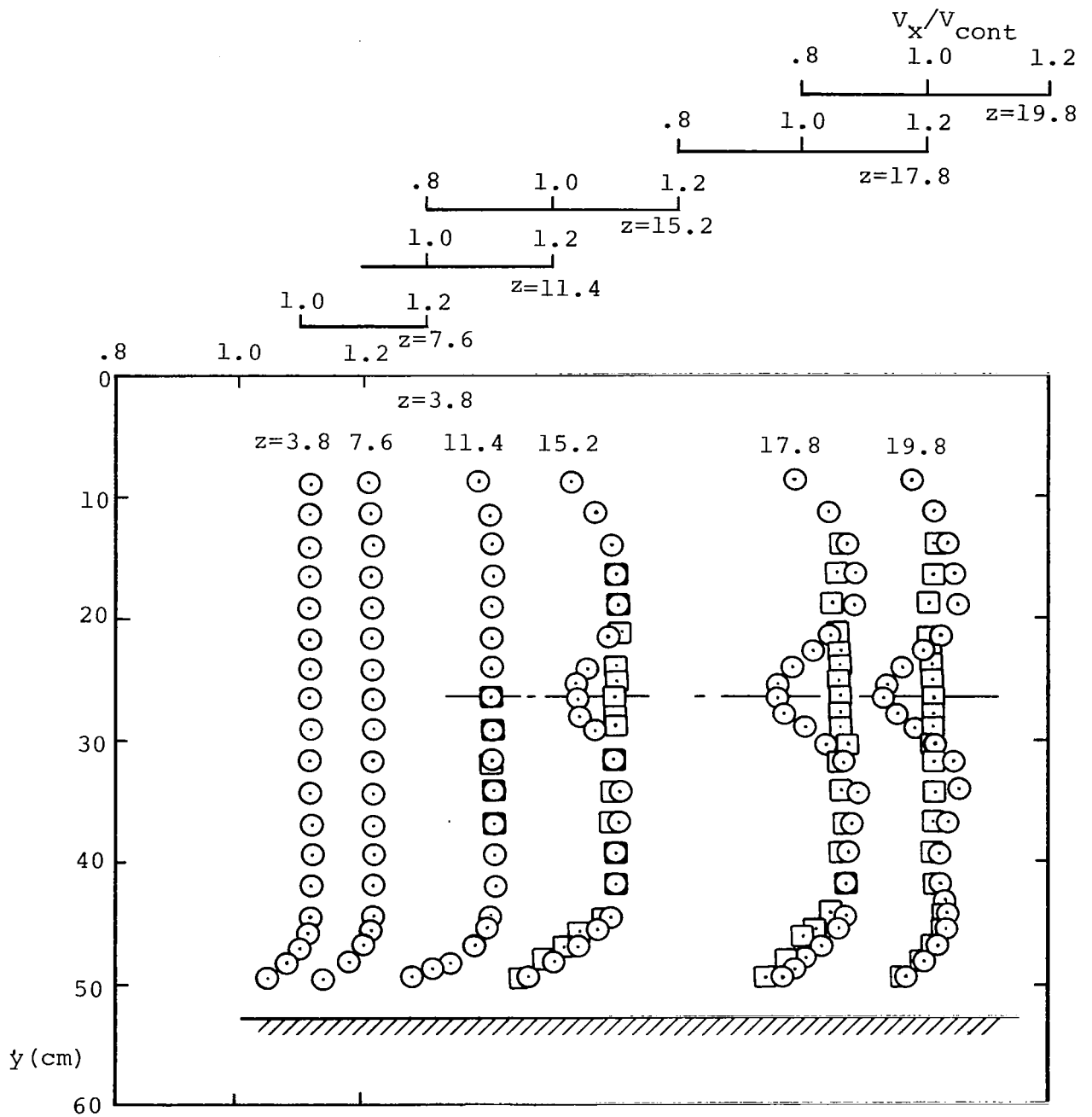
(a) -  $19.8 \leq z \leq -12.7$

Figure 21.- Axial velocity profiles, station 38.  
Average  $V_{cont} = 23.2$  mps.



(b)  $-10.2 \leq z \leq 0$

Figure 21.- (Continued)

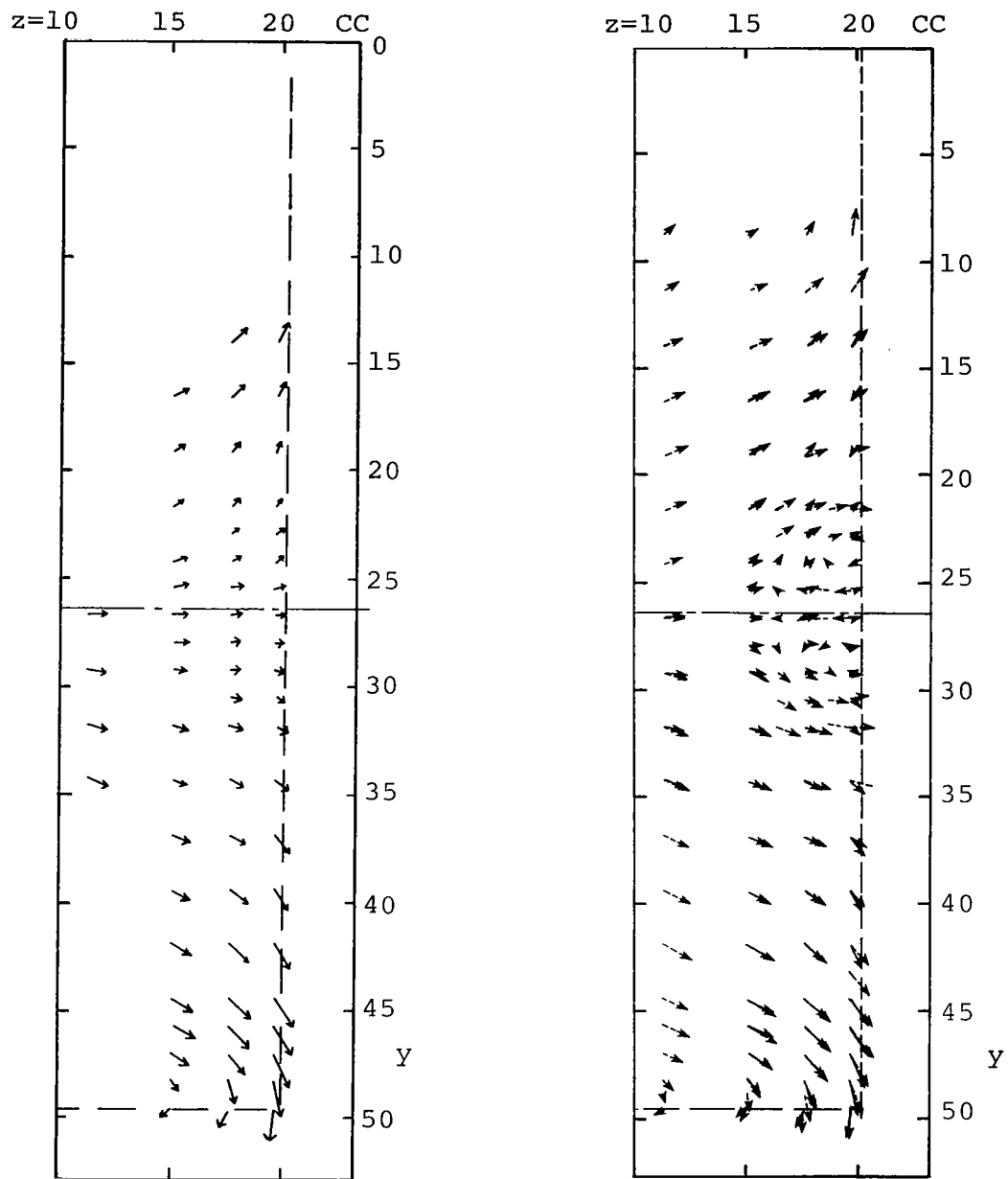


Plenum Thermister Position

- Center line, CC side
- Center line, top

(c)  $z > 0$

Figure 21.- (Concluded)



(a) Thermister removed from CC-wall center line

(b) Overlay of results with (→) and without (↔) thermister at CC-wall center line

Figure 22.- Effect of the plenum thermister on the velocity vectors at station 38.

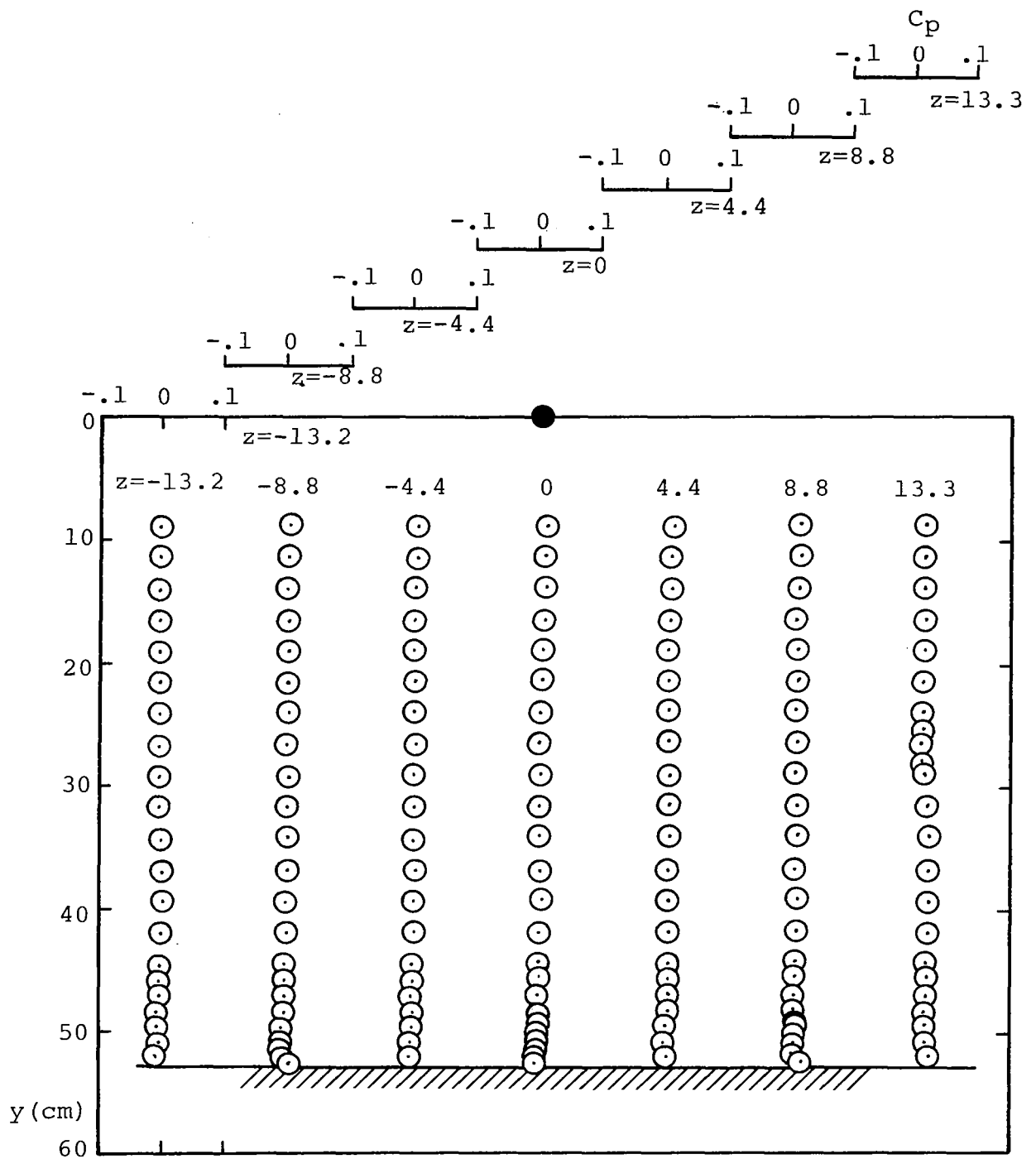
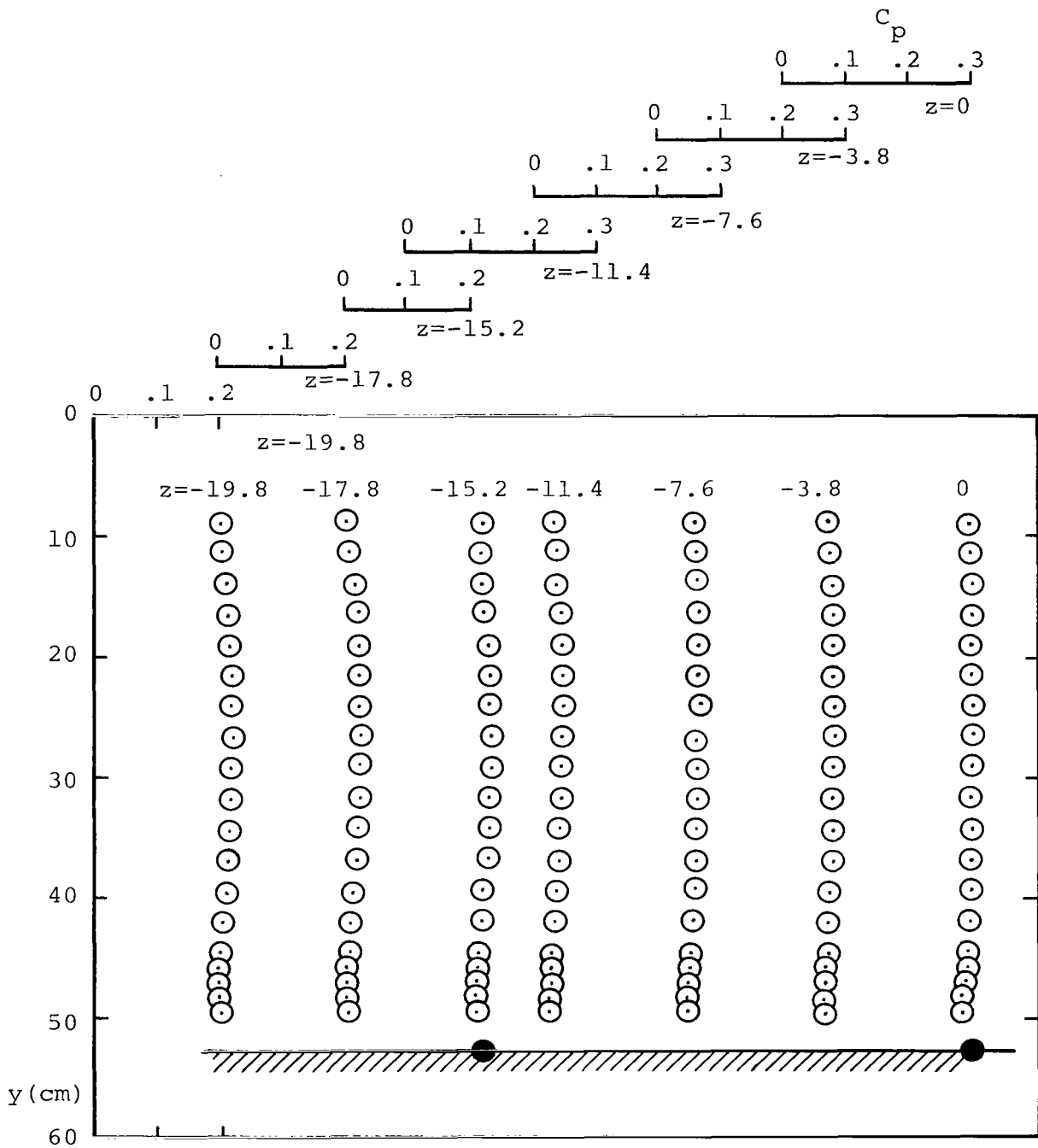


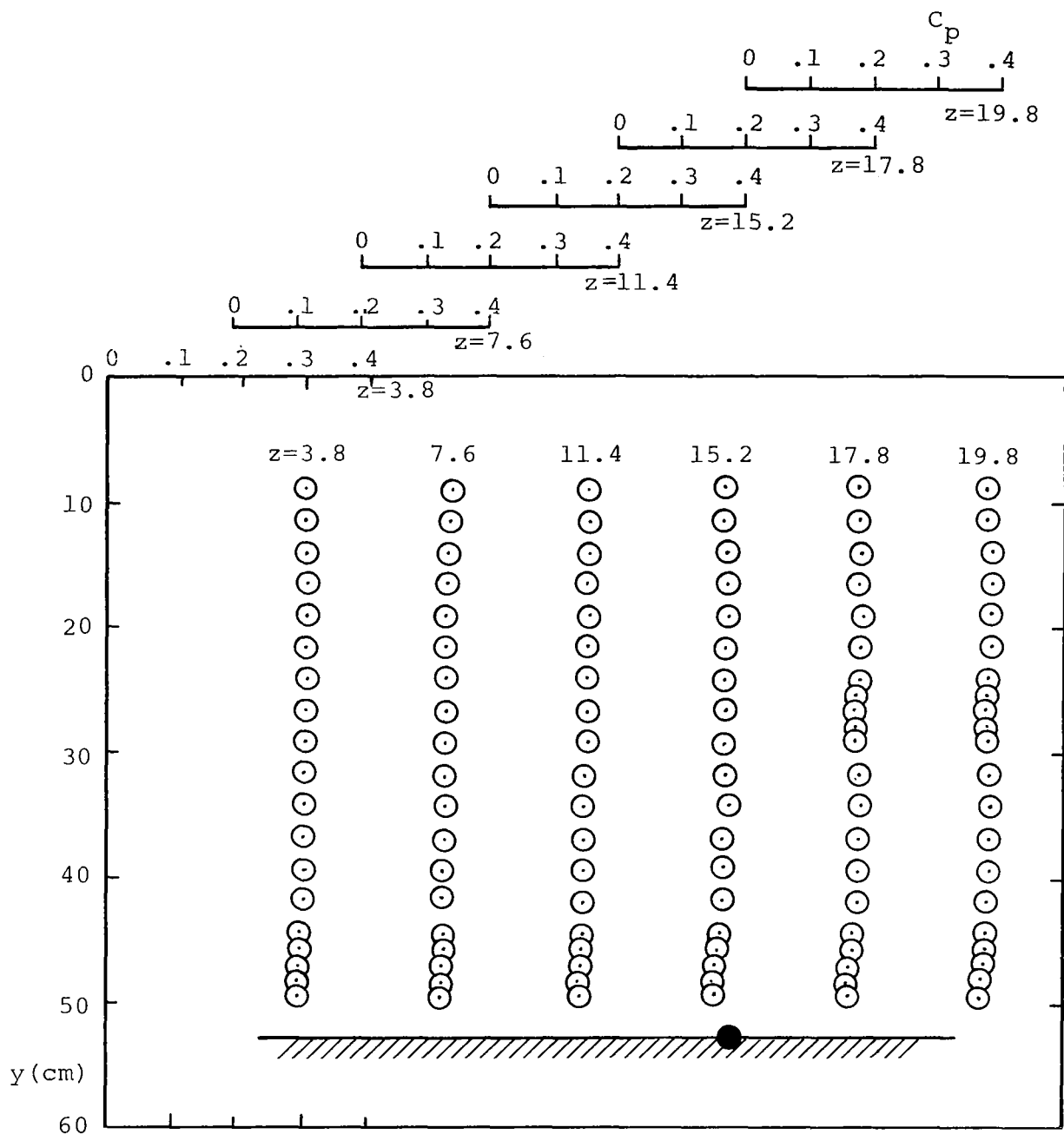
Figure 23.- Static pressure profiles, station 0.



○, Five-hole probe; ●, Wall tap

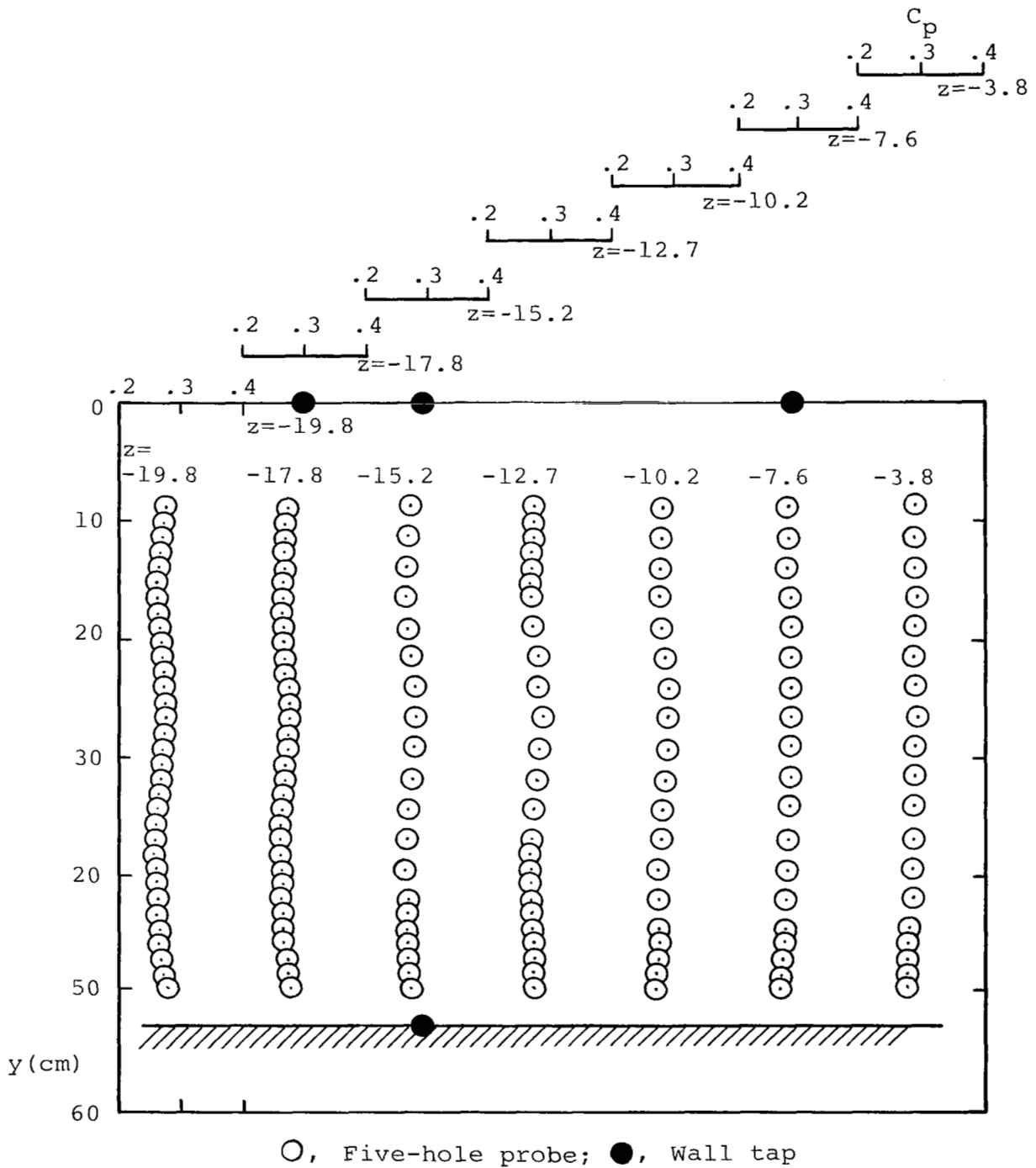
(a)  $z \leq 0$

Figure 24.- Static pressure profiles, station 28



(b)  $z > 0$

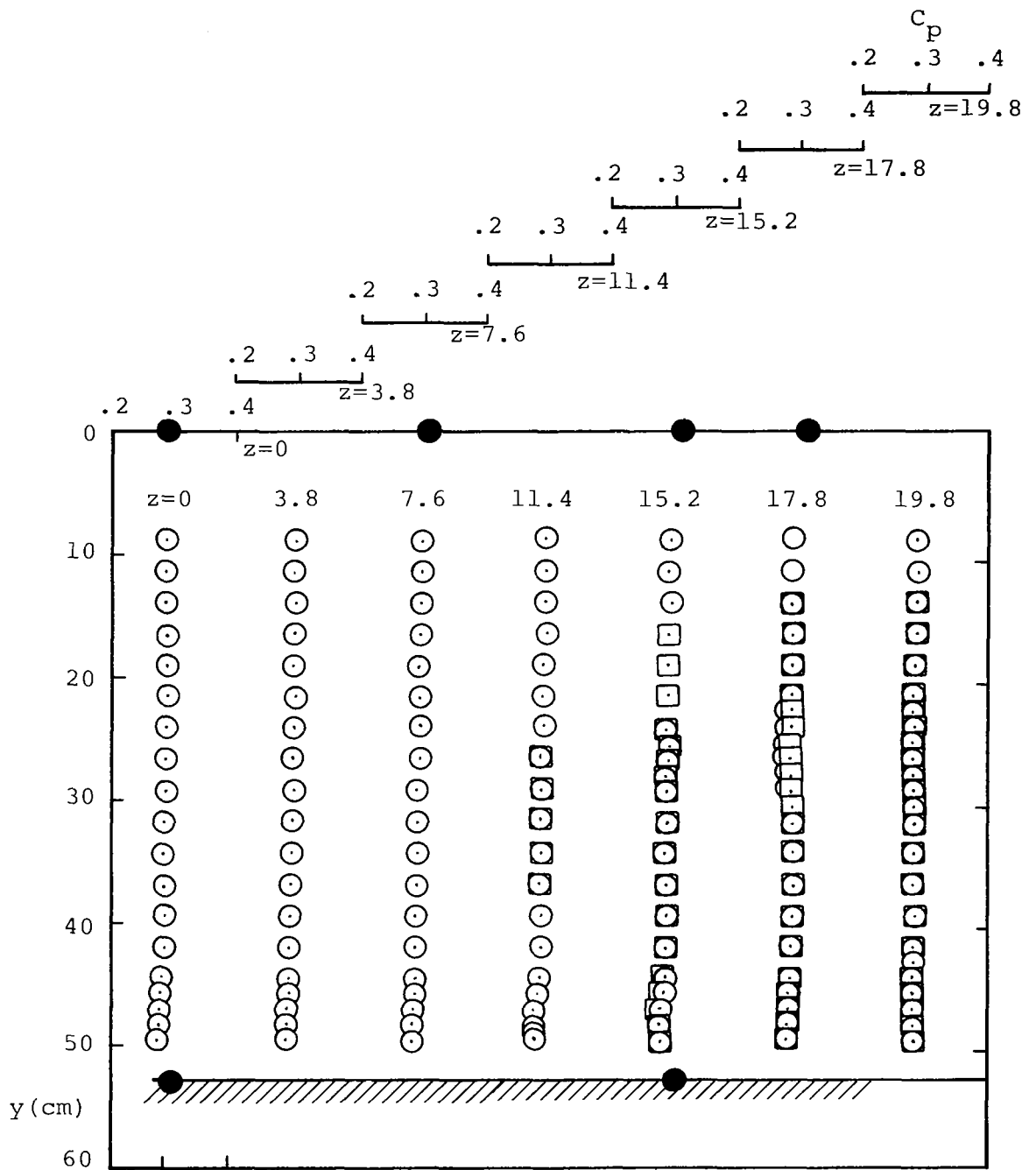
Figure 24.- (Concluded)



(a)  $z < 0$

Figure 25.- Static pressure profiles, station 38.





Plenum Thermister Position

○ Center line, CC side

□ Center line, top

(b)  $z \geq 0$

Figure 25.- (Concluded)

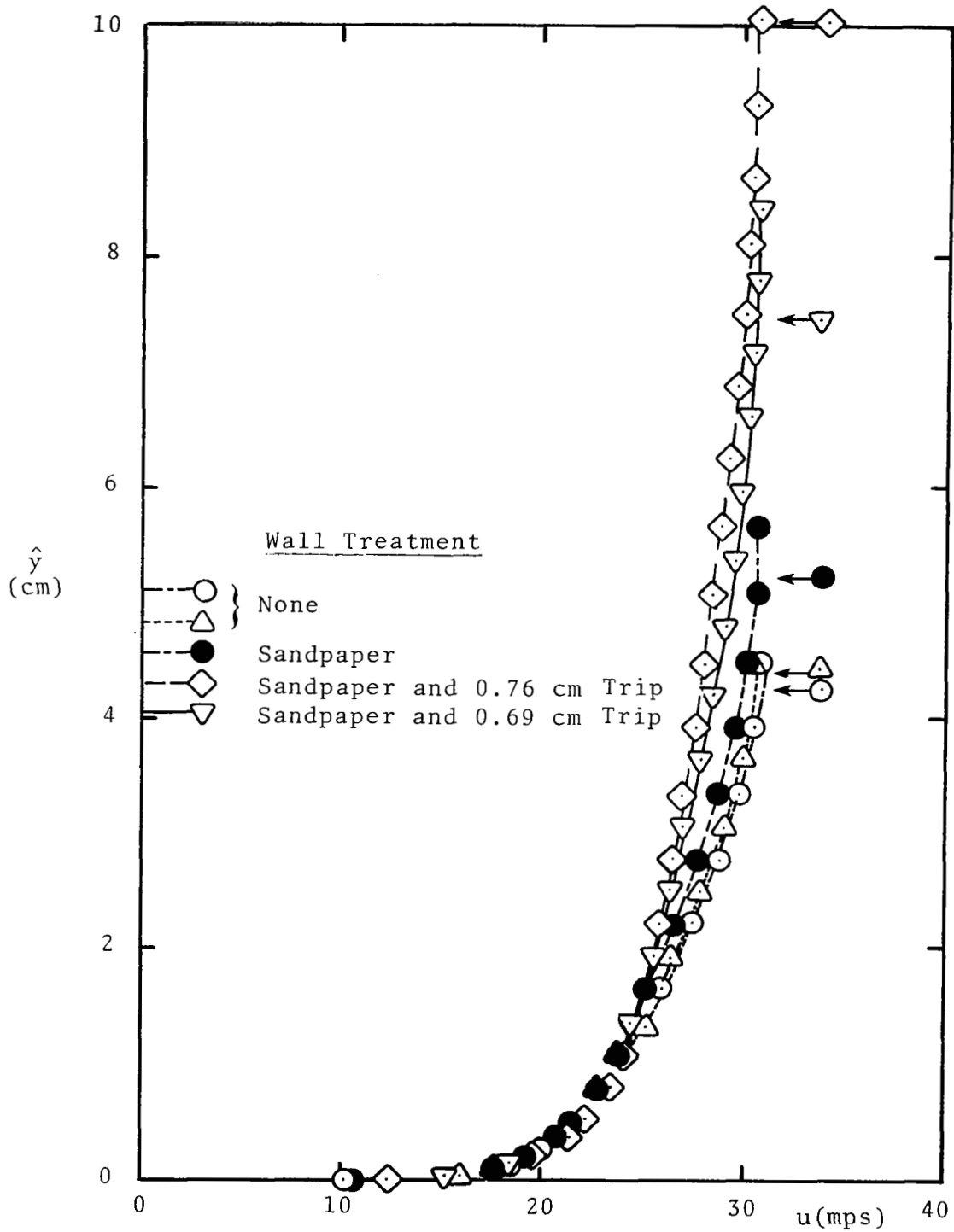


Figure 26.- Velocity profiles -  $u$  vs.  $\hat{y}$ .

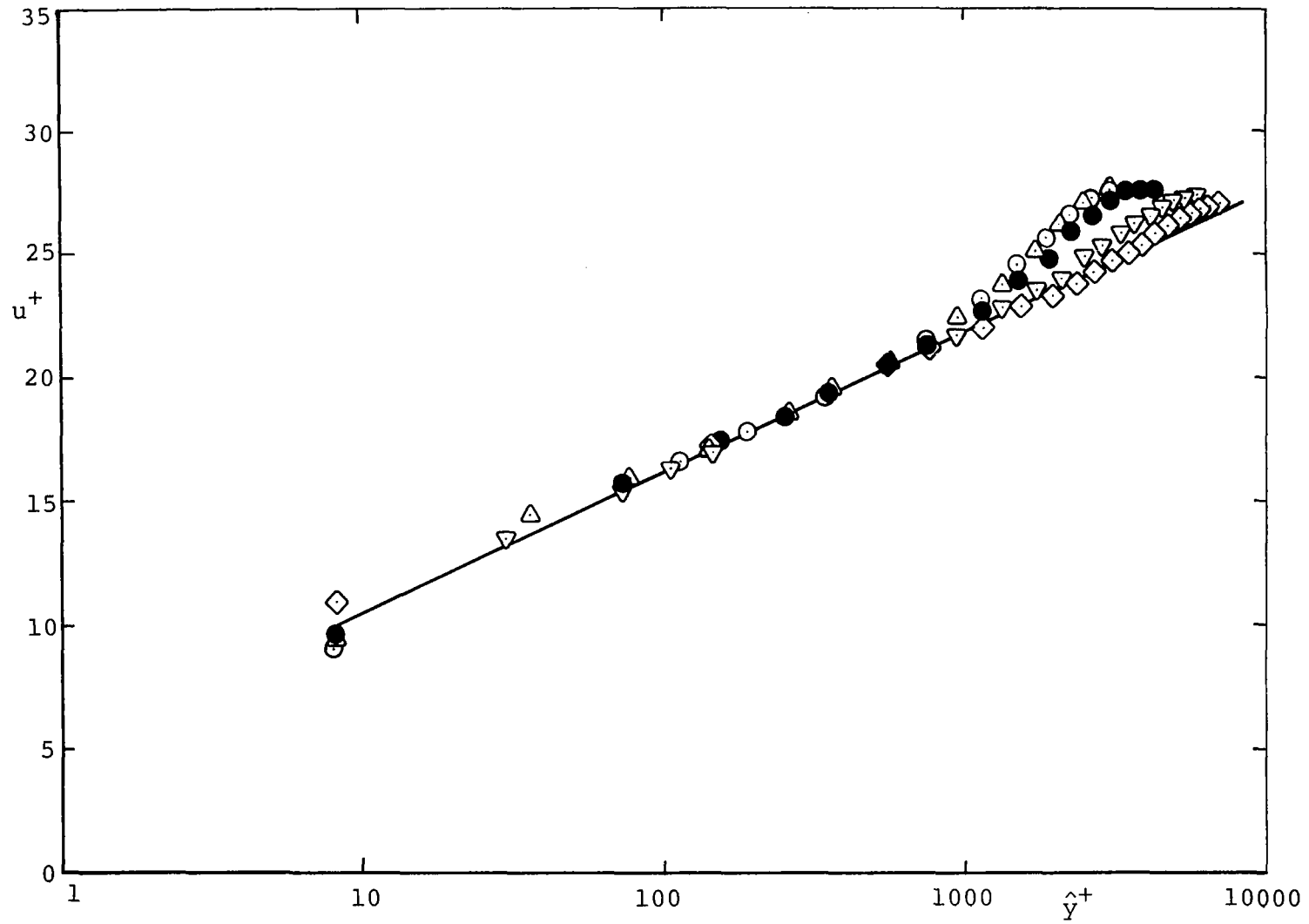


Figure 27.- Velocity profiles - wall variables. See figure 26 for symbol definitions.

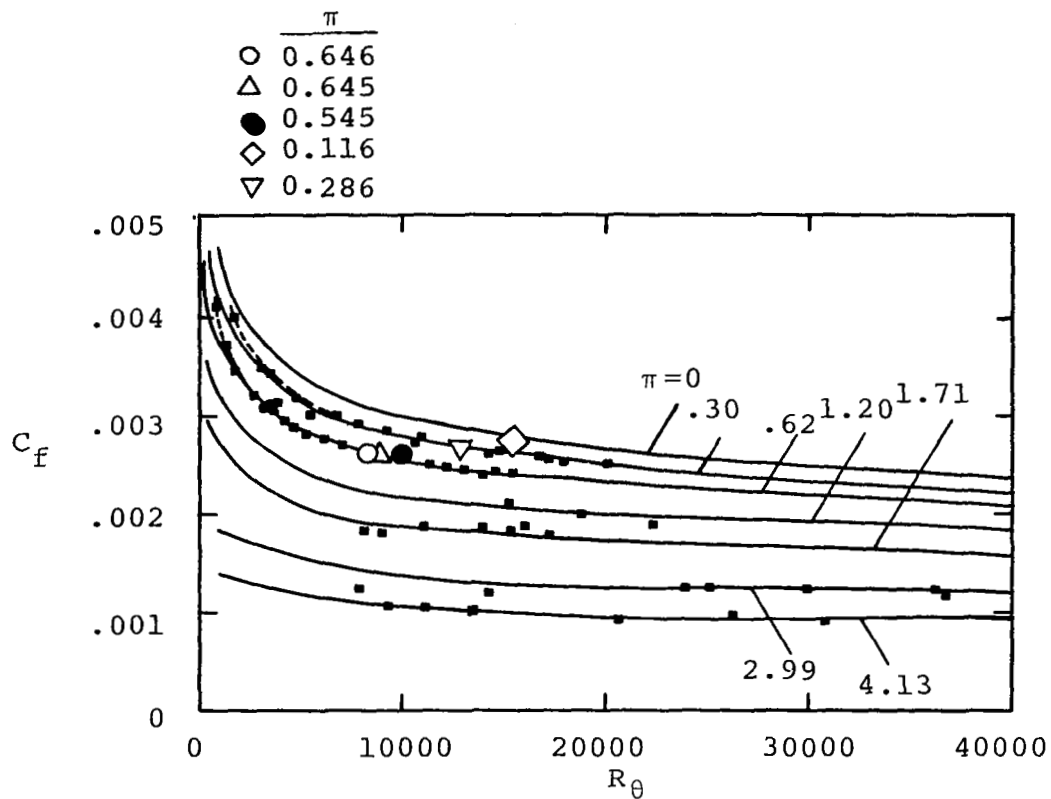


Figure 28.-  $C_f$  vs  $R_\theta$  for equilibrium flows (reproduced from ref. 6). See fig. 26 for symbol definitions.

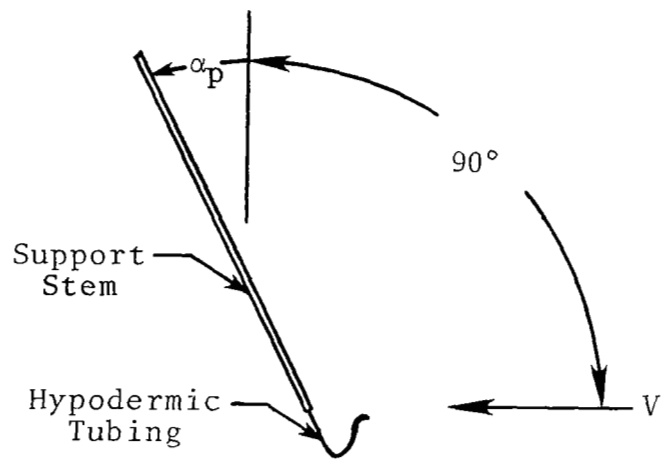


Figure 29.- Boundary-layer probe.

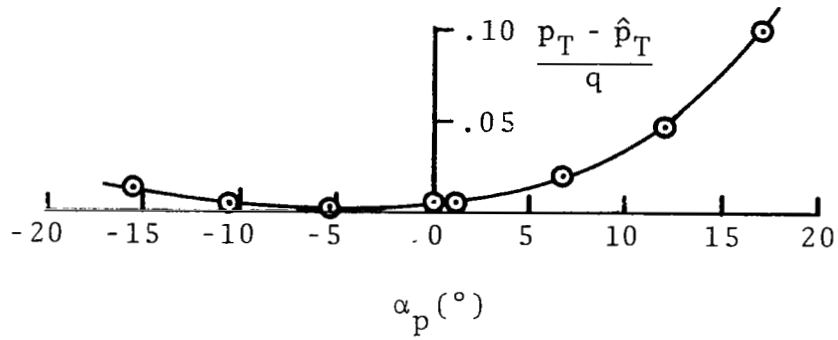


Figure 30.- Boundary-layer-probe pitch sensitivity.

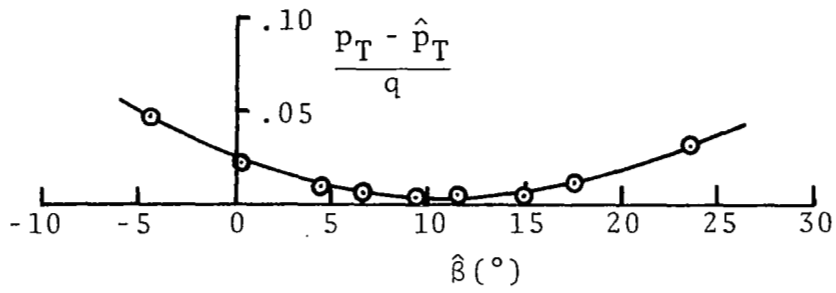


Figure 31.- Boundary-layer-probe yaw sensitivity.

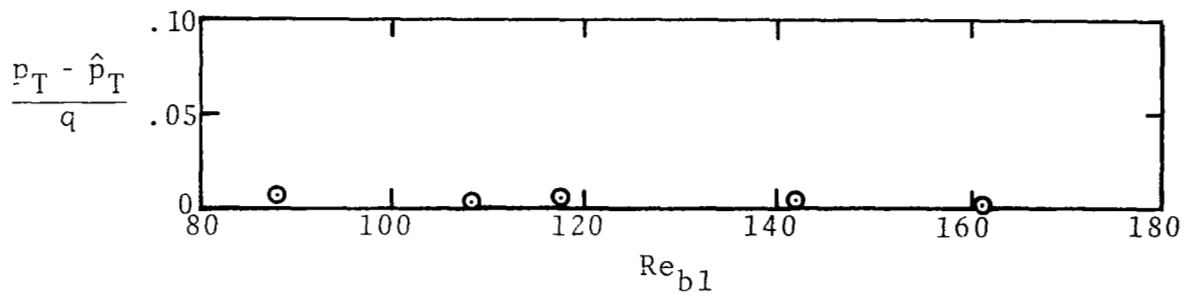


Figure 32.- Boundary-layer-probe Reynolds-number sensitivity.

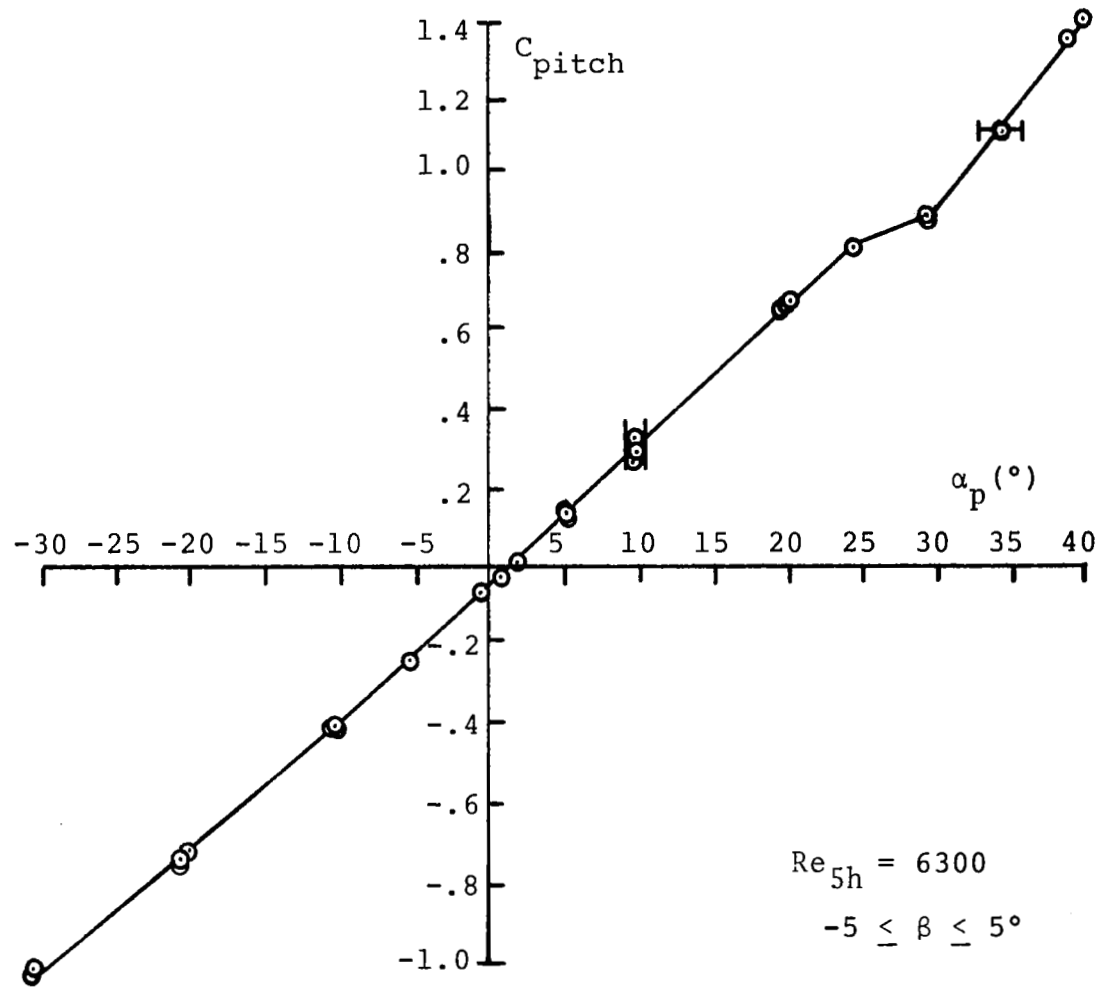


Figure 33.- Five-hole-probe pitch coefficient.



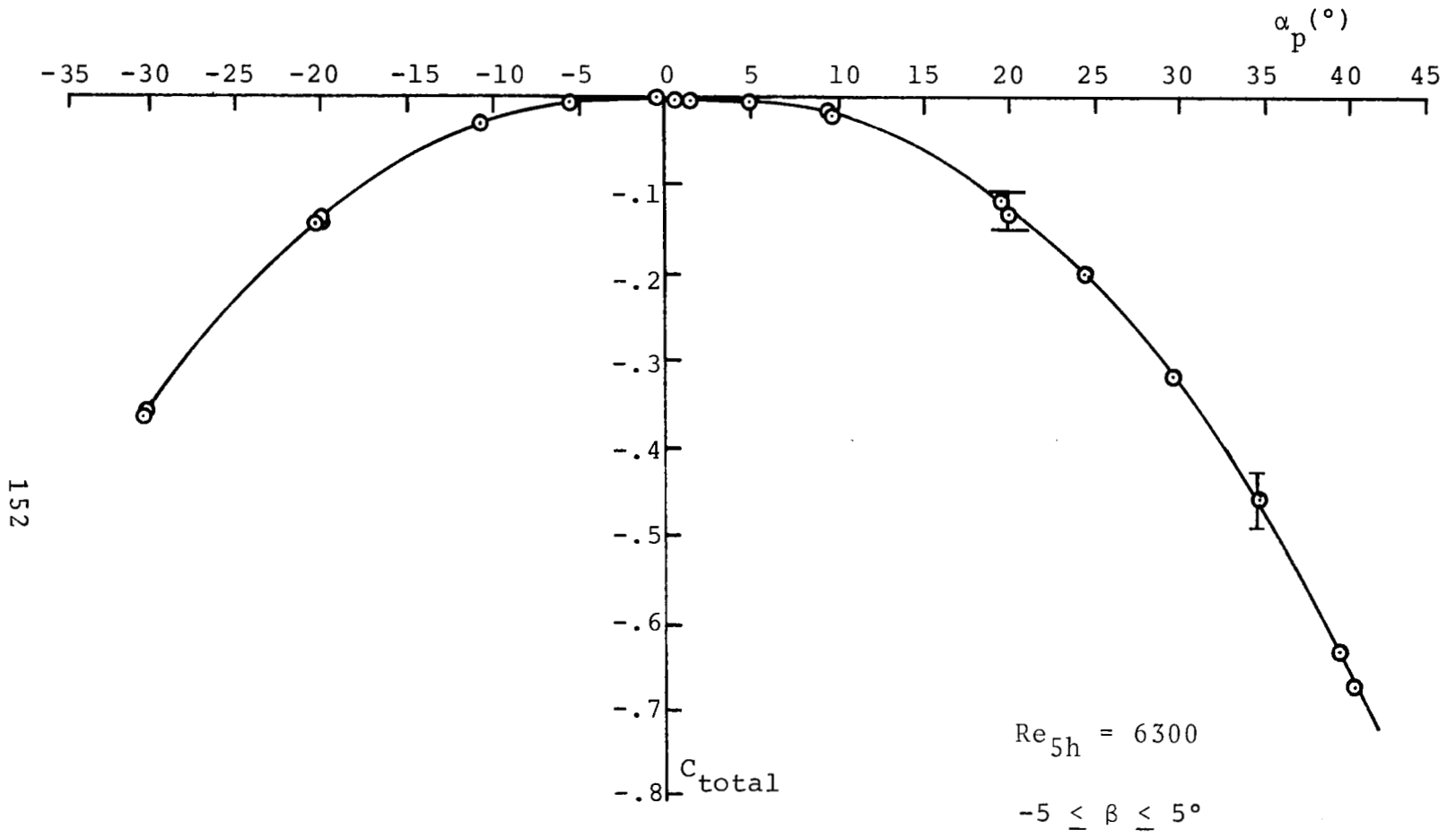


Figure 34.- Five-hole-probe total pressure coefficient.

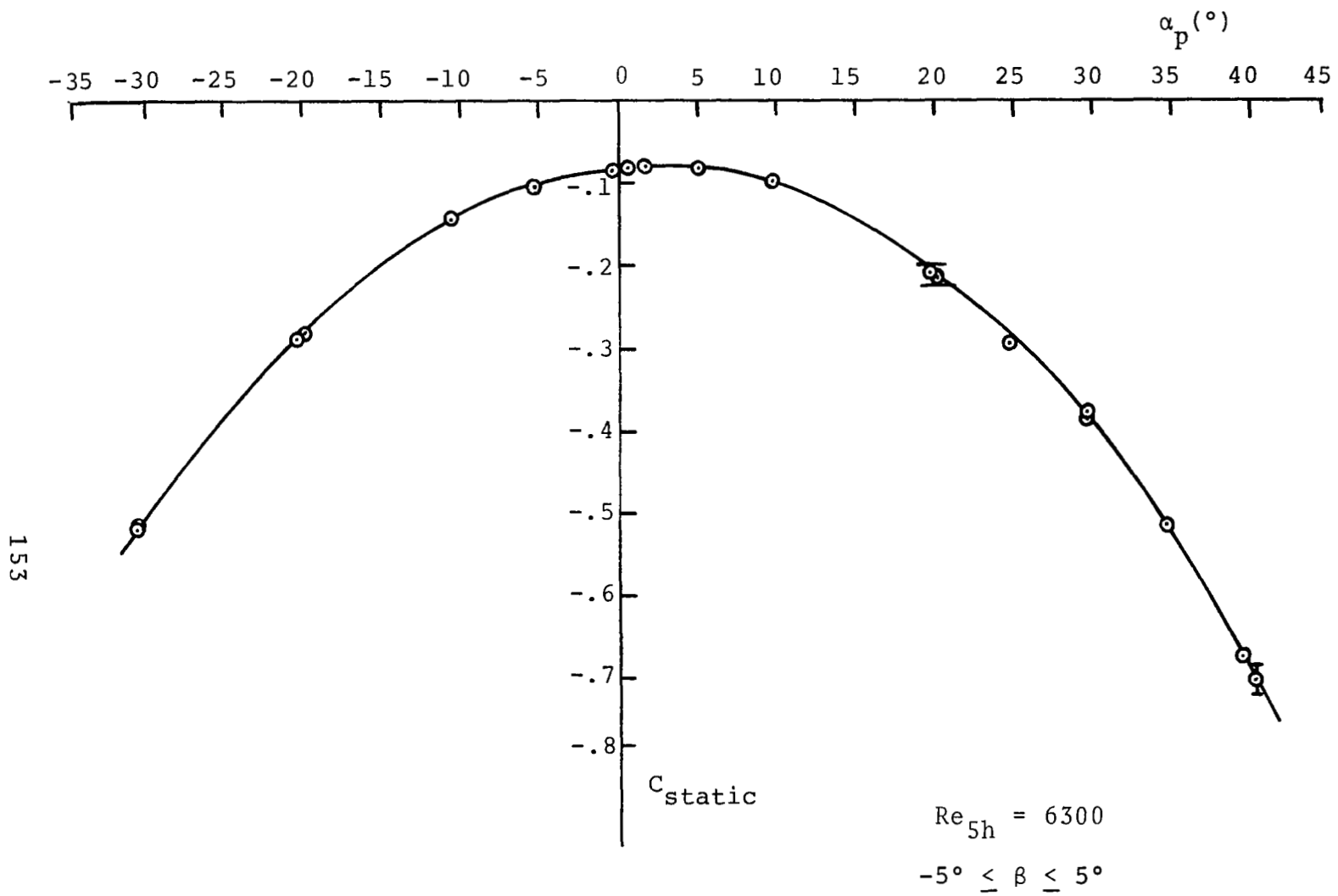


Figure 35.- Five-hole-probe static pressure coefficient.

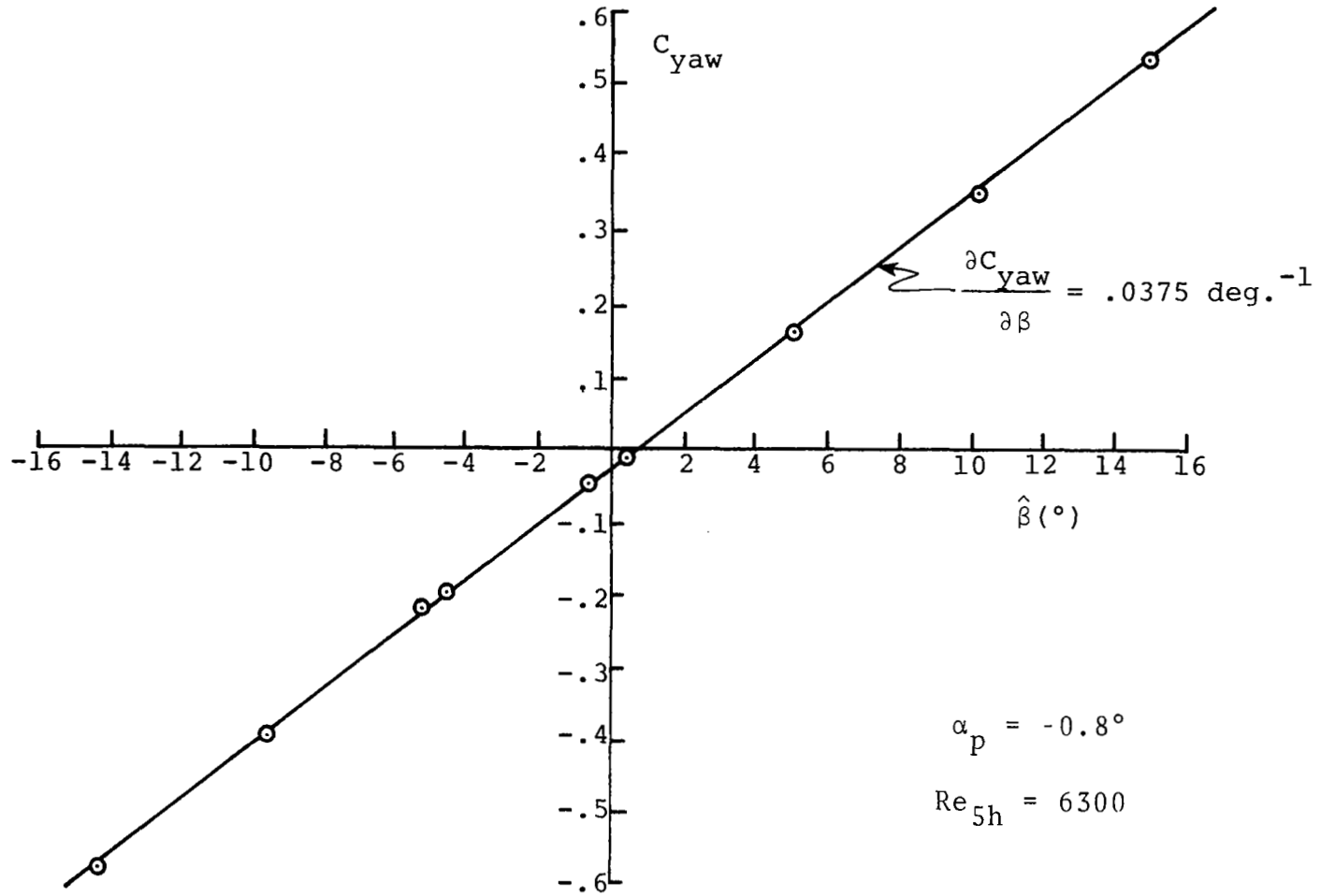


Figure 36.- Five-hole-probe yaw coefficient.

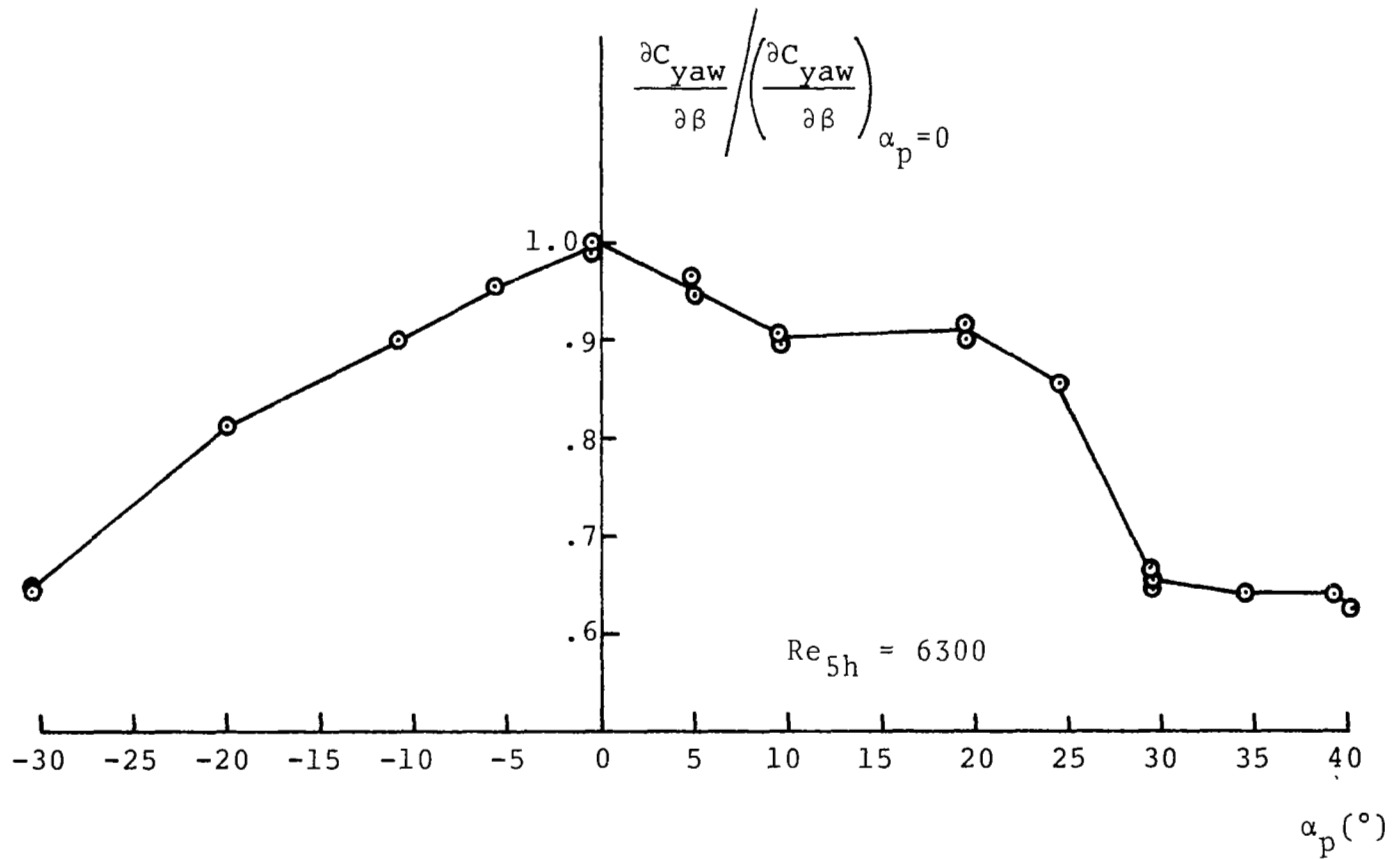
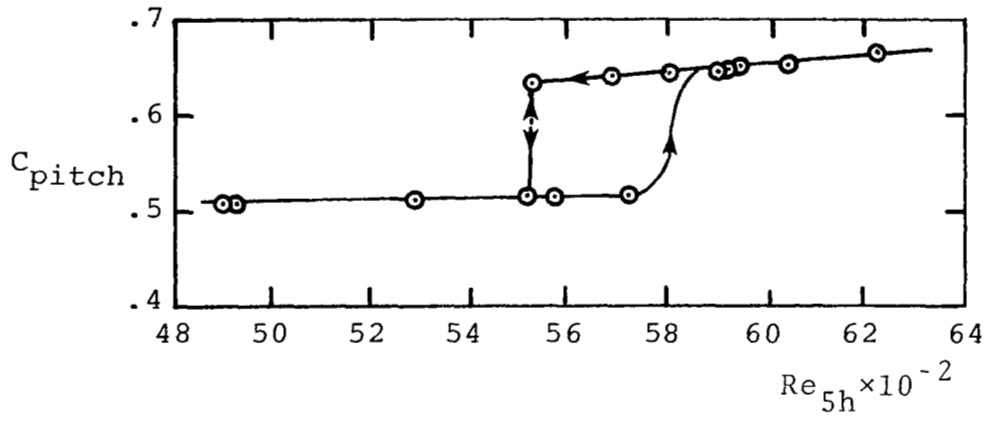
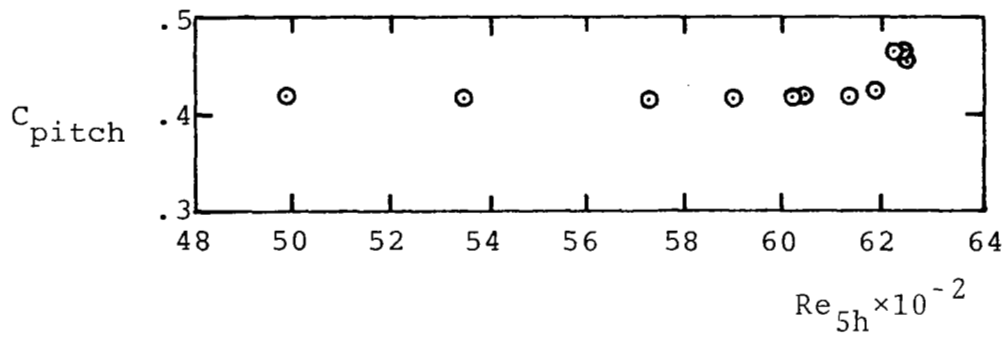


Figure 37.- Effect of pitch on the yaw sensitivity of the five-hole probe.

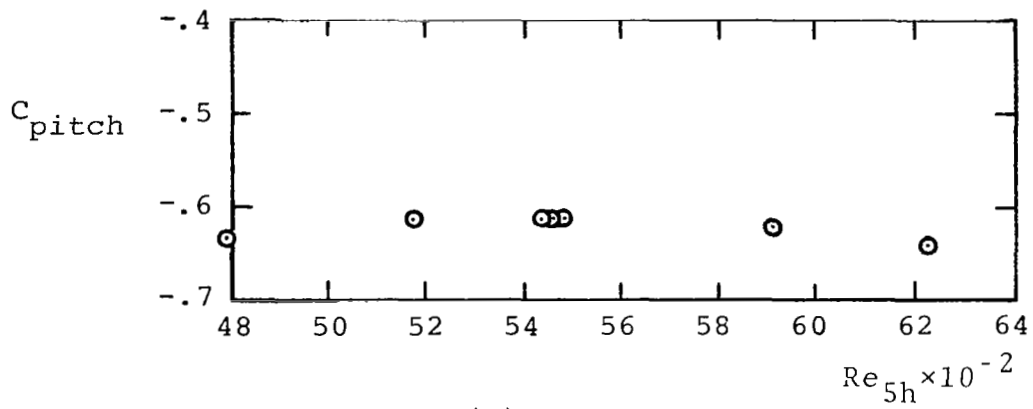


(a)  $\alpha_p = 20.0^\circ$



(b)  $\alpha_p = 15.0^\circ$

Figure 38.- Reynolds-number dependence of five-hole-probe pitch coefficient for large pitch angle.



(c)  $\alpha_p = -15.1^\circ$

Figure 38.- (Concluded)

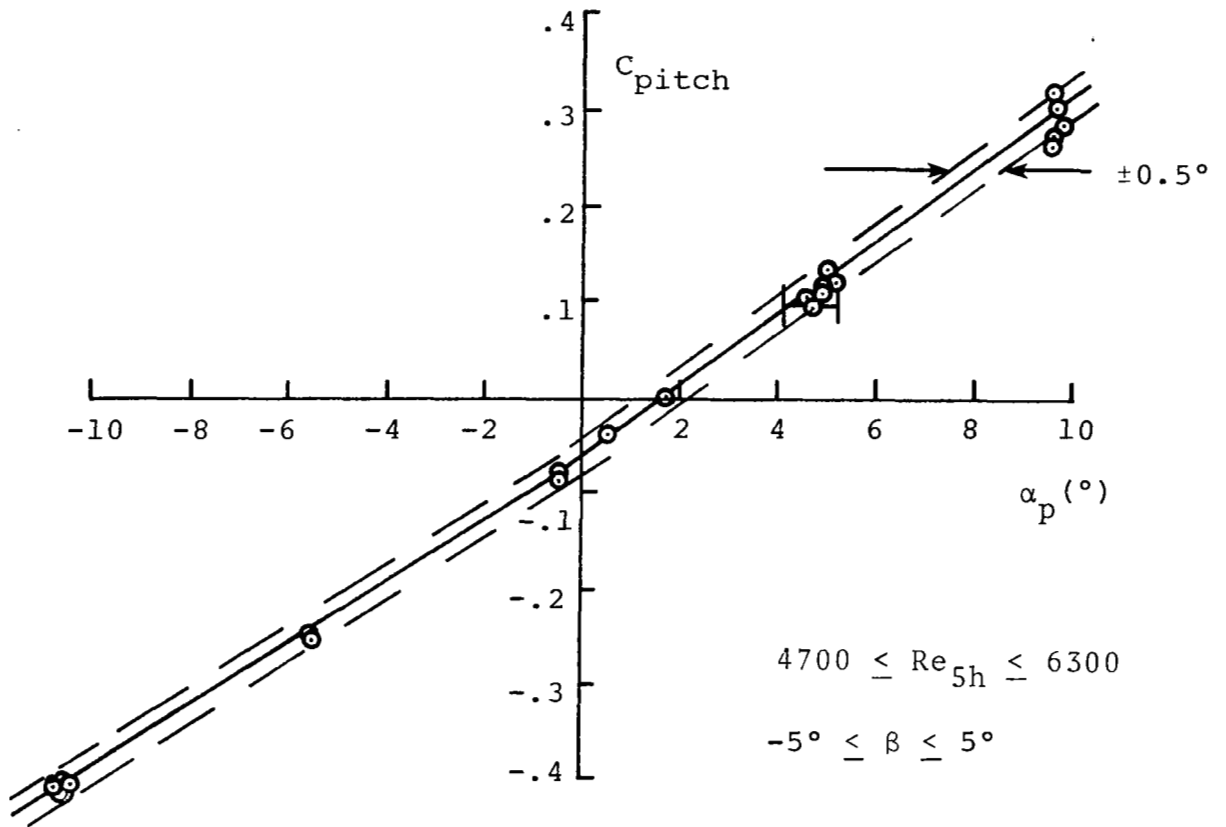


Figure 39.- Reynolds number dependence of a five-hole-probe pitch coefficient,  $-10^{\circ} \leq \alpha_p \leq 10^{\circ}$ .

1. Report No. NASA CR-3634	2. Government Accession No.	3. Recipient's Catalog No.	
4. Title and Subtitle <b>MEAN-FLOW MEASUREMENTS OF THE FLOW FIELD DIFFUSING BEND</b>		5. Report Date November 1982	6. Performing Organization Code <b>640/C</b>
		8. Performing Organization Report No. <b>NEAR TR 271</b>	
7. Author(s) <b>O. J. McMillan</b>		10. Work Unit No.	
9. Performing Organization Name and Address <b>Nielsen Engineering &amp; Research, Inc. 510 Clyde Avenue Mountain View, California 94043</b>		11. Contract or Grant No. <b>NAS3-22113</b>	
		13. Type of Report and Period Covered <b>Contractor Report</b>	
12. Sponsoring Agency Name and Address <b>National Aeronautics and Space Administration Cleveland, Ohio 44135</b>		14. Sponsoring Agency Code <b>505-32-2A</b> (E-1367)	
		15. Supplementary Notes <b>Final report. Project Manager, Donald R. Boldman, Fluid Mechanics and Acoustics Division, NASA Lewis Research Center, Cleveland, Ohio 44135.</b>	
16. Abstract <p>Time-average measurements of the low-speed turbulent flow in a diffusing bend are presented. The experimental geometry consists of parallel top and bottom walls and curved diverging side walls. The turning of the center line of this channel is 40°, the area ratio is 1.5 and the ratios of height and center-line length to throat width are 1.5 and 3, respectively. The diffusing bend is preceded and followed by straight constant-area sections in which measurements were also taken. The inlet boundary layers on the parallel walls are artificially thickened and occupy about 30% of the channel height; those on the side walls develop naturally and are about half as thick. The free-stream speed at the inlet was approximately 30 m/sec for all the measurements. Inlet boundary-layer mean-velocity and turbulence-intensity profiles are presented, as are data for wall static pressures, and at six cross sections, surveys of the velocity-vector and static-pressure fields. The flow-field surveys were done with a five-hole probe, the boundary-layer mean-velocity profiles with a flattened Pitot probe, and the intensity profiles with a single-sensor hot wire anemometer. The dominant feature of the flow field is shown to be a pair of counter-rotating streamwise vortices formed by the cross-stream pressure gradient in the bend on which an overall deceleration is superimposed. No separation or reverse flow was detected.</p>			
17. Key Words (Suggested by Author(s)) <b>Secondary flow Ducts - intake systems Curved diffusers</b>		18. Distribution Statement <b>Unclassified - unlimited STAR Category 02</b>	
19. Security Classif. (of this report) <b>Unclassified</b>	20. Security Classif. (of this page) <b>Unclassified</b>	21. No. of Pages <b>165</b>	22. Price* <b>A08</b>